US012040417B2

(12) **United States Patent**
Cardwell et al.

(10) **Patent No.: US 12,040,417 B2**
(45) **Date of Patent: Jul. 16, 2024**

(54) **POWER PHOTODIODE STRUCTURES AND DEVICES**

(71) Applicant: **SLT Technologies, Inc.**, Los Angeles, CA (US)

(72) Inventors: **Drew W. Cardwell**, Camas, WA (US); **Mark P. D'Evelyn**, Vancouver, WA (US)

(73) Assignee: **SLT Technologies, Inc.**, Los Angeles, CA (US)

(*) Notice: Subject to any disclaimer, the term of this patent is extended or adjusted under 35 U.S.C. 154(b) by 0 days.

(21) Appl. No.: **18/059,293**

(22) Filed: **Nov. 28, 2022**

(65) **Prior Publication Data**

US 2023/0108564 A1 Apr. 6, 2023

Related U.S. Application Data

(63) Continuation of application No. 17/151,109, filed on Jan. 15, 2021, now Pat. No. 11,569,398, which is a (Continued)

(51) **Int. Cl.**
H01L 31/0232 (2014.01)
G02B 6/42 (2006.01)
(Continued)

(52) **U.S. Cl.**
CPC ***H01L 31/02327*** (2013.01); ***G02B 6/4206*** (2013.01); ***H01L 31/02161*** (2013.01);
(Continued)

(58) **Field of Classification Search**
CPC H01L 31/02327; H01L 31/02161; H01L 31/022408; H01L 31/03048;
(Continued)

(56) **References Cited**

U.S. PATENT DOCUMENTS

5,883,988 A 3/1999 Yamamoto et al.
5,937,274 A 8/1999 Kondow et al.
(Continued)

FOREIGN PATENT DOCUMENTS

CN 107046071 A 8/2017
JP H11500273 A 1/1999
(Continued)

OTHER PUBLICATIONS

P. Żyłka and M. Guzowski, "Making Power over Fiber Supply of Microelectronic Sensor Devices Simpler," 2018 XV International Scientific Conference on Optoelectronic and Electronic Sensors (COE), Warsaw, Poland, 2018, pp. 1-4, doi: 10.1109/COE.2018.8435164 (Year: 2018).*
(Continued)

Primary Examiner — Sitaramarao S Yechuri
(74) *Attorney, Agent, or Firm* — Patterson + Sheridan, LLP

(57) **ABSTRACT**

According to the present disclosure, techniques related to manufacturing and applications of power photodiode structures and devices based on group-III metal nitride and gallium-based substrates are provided. More specifically, embodiments of the disclosure include techniques for fabricating photodiode devices comprising one or more of GaN, AlN, InN, InGaN, AlGaN, and AlInGaN, structures and devices. Such structures or devices can be used for a variety of applications including optoelectronic devices, photodiodes, power-over-fiber receivers, and others.

20 Claims, 58 Drawing Sheets

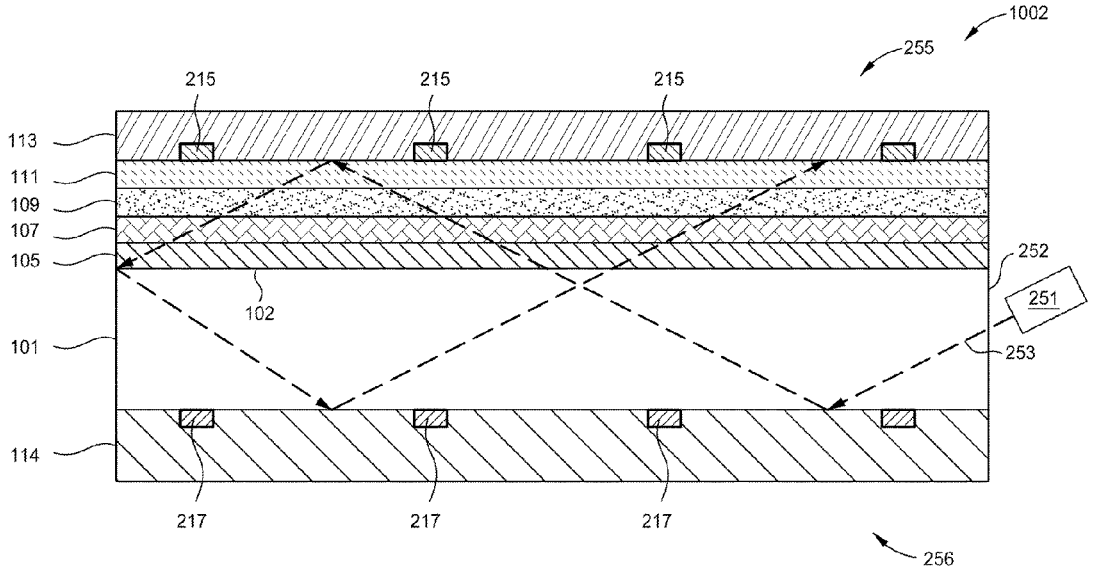

Related U.S. Application Data

continuation-in-part of application No. 16/930,250, filed on Jul. 15, 2020, now Pat. No. 11,444,216.

(60) Provisional application No. 62/978,281, filed on Feb. 18, 2020, provisional application No. 62/874,487, filed on Jul. 15, 2019.

(51) **Int. Cl.**

H01L 31/0216	(2014.01)
H01L 31/0224	(2006.01)
H01L 31/0304	(2006.01)
H01L 31/0352	(2006.01)
H01L 31/036	(2006.01)
H01L 31/109	(2006.01)
H01L 31/18	(2006.01)

(52) **U.S. Cl.**
CPC ***H01L 31/022408*** (2013.01); ***H01L 31/03048*** (2013.01); ***H01L 31/035236*** (2013.01); ***H01L 31/036*** (2013.01); ***H01L 31/109*** (2013.01); ***H01L 31/1892*** (2013.01)

(58) **Field of Classification Search**
CPC H01L 31/035236; H01L 31/036; H01L 31/109; H01L 31/1892; H01L 31/105; H01L 31/1852; G02B 6/4206; G02B 6/4214; H02J 50/30
See application file for complete search history.

(56) **References Cited**

U.S. PATENT DOCUMENTS

6,297,495	B1	10/2001	Bulovic et al.	
6,333,458	B1	12/2001	Forrest et al.	
6,440,769	B2 *	8/2002	Peumans	G02B 19/0023 136/246
6,806,508	B2	10/2004	D'Evelyn et al.	
7,119,372	B2	10/2006	Stokes et al.	
8,148,801	B2	4/2012	D'Evelyn	
8,455,894	B1 *	6/2013	D'Evelyn	H01L 33/405 257/E33.068
8,866,149	B2	10/2014	Holder et al.	
9,917,227	B1	3/2018	Hurni et al.	
2004/0008952	A1	1/2004	Kragl	
2004/0126053	A1 *	7/2004	Ouchi	G02B 6/12004 385/14
2005/0025443	A1 *	2/2005	Nakaji	H01L 31/105 257/431
2006/0000976	A1	1/2006	Brouns	
2006/0255341	A1	11/2006	Pinnington et al.	
2008/0123198	A1	5/2008	Fujita	
2010/0147382	A1	6/2010	Chiang et al.	
2013/0250991	A1	9/2013	Homewood et al.	
2014/0077322	A1 *	3/2014	Wertsberger	H01L 31/055 257/432
2014/0147650	A1	5/2014	Jiang et al.	
2014/0353713	A1	12/2014	Kuh et al.	
2015/0146757	A1	5/2015	Ohki et al.	
2015/0221803	A1	8/2015	Suarez Arias	
2016/0020284	A1	1/2016	D'Evelyn et al.	
2018/0195206	A1	7/2018	Jiang et al.	
2019/0088495	A1	3/2019	Youtsey et al.	
2019/0115497	A1	4/2019	Zhang et al.	
2019/0288132	A1	9/2019	Wang et al.	
2019/0305164	A1 *	10/2019	Vawter	H01L 31/1892

FOREIGN PATENT DOCUMENTS

WO	2002054129	7/2002	
WO	WO-2005060010 A1 *	6/2005	H01L 31/107
WO	2014141028 A1	9/2014	

OTHER PUBLICATIONS

A. Basanskaya, "Electricity over glass [fiber optic to transfer electric power]," in IEEE Spectrum, vol. 42, No. 10, pp. 18-18, Oct. 2005, doi: 10.1109/MSPEC.2005.1515953 (Year: 2005).*

G. Bottger et al., "Optically Powered Video Camera Link," 33rd European Conference and Exhibition of Optical Communication, Berlin, Germany, 2007, pp. 1-2 (Year: 2007).*

J. D. López-Cardona, C. Vázquez, D. S. Montero and P. C. Lallana, "Remote Optical Powering Using Fiber Optics in Hazardous Environments," in Journal of Lightwave Technology, vol. 36, No. 3, pp. 748-754, 1 Feb. 1, 2018, doi: 10. 1109/JLT.2017.2776399 (Year: 2018).*

Non-Final Office Action for U.S. Appl. No. 17/151,110 dated Mar. 17, 2022.

Non-Final Office Action for U.S. Appl. No. 17/151,109 dated Apr. 11, 2022.

Non-Final Office Action dated Apr. 11, 2022 for U.S. Appl. No. 17/151,109.

European Patent Application No. 21707436.8, Office Action dated Aug. 24, 2023, 6 pages.

Carlo De Santi et al. "GaN-Based Laser Wireless Power Transfer System", Materials 2018, 11, 153; doi: 10.3390/ma11010153.

"Improved Photovoltaic Effects of a Vertical-Type InGaN/GaN Multiple Quantum Well Solar Cell", Si-Young Bae et al 2011 Jpn. J. Appl. Phys. 50 092301.

J. Bai et al. "Efficiency enhancement of InGaN/GaN solar cells with nanostructures", Appl. Phys. Lett. 104, 051129 (2014); https://doi.org/10.1063/1.4864640 Submitted: Dec. 18, 2013 . Accepted: Jan. 23, 2014 . Published Online: Feb. 7, 2014.

Xiao-Mei Cai et al. "Fabrication and characterization of InGaN p-i-n homojunction solar cell", Appl. Phys. Lett. 95, 173504 (2009); https://doi.org/10.1063/1.3254215 Submitted: Jul. 24, 2009 . Accepted: Oct. 5, 2009 . Published Online: Oct. 28, 2009.

X. Chen et al. "Growth, fabrication, and characterization of InGaN solar cells", p hys. stat. sol. (a) 205, No. 5, 1103-1105 (2008) / DOI 10.1002/pssa.200778695.

Zhaoying Chen et al. "Positive temperature coefficient of photovoltaic efficiency in solar cells based on InGaN/GaN MQWs", Appl. Phys. Lett. 109, 062104 (2016); https://doi.org/10.1063/1.4960765 Submitted: Jul. 2, 2016 . Accepted: Jul. 26, 2016 . Published Online: Aug. 10, 2016.

Sang-Bae Choi, "Effect of indium composition on carrier escape in InGaN/GaN multiple quantum well solar cells", Appl. Phys. Lett. 103, 033901 (2013); https://doi.org/10.1063/1.4813623 Submitted: Jun. 4, 2013 . Accepted: Jun. 19, 2013 . Published Online: Jul. 15, 2013.

R. Dahal et al. "InGaN/GaN multiple quantum well concentrator solar cells", Appl. Phys. Lett. 97, 073115 (2010); https://doi.org/10.1063/1.3481424 Submitted: Jul. 8, 2010 . Accepted: Aug. 1, 2010 . Published Online: Aug. 19, 2010.

R. Dahal et al. "InGaN/GaN multiple quantum well solar cells with long operating wavelengths", Appl. Phys. Lett. 94, 063505 (2009); https://doi.org/10.1063/1.3081123 Submitted: Dec. 9, 2008 . Accepted: Jan. 20, 2009 . Published Online: Feb. 10, 2009.

Young, Nathan "Improving Efficiency of III-N Quantum Well Based Optoelectronic Devices through Active" Region Design and Growth Techniques 2015.

Robert Farrell et al. "High quantum efficiency InGaN/GaN multiple quantum well solar cells with spectral response extending out to 520 nm", Article in Applied Physics Letters • May 2011.

Guangxu Ju, "Role of threading dislocations in strain relaxation during GaInN growth monitored by real-time X-ray reflectivity", Article in Applied Physics Letters • Jun. 2017.

Y. El Gmili et al. "Multilayered InGaN/GaN structure vs. single InGaN layer for solar cell applications: A comparative study" Science Direct. Acta Materialia 61 (2013) 6587-6596.

Ray-Hua Horng et al. "Improved Conversion Efficiency of GaN/InGaN Thin-Film Solar Cells", IEEE Electron Device Letters, vol. 30, No. 7, Jul. 2009.

Omkar Jani et al. "Characterization and Analysis of InGaN Photovoltaic Devices", 0-7803-8707-4/05/$20.00 02005 IEEE.

(56) **References Cited**

OTHER PUBLICATIONS

Omkar Jani, "Design and characterization of solar cells", Appl. Phys. Lett. 91, 132117 (2007); https://doi.org/10.1063/1.2793180 Submitted: Jul. 22, 2007 . Accepted: Sep. 11, 2007 . Published Online: Sep. 28, 2007.
Omkar Jani1 et al. "Design, Growth, Fabrication and Characterization of High-Band Gap InGaN/GaN Solar Cells", 1-4244-0016-3/06/$20.00 © 2006 IEEE.
Omkar K. Jani, "Development of Wide-Band Gap InGaN Solar Cells for High-Efficiency Photovoltaics", 2008.
Ming-Jer Jeng et al. "Effect of Silicon Doping on Performance of 30-Pair InxGa1¬xN/GaN Quantum Well Solar Cells", Japanese Journal of Applied Physics 49 (2010) 052302.
Ming-Jer Jeng, "Influence of Polarization on the Efficiency of InxGa1 xN/GaN p-i-n Solar Cells", Japanese Journal of Applied Physics 49 (2010) 128001.
Asghar Asgari et al. "Temperature dependence of InGaN/GaN multiple quantum well based high efficiency solar cell", Solar Energy Materials & Solar Cells 95 (2011) 3124-3129.
Yen-Kuang Kuo et al. "Numerical Study of the Effects of Hetero-Interfaces, Polarization Charges, and Step-Graded Interlayers on the Photovoltaic Properties of (0001) Face GaN/InGaN p-i-n Solar Cell", IEEE Journal of Quantum Electronics, vol. 48, No. 3, Mar. 2012.
Yousuke Kuwahara et al. "GaInN-Based Solar Cells Using Strained-Layer GaInN/GaInN Superlattice Active Layer on a Freestanding GaN Substrate", Applied Physics Express 4 (2011) 021001.
Yosuke Kuwahara et al. "Realization of Nitride-Based Solar Cell on Freestanding GaN Substrate", 2010 Appl. Phys. Express 3 111001.
J. R. Lang, et al. "High external quantum efficiency and fillfactor InGaN/GaN heterojunction solar cells grown by –based molecular beam epitaxy", Appl. Phys. Lett. 98, 131115 (2011); https://doi.org/10.1063/1.3575563 Submitted: Mar. 3, 2011 . Accepted: Mar. 21, 2011 . Published Online: Apr. 1, 2011.
Z. Q. Li et al. "Effects of polarization charge on the photovoltaic properties of InGaN solar cells", Phys. Status Solidi A 208, No. 4, 928-931 (2011) / DOI 10.1002/pssa.201026489.
Na Lu, "III-nitrides for energy production: photovoltaic and thermoelectric applications", Semicond. Sci. Technol. 28 (2013) 074023 (11pp).
Elison Matioli et al. "High internal and external quantum efficiency InGaN/GaN solar cells", Applied Physics Letters 98, 021102 (2011).
Anna Mukhtarova et al. "Dependence of the photovoltaic performance of pseudomorphic InGaN/GaN multiple-quantum-well solar cells on the active region thickness", Appl. Phys. Lett. 108, 161907 (2016); https://doi.org/10.1063/1.4947445 Submitted: Feb. 22, 2016 . Accepted: Apr. 12, 2016 . Published Online: Apr. 22, 2016.
Carl J. Neufeld et al. "Effect of doping and polarization on carrier collection in InGaN quantum well solar cells", Appl. Phys. Lett. 98, 243507 (2011); https://doi.org/10.1063/1.3595487 Submitted: Mar. 24, 2011 . Accepted: May 9, 2011 . Published Online: Jun. 16, 2011.
Carl J. Neufeld et al. "High quantum efficiency InGaN/GaN solar cells with 2.95 eV band gap", Appl. Phys. Lett. 93, 143502 (2008); https://doi.org/10.1063/1.2988894 Submitted: Aug. 19, 2008 . Accepted: Sep. 3, 2008 . Published Online: Oct. 8, 2008.
Carl Neufeld et al. "Effect of doping and polarization on carrier collection in InGaN quantum well solar cells", Article in Applied Physics Letters • Jul. 2011, DOI: 10.1063/1.3595487 • Source: IEEE Xplore.
Cyril Pernot et al. "Solar-Blind UV Photodetectors Based on GaN/AlGaN p-i-n Photodiodes", Jpn. J. Appl. Phys. vol. 39 (2000) pp. L 387-L 389, Part 2, No. 5A, May 1, 2000, The Japan Society of Applied Physics.
L. Redaelli et al. "Effect of the quantum well thickness on the performance of InGaN photovoltaic cells", Appl. Phys. Lett. 105, 131105 (2014); https://doi.org/10.1063/1.4896679 Submitted: Jul. 29, 2014 . Accepted: Sep. 16, 2014 . Published Online: Sep. 29, 2014.
Daisuke Iida et al. "Analysis of strain relaxation process in GaInN/GaN heterostructure by in situ X-ray diffraction monitoring during metalorganic vapor-phase epitaxial growth", Article in physica status solidi (RRL)—Rapid Research Letters • Mar. 2013.
Liwen Sang et al. "Enhanced performance of InGaN solar cell by using a super-thin AlN interlayer", Appl. Phys. Lett. 99, 161109 (2011); https://doi.org/10.1063/1.3654155 Submitted: Sep. 4, 2011 . Accepted: Sep. 30, 2011 . Published Online: Oct. 19, 2011.
Jinn-Kong Sheu et al, "Demonstration of GaN-Based Solar Cells With GaN/InGaN Superlattice Absorption Layers", IEEE Electron Device Letters, vol. 30, No. 3, Mar. 2009.
Ehsan Vadiee, et al. "Evaluating the performance of InGaN/GaN multi-quantum-well solar cells operated at elevated temperatures via DC and small-signal AC analysis", Japanese Journal of Applied Physics 58, 101003 (2019).
Sirona Valdueza-Felip et al. "Photovoltaic Response of InGaN/GaN Multiple-Quantum Well Solar Cells", Japanese Journal of Applied Physics 52 (2013) 08JH05.
Noriyuki Watanabe et al. "Barrier Thickness Dependence of Photovoltaic Characteristics of InGaN/GaN Multiple Quantum Well Solar Cells", 2012 Jpn. J. Appl. Phys. 51 10ND10.
Noriyuki Watanabe et al. "Influence of InGaN/GaN multiple quantum well structure on photovoltaic characteristics of solar cell", 2014 Jpn. J. Appl. Phys. 53 112301.
J. J. Wierer, et al. "Influence of barrier thickness on the performance of InGaN/GaN multiple quantum well solar cells", Appl. Phys. Lett. 100, 111119 (2012); https://doi.org/10.1063/1.3695170 Submitted: Jan. 24, 2012 . Accepted: Mar. 1, 2012 . Published Online: Mar. 16, 2012.
Zhang Xiao-Bin et al. "InGaN/GaN multiple quantum well solar cells with an enhanced open-circuit voltage", 2011 Chinese Phys. B 20 028402.
C. C. Yang et al. "Enhancement of the conversion efficiency of GaN-based photovoltaic devices with AlGaN/InGaN absorption layers", Appl. Phys. Lett. 97, 021113 (2010); https://doi.org/10.1063/1.3463469, Submitted: Apr. 24, 2010 . Accepted: Jun. 22, 2010 . Published Online: Jul. 16, 2010.
J. Yang, et al. "Photovoltaic response of InGaN/GaN multi-quantum well solar cells enhanced by inserting thin GaN cap layers", Journal of Alloys and Compounds 635 (2015) 82-86.
N. G. Young et al. "High-performance broadband optical coatings on InGaN/GaN solar cells for multijunction device Integration", Appl. Phys. Lett. 104, 163902 (2014); https://doi.org/10.1063/1.4873117 Submitted: Mar. 12, 2014 . Accepted: Apr. 11, 2014 . Published Online: Apr. 22, 2014.
N. G. Young et al. "High performance thin quantum barrier InGaN/GaN solar cells on sapphire and bulk (0001) GaN substrates", Appl. Phys. Lett. 103, 173903 (2013); https://doi.org/10.1063/1.4826483 Submitted: Aug. 16, 2013 . Accepted: Oct. 6, 2013 . Published Online: Oct. 22, 2013.
Xinhe Zheng et al. High-quality InGaN/GaN heterojunctions and their photovoltaic effects, Phys. Lett. 93, 261108 (2008); https://doi.org/10.1063/1.3056628 Submitted: Oct. 30, 2008 . Accepted: Dec. 4, 2008 . Published Online: Dec. 29, 2008.
International Search Report dated Apr. 19, 2021, Application No. PCT/US2020/066900.
Asgari, A., Khalili, K. (2011). Temperature dependence of InGaN/GaN multiple quantum well based high efficiency solar cell. Solar Energy Materials and Solar Cells, 95(11), 3124-3129. https://doi.org/10.1016/j.solmat.2011.07.001.
Bae, S.-Y., Shim, J.-P., Lee, D.-S., Jeon, S.-R., Namkoong, G. (2011). Improved Photovoltaic Effects of a Vertical-Type InGaN/GaN Multiple Quantum Well Solar Cell. Japanese Journal of Applied Physics, 50(98), 092301.
Bai, J., Yang, C. C., Athanasiou, M., Wang, T. (2014). Efficiency enhancement of InGaN/GaN solar cells with nanostructures. Applied Physics Letters, 104(5), 051129. https://doi.org/10.1063/1.4864640.
Cai, X. M., Zeng, S. W., Zhang, B. P. (2009). Fabrication and characterization of InGaN p-i-n homojunction solar cell. Applied Physics Letters, 95(17), 173504. https://doi.org/10.1063/1.3254215.
Chen, X., Matthews, K. D., Hao, D., Schaff, W. J., Eastman, L. F. (2008). Growth, fabrication, and characterization of InGaN solar cells. Physica Status Solidi (A) Applications and Materials Science, 205(5), 1103-1105. https://doi.org/10.1002/pssa.200778695.

(56) **References Cited**

OTHER PUBLICATIONS

Chen, Z., Zheng, X., Li, Z., Wang, P., Rong, X., Wang, T., Yang, X., Xu, F., Qin, Z., Ge, W., Shen, B., Wang, X. (2016). Positive temperature coefficient of photovoltaic efficiency in solar cells based on InGaN/GaN MQWs. Applied Physics Letters, 109(6), 062104. https://doi.org/10.1063/1.4960765.

Choi, S. B., Shim, J. P., Kim, D. M., Jeong, H. Il, Jho, Y. D., Song, Y. H., Lee, D. S. (2013). Effect of indium composition on carrier escape in InGaN/GaN multiple quantum well solar cells. Applied Physics Letters, 103(3), 033901. https://doi.org/10.1063/1.4813623.

Dahal, R., Li, J., Aryal, K., Lin, J. Y., Jiang, H. X. (2010). InGaN/GaN multiple quantum well concentrator solar cells. Applied Physics Letters, 97(7), 073115. https://doi.org/10.1063/1.3481424.

Dahal, R., Pantha, B., Li, J., Lin, J. Y., Jiang, H. X. (2009). InGaN/GaN multiple quantum well solar cells with long operating wavelengths. Applied Physics Letters, 94(6), 063505. https://doi.org/10.1063/1.3081123.

De Santi, C., Meneghini, M., Caria, A., Dogmus, E., Zegaoui, M., Medjdoub, F., Kalinic, B., Cesca, T., Meneghesso, G., Zanoni, E. (2018). GaN-based laser wireless power transfer system. Materials, 11(1), 153. https://doi.org/10.3390/ma11010153.

El Gmili, Y., Orsal, G., Pantzas, K., Moudakir, T., Sundaram, S., Patriarche, G., Hester, J., Ahaitouf, A., Salvestrini, J. P., Ougazzaden, A. (2013). Multilayered InGaN/GaN structure vs. single InGaN layer for solar cell applications: A comparative study. Acta Materialia, 61(17), 6587-6596. https://doi.org/10.1016/j.actamat.2013.07.041.

Farrell, R. M., Neufeld, C. J., Cruz, S. C., Lang, J. R., Iza, M., Keller, S., Nakamura, S., Denbaars, S. P., Mishra, U. K., Speck, J. S. (2011). High quantum efficiency InGaN/GaN multiple quantum well solar cells with spectral response extending out to 520 nm. Applied Physics Letters, 98(20), 201107. https://doi.org/10.1063/1.3591976.

Horng, R. H., Lin, S. T., Tsai, Y. L., Chu, M. T., Liao, W. Y., Wu, M. H., Lin, R. M., Lu, Y. C. (2009). Improved conversion efficiency of GaN/InGaN thin-film solar cells. IEEE Electron Device Letters, 30(7), 724-726. https://doi.org/10.1109/LED.2009.2021414.

Ida, D., Kondo, Y., Sowa, M., Sugiyama, T., Iwaya, M., Takeuchi, T., Kamiyama, S., Akasaki, I. (2013). Analysis of strain relaxation process in GaInN/GaN heterostructure by in situ X-ray diffraction monitoring during metalorganic vapor-phase epitaxial growth. Physica Status Solidi—Rapid Research Letters, 7(3), 211-214. https://doi.org/10.1002/pssr.201307023.

Jani, O. K. (2008). Development of Wide-Band Gap InGaN Solar Cells for High-Efficiency Photovoltaics A Dissertation Presented to The Academic Faculty. Georgia Institute of Technology.

Jani, O., Ferguson, I., Honsberg, C., Kurtz, S. (2007). Design and characterization of GaNInGaN solar cells. Applied Physics Letters, 91(13), 132117. https://doi.org/10.1063/1.2793180.

Jani, O., Honsberg, C., Asghar, A., Nicol, D., Ferguson, I., Doolittle, A., Kurtz, S. (2005). Characterization and Analysis of InGaN Photovoltaic Devices. Conference Record of the Thirty-First IEEE Photovoltaic Specialists Conference, 37-42. https://doi.org/10.1109/PVSC.2005.1488064.

Jani, O., Honsberg, C., Huang, Y., Song, J.-O., Ferguson, I., Namkoong, G., Trybus, E., Doolittle, A., Kurtz, S. (2006). Design, Growth, Fabrication and Characterization of High-Band Gap InGaN/GaN Solar Cells. IEEE 4th World Conference on Photovoltaic Energy Conference, 20-25. https://doi.org/10.1109/WCPEC.2006.279337.

Jeng, M. J. (2010). Influence of polarization on the efficiency of InxGa 1-xN/GaN p-i-n solar cells. Japanese Journal of Applied Physics, 49(12), 128001. https://doi.org/10.1143/JJAP.49.128001.

Jeng, M. J., Su, T. W., Lee, Y. L., Chang, Y. H., Chang, L. B., Lin, R. M., Jiang, J. H., Lu, Y. C. (2010). Effect of silicon doping on performance of 30-pair InxGa 1-xN/GaN quantum well solar cells. Japanese Journal of Applied Physics, 49(5 Part 1), 0523021-0523024. https://doi.org/10.1143/JJAP.49.052302.

Ju, G., Tabuchi, M., Takeda, Y., Amano, H. (2017). Role of threading dislocations in strain relaxation during GaInN growth monitored by real-time X-ray reflectivity. Applied Physics Letters, 110(26), 262105. https://doi.org/10.1063/1.4990687.

Kuo, Y. K., Chang, J. Y., Shih, Y. H. (2012). Numerical study of the effects of hetero-interfaces, polarization charges, and step-graded interlayers on the photovoltaic properties of (0001) face GaN/InGaN p-i-n solar cell. IEEE Journal of Quantum Electronics, 48(3), 367-374. https://doi.org/10.1109/JQE.2011.2181972.

Kuwahara, Y., Fujii, T., Fujiyama, Y., Sugiyama, T., Iwaya, M., Takeuchi, T., Kamiyama, S., Akasaki, I., Amano, H. (2010). Realization of nitride-based solar cell on freestanding GaN substrate. Applied Physics Express, 3(11), 111001. https://doi.org/10.1143/APEX.3.111001.

Kuwahara, Y., Fujii, T., Sugiyama, T., Iida, D., Isobe, Y., Fujiyama, Y., Morita, Y., Iwaya, M., Takeuchi, T., Kamiyama, S., Akasaki, I., Amano, H. (2011). GaInN-based solar cells using strained-layer GaInN/GaInN superlattice active layer on a freestanding GaN substrate. Applied Physics Express, 4(2), 021001. https://doi.org/10.1143/APEX.4.021001.

Lang, J. R., Neufeld, C. J., Hurni, C. A., Cruz, S. C., Matioli, E., Mishra, U. K., Speck, J. S. (2011). High external quantum efficiency and fill-factor InGaN/GaN heterojunction solar cells grown by NH3-based molecular beam epitaxy. Applied Physics Letters, 98(13), 131115. https://doi.org/10.1063/1.3575563.

Li, Z. Q., Lestradet, M., Xiao, Y. G., Li, S. (2011). Effects of polarization charge on the photovoltaic properties of InGaN solar cells. Physica Status Solidi (A) Applications and Materials Science, 208(4), 928-931. https://doi.org/10.1002/pssa.201026489.

Lu, N., Ferguson, I. (2013). III-nitrides for energy production: Photovoltaic and thermoelectric applications. In Semiconductor Science and Technology (vol. 28, Issue 7, pp. 1-11). https://doi.org/10.1088/0268-1242/28/7/074023.

Matioli, E., Neufeld, C., Iza, M., Cruz, S. C., Al-Heji, A. A., Chen, X., Farrell, R. M., Keller, S., DenBaars, S., Mishra, U., Nakamura, S., Speck, J., Weisbuch, C. (2011). High internal and external quantum efficiency InGaN/GaN solar cells. Applied Physics Letters, 98(2), 021102. https://doi.org/10.1063/1.3540501.

Mukhtarova, A., Valdueza-Felip, S., Redaelli, L., Durand, C., Bougerol, C., Monroy, E., Eymery, J. (2016). Dependence of the photovoltaic performance of pseudomorphic InGaN/GaN multiple-quantum-well solar cells on the active region thickness. Applied Physics Letters, 108(16), 161907. https://doi.org/10.1063/1.4947445.

Neufeld, C. J., Cruz, S. C., Farrell, R. M., Iza, M., Lang, J. R., Keller, S., Nakamura, S., Denbaars, S. P., Speck, J. S., Mishra, U. K. (2011). Effect of doping and polarization on carrier collection in InGaN quantum well solar cells. Applied Physics Letters, 98(24), 243507. https://doi.org/10.1063/1.3595487.

Neufeld, C. J., Toledo, N. G., Cruz, S. C., Iza, M., DenBaars, S. P., Mishra, U. K. (2008). High quantum efficiency InGaN/GaN solar cells with 2.95 eV band gap. Applied Physics Letters, 93(14), 143502. https://doi.org/10.1063/1.2988894.

Pernot, C., Hirano, A., Iwaya, M., Detchprohm, T., Amano, H., Akasaki, I. (2000). Solar-Blind UV Photodetectors Based on GaN/AlGaN p-i-n Photodiodes. Jpn. J. Appl. Phys, 39(Part 2, No. 5A), L387-L 389.

Redaelli, L., Mukhtarova, A., Valdueza-Felip, S., Ajay, A., Bougerol, C., Himwas, C., Faure-Vincent, J., Durand, C., Eymery, J., Monroy, E. (2014). Effect of the quantum well thickness on the performance of InGaN photovoltaic cells. Applied Physics Letters, 105(13), 131105. https://doi.org/10.1063/1.4896679.

Sang, L., Liao, M., Ikeda, N., Koide, Y., Sumiya, M. (2011). Enhanced performance of InGaN solar cell by using a super-thin AlN interlayer. Applied Physics Letters, 99(16), 161109. https://doi.org/10.1063/1.3654155.

Sheu, J. K., Yang, C. C., Tu, S. J., Chang, K. H., Lee, M. L., Lai, W. C., Peng, L. C. (2009). Demonstration of GaN-based solar cells with GaN/InGaN superlattice absorption layers. IEEE Electron Device Letters, 30(3), 225-227. https://doi.org/10.1109/LED.2008.2012275.

Vadiee, E., Fischer, A. M., Clinton, E. A., McFavilen, H., Patadia, A., Arena, C., Ponce, F. A., King, R. R., Honsberg, C. B., Doolittle, W. A. (2019). Evaluating the performance of InGaN/GaN multi-quantum-well solar cells operated at elevated temperatures via DC

(56) **References Cited**

OTHER PUBLICATIONS

and small-signal AC analysis. Japanese Journal of Applied Physics, 58(10), 101003. https://doi.org/10.7567/1347-4065/ab3b66.
Valdueza-Felip, S., Mukhtarova, A., Pan, Q., Altamura, G., Grenet, L., Durand, C., Bougerol, C., Peyrade, D., Gonzalez-Posada, F., Eymery, J., Monroy, E. (2013). Photovoltaic response of InGaN/GaN multiple-quantum well solar cells. Japanese Journal of Applied Physics, 52(8 Part 2), 08JH05. https://doi.org/10.7567/JJAP.52.08JH05.
Watanabe, N., Mitsuhara, M., Yokoyama, H., Liang, J., Shigekawa, N. (2014). Influence of InGaN/GaN multiple quantum well structure on photovoltaic characteristics of solar cell. Japanese Journal of Applied Physics, 53(11), 112301. https://doi.org/10.7567/JJAP.53.112301.
Watanabe, N., Yokoyama, H., Shigekawa, N., Sugita, K. I., Yamamoto, A. (2012). Barrier thickness dependence of photovoltaic characteristics of InGaN/GaN multiple quantum well solar cells. Japanese Journal of Applied Physics, 51 (10S), 10ND10. https://doi.org/10.1143/JJAP.51.10ND10.
Wierer, J. J., Koleske, D. D., Lee, S. R. (2012). Influence of barrier thickness on the performance of InGaN/GaN multiple quantum well solar cells. Applied Physics Letters, 100(11), 11111. https://doi.org/10.1063/1.3695170.
Yang, C. C., Sheu, J. K., Liang, X. W., Huang, M. S., Lee, M. L., Chang, K. H., Tu, S. J., Huang, F. W., Lai, W. C. (2010). Enhancement of the conversion efficiency of GaN-based photovoltaic devices with AlGaN/InGaN absorption layers. Applied Physics Letters, 97(2), 021113. https://doi.org/10.1063/1.3463469.
Yang, J., Zhao, D. G., Jiang, D. S., Chen, P., Zhu, J. J., Liu, Z. S., Le, L. C., He, X. G., Li, X. J., Yang, H., Zhang, Y. T., Du, G. T. (2015). Photovoltaic response of InGaN/GaN multi-quantum well solar cells enhanced by inserting thin GaN cap layers. Journal of Alloys and Compounds, 635, 82-86. https://doi.org/10.1016/j.jallcom.2015.02.052.
Young, N. G., Farrell, R. M., Hu, Y. L., Terao, Y., Iza, M., Keller, S., Denbaars, S. P., Nakamura, S., Speck, J. S. (2013). High performance thin quantum barrier InGaN/GaN solar cells on sapphire and bulk (0001) GaN substrates. Applied Physics Letters, 103(17), 173903. https://doi.org/10.1063/1.4826483.
Young, N. G., Perl, E. E., Farrell, R. M., Iza, M., Keller, S., Bowers, J. E., Nakamura, S., Denbaars, S. P., Speck, J. S. (2014). High-performance broadband optical coatings on InGaN/GaN solar cells for multijunction device integration. Applied Physics Letters, 104(16), 163902. https://doi.org/10.1063/1.4873117.
Young, N. G. (2015). Improving Efficiency of III-N Quantum Well Based Optoelectronic Devices through Active Region Design and Growth Techniques. University of California Santa Barbara .
Zhang, X. Bin, Wang, X. L., Xiao, H. L., Yang, C. B., Hou, Q. F., Yin, H. B., Chen, H., Wang, Z. G. (2011). InGaN/GaN multiple quantum well solar cells with an enhanced open-circuit voltage. Chinese Physics B, 20(2), 028402. https://doi.org/10.1088/1674-1056/20/2/028402.
Zhang, Y., Kappers, M. J., Zhu, D., Oehler, F., Gao, F., Humphreys, C. J. (2013). The effect of dislocations on the efficiency of InGaN/GaN solar cells. Solar Energy Materials and Solar Cells, 117, 279-284. https://doi.org/10.1016/j.solmat.2013.06.022.
Zheng, X., Horng, R. H., Wuu, D. S., Chu, M. T., Liao, W. Y., Wu, M. H., Lin, R. M., Lu, Y. C. (2008). High-quality InGaN/GaN heterojunctions and their photovoltaic effects. Applied Physics Letters, 93(26), 261108. https://doi.org/10.1063/1.3056628.
International Search Report dated Sep. 4, 2020, Application No. PCT/US2020/042205.
International Search Report dated Oct. 18, 2021, Application No. PCT/US2021/013760.
U.S. Office Action for U.S. Appl. No. 16/930,250 dated Dec. 15, 2021, 19 pages.
Chinese Application No. 202180015546.2, Office Action and Search Report dated Dec. 7, 2023, 15 pages.
L. J. Meyer, "Using fiber optics with analog RF signals," IEEE 39th Vehicular Technology Conference, San Francisco, CA, USA, 1989, pp. 398-400vol.1, doi: 10.1109NETEC.1989.40106.
X. Zhou et al., "Vertically Integrated Optical Sensor With Photoconductive Gain > 10 and Fill Factor> 70%," in IEEE Electron Device Letters, vol. 39, No. 3, pp. 386-389, Mar. 2018, doi: 10.1109/LED.2018.2792003.
C. Budelmann, "Opto-Electronic Sensor Network Powered Over Fiber for Harsh Industrial Applications," in IEEE Transactions on Industrial Electronics, vol. 65, No. 2, pp. 1170-1177, Feb. 2018, doi: 10.1109/TIE.2017.2733479.

* cited by examiner

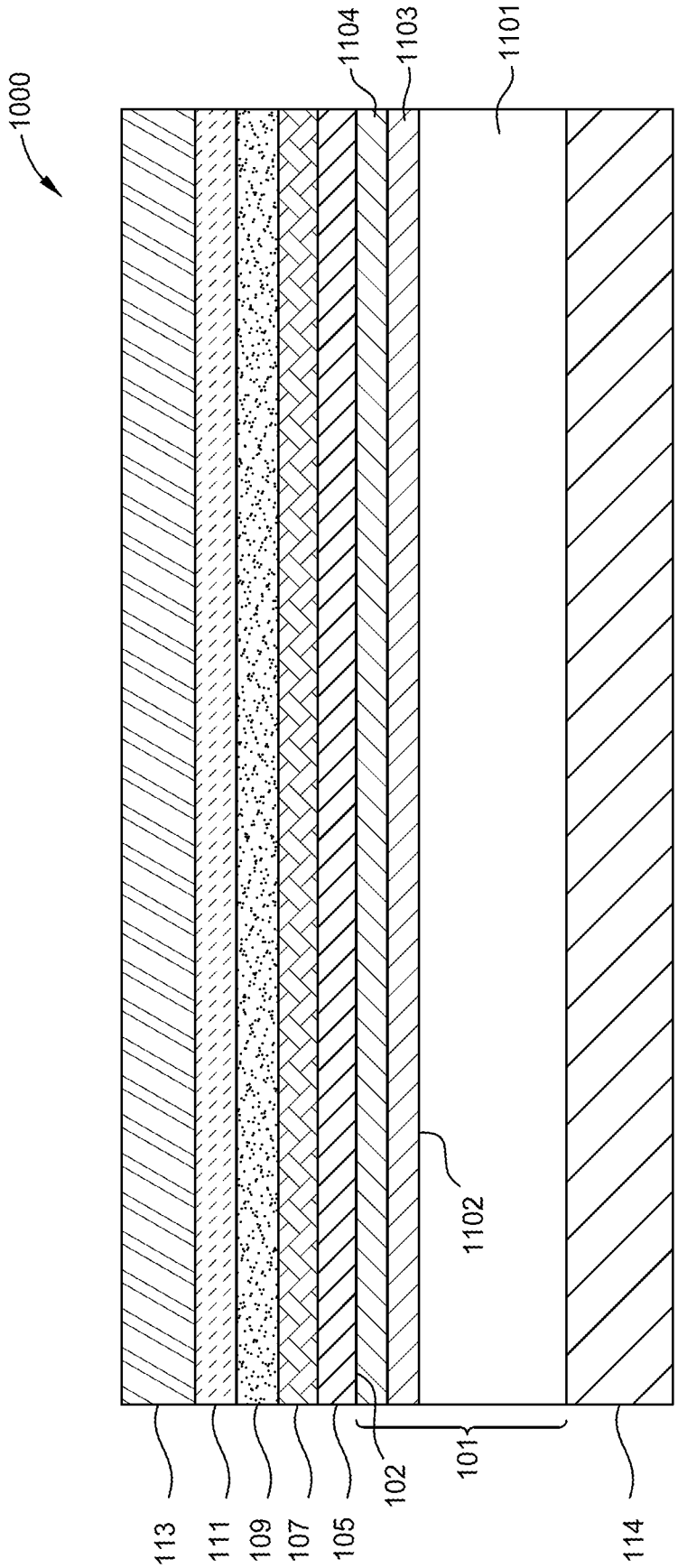

FIG. 1

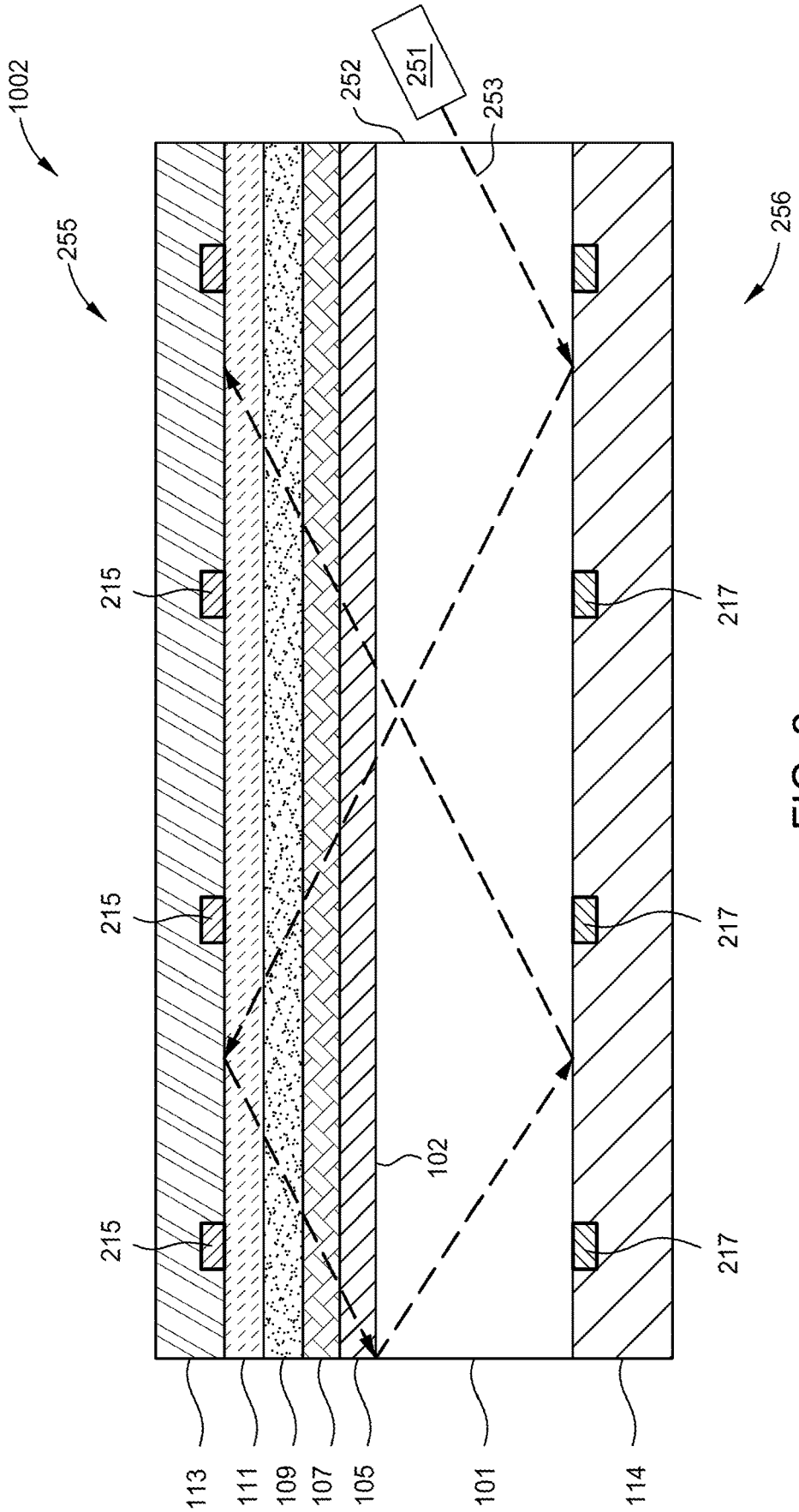
1002
255
256
251
252
253
215
215
215
217
217
217
102
113
111
109
107
105
101
114

FIG. 2

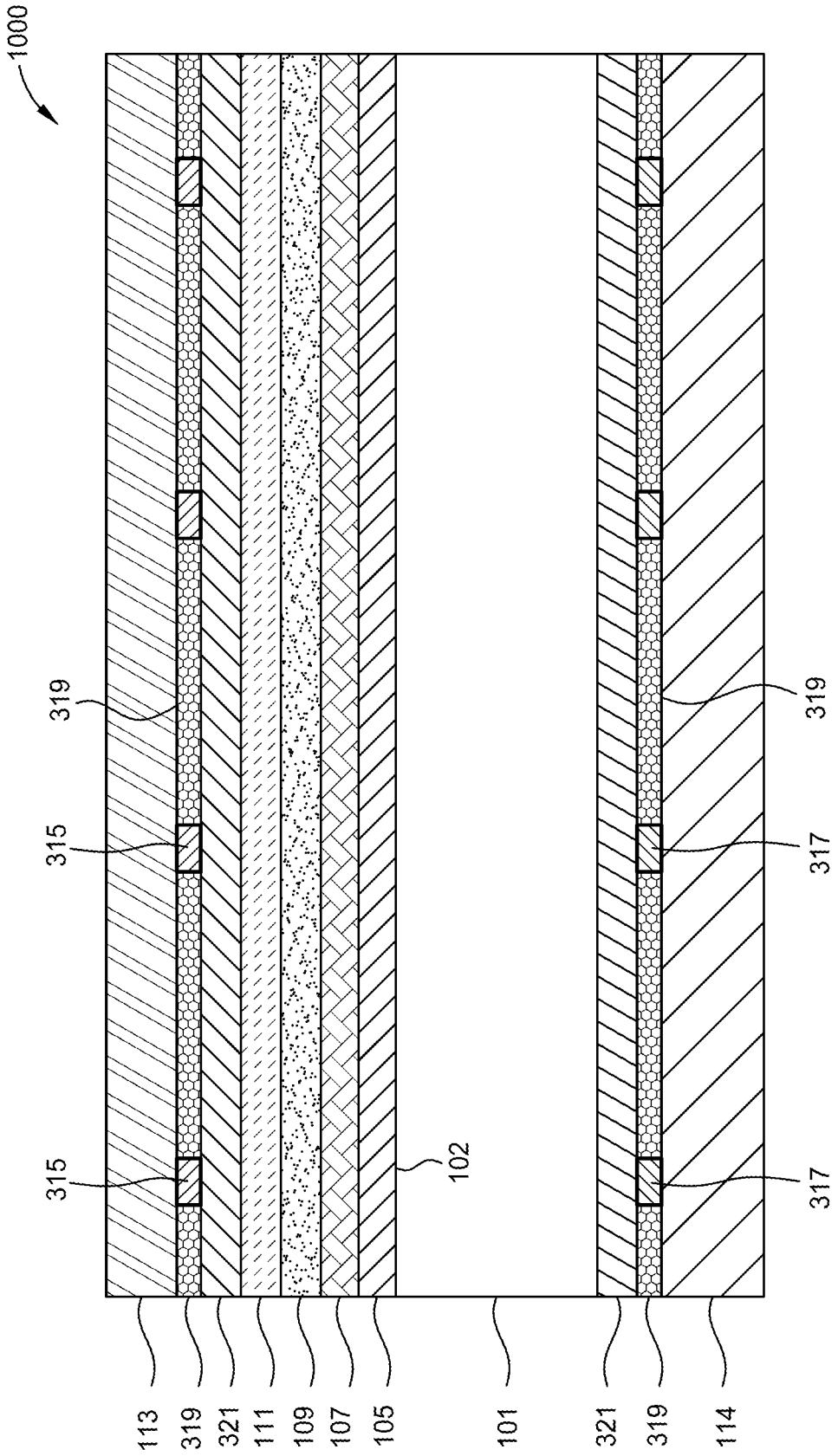
1000
319
315
315
102
319
317
317
113
319
321
111
109
107
105
101
321
319
114

FIG. 3

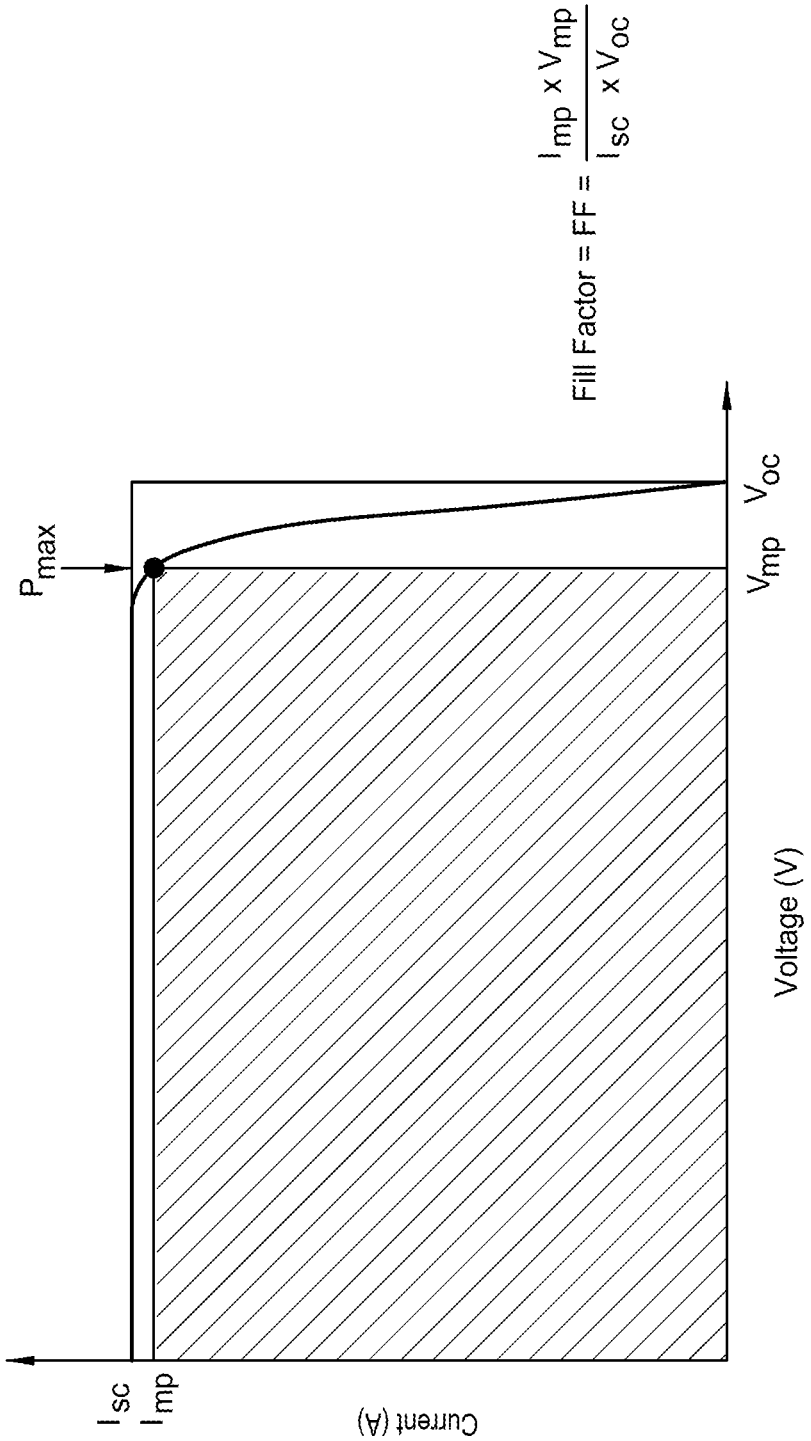
Fill Factor = FF = $\frac{I_{mp} \times V_{mp}}{I_{sc} \times V_{oc}}$
P_{max}
V_{oc}
V_{mp}
Voltage (V)
I_{sc}
I_{mp}
Current (A)

FIG. 4

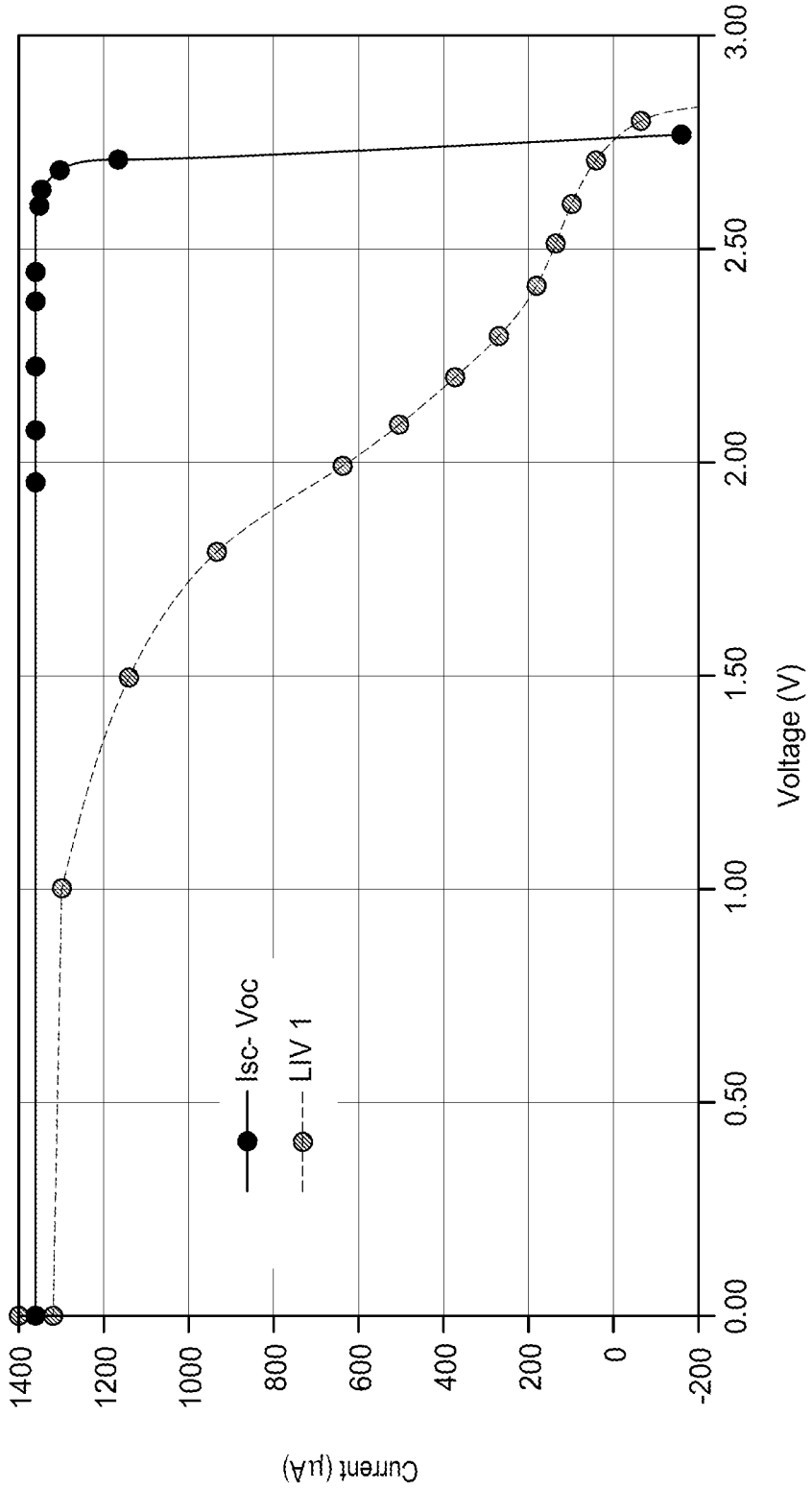
Current (μA)
1400
1200
1000
800
600
400
200
0
-200
0.00
0.50
1.00
1.50
2.00
2.50
3.00
Voltage (V)
Isc- Voc
LIV 1

FIG. 5

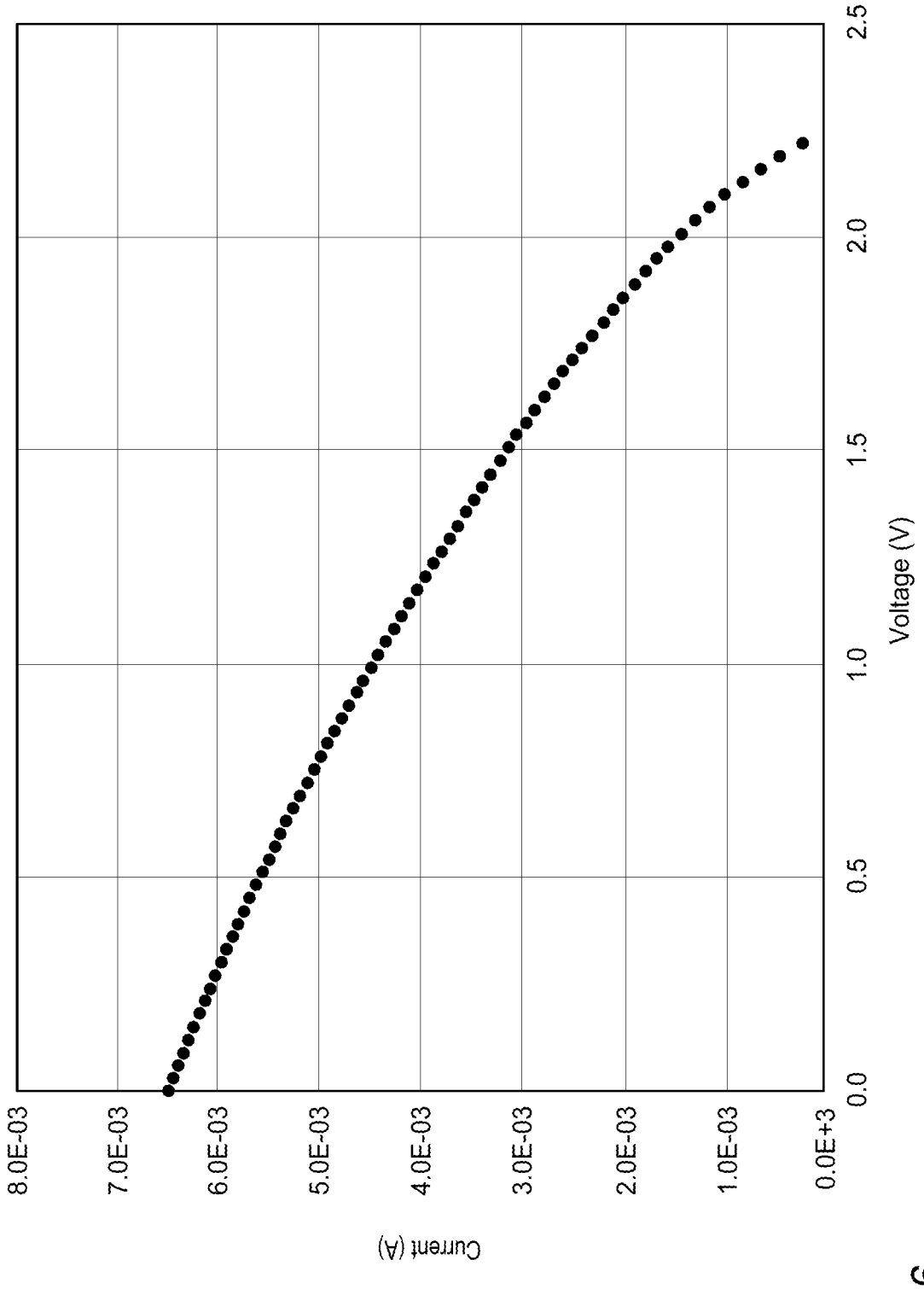
8.0E-03
7.0E-03
6.0E-03
5.0E-03
4.0E-03
3.0E-03
2.0E-03
1.0E-03
0.0E+3
Current (A)
0.0
0.5
1.0
1.5
2.0
2.5
Voltage (V)

FIG. 6

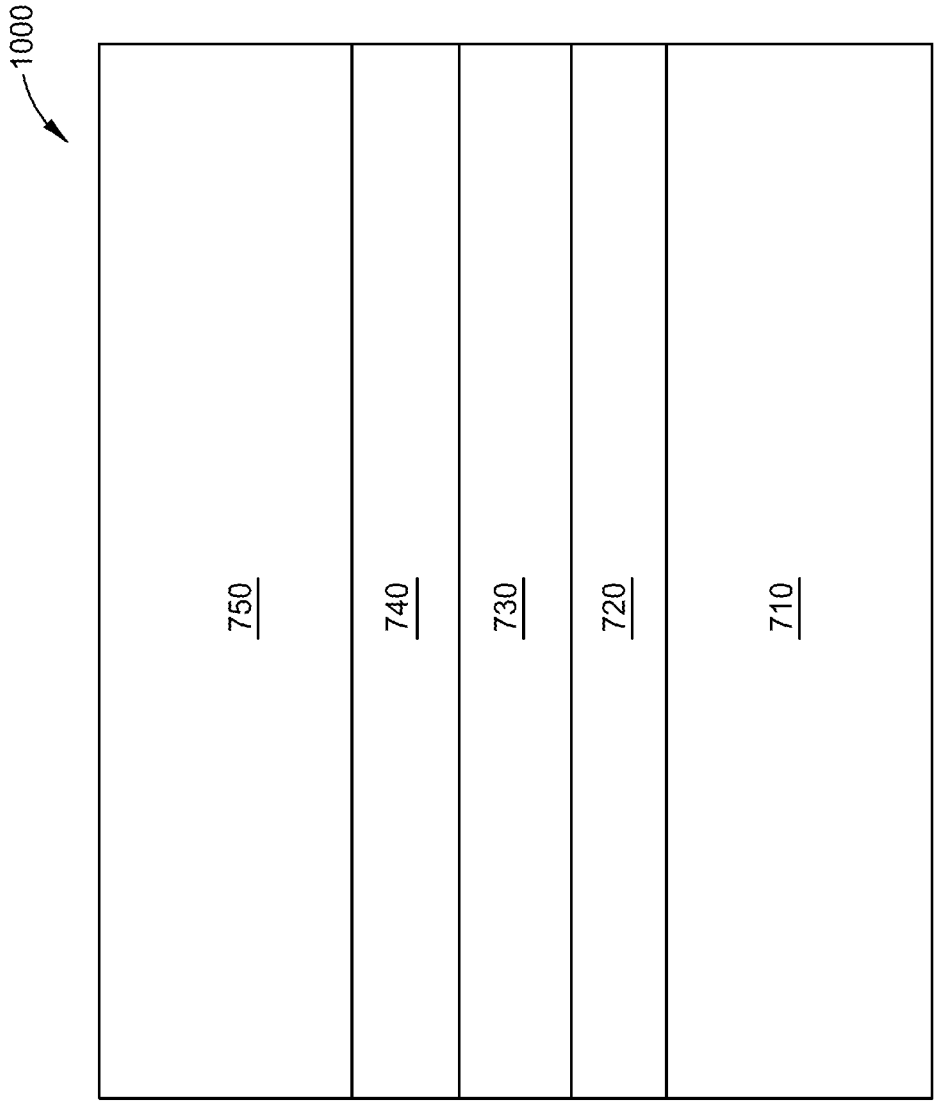

FIG. 7

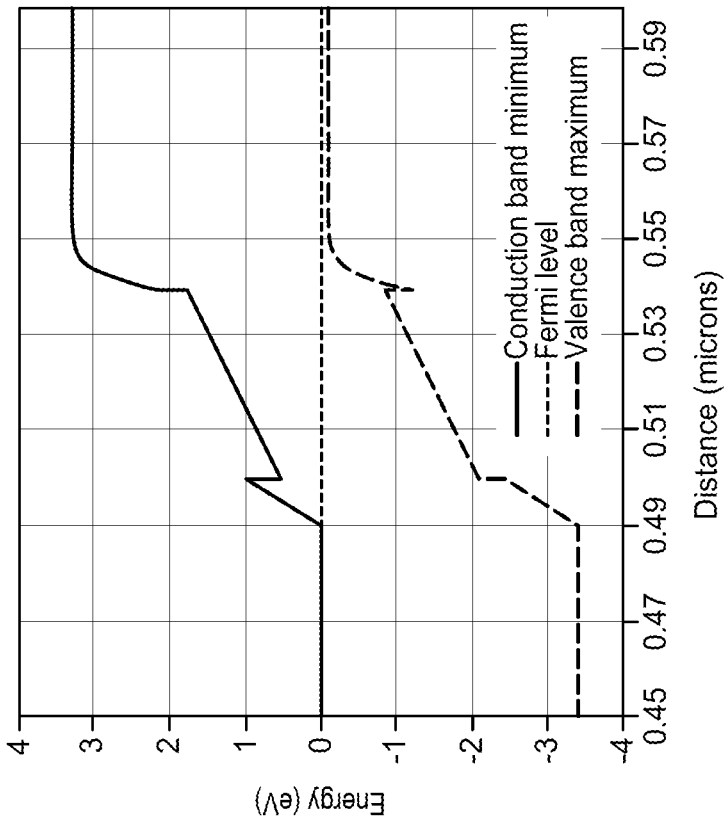
Energy (eV)
4
3
2
1
0
-1
-2
-3
-4
0.45
0.47
0.49
0.51
0.53
0.55
0.57
0.59
Distance (microns)
Conduction band minimum
Fermi level
Valence band maximum

FIG. 8B

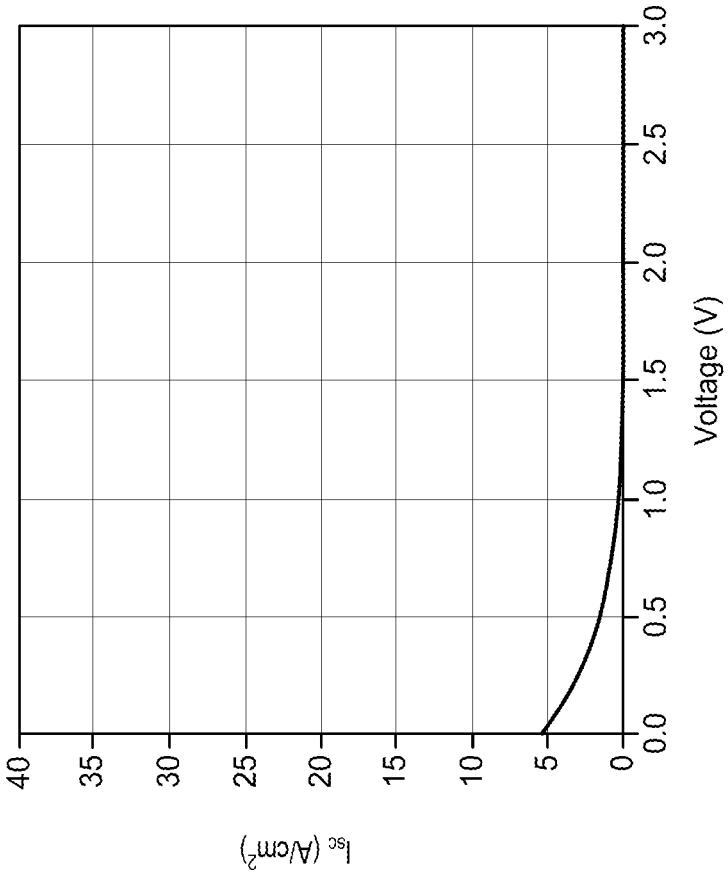
Isc (A/cm2)
40
35
30
25
20
15
10
5
0
0.0
0.5
1.0
1.5
2.0
2.5
3.0
Voltage (V)

FIG. 8A

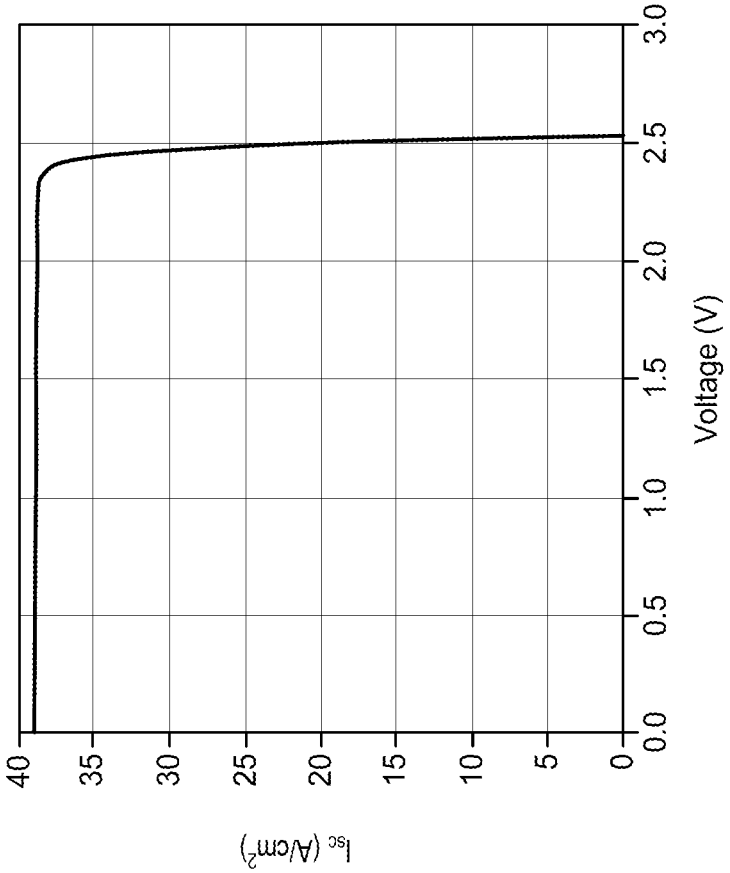
Isc (A/cm²)
40
35
30
25
20
15
10
5
0
0.0
0.5
1.0
1.5
2.0
2.5
3.0
Voltage (V)

FIG. 9A

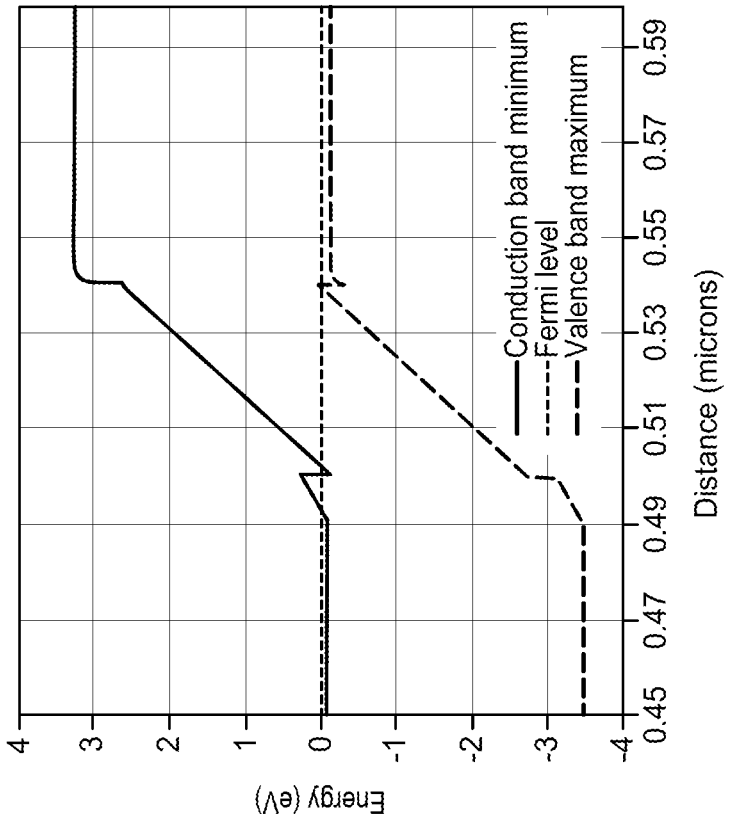
Energy (eV)
4
3
2
1
0
-1
-2
-3
-4
0.45
0.47
0.49
0.51
0.53
0.55
0.57
0.59
Distance (microns)
Conduction band minimum
Fermi level
Valence band maximum

FIG. 9B

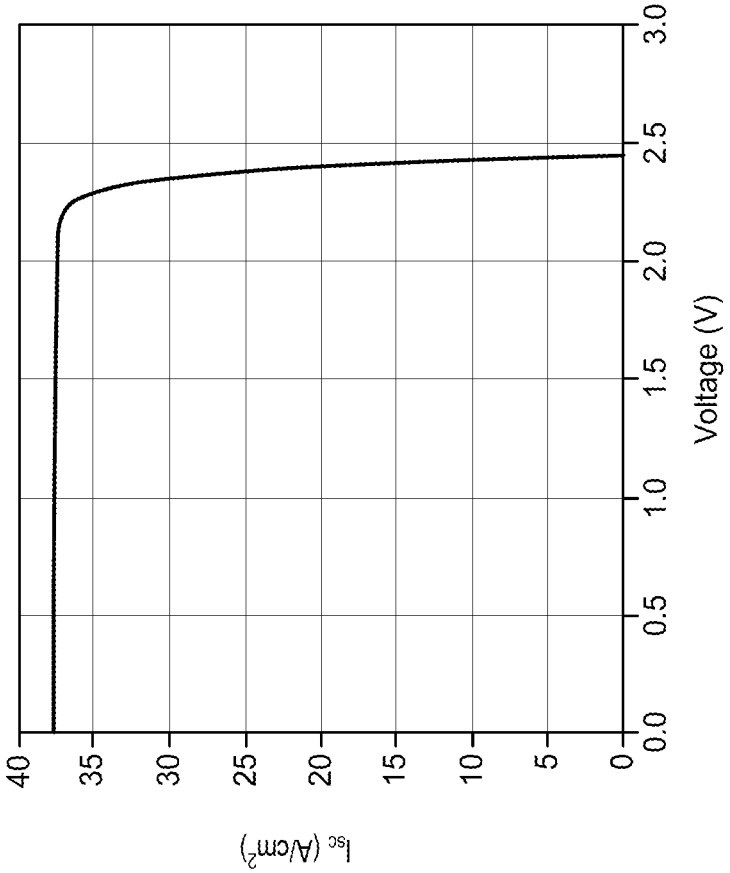

FIG. 10A

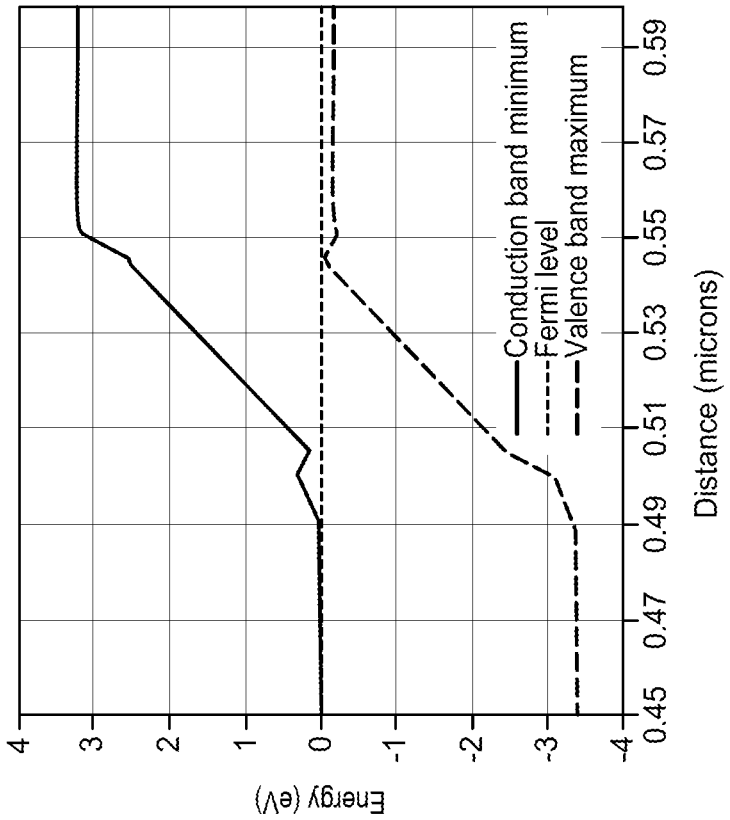

FIG. 10B

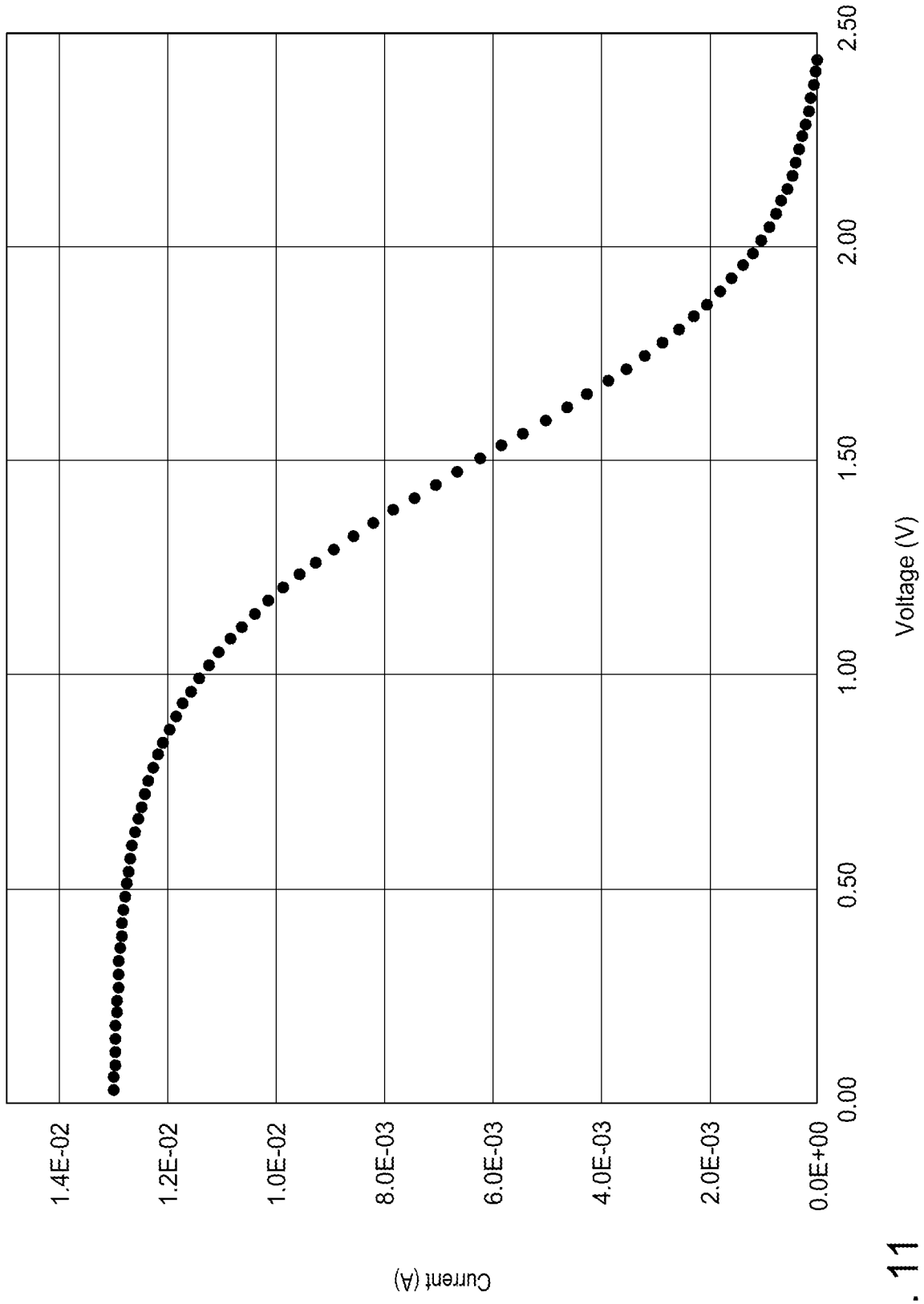
1.4E-02
1.2E-02
1.0E-02
8.0E-03
6.0E-03
4.0E-03
2.0E-03
0.0E+00
Current (A)
0.00
0.50
1.00
1.50
2.00
2.50
Voltage (V)

FIG. 11

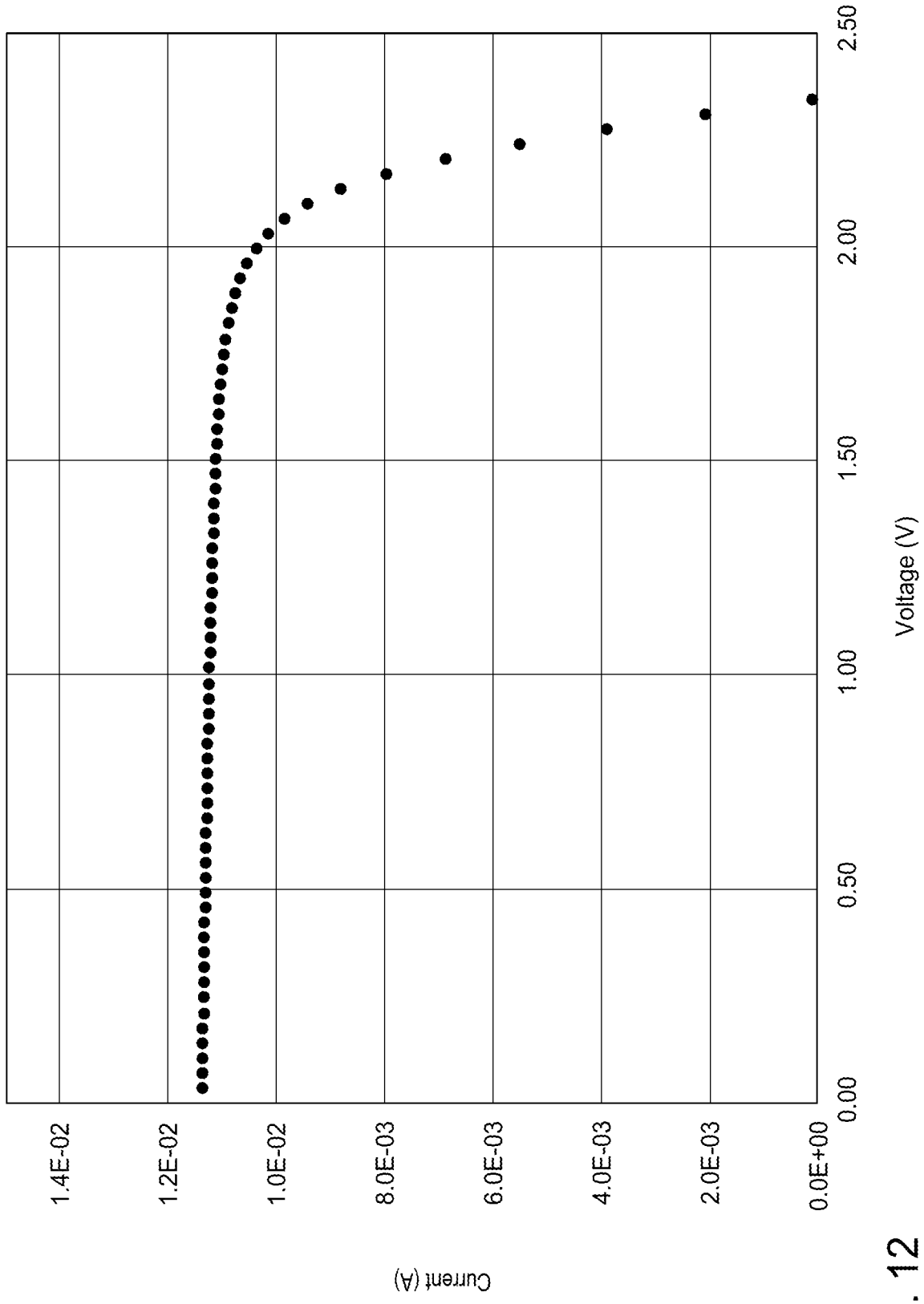
1.4E-02
1.2E-02
1.0E-02
8.0E-03
6.0E-03
4.0E-03
2.0E-03
0.0E+00
Current (A)
0.00
0.50
1.00
1.50
2.00
2.50
Voltage (V)

FIG. 12

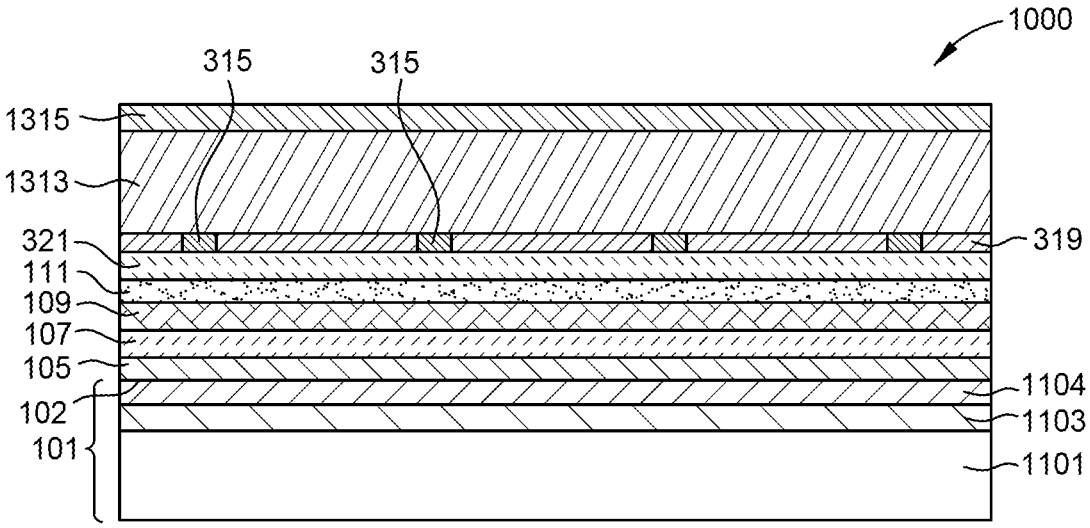
1000
315
315
1315
1313
321
319
111
109
107
105
1104
102
1103
101
1101

FIG. 13A

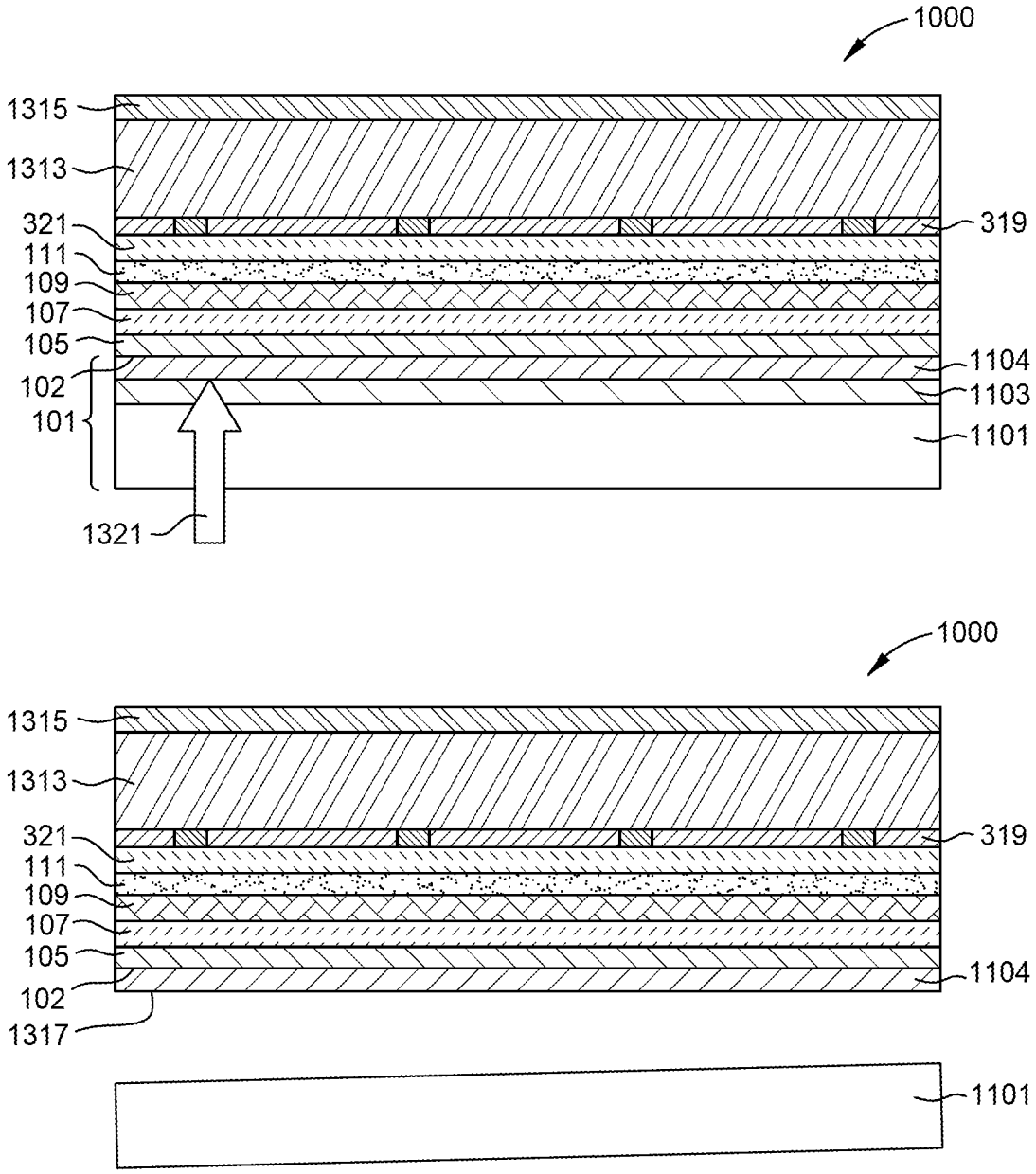
1000
1315
1313
321
111
109
107
105
102
101
319
1104
1103
1101
1321
1000
1315
1313
321
111
109
107
105
102
1317
319
1104
1101

FIG. 13B

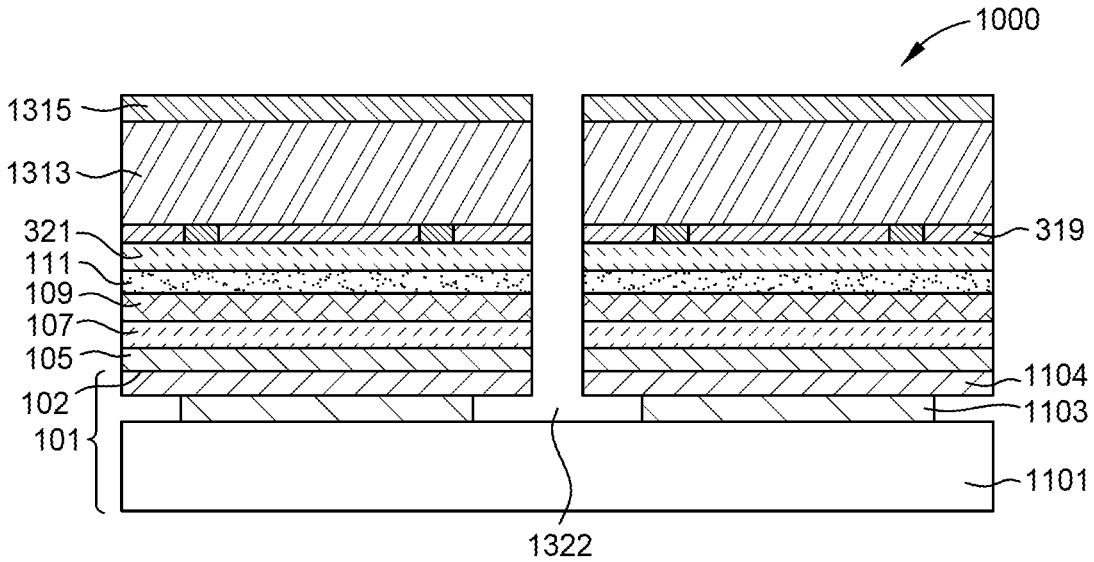
1000
1315
1313
321
111
109
107
105
102
101
319
1104
1103
1101
1322

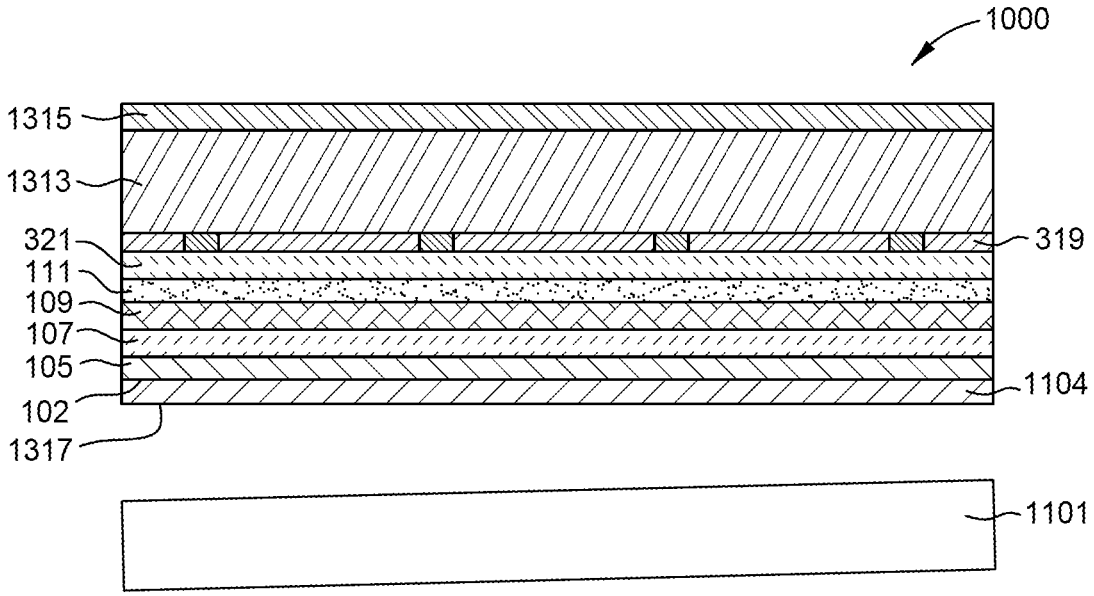
1000
1315
1313
321
111
109
107
105
102
1317
319
1104
1101

FIG. 13C

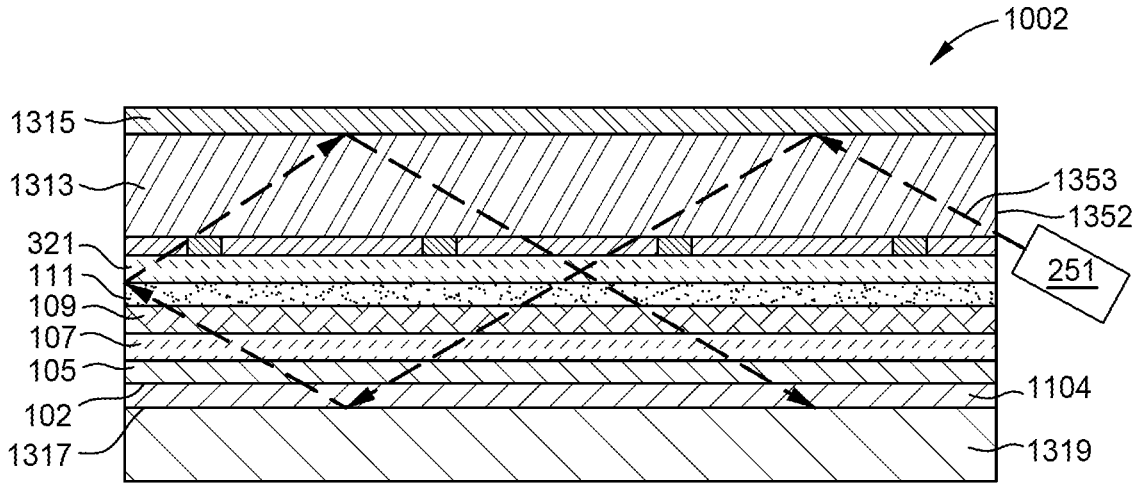

FIG. 13D

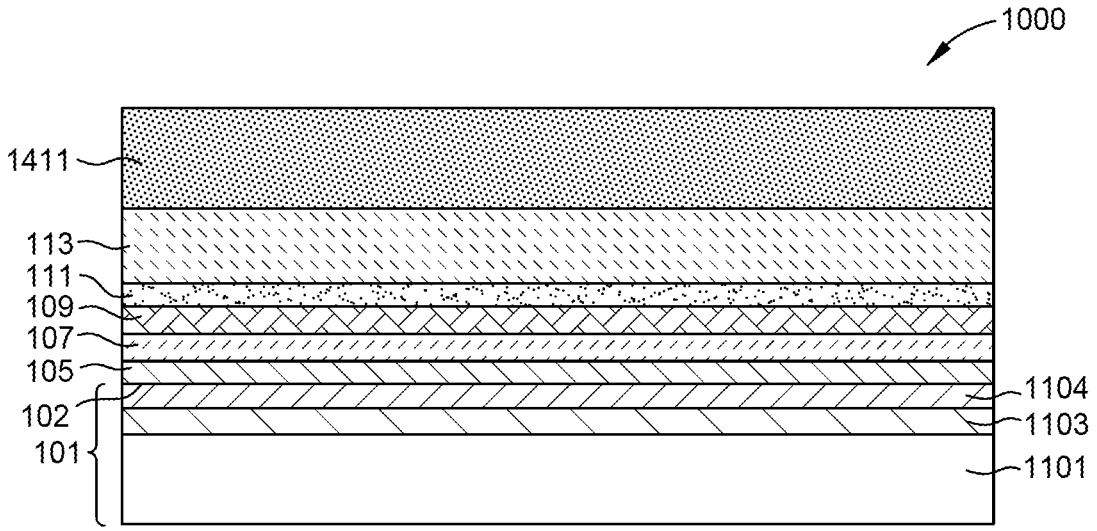

FIG. 14A

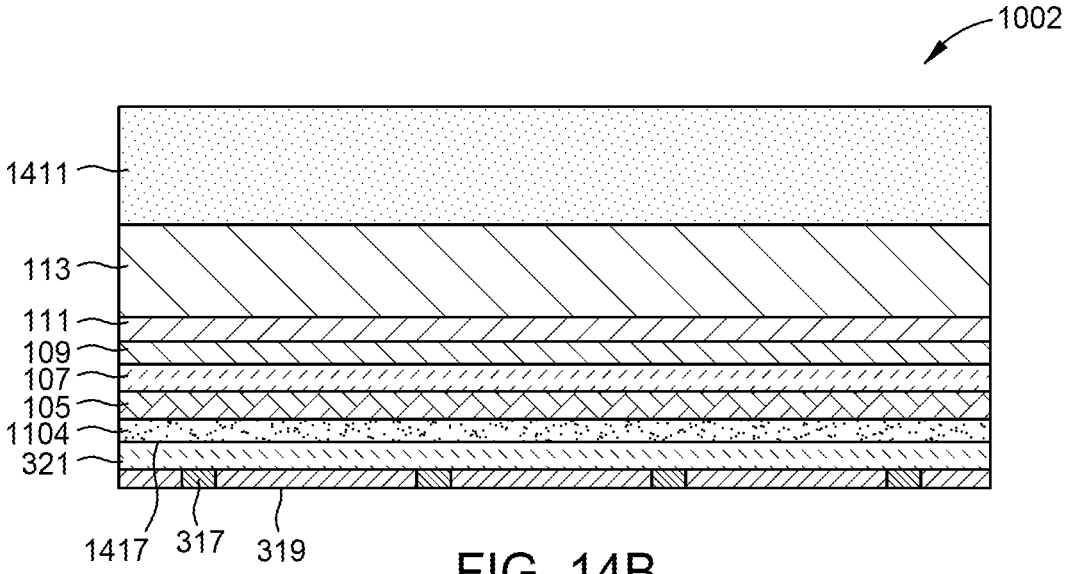

FIG. 14B

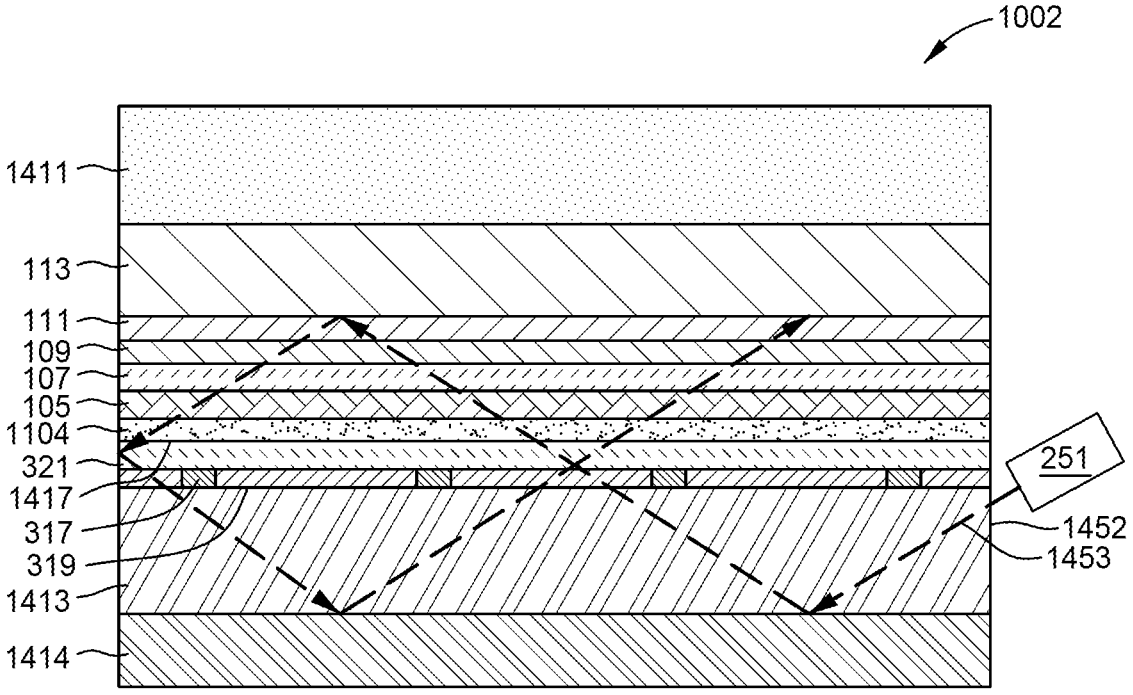

FIG. 14C

Crystallographic orientation	N-type doping layer	N-type cladding layer			Absorber Layer	P-type cladding layer			P-type doping layer	Fill factor	V_{oc}
	doping (cm^{-3})	% In	thickness (nm)	doping (cm^{-3})	% In	% In	thickness (nm)	doping (cm^{-3})	doping (cm^{-3})	%	(V)
(0001)	2.00E+19				18				2.00E+19	6	2.53
(0001)	1.50E+19				18				6.00E+20	18	2.52
(0001)	1.50E+19	8	3	1.50E+19	18				6.00E+20	86	2.45
(0001)	3.50E+19				18				5.00E+19	63	2.53
(0001)	3.50E+19				18				6.00E+19	69	2.53
(0001)	3.50E+19				18				8.00E+19	76	2.53
(0001)	3.50E+19				18				1.20E+20	84	2.53
(0001)	3.50E+19				18				2.00E+20	89	2.53
(0001)	3.50E+19				18				4.00E+20	92	2.53
(0001)	3.50E+19				18				6.00E+20	92	2.53
(0001)	4.50E+19				18				1.20E+20	85	2.53
(0001)	4.50E+19				18				2.00E+20	91	2.53
(0001)	2.00E+19				12				8.00E+18	49	2.78
(0001)	2.00E+19				12				1.30E+19	69	2.78
(0001)	2.00E+19				12				2.00E+19	80	2.78
(0001)	2.00E+19				12				1.00E+20	93	2.78
(0001)	2.00E+19				12	0	10	5.00E+18	8.00E+18	28	2.77
(0001)	2.00E+19				12	0	10	5.00E+18	2.00E+19	38	2.77
(0001)	2.00E+19				12	0	3	5.00E+18	2.00E+19	66	2.78
(0001)	2.00E+19				12	0	3	5.00E+18	1.00E+20	82	2.78
(0001)	2.00E+19				12	6	3	5.00E+18	1.00E+20	93	2.78
(0001)	2.00E+19	0	3	5.00E+18	12	6	3	5.00E+18	1.00E+20	81	2.78
(0001)	2.00E+19	6	3	5.00E+18	12	6	3	5.00E+18	1.00E+20	90	2.74
(0001)	1.50E+16	0→18	10	1.50E+16	18				2.00E+20	16	2.44
(0001)	1.50E+17	0→18	10	1.50E+17	18				2.00E+20	83	2.44
(0001)	1.50E+18	0→18	10	1.50E+18	18				2.00E+20	86	2.45
(0001)	1.50E+17	0→18	5	1.50E+17	18				2.00E+20	16	2.52
(0001)	1.50E+18	0→18	5	1.50E+18	18				2.00E+20	86	2.45
(0001)	1.50E+18	0→18	5	1.50E+18	18				5.00E+19	58	2.47
(0001)	1.50E+18	0→18	5	1.50E+18	18	0→18	5	5.00E+19	5.00E+19	89	2.45
(000-1)	1.00E+18				12				1.00E+18	94	2.78
(000-1)	1.00E+16				18				1.00E+16	93	2.53
(000-1)	1.00E+17				18				1.00E+17	94	2.53
(000-1)	1.00E+18				18				1.00E+18	94	2.53
(10-10)	4.00E+18				18				4.00E+18	58	2.53
(10-10)	8.00E+18				18				8.00E+18	78	2.53
(10-10)	1.20E+19				18				1.20E+19	84	2.53
(10-10)	2.00E+19				18				2.00E+19	90	2.53
(10-10)	2.00E+19				12				2.00E+19	94	2.78
(30-3-1)	1.00E+18				12				1.00E+18	94	2.78
(30-3-1)	1.00E+18				18				1.00E+18	57	2.53
(30-3-1)	8.00E+18				18				8.00E+18	89	2.53
(30-3-1)	1.20E+19				18				1.20E+19	91	2.53

FIG. 15

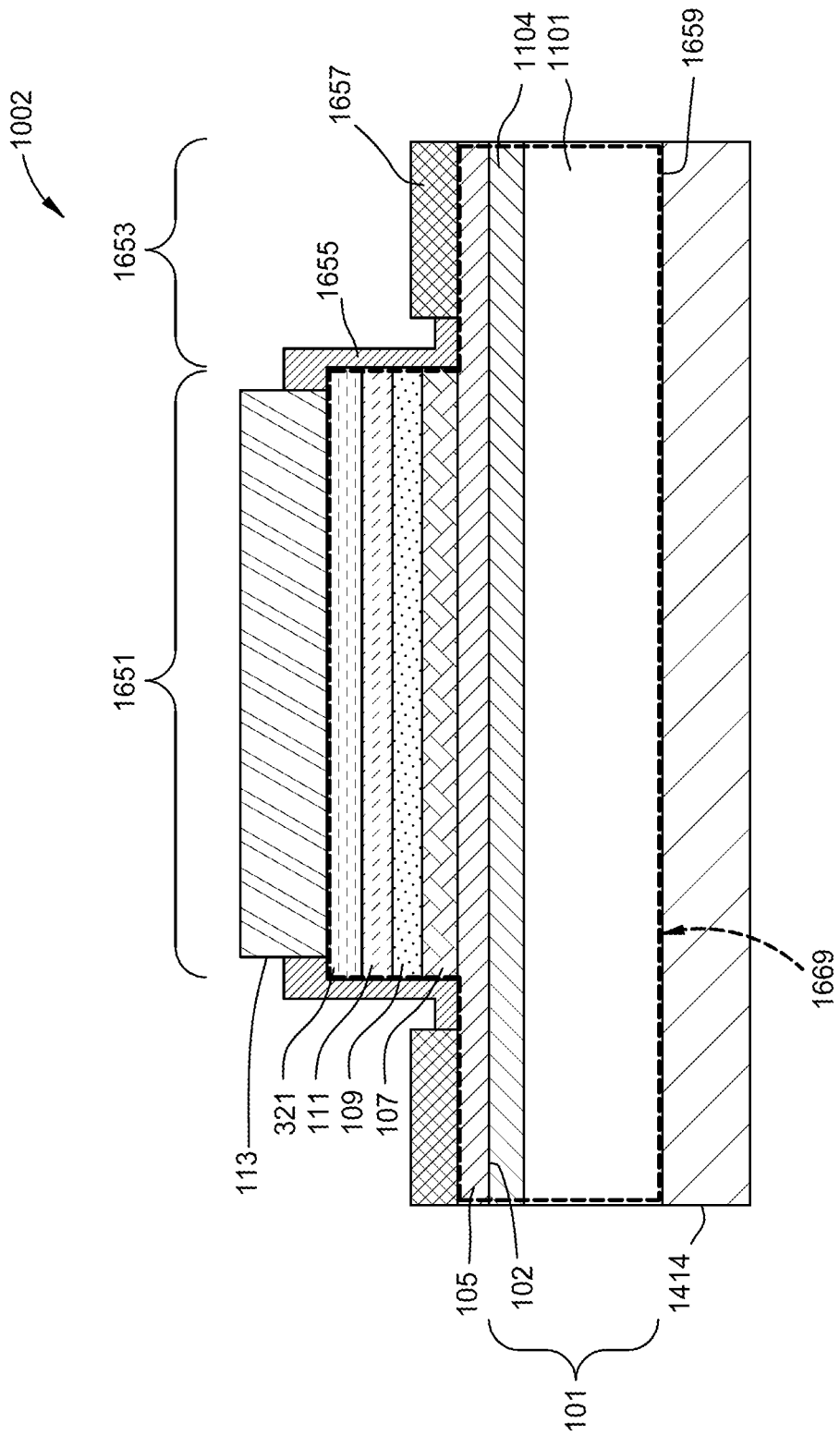
1002
1653
1651
1657
1655
1104
1101
1659
1669
113
321
111
109
107
105
102
1414
101

FIG. 16A

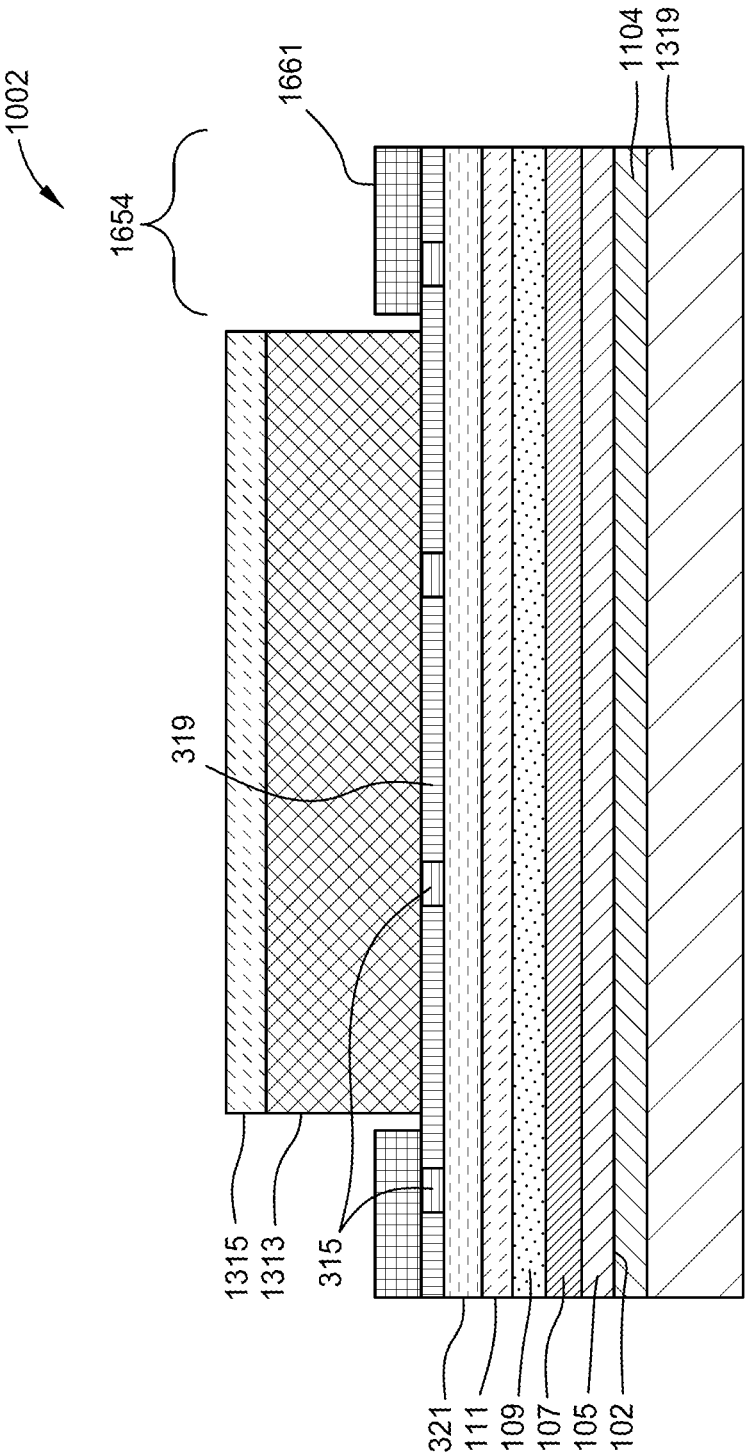
1002
1654
1661
1104
1319
319
1315
1313
315
321
111
109
107
105
102

FIG. 16B

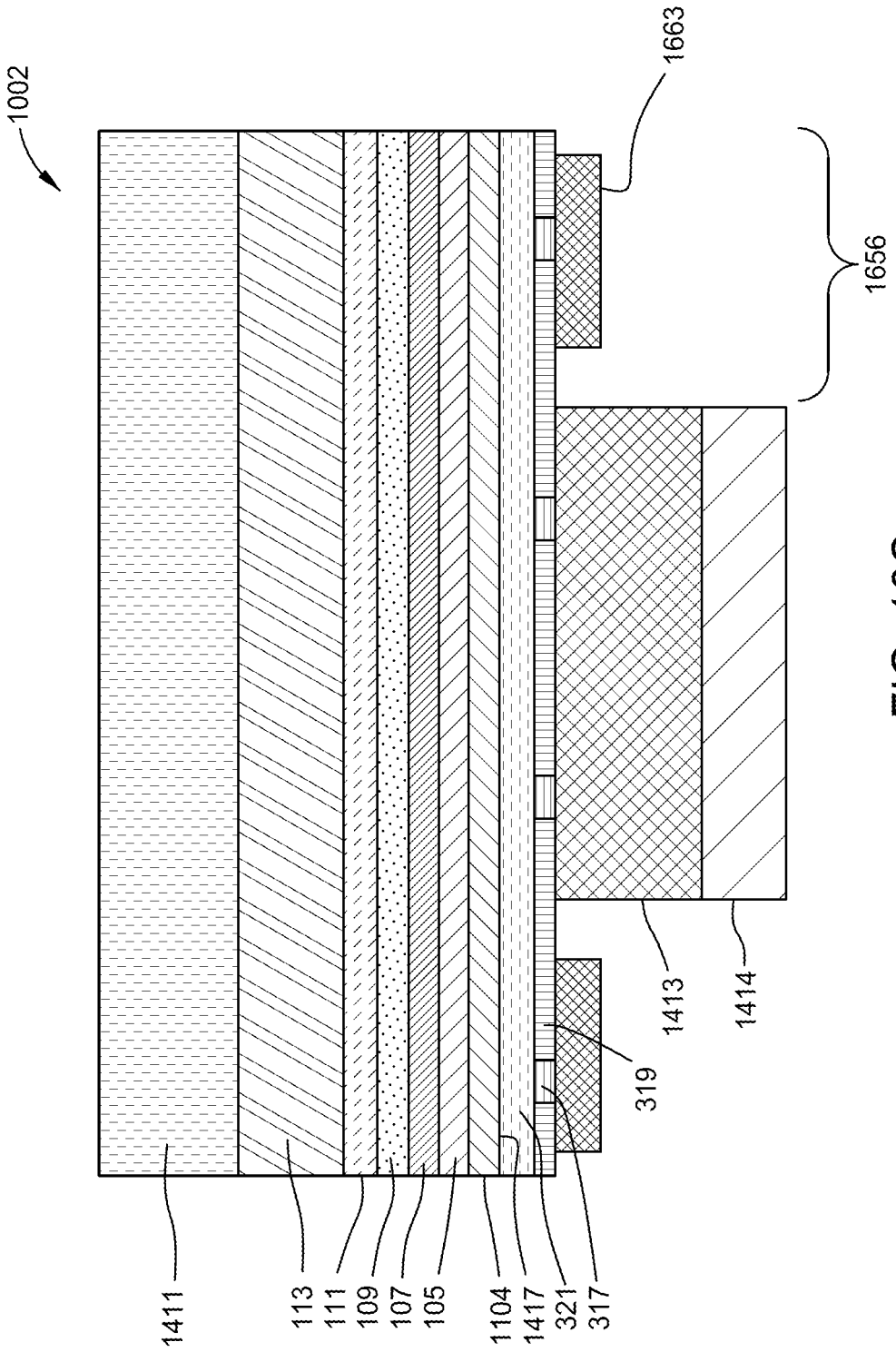
1002
1411
113
111
109
107
105
1104
1417
321
317
319
1413
1414
1656
1663

FIG. 16C

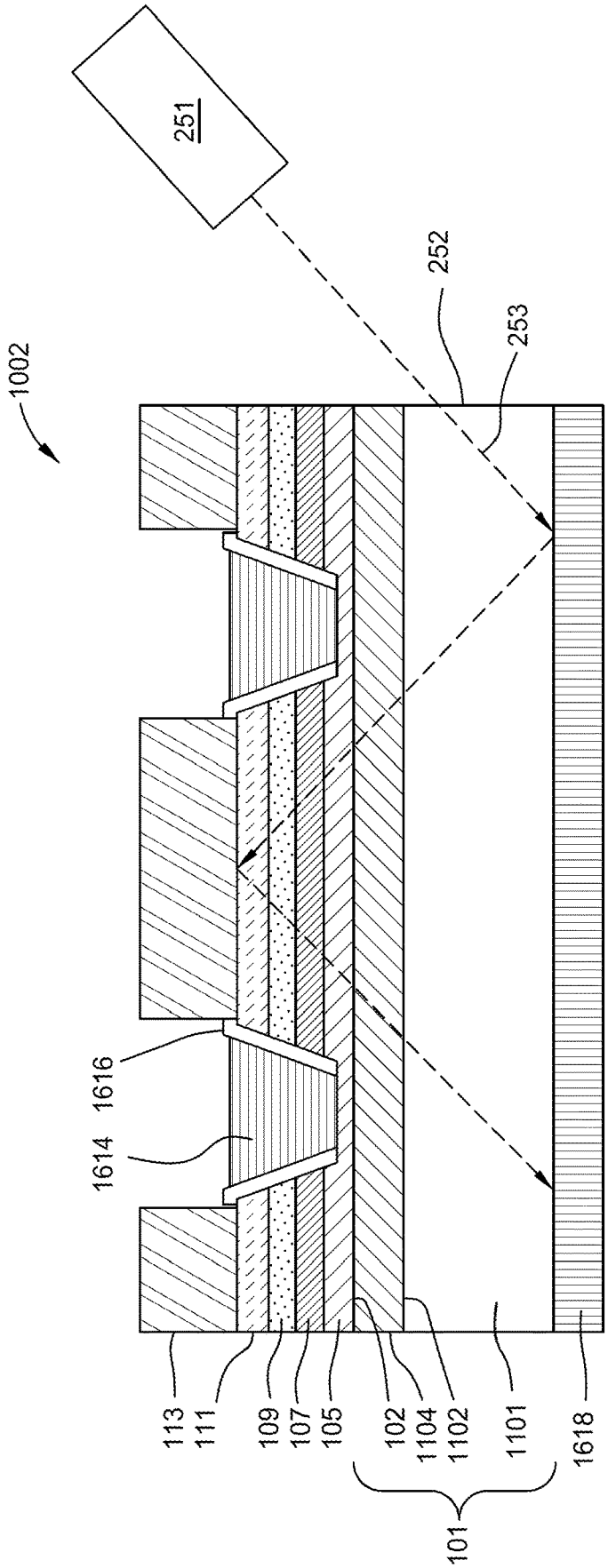
1002
251
252
253
1616
1614
113
111
109
107
105
102
1104
1102
1101
1618
101

FIG. 17A

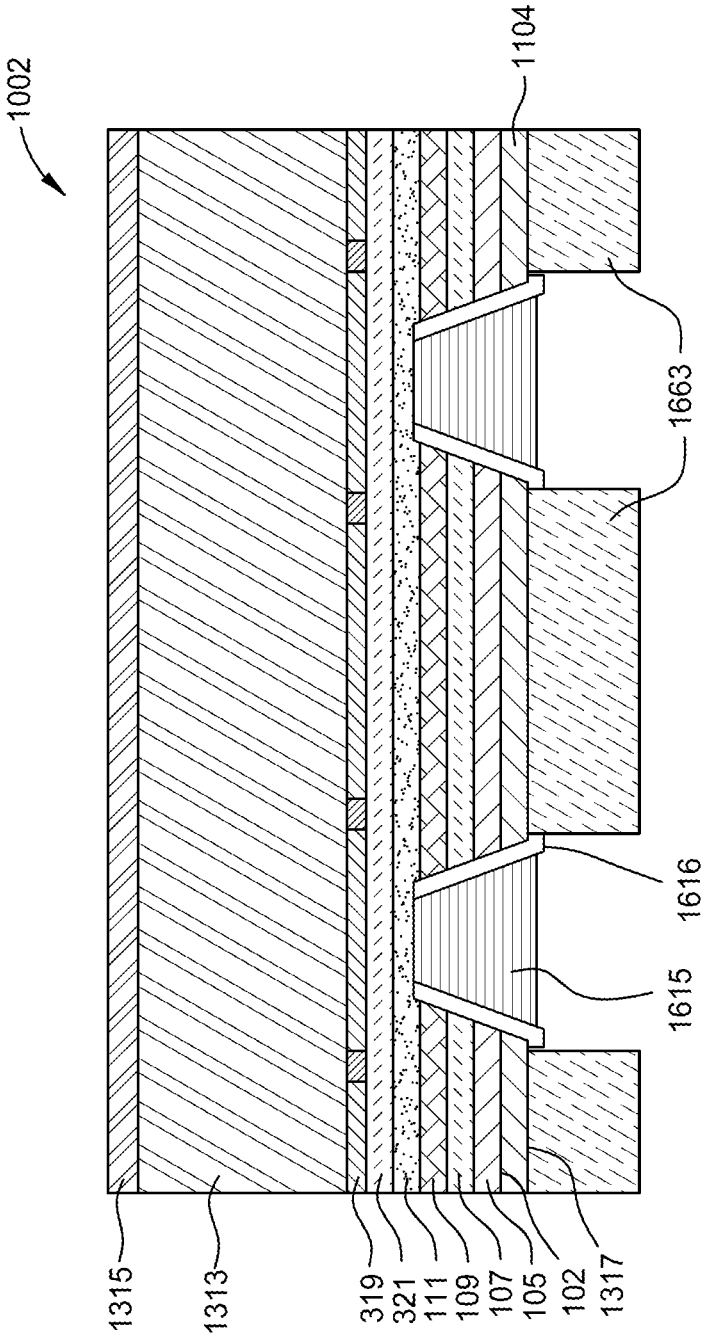
1002
1315
1313
319
321
111
109
107
105
102
1317
1615
1616
1663
1104

FIG. 17B

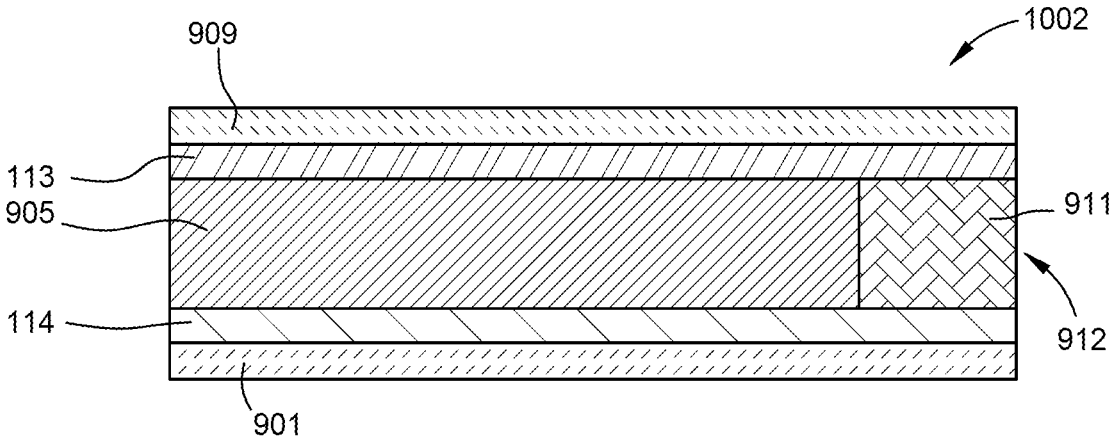

FIG. 18A

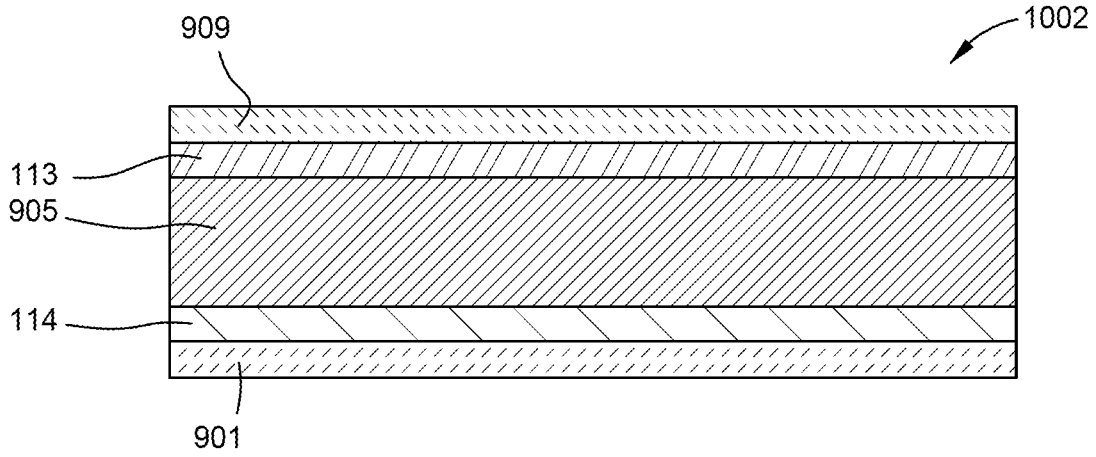

FIG. 18B

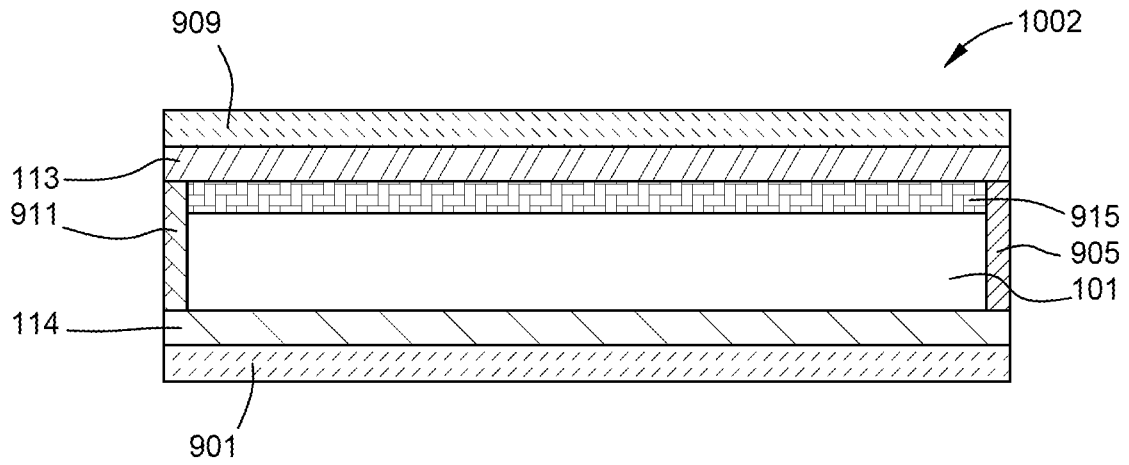

FIG. 18C

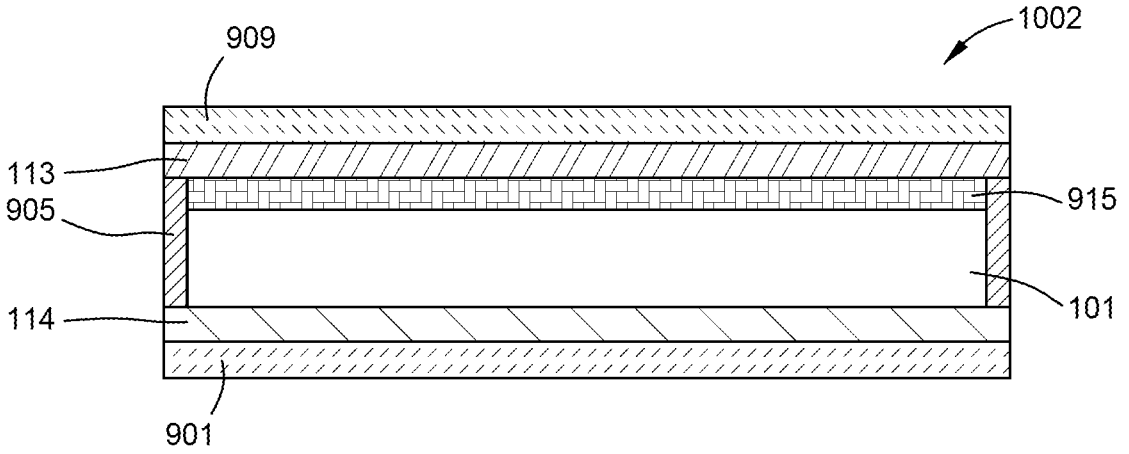

FIG. 18D

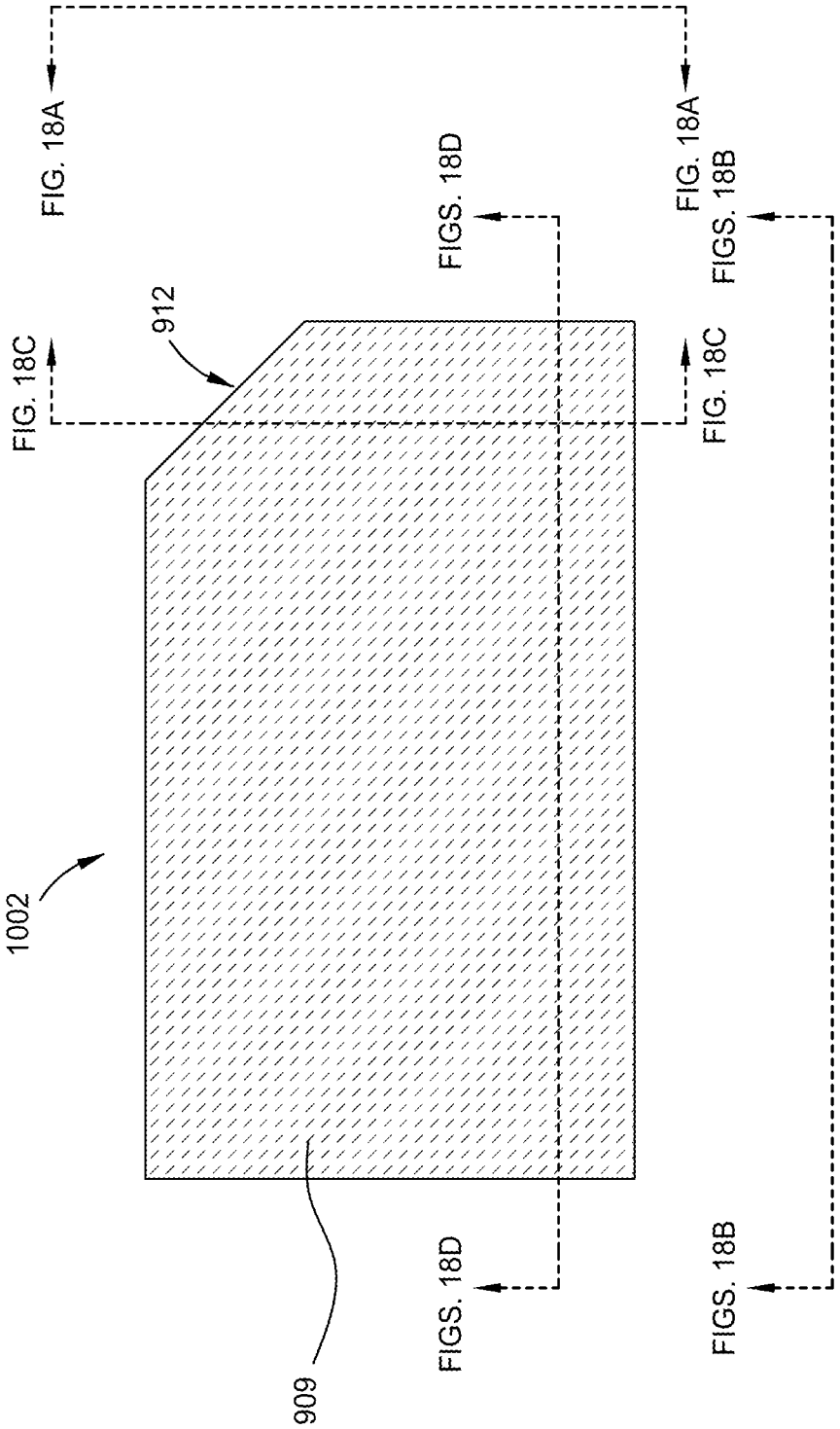
FIG. 18A
FIG. 18A
FIGS. 18D
FIGS. 18B
912
FIG. 18C
FIG. 18C
1002
909
FIGS. 18D
FIGS. 18B

FIG. 18E

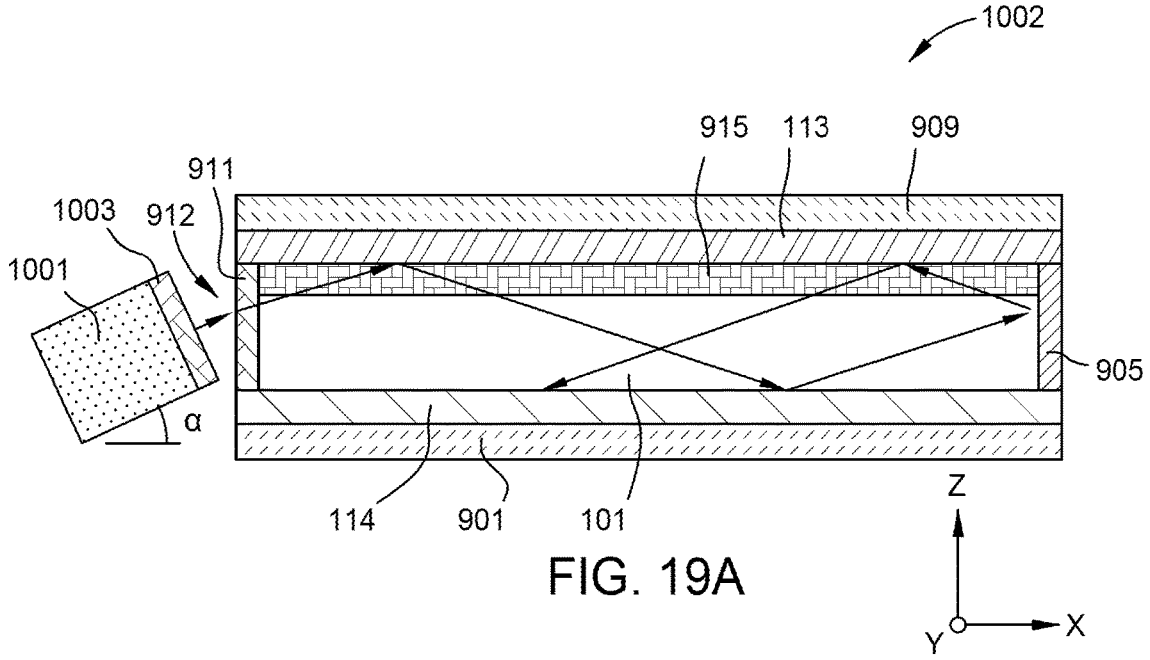

FIG. 19A

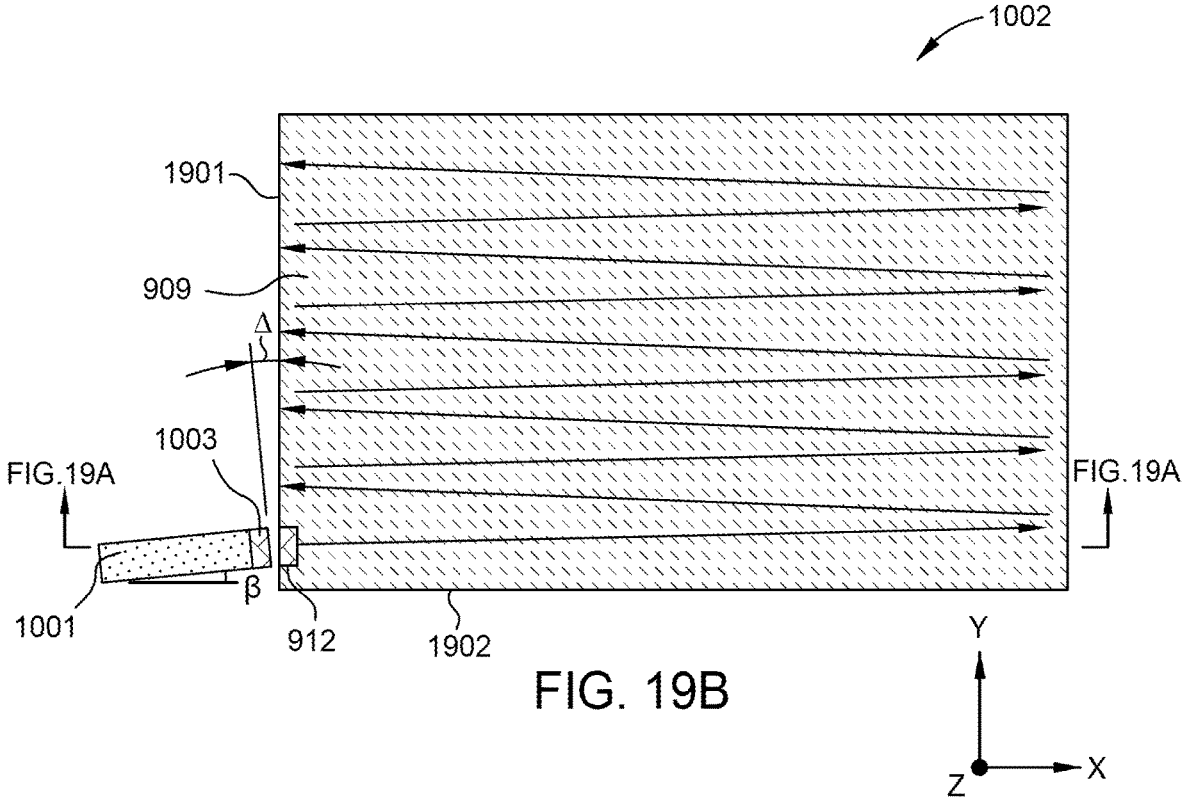

FIG. 19B

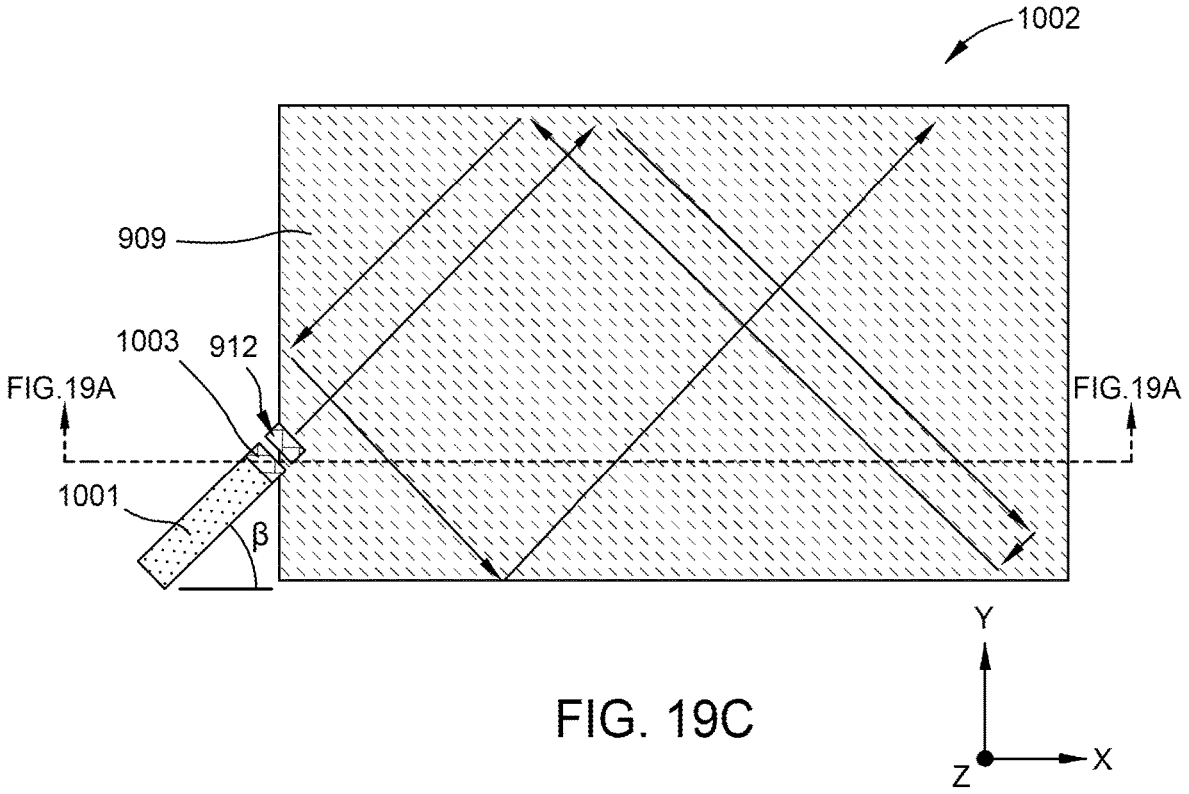

FIG. 19C

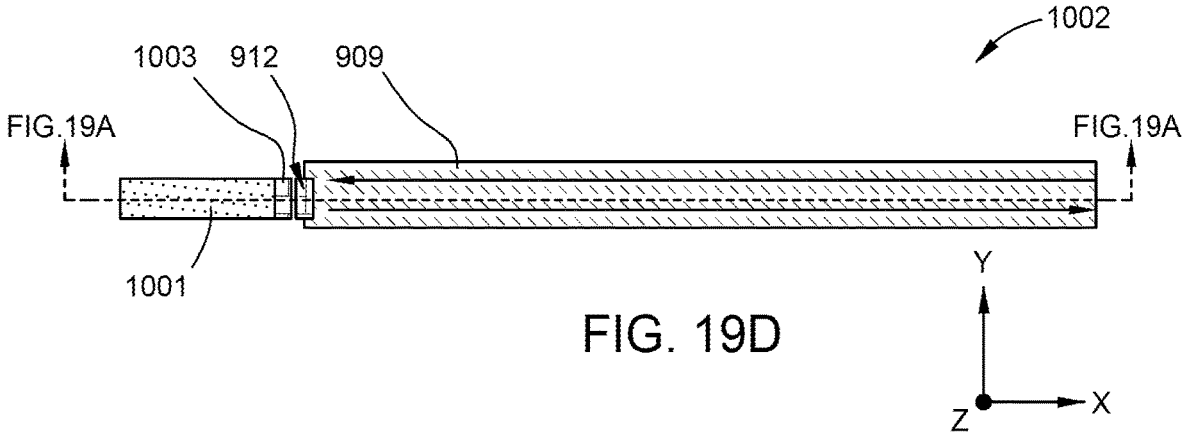

FIG. 19D

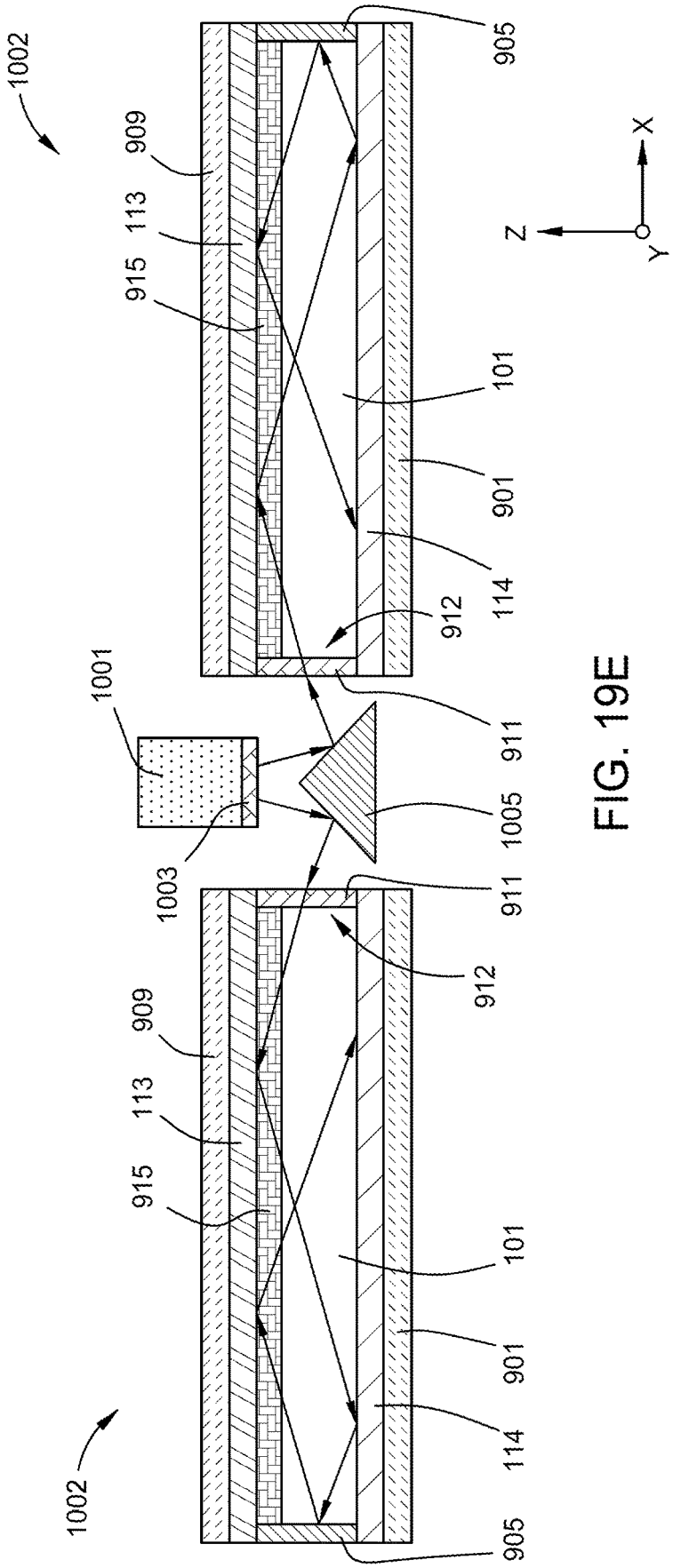

FIG. 19E

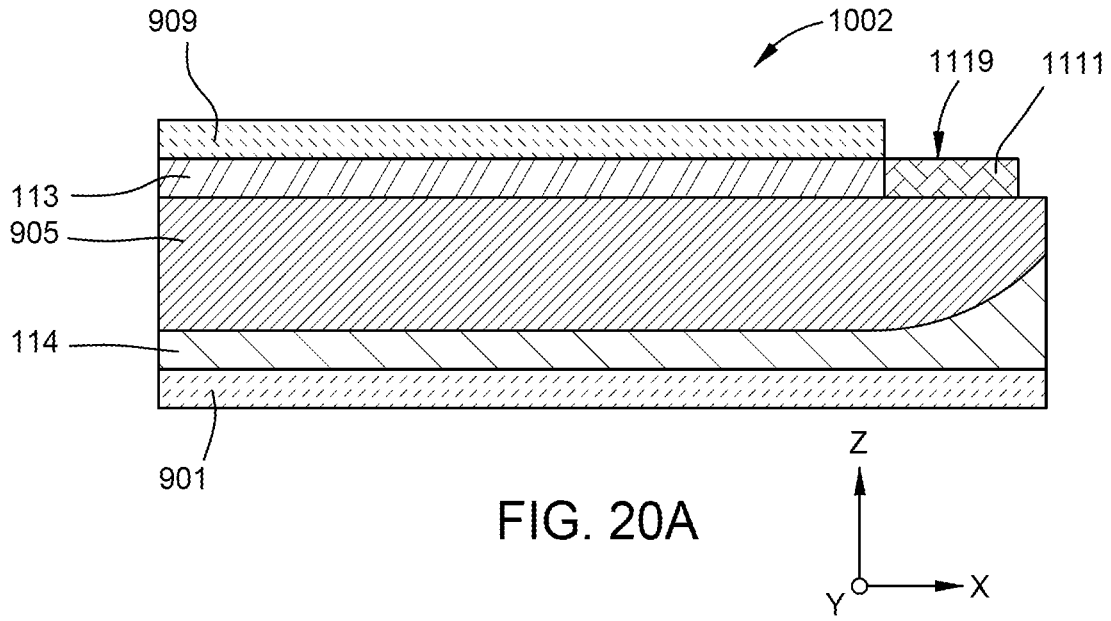

FIG. 20A

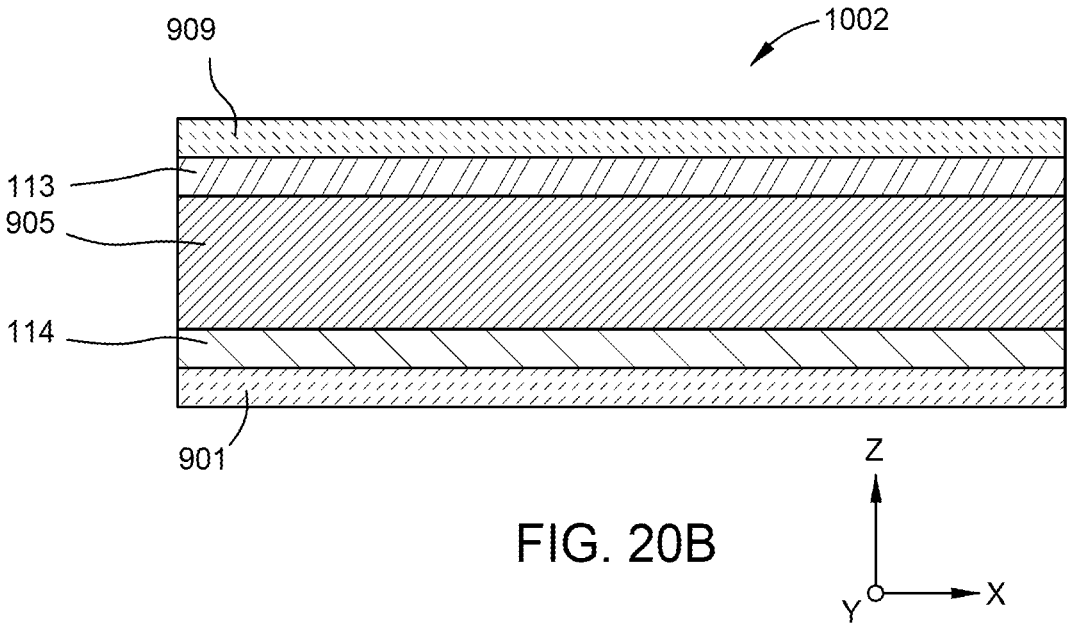

FIG. 20B

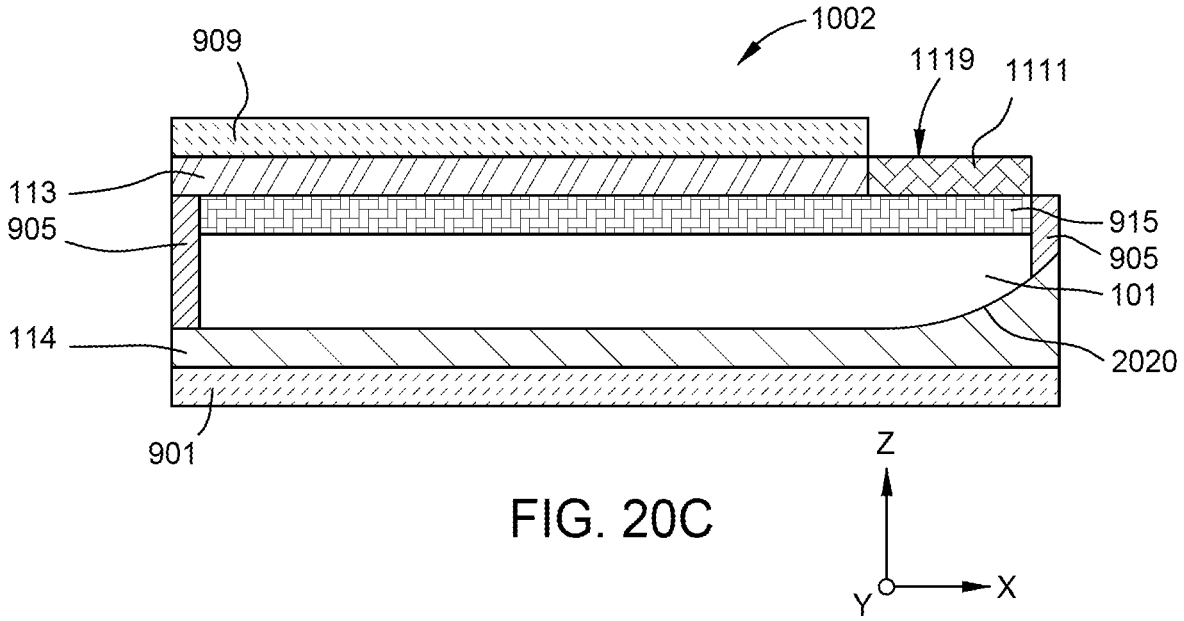

FIG. 20C

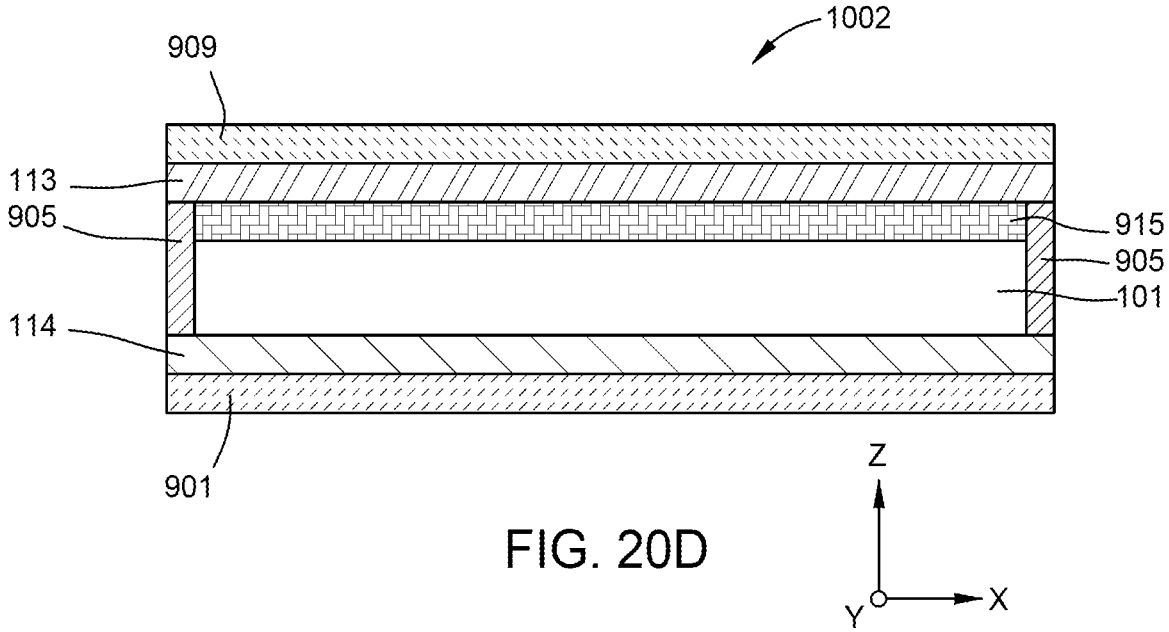

FIG. 20D

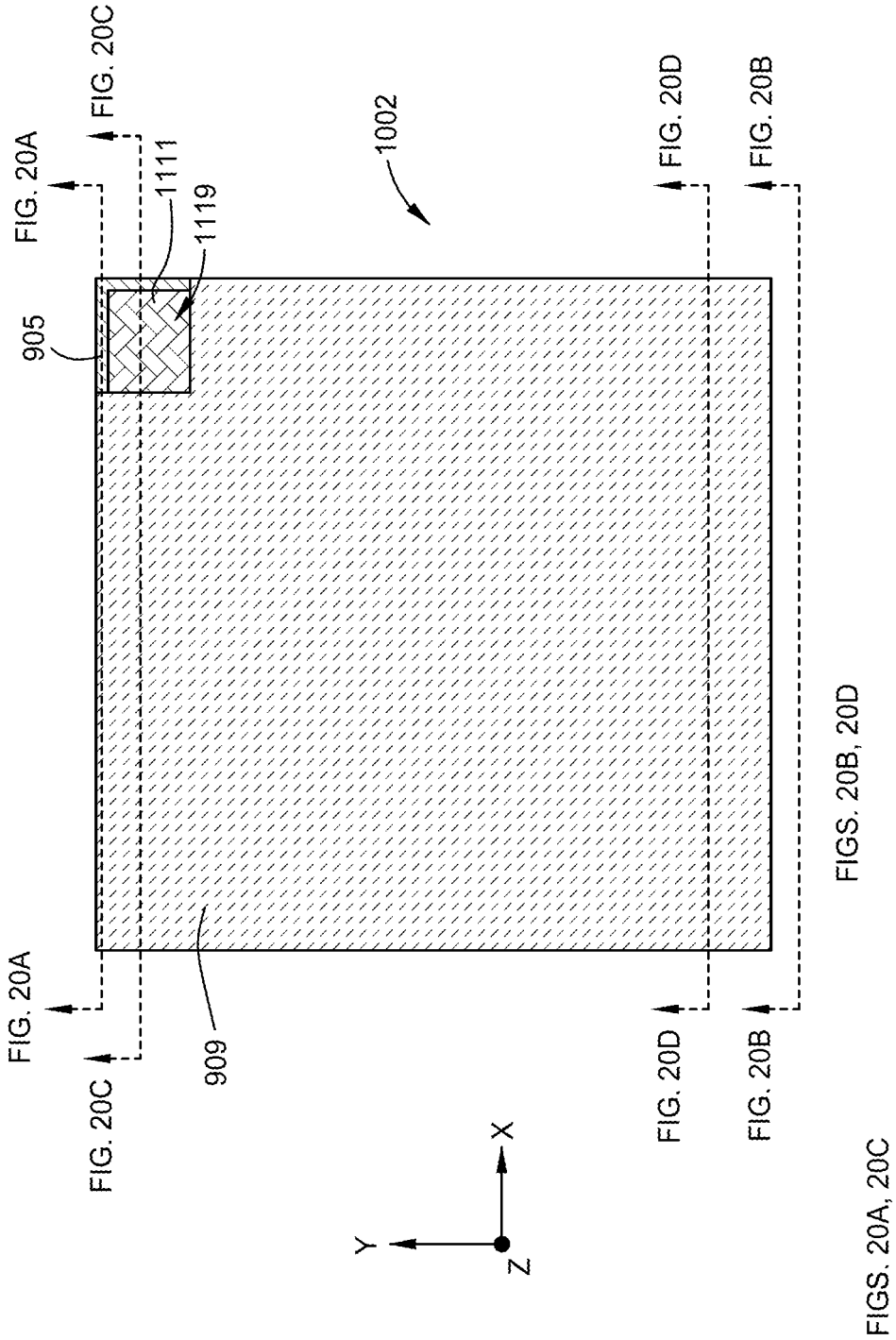
FIG. 20A
FIG. 20C
1111
1119
1002
FIG. 20D
FIG. 20B
905
909
FIG. 20A
FIG. 20C
FIG. 20D
FIG. 20B
X
Y
Z
FIGS. 20B, 20D
FIGS. 20A, 20C

FIG. 20E

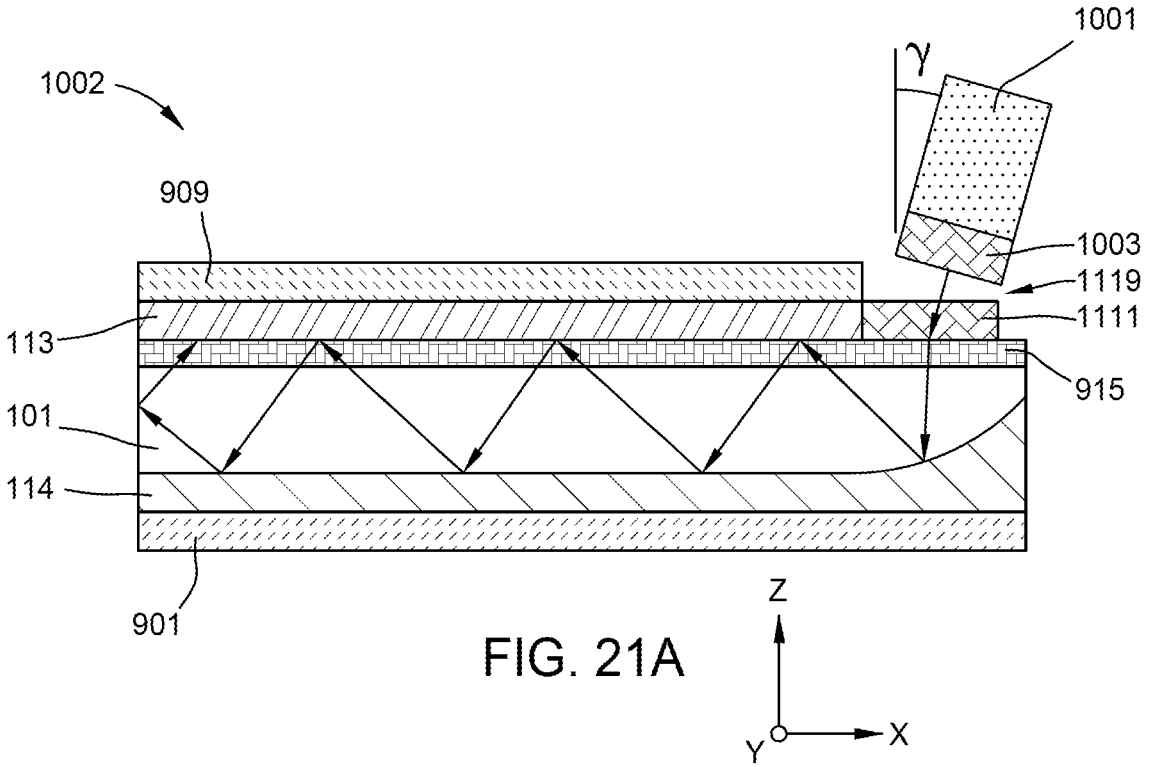

FIG. 21A

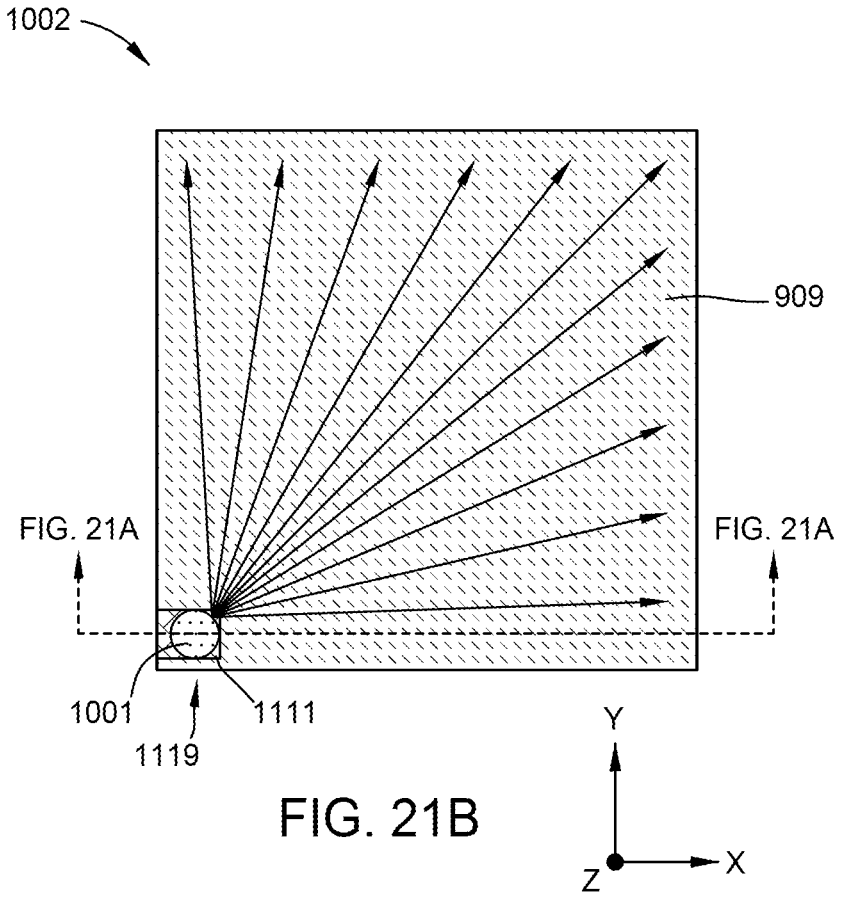

FIG. 21B

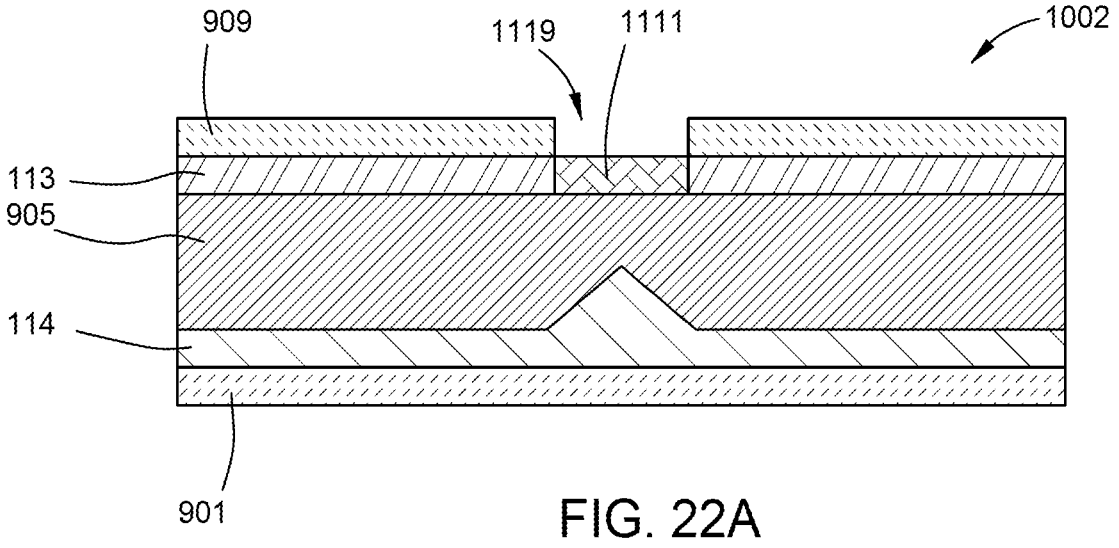

FIG. 22A

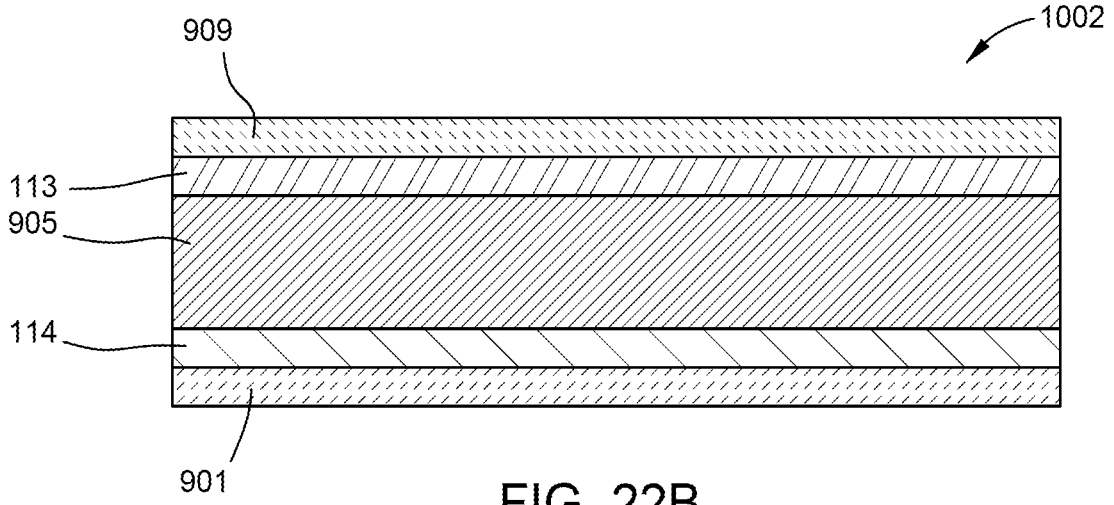

FIG. 22B

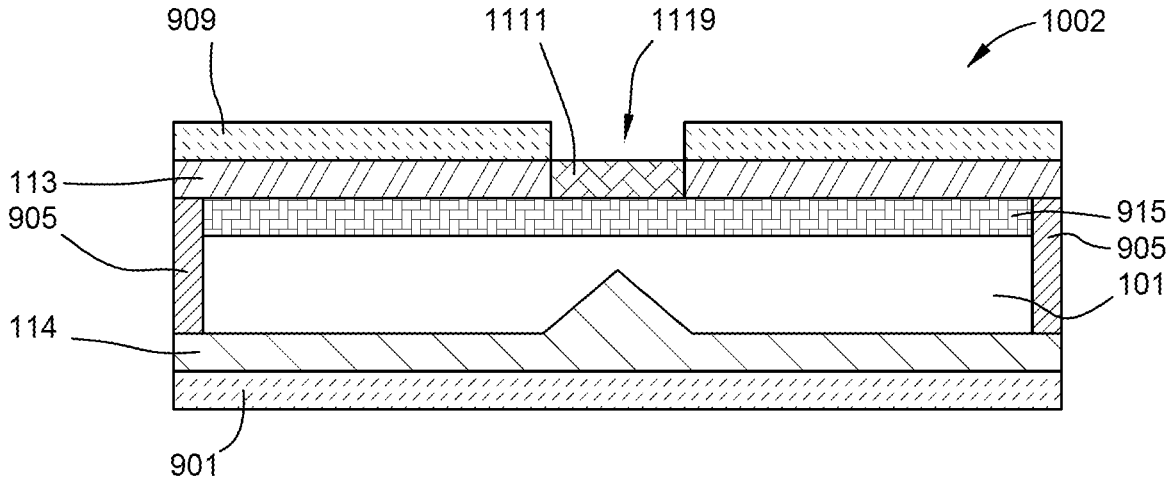

FIG. 22C

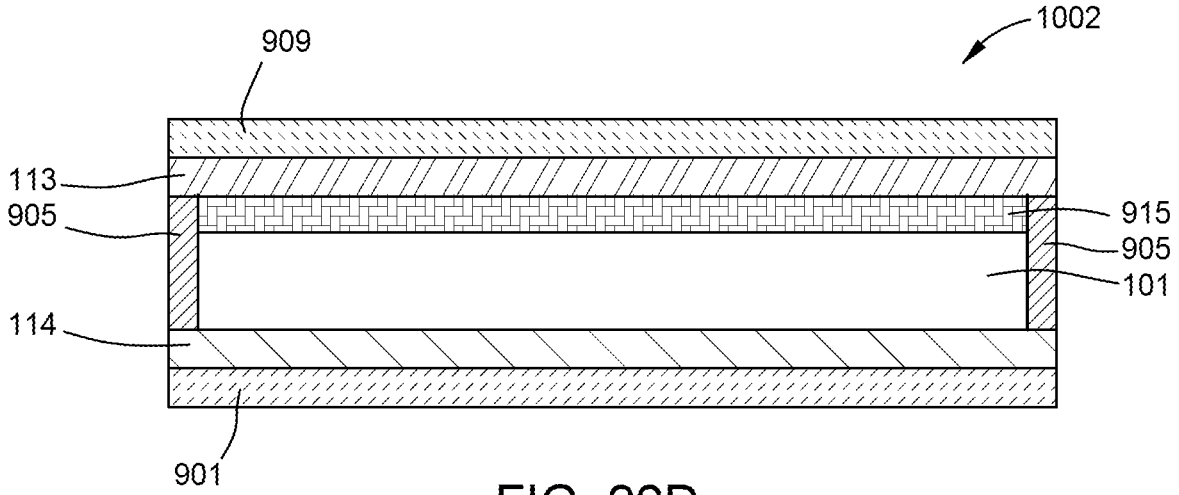

FIG. 22D

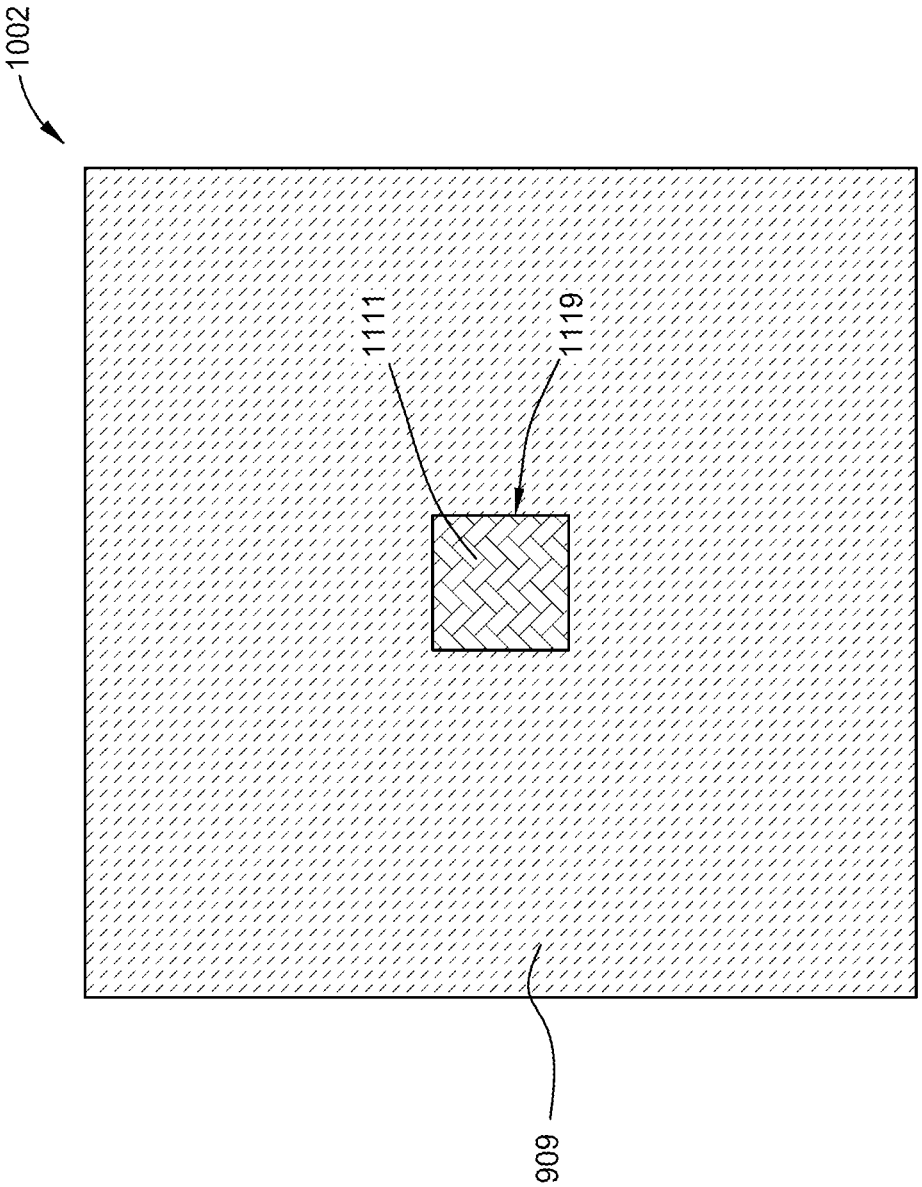

FIG. 22E

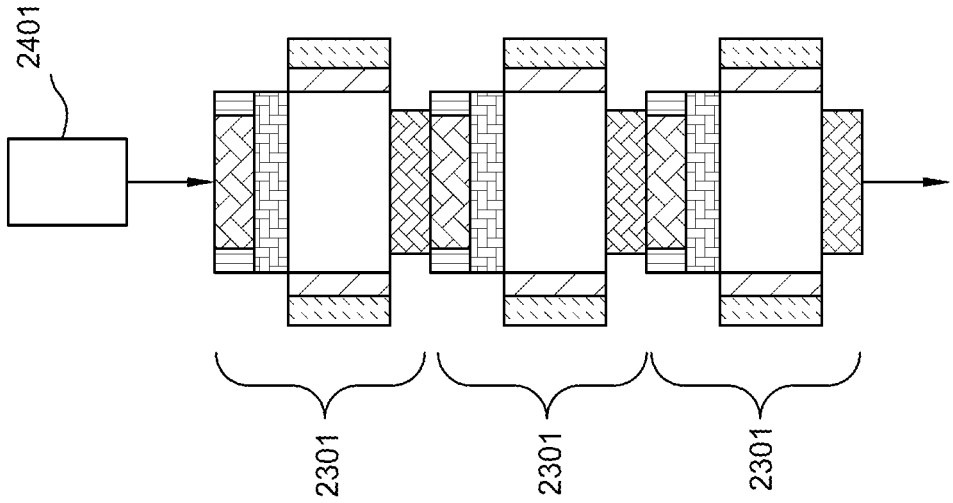

FIG. 23B

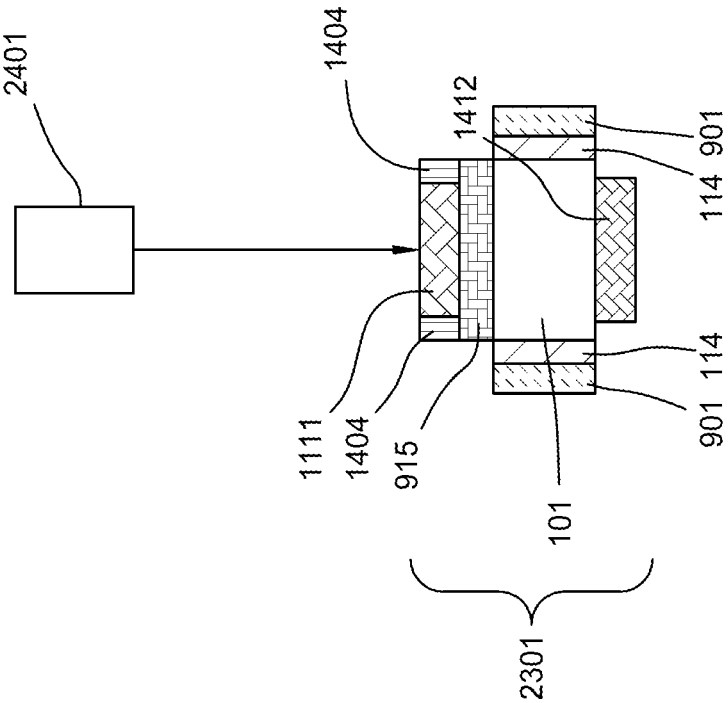

FIG. 23A

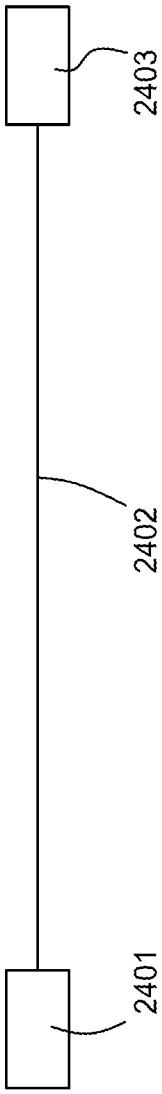

FIG. 24A

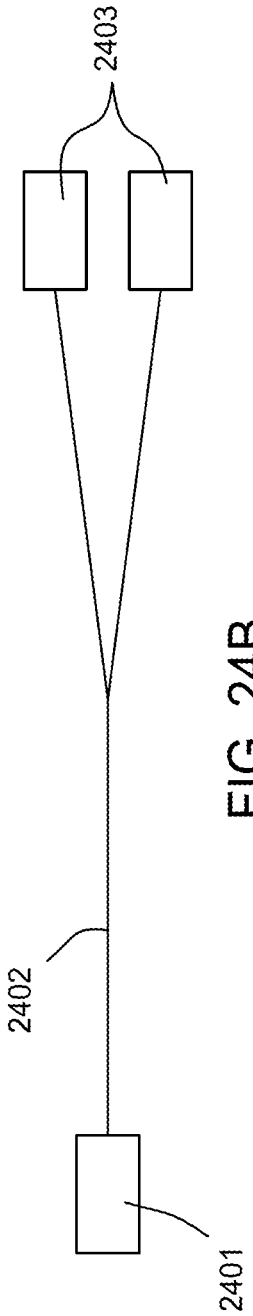

FIG. 24B

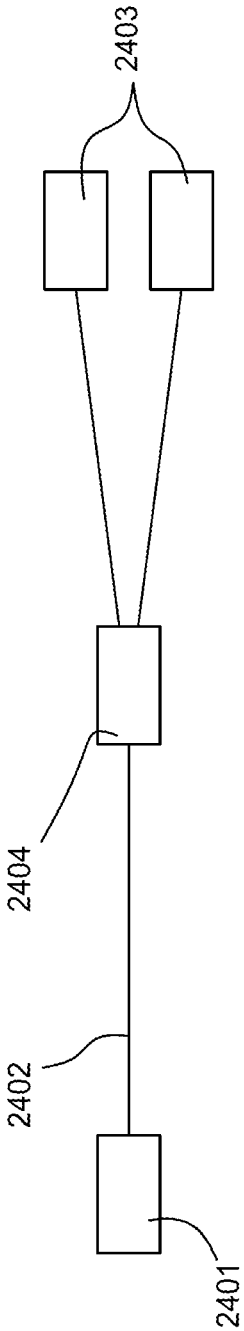

FIG. 24C

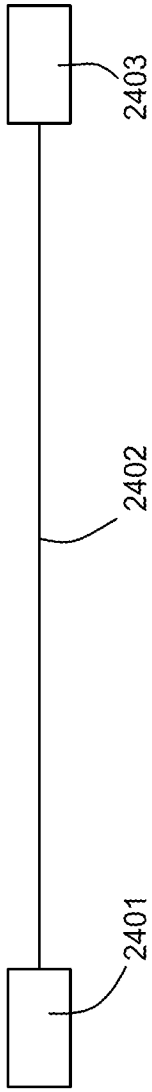

FIG. 25A

FIG. 25B

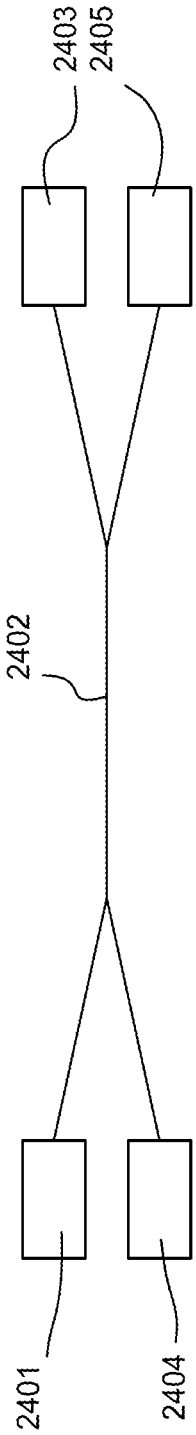

FIG. 25C

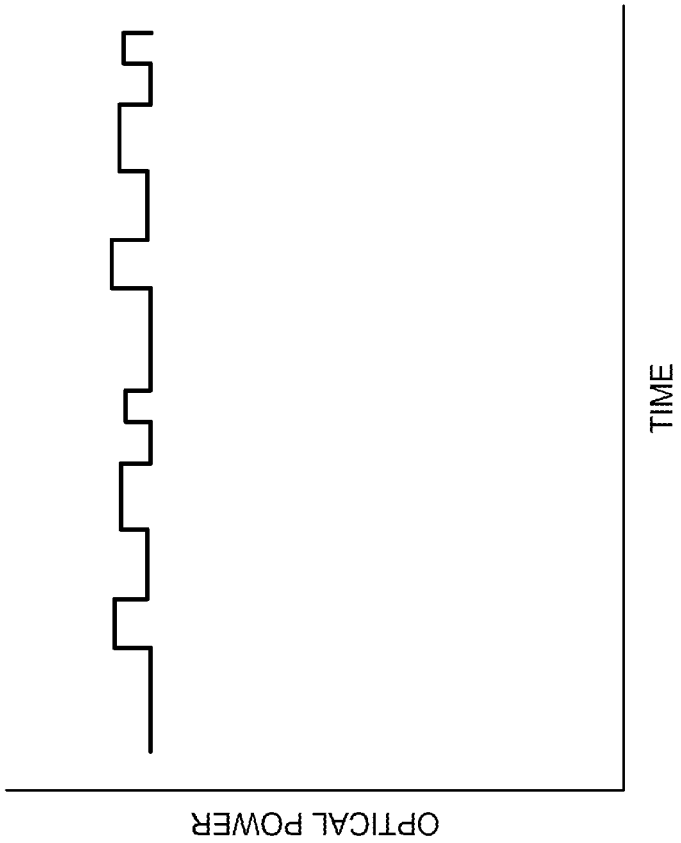

FIG. 25D

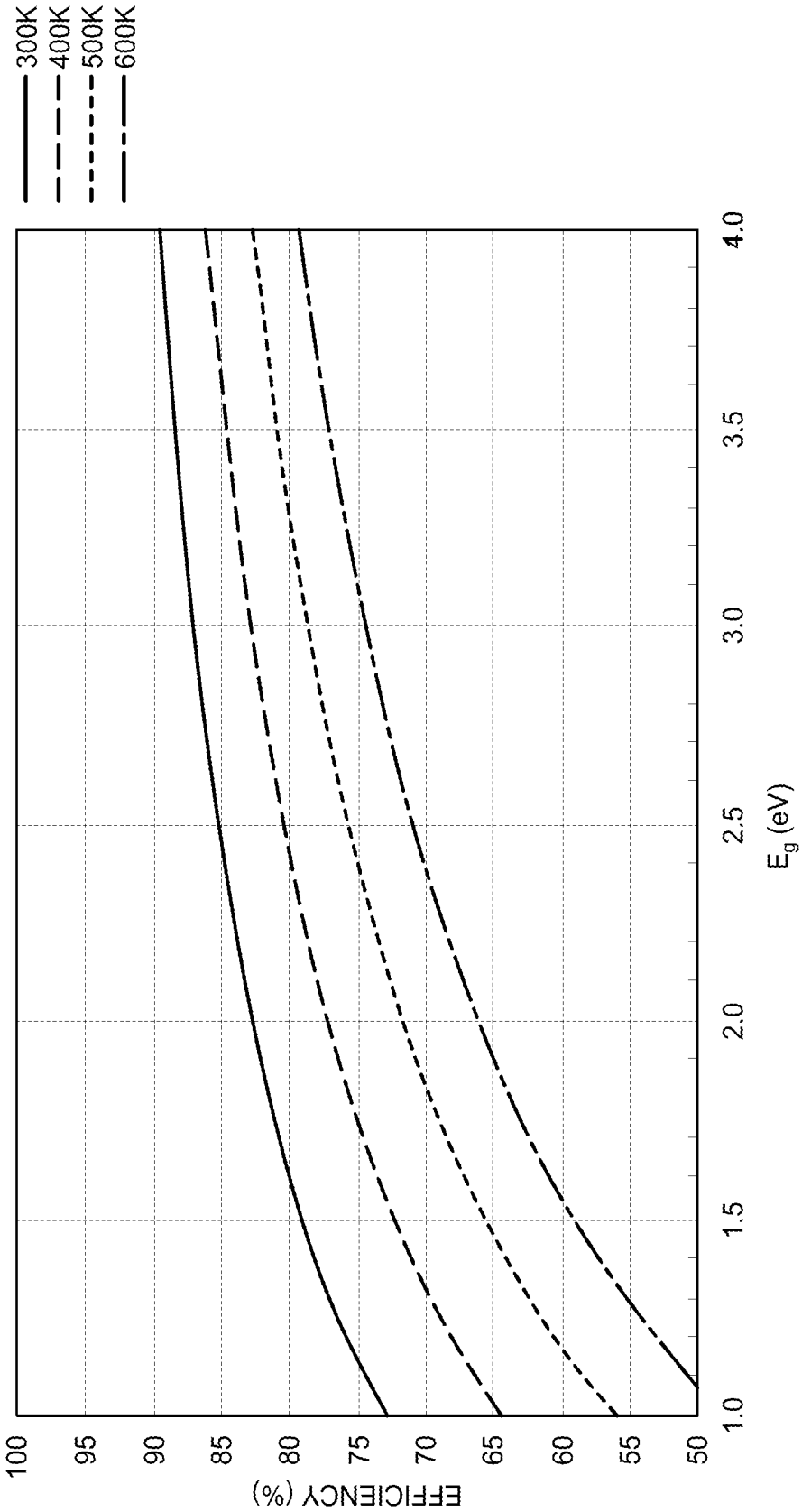
300K
400K
500K
600K
EFFICIENCY (%)
100
95
90
85
80
75
70
65
60
55
50
1.0
1.5
2.0
2.5
3.0
3.5
4.0
E_g (eV)

FIG. 26

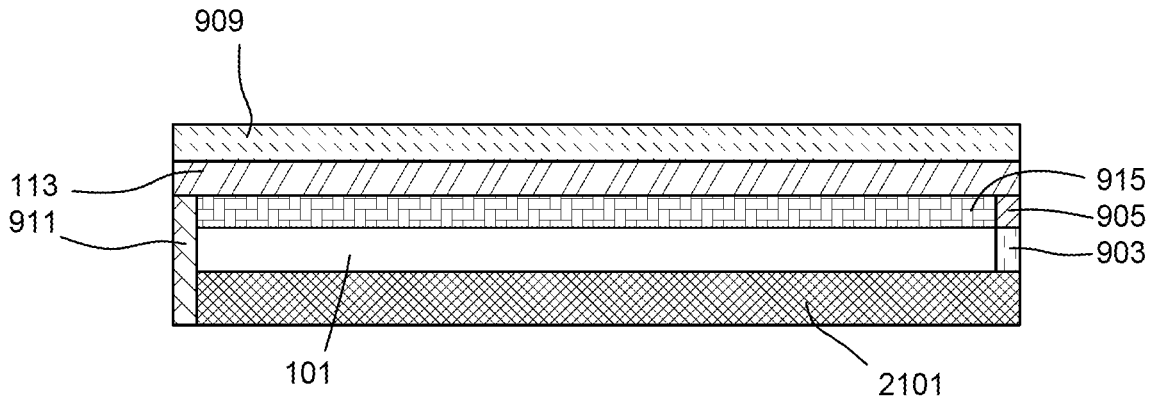

FIG. 27A

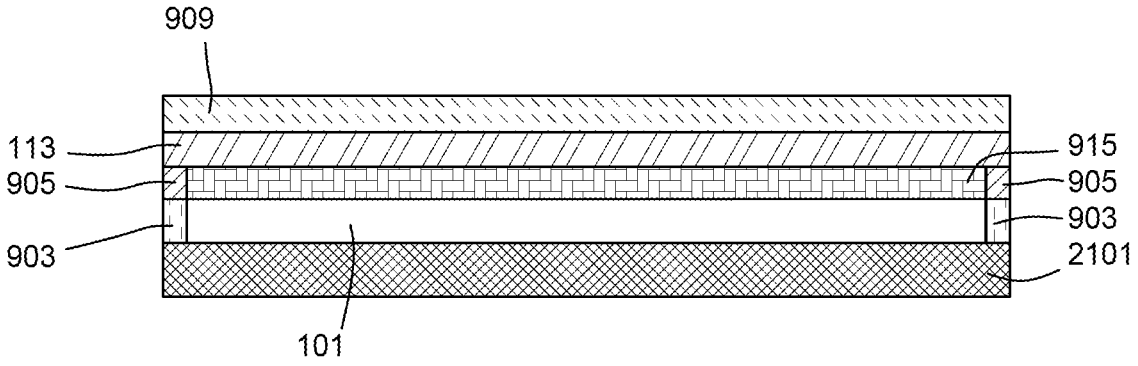

FIG. 27B

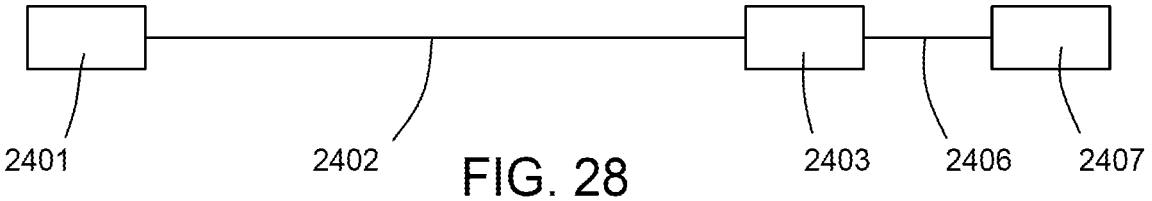

FIG. 28

Items	Value	Units
absorption coefficient of absorber layer, α_{abslay}	1.0E+05	cm^{-1}
absorber layer thickness	4.0E-06	cm
absorber layer refractive index for angle calc, n_{abs}	2.55	
absorption coefficient of substrate, α_{sub}	0.4	cm^{-1}
substrate thickness	0.05	cm
substrate refractive index, n_{sub}	2.45	
top surface reflectance, R_{ts}	85	%
bottom surface reflectance, R_{bs}	94	%
angle in substrate relative to bottom surface, θ	15	degrees

FIG. 29A

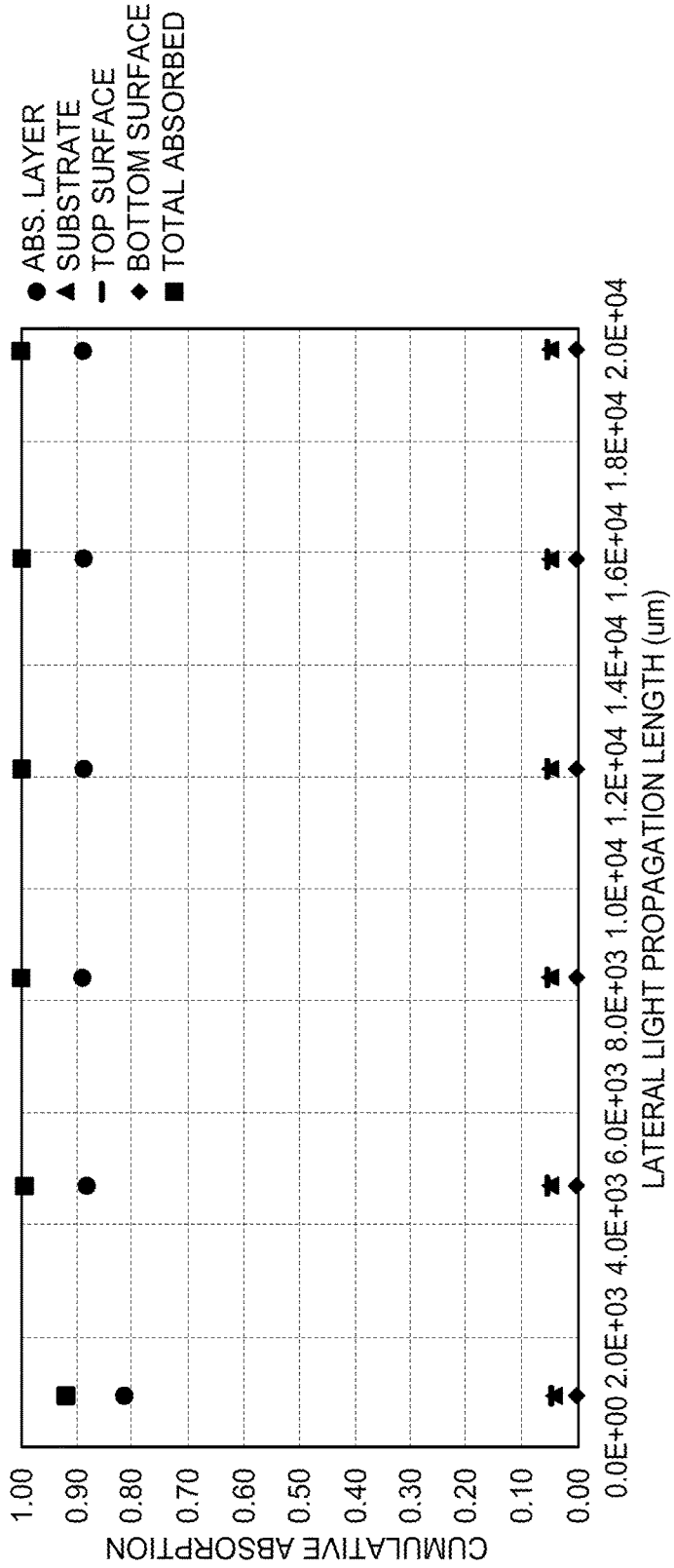

FIG. 29B

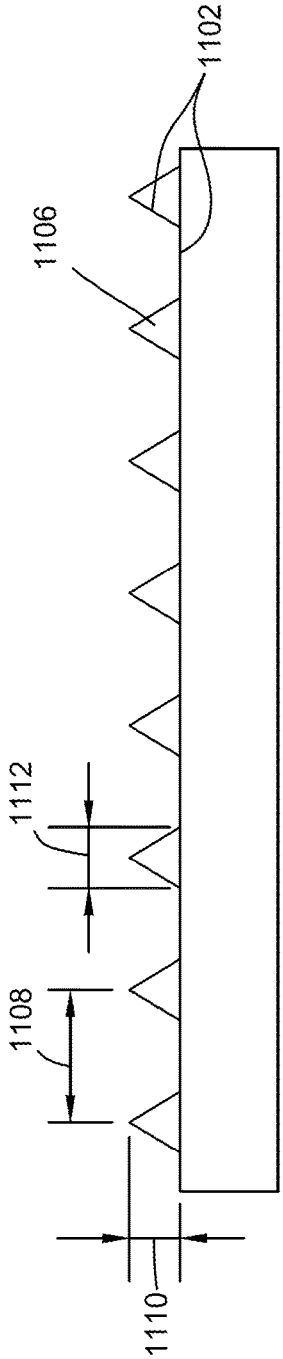

FIG. 30

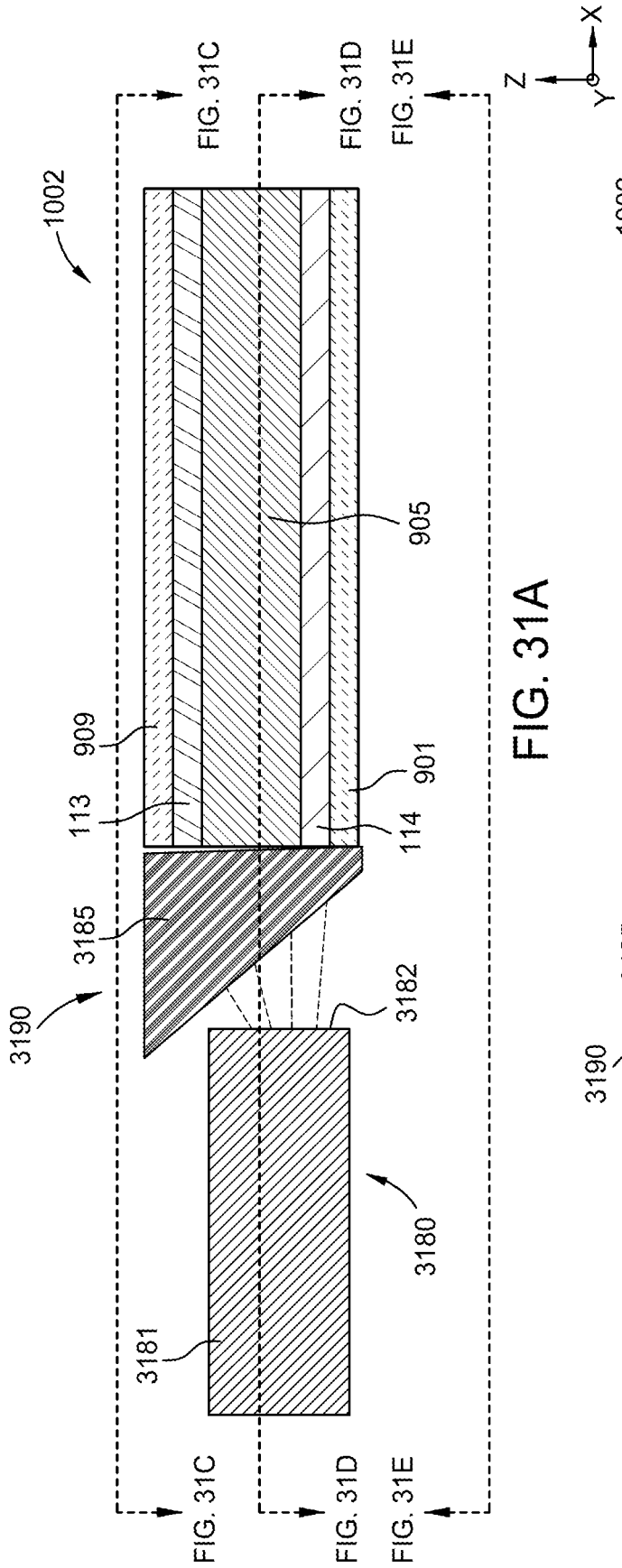

FIG. 31A

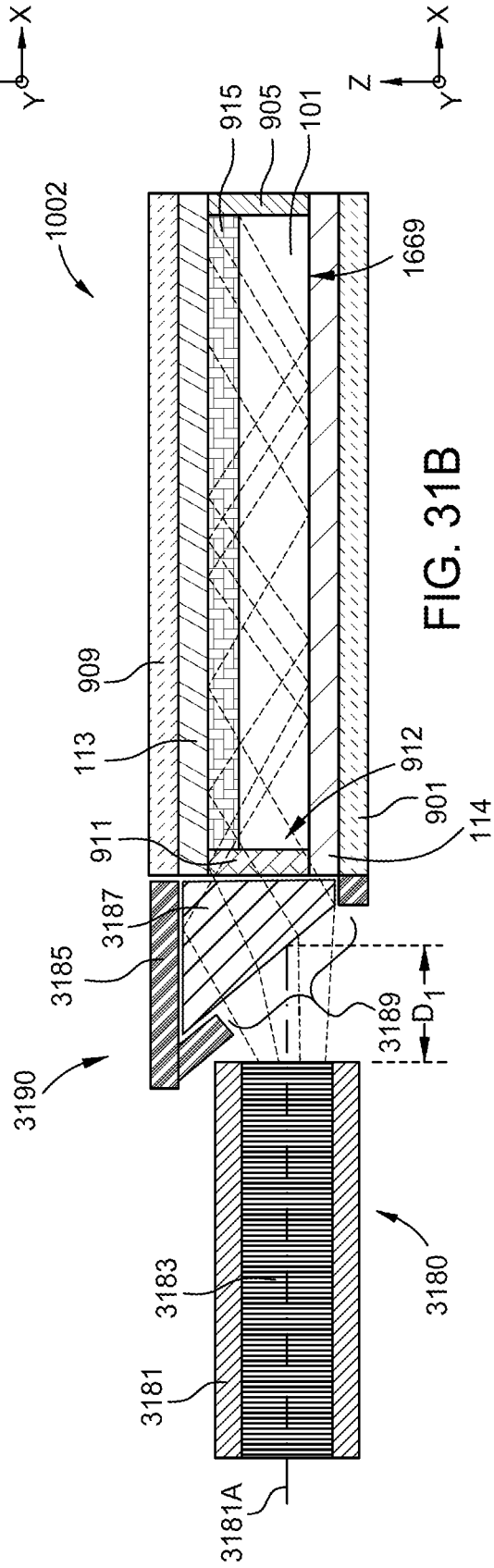

FIG. 31B

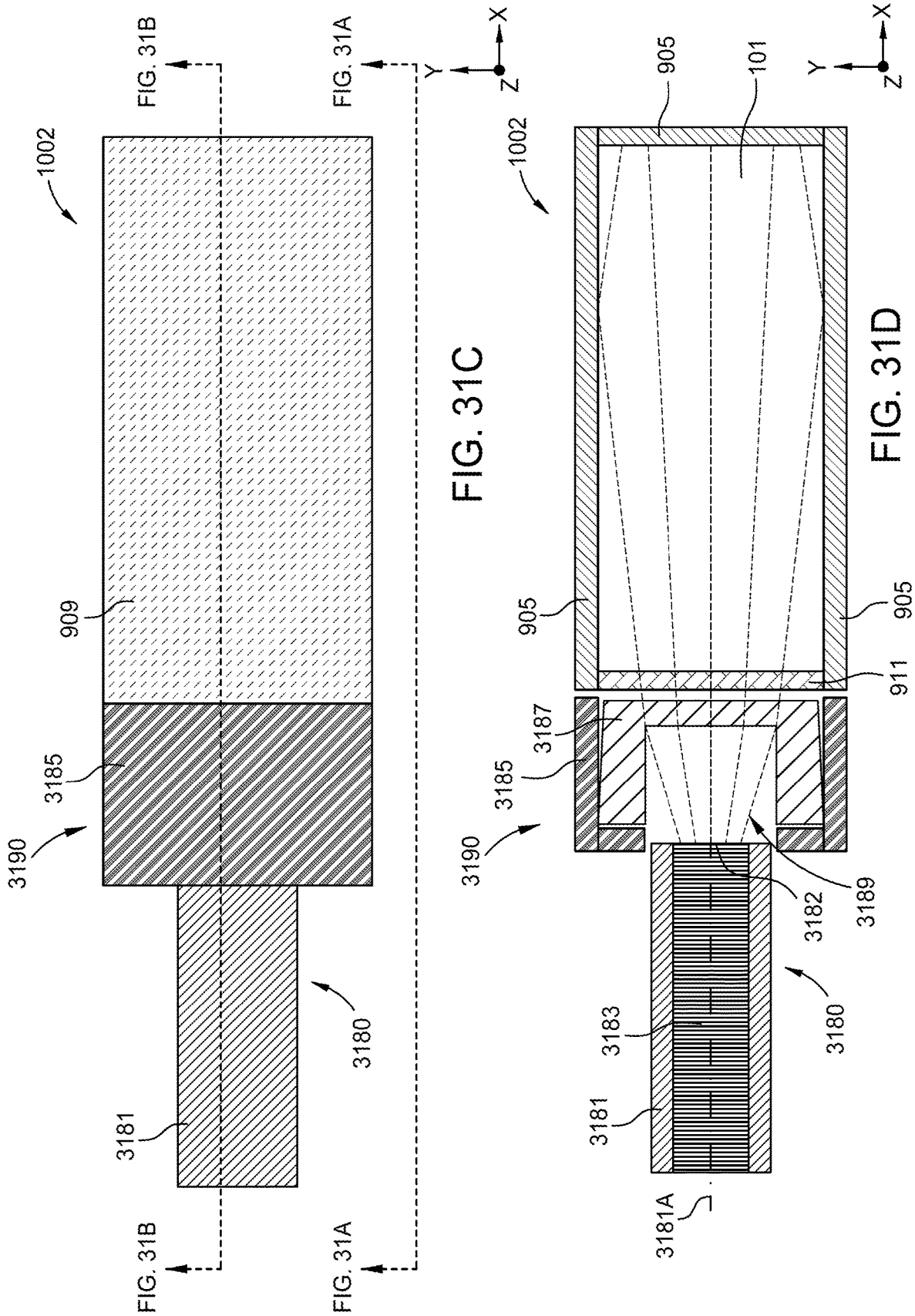
FIG. 31B
FIG. 31A
X
Y
Z
1002
909
3185
3190
3180
3181
FIG. 31B
FIG. 31A
FIG. 31C
905
101
X
Y
Z
1002
905
905
911
3187
3185
3190
3182
3189
3183
3180
3181
3181A
FIG. 31D

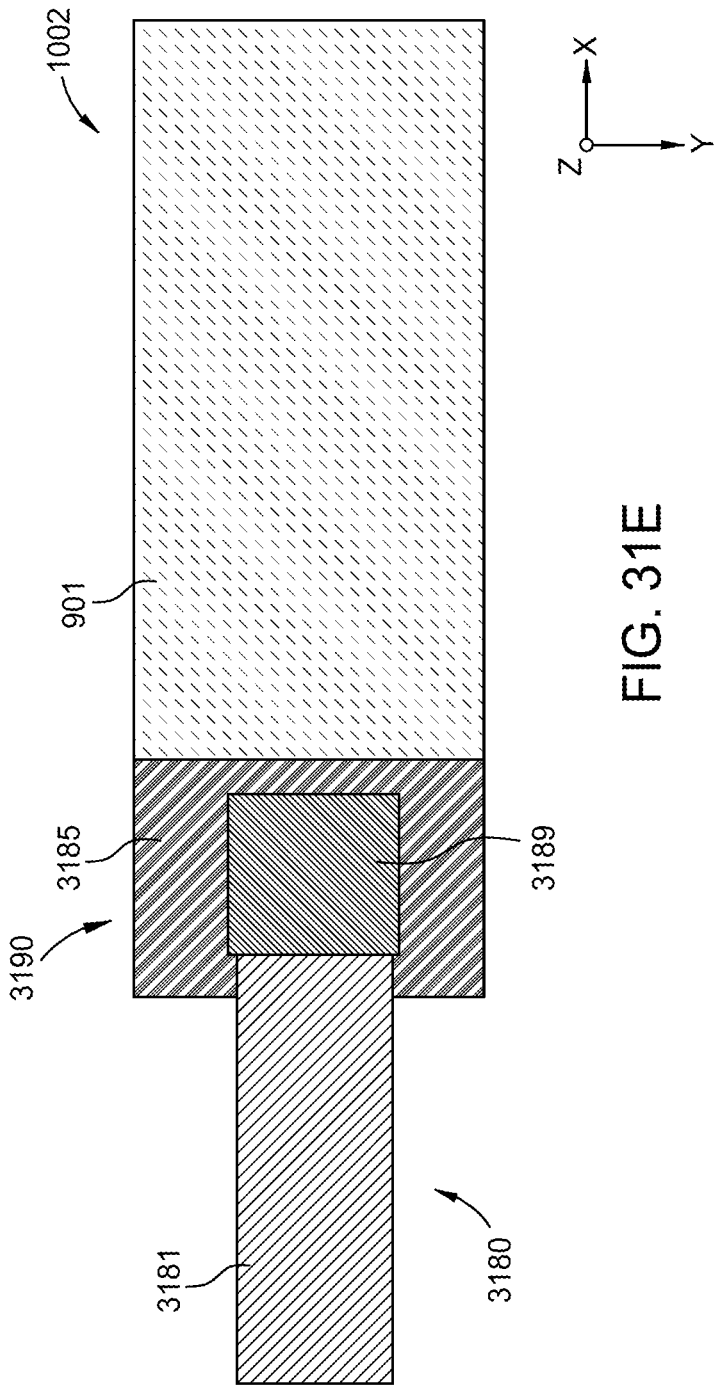

FIG. 31E

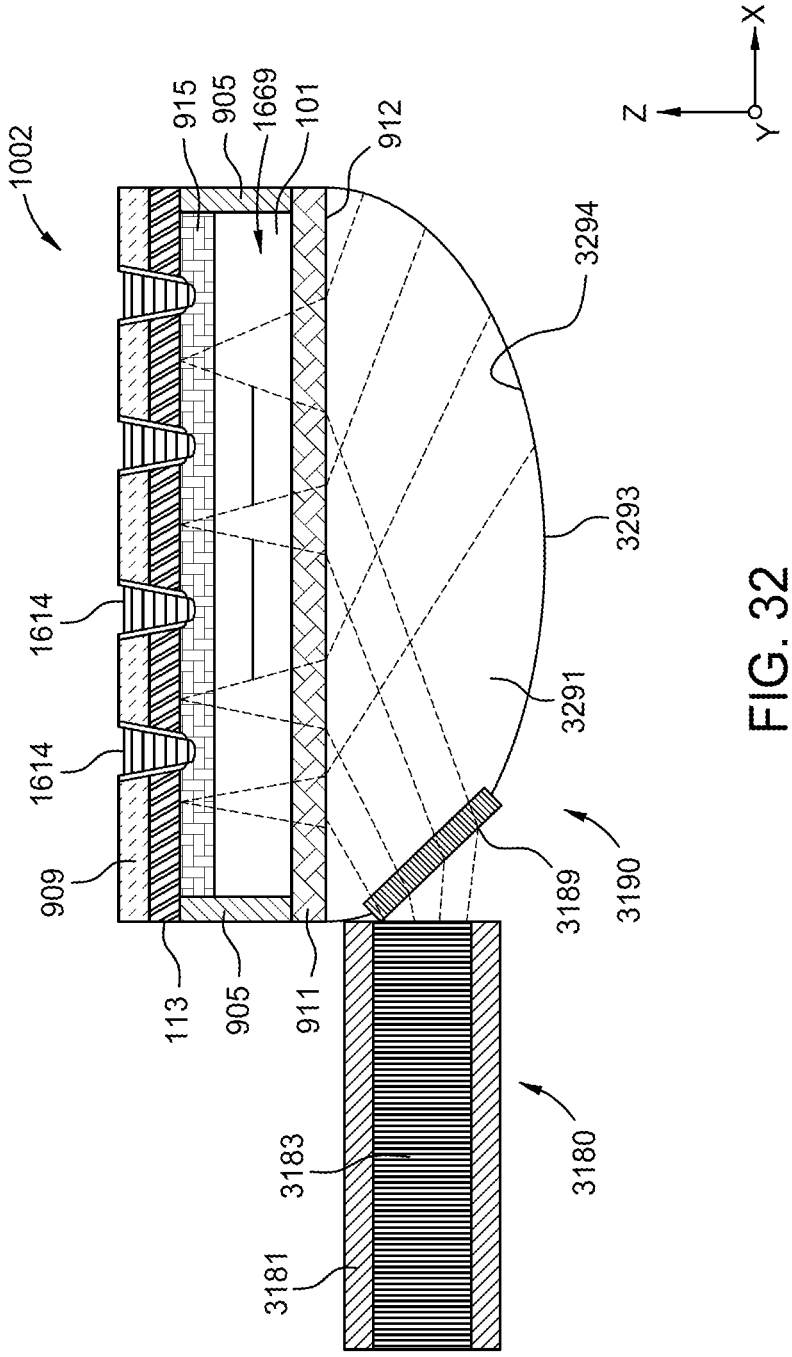
1002
915
905
1669
101
912
Z
X
Y
3294
3293
3291
1614
1614
909
113
905
911
3189
3190
3183
3181
3180

FIG. 32

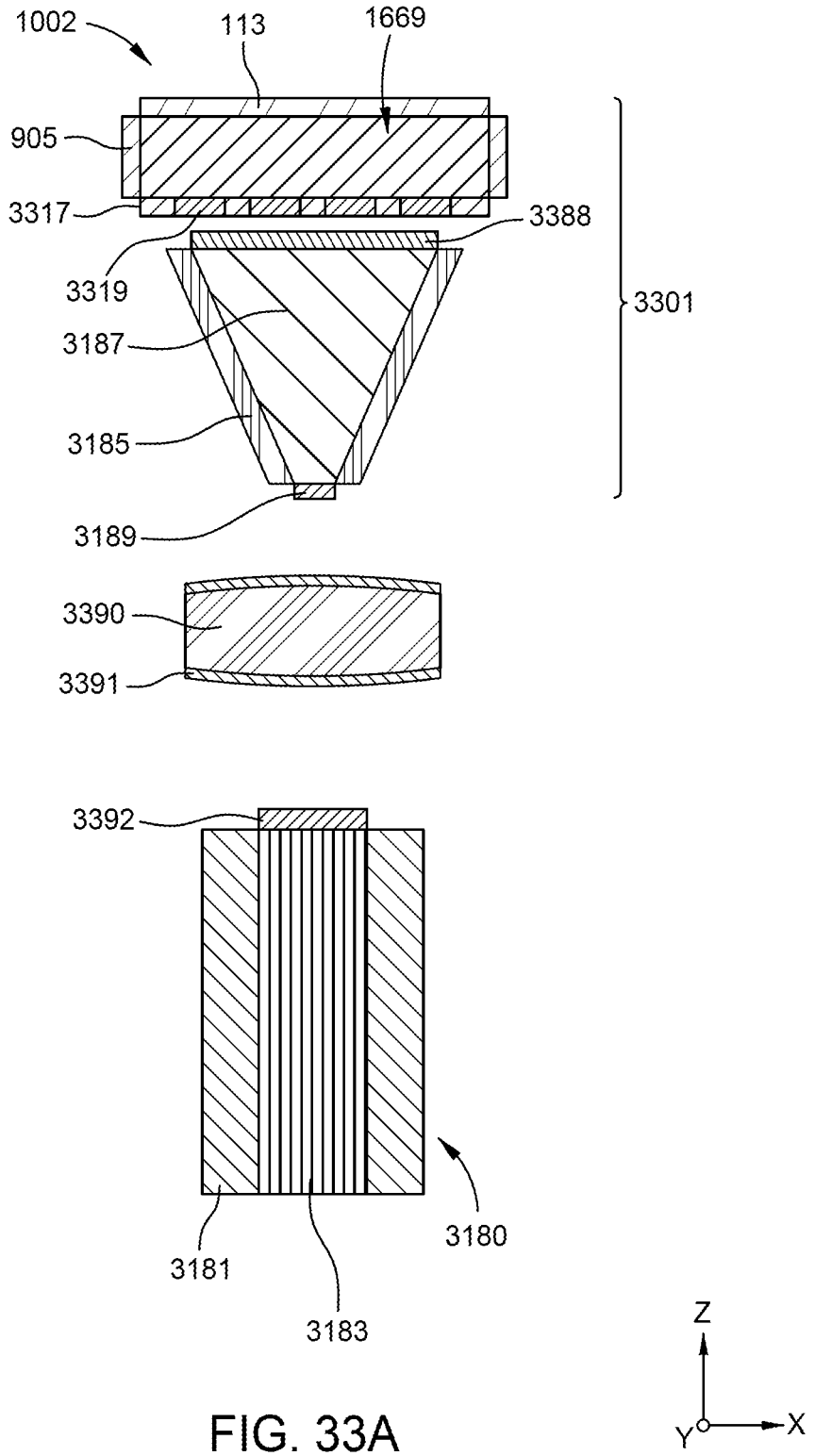
1002
113
1669
905
3317
3388
3319
3301
3187
3185
3189
3390
3391
3392
3180
3181
3183
Z
Y
X

FIG. 33A

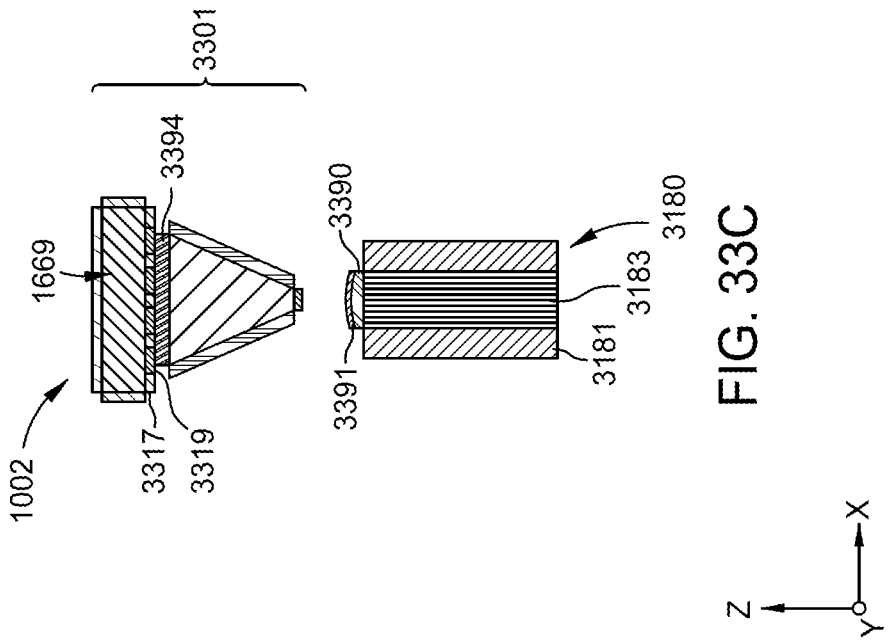

FIG. 33C

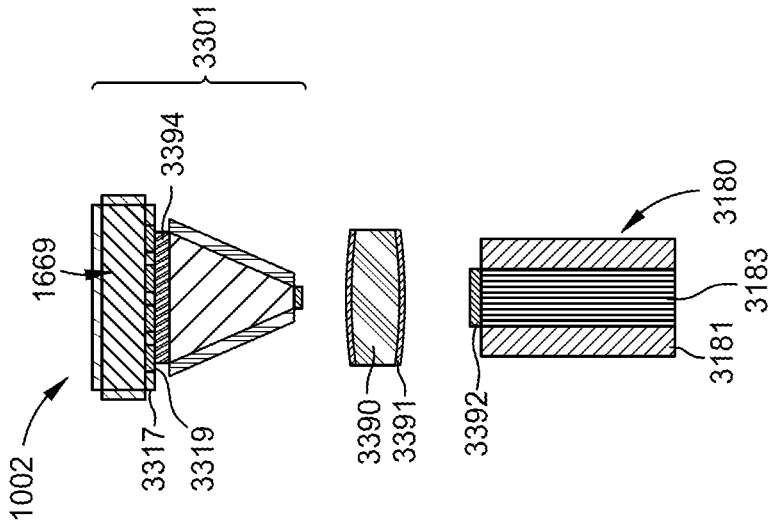

FIG. 33B

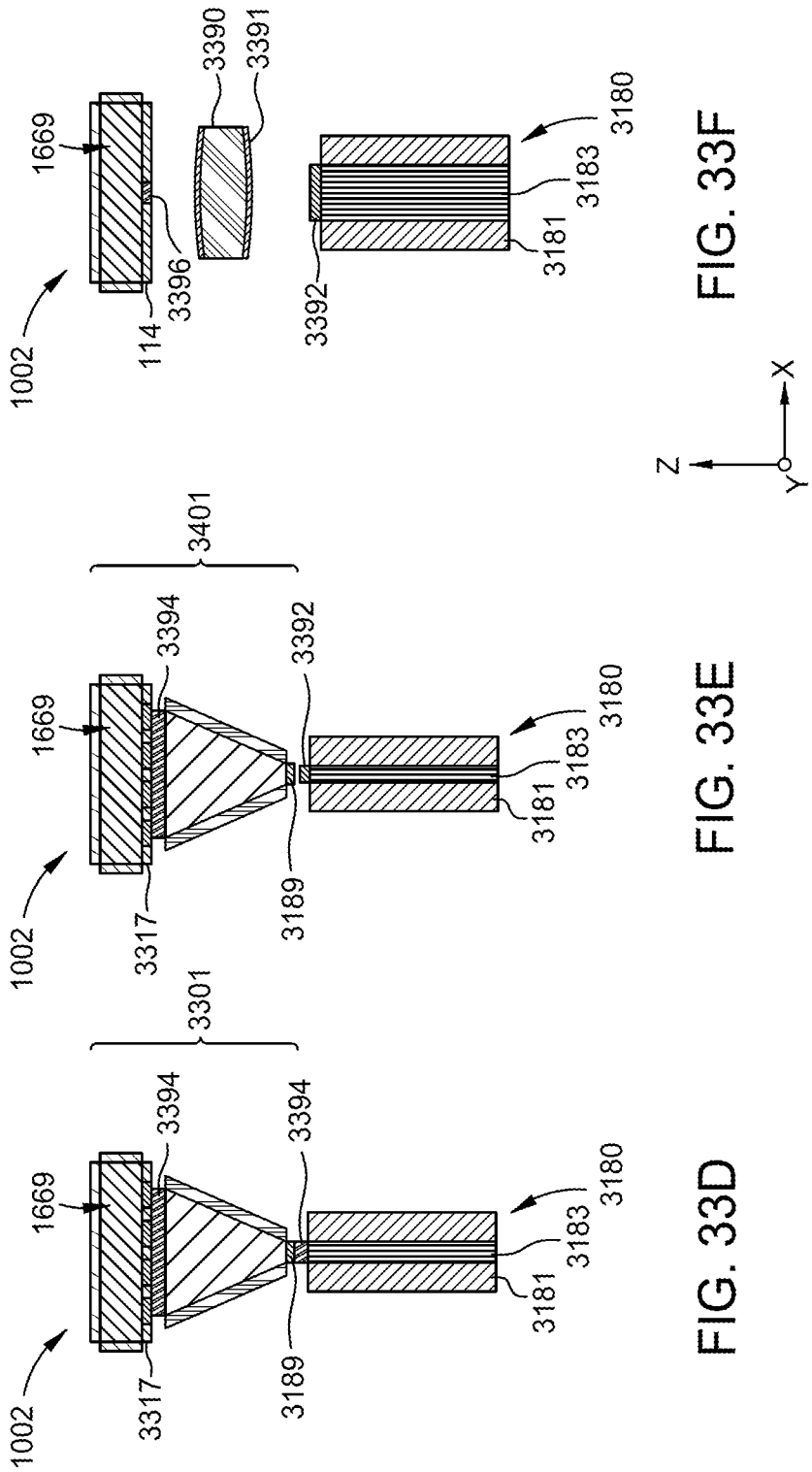

FIG. 33D

FIG. 33E

FIG. 33F

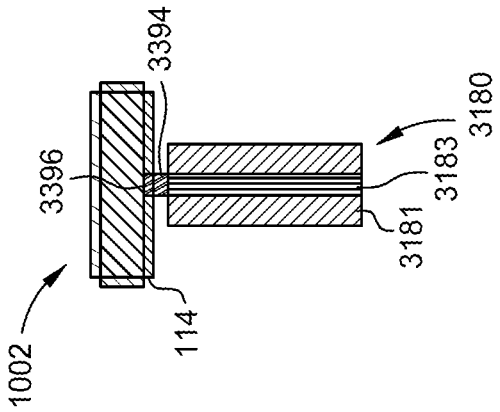

FIG. 33I

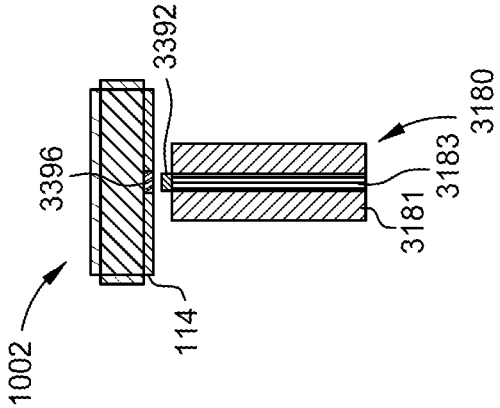

FIG. 33H

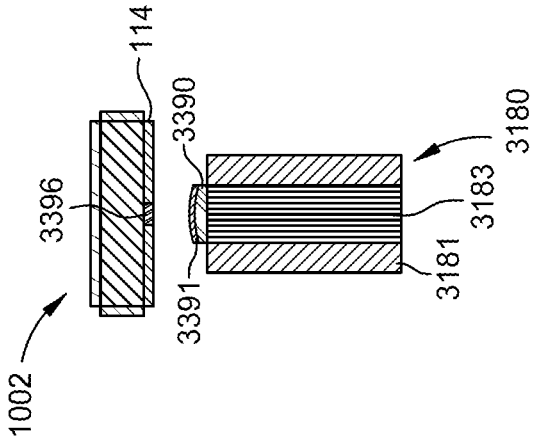

FIG. 33G

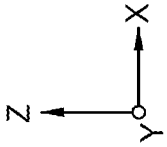

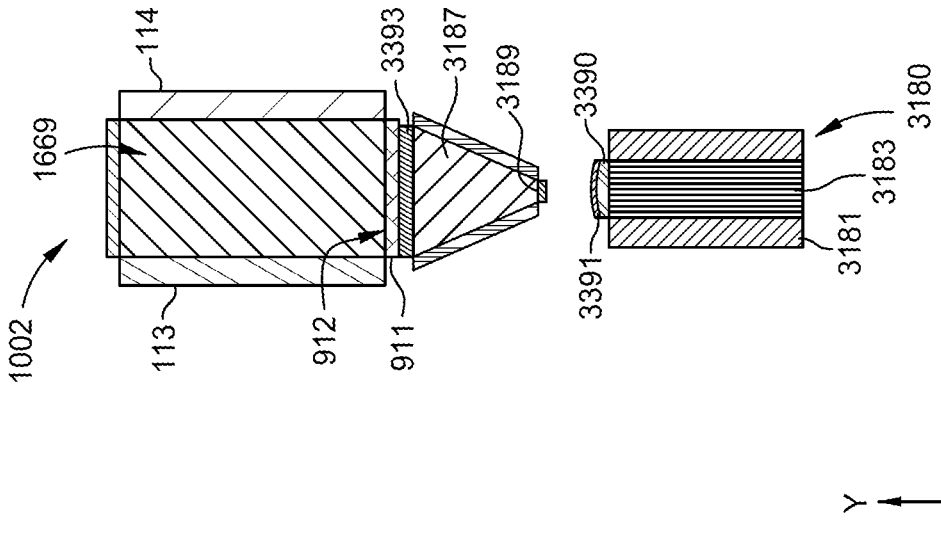

FIG. 34C

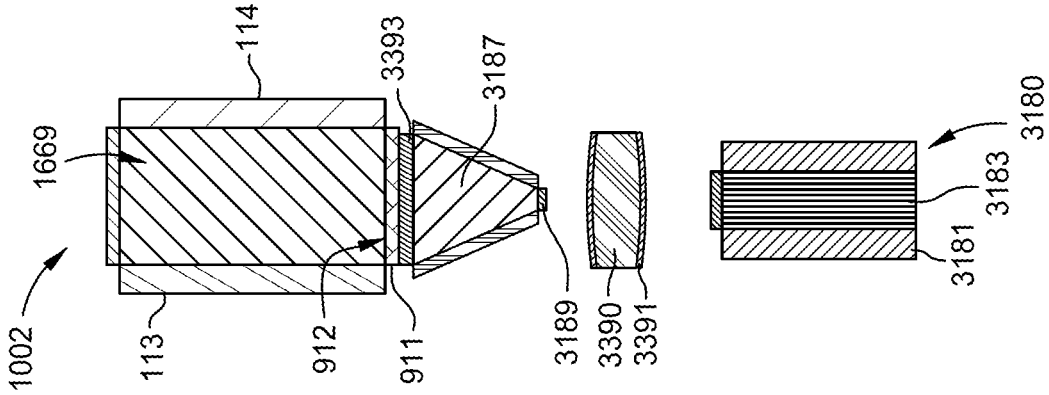

FIG. 34B

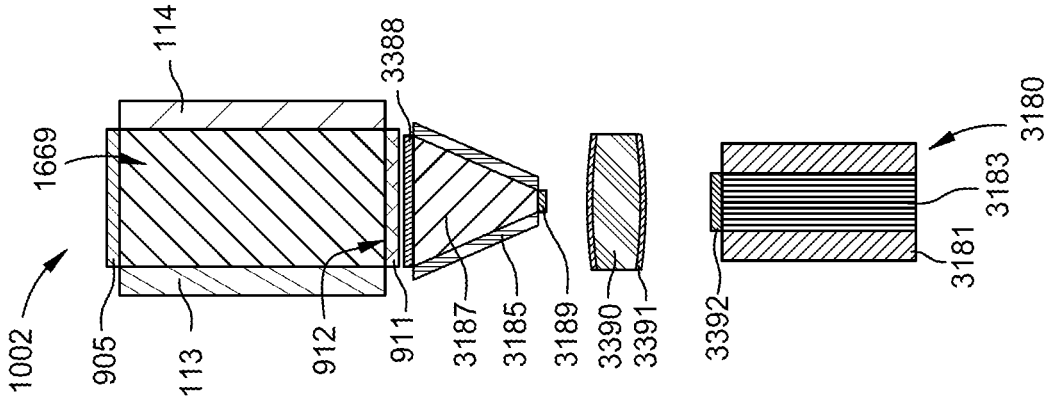

FIG. 34A

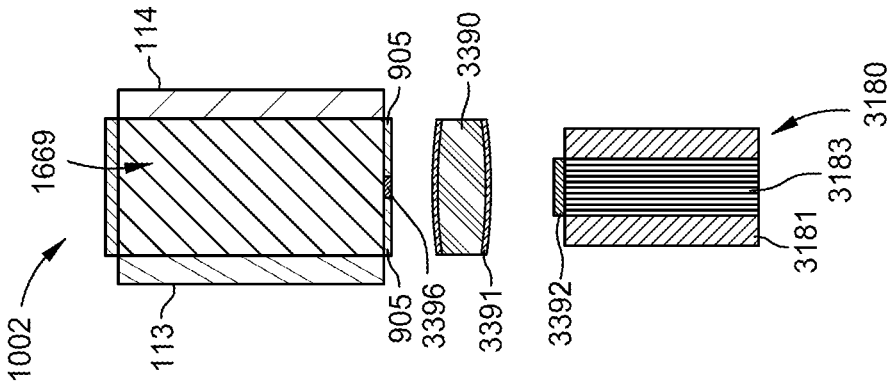

FIG. 34F

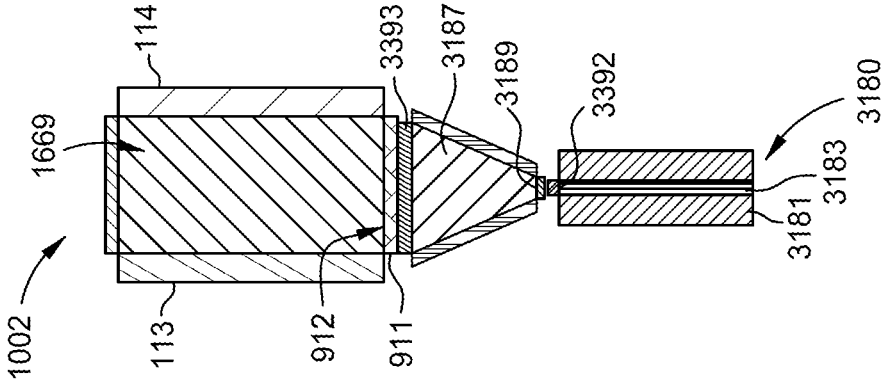

FIG. 34E

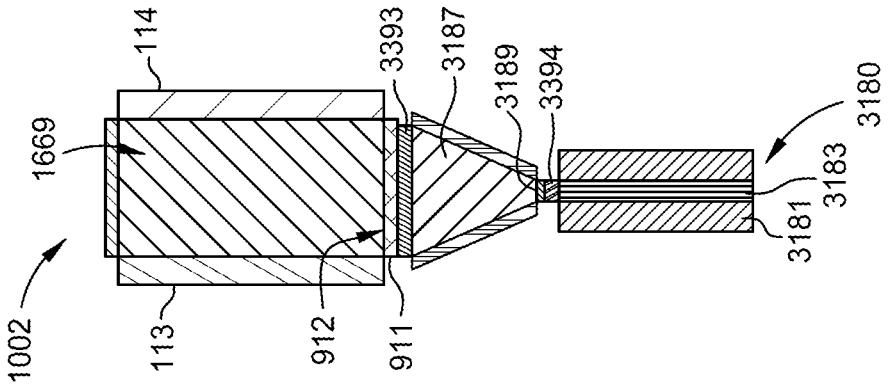

FIG. 34D

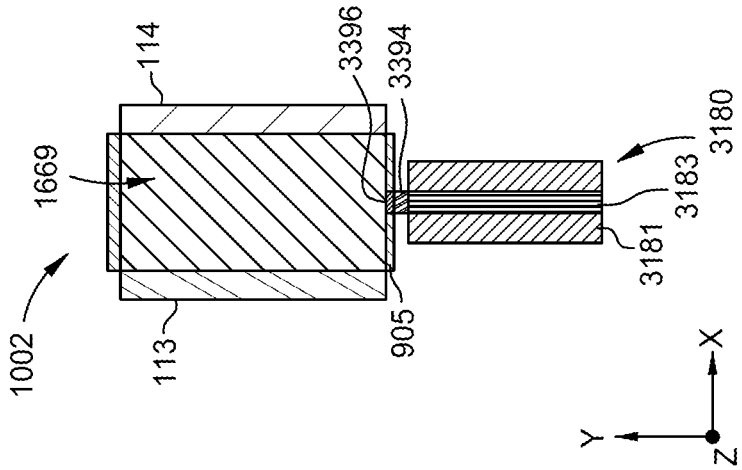

FIG. 34I

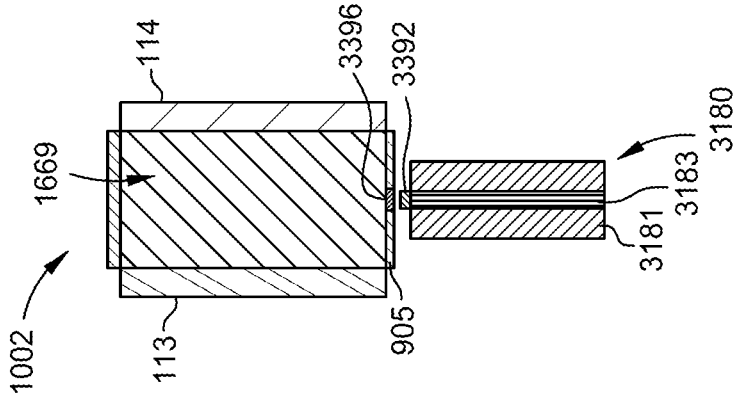

FIG. 34H

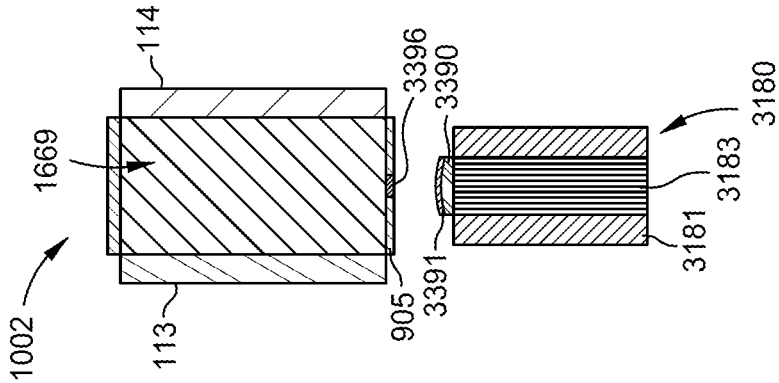

FIG. 34G

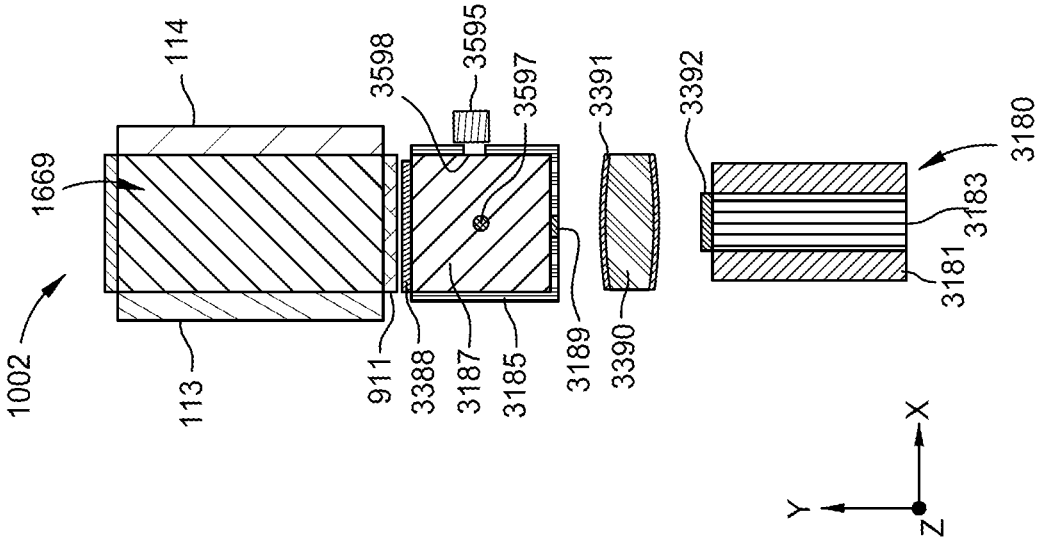

FIG. 35C

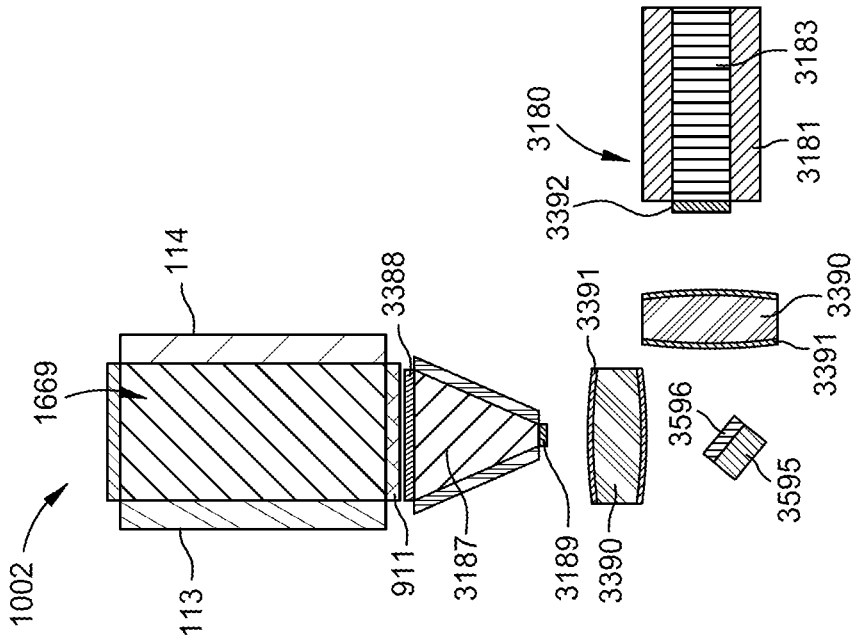

FIG. 35B

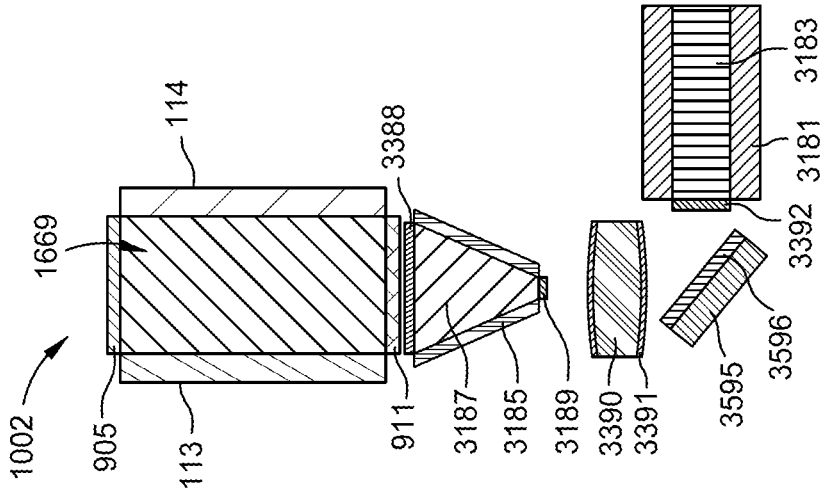

FIG. 35A

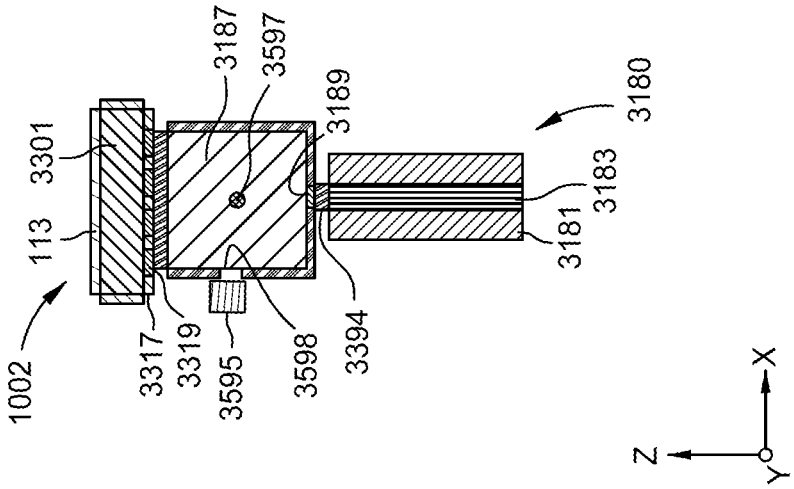

FIG. 35F

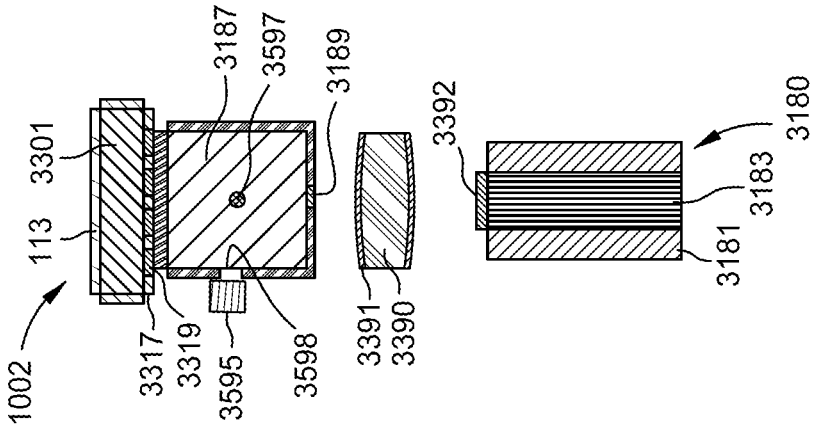

FIG. 35E

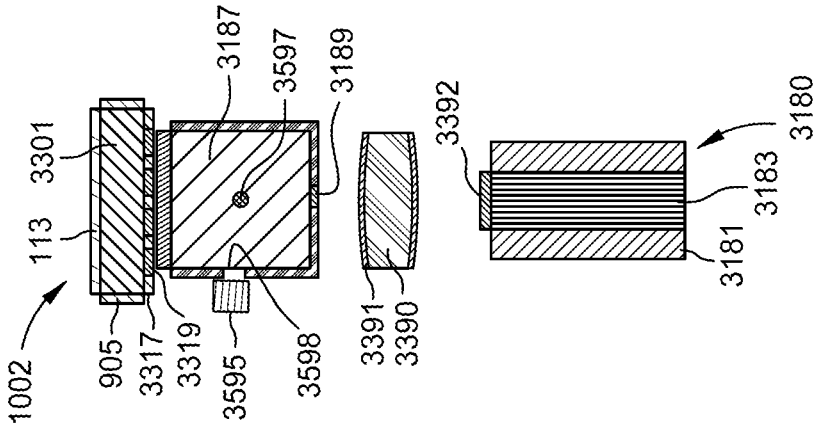

FIG. 35D

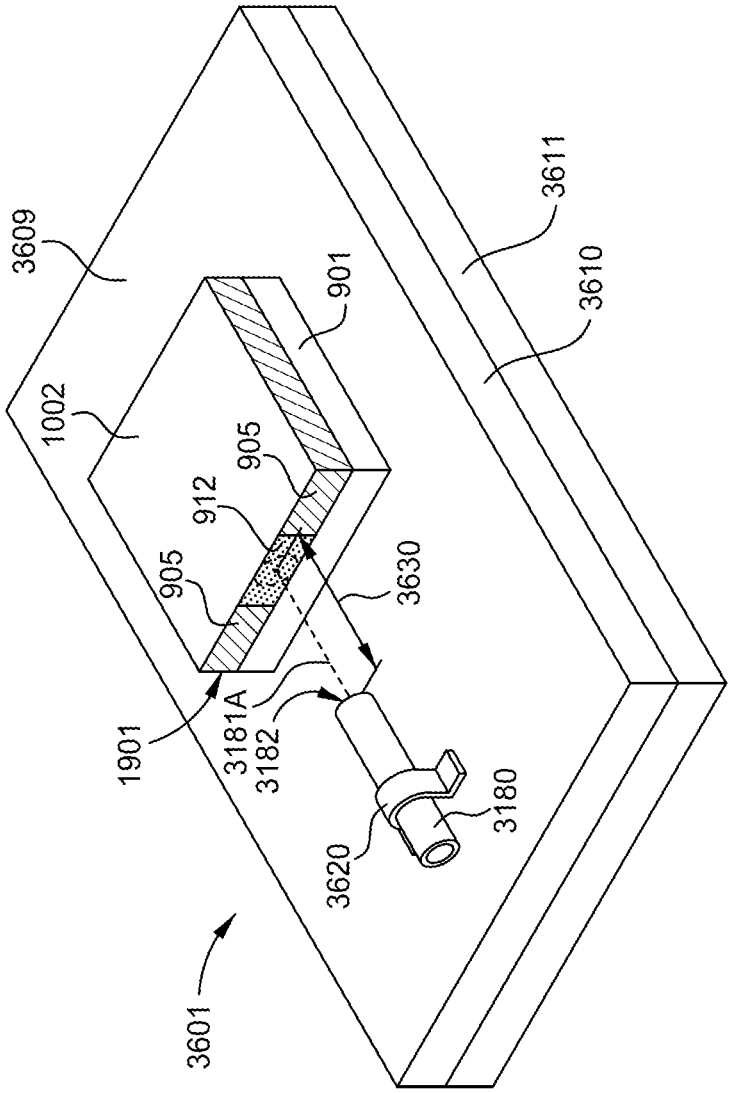
3609
1002
1901
3601
905
912
905
901
3181A
3182
3620
3630
3180
3611
3610

FIG. 36

POWER PHOTODIODE STRUCTURES AND DEVICES

CROSS-REFERENCE TO RELATED APPLICATIONS

This patent application continuation of U.S. patent application Ser. No. 17/151,109, filed Jan. 15, 2021, which is a continuation-in-part of U.S. patent application Ser. No. 16/930,250, filed Jul. 15, 2020, which claims the benefit of U.S. Provisional Application No. 62/874,487, filed Jul. 15, 2019. The U.S. patent application Ser. No. 17/151,109 also claims the benefit of U.S. Provisional Application No. 62/978,281, filed Feb. 18, 2020. Each of these patent applications are incorporated by reference herein.

BACKGROUND

Field

This disclosure relates generally to techniques for transmitting power through optical fibers and, in particular, to techniques for high current density power photodiode structures and devices fabricated on bulk gallium and nitrogen containing polar, semipolar, or nonpolar materials. The invention can be applied to applications involving conversion of light energy to electrical energy, particularly via optical fibers, other optoelectronic devices, and similar products.

Description of the Related Art

Electrical power is typically transmitted over a wire, for example, a copper wire. However, such wires can be heavy, cumbersome, and expensive, and the transmitted power can be subject to electromagnetic interference. Some of these limitations can be overcome by transmitting power over an optical fiber but, unfortunately, with current capability such approaches are not yet commercially viable. In addition, current approaches generally involve light at infrared wavelengths, which has certain disadvantages over visible light, or visible optical radiation, such as greater sensitivity to temperature variations in the surrounding environment.

Gallium nitride (GaN) based optoelectronic and electronic devices are of tremendous commercial importance. The best-developed of these devices include light emitting diodes (LEDs) and laser diodes, and GaN-based power diodes and transistors are becoming increasingly important. There is also interest in emerging applications. De Santi, and coauthors [Materials 11, 153 (2018)] described an application whereby electrical power is converted to optical power using a laser diode, the optical power is coupled to an optical fiber and transmitted to a remote location, then the optical power is converted back to electrical power using a photodiode. Both the laser diode and the photodiode were based on GaN-on-sapphire devices and the system performance was relatively poor. The photodiode was a particular challenge, with a reported efficiency of 17%. GaN-based solar cells have also been reported by a number of groups, typically utilizing GaN-on-sapphire structures for low power (ca. one sun) applications. Even concentrator solar cell structures, which are well known in the art for other materials systems, are only able to generate substantially lower current densities than those that are the principal focus of the current invention.

In the case of laser diodes, it is well known that superior performance and reliability can be obtained in GaN-on-GaN

devices, which have greatly reduced defect densities and have undergone many years of optimization and improvement. In the case of photodiodes, considerably less work has been done. For example, D'Evelyn et al. [U.S. Pat. No. 6,806,508] disclosed a GaN-on-GaN photodiode that was intended for photodetector applications rather than for power diode applications.

Related applications have been disclosed using GaAs-based lasers and photodiodes, at wavelengths in the near-infrared. However, due to its larger bandgap, photodiodes based on the nitrides should enable considerably higher open-circuit voltages and superior efficiencies at elevated temperatures and at high input power levels, relative to corresponding GaAs-based devices and systems.

From the above, it is seen that techniques for improving GaN-based power photodiodes and methods for optical coupling thereto are highly desirable. There is also a need for systems, device(s) and methods that solve the problems described above.

SUMMARY

Embodiments of the disclosure may provide a photodiode structure, including a substrate having a first surface and a second surface, wherein the second surface of the substrate is opposite to the first surface, the substrate is a single-crystalline group-III metal nitride, and the first surface of the substrate has a crystallographic orientation within 5 degrees of (0001) +c-plane, {10-10} m-plane, or a semipolar plane selected from one of {11-2±2}, {60-6±1}, {50-5±1}, {40-4±1}, {30-3±1}, {50-5±2}, {70-7±3}, {20-2±1}, {30-3±2}, {40-4±3}, {50-5±4}, {10-1±1}, {1 0 −1 ±2}, {1 0 −1 ±3}, or differs from (000-1) by between 2 degrees and 5 degrees. The photodiode structure also includes an n-type layer and a p-type layer that are disposed over the first surface of the substrate, wherein the n-type layer and the p-type layer each comprise $Al_xIn_yGa_{1-x-y}N$, where $0 \le x, y, x+y \le 1$, and have a dopant concentration of at least 1×10^{17} cm^{-3}, one or more absorber layers disposed between the n-type and the p-type layers, wherein the one or more absorber layers comprise $Al_xIn_yGa_{1-x-y}N$, where $0 \le x, y, x+y \le 1$ and have a dislocation density below about 10^9 cm^{-2}, a p-side electrical contact layer disposed over the p-type layer, wherein the p-side electrical contact layer has an average reflectance of at least 70% for at least one wavelength between 390 nanometers and 460 nanometers and a contact resistance below 3×10^{-3} Ωcm^2, an n-side electrical contact layer disposed over the second surface of the substrate, wherein the n-side electrical contact layer has an average reflectance of at least 70% for at least one wavelength between 390 nanometers and 460 nanometers and a contact resistance below 1×10^{-3} Ωcm^2; and a light receiving surface, wherein the light receiving surface is aligned to cause light, having at least one wavelength between 390 nanometers and 460 nanometers and incident on the light receiving surface at an angle, to be reflected at least once from the n-side electrical contact layer and from the p-side electrical contact layer. The photodiode structure may also be characterized by a fill factor of at least 50% under an illumination level producing a current density of at least 10 A cm^{-2}.

Embodiments of the disclosure may further provide a photodiode structure, including one or more absorber layers, wherein the one or more absorber layers comprise $Al_xIn_yGa_{1-x-y}N$, where $0 \le x, y, x+y \le 1$, an n-type layer and a p-type layer, wherein the one or more absorber layers being disposed over the n-type layer and the p-type layer being disposed over the one or more absorber layers, a carrier

substrate having a first surface and a second surface, wherein the first surface of the carrier substrate being disposed over the p-type layer or under the n-type layer, a p-side electrical contact layer placed in electrical contact with the p-type layer, wherein the p-side electrical contact layer has a contact resistance below 3×10^{-3} Ωcm^2, a p-side reflector layer disposed on one of the p-type layer and the second surface of the carrier substrate, the p-side reflector layer having an average reflectance of at least 70% for at least one wavelength between 390 nanometers and 460 nanometers, an n-side electrical contact layer placed in electrical contact with the n-type layer, wherein the n-side electrical contact layer has a contact resistance below 1×10^{-3} Ωcm^2, an n-side reflector layer disposed over one of the n-side layer and the second surface of the carrier substrate, the n-side reflector layer having an average reflectance of at least 70% for at least one wavelength between 390 nanometers and 460 nanometers, and a light receiving surface, wherein the light receiving surface is aligned to cause light, having at least one wavelength between 390 nanometers and 460 nanometers and incident on the light receiving surface at an angle, to be reflected at least once from the n-side reflector layer and from the p-side reflector layer. The n-type layer and the p-type layer each comprise $Al_xIn_yGa_{1-x-y}N$, where $0\leq x, y, x+y\leq 1$, and have a dopant concentration of at least 1×10^{16} cm^{-3}. The carrier substrate being substantially transparent at wavelengths between 390 nanometers and 460 nanometers.

Embodiments of the disclosure may further provide a photodiode structure, including a substrate having a first surface, a second surface and a third surface, an n-type layer and a p-type layer that are disposed over the first surface of the substrate, one or more absorber layers disposed between the n-type and the p-type layers, a p-type electrode layer disposed over the p-type layer, an n-type electrode layer disposed over the second surface of the substrate, and a light receiving surface, wherein the third surface comprises the light receiving surface and is configured to cause light received therethrough to be reflected at least once between the n-type electrode layer and the p-type electrode layer. The n-type electrode layer includes an array of openings formed therein, and has an average reflectance of at least 70% at wavelengths between 390 nanometers and 460 nanometers. The p-type electrode layer includes an array of openings formed therein, and has an average reflectance of at least 70% at wavelengths between 390 nanometers and 460 nanometers. The one or more absorber layers include an $Al_xIn_yGa_{1-x-y}N$ material, where $0\leq x, y, x+y\leq 1$ and have a dislocation density below about 10^9 cm^{-2}. The n-type layer and the p-type layer each include an $Al_xIn_yGa_{1-x-y}N$ material, where $0\leq x, y, x+y\leq 1$; and have a dopant concentration of at least 1×10^{16} cm^{-3}. The second surface of the substrate is opposite to the first surface, the third surface of the substrate is aligned at an angle to the first and second surfaces, the substrate is a single-crystalline group-III metal nitride, and the first surface of the substrate has a crystallographic orientation within 5 degrees of (0001) +c-plane, {10-10} m-plane, or a semipolar plane selected from one of {11-2±2}, {60-6±1}, {50-5±1}, {40-4±1}, {30-3±1}, {50-5±2}, {70-7±3}, {20-2±1}, {30-3±2}, {40-4±3}, {50-5±4}, {10-1±1}, {1 0 −1 ±2}, {1 0 −1 ±3}, or differs from (000-1) by between 2 degrees and 5 degrees.

Embodiments of the disclosure may include a photodiode structure, comprising one or more absorber layers lying between n-type and p-type layers, each of the absorber and n-type and p-type layers comprising $Al_xIn_yGa_{1-x-y}N$, where $0\leq x, y, x+y\leq 1$ and having a dislocation density below about 10^9 cm^{-2}, each of the first and second non-absorber layers being characterized by a dopant concentration of at least 1×10^{16} cm^{-3}, wherein the absorber layer is configured for efficient power conversion of light having a wavelength between about 390 nanometers and 460 nanometers; and the structure is characterized by a fill factor of at least 50% under an illumination level producing a current density of at least 10 A cm^{-2}.

Embodiments of the disclosure may further provide an optical device, comprising a die that comprises one or more absorber layers disposed between an first non-absorber layer and a second non-absorber layer, each of the one or more absorber layers and the first and second non-absorber layers comprising $Al_xIn_yGa_{1-x-y}N$, where $0\leq x, y, x+y\leq 1$ and having a dislocation density below about 10^{10} cm^{-2}; wherein the one or more absorber layers each have a thickness, measured in a first direction, and an absorber layer surface that is parallel to a first plane and oriented normal to the first direction, and the die having an device cavity region having an optical window, the device cavity region comprising at least two opposing reflective members that are configured to cause internal reflection of electromagnetic radiation entering through the optical window to pass through the one or more absorber layers at least two or more times.

Embodiments of the disclosure may further provide an optical device, comprising a die that comprises an optical window and at least two absorber layers that are disposed between an n-type first non-absorber layer and a second non-absorber layer, each of the absorber and non-absorber layers comprising $Al_xIn_yGa_{1-x-y}N$, where $0\leq x, y, x+y\leq 1$ and having a dislocation density below about 10^{10} cm^{-2}; wherein a separate n-contact is disposed on the first non-absorber layer and a p-type contact is disposed on the second non-absorber layer.

Embodiments of the disclosure may further provide a power-over-fiber module that comprises at least one laser diode, at least one optical fiber, and at least one photodiode. The laser diode comprises at least one active layer comprising $Al_xIn_yGa_{1-x-y}N$, where $0\leq x, y, x+y\leq 1$ and having a dislocation density below about 10^7 cm^{-2}. The laser diode is configured to have an emission wavelength between about 400 nanometers and about 500 nanometers. The photodiode comprises at least one absorber layer comprising $Al_xIn_yGa_{1-x-y}N$, where $0\leq x, y, x+y\leq 1$ and having a dislocation density below about 10^{10} cm^{-2}. The photodiode is configured to have absorber layer bandgap wavelengths that are between about 400 nanometers and about 550 nanometers.

Embodiments of the disclosure may further provide a power-over-fiber system, comprising at least one laser diode, at least one optical fiber, and at least one photodiode, wherein the electrical power from the photodiode is used to power an Internet-of-Things sensor or actuator or a personal electronic device. The laser diode comprises at least one active layer comprising $Al_xIn_yGa_{1-x-y}N$, where $0\leq x, y, x+y\leq 1$ and having a dislocation density below about 10^7 cm^{-2}. The laser diode is configured to have an emission wavelength between about 400 nanometers and about 500 nanometers. The photodiode comprises at least one absorber layer comprising $Al_xIn_yGa_{1-x-y}N$, where $0\leq x, y, x+y\leq 1$ and having a dislocation density below about 10^{10} cm^{-2}. The photodiode is configured to have absorber layer bandgap wavelengths that are between about 400 nanometers and about 550 nanometers.

The power-over-fiber module or power-over-fiber system may further comprise at least one optical dispensing device, and/or control modules to modulate the laser diode power at at least one controlled AC frequency and to separate the photodiode signal into a DC power component and an AC

signal component at the at least one controlled frequency. In some cases, the amplitude of the modulated AC component of the laser diode power and of the photodiode power is less than 10% of the corresponding DC components. In some embodiments, the AC signal component is modulated at an audio frequency and the module is coupled to a headphone or to an audio speaker. In some embodiments, the AC signal component at the at least one controlled frequency is detected using the same photodiode that also converts the DC power component into electrical power. In some embodiments, the AC signal component at the at least one controlled frequency is detected using a separate, signal photodetector device. In some embodiments, the separate, signal photodetector device is positioned between an end of the optical fiber and the one photodiode. In some embodiments, the separate, signal photodetector device is positioned proximate to an optical coupling member, the optical coupling member being positioned between an end of the optical fiber and the one photodiode. In some embodiments, the power-over-fiber system further comprises an internal reflector within the optical coupling member, the internal reflector comprising at least one of a metal, a dielectric, and a void and has a maximum dimension less than about 1 millimeter.

In some embodiments of the power-over-fiber module or power-over-fiber system, the optical fiber has a branched structure. In some embodiments of the power-over-fiber module or power-over-fiber system, the at least one laser diode comprises at least two laser diodes, the at least one photodiode comprises at least two photodiodes, and is the module configured to enable signal communication in at least two different directions. In some embodiments, at least one photodiode is configured for both input and output optical power. In some embodiments of the power-over-fiber module, at least one non-rigid or non-contact optical coupling is used to accommodate rotation of the photodiode relative to the laser diode. In some embodiments, the power-over-fiber system further includes a lighting system that comprises at least one of a phosphor, a heat sink, a reflective or transmissive optic for shaping the far-field distribution of light, a sensor, and a control system. The lighting system may comprise a luminaire.

Embodiments of the disclosure may further provide an optical assembly, comprising a first die comprising one or more absorber layers disposed between an first non-absorber layer and a second non-absorber layer, wherein each of the one or more absorber layers and the first and second non-absorber layers comprising $Al_xIn_yGa_{1-x-y}N$, where $0 \leq x$, y, $x+y \leq 1$ and having a dislocation density below about 10^{10} cm^{-2}, an optical cavity region having an optical window, and a fixture that is configured to position a first end of an optical fiber a first distance from a surface of the optical window of the first die. The one or more absorber layers each have a thickness, measured in a first direction, and an absorber layer surface that is parallel to a first plane and oriented normal to the first direction. The optical cavity region comprising a device cavity region, the device cavity region comprising the one or more absorber layers, the first non-absorber layer, the second non-absorber layer, and at least two opposing reflective members that are configured to cause internal reflection of electromagnetic radiation entering through the optical window to pass through the device cavity region at least two or more times.

Embodiments of the disclosure may further provide an optical assembly, comprising a first die comprising one or more absorber layers disposed between an first non-absorber layer and a second non-absorber layer, wherein each of the one or more absorber layers and the first and second non-absorber layers comprising $Al_xIn_yGa_{1-x-y}N$, where $0 \leq x$, y, $x+y \leq 1$ and having a dislocation density below about 10^{10} cm^{-2}, and having a device cavity region having an optical window. The optical assembly will further include an optical element that is configured to receive optical radiation from an optical fiber and transmit the received optical radiation to at least a portion of the optical window. The one or more absorber layers each have a thickness, measured in a first direction, and an absorber layer surface that is parallel to a first plane and oriented normal to the first direction. The device cavity region comprising at least two opposing reflective members that are configured to cause internal reflection of electromagnetic radiation entering through the optical window to pass through the one or more absorber layers at least two or more times.

BRIEF DESCRIPTION OF THE DRAWINGS

So that the manner in which the above recited features of the present disclosure can be understood in detail, a more particular description of the disclosure, briefly summarized above, may be had by reference to embodiments, some of which are illustrated in the appended drawings. It is to be noted, however, that the appended drawings illustrate only exemplary embodiments and are therefore not to be considered limiting of its scope, and may admit to other equally effective embodiments.

FIG. **1** is a simplified diagram illustrating a nitride-based power photodiode structure that has been prepared according to an embodiment of the present disclosure.

FIG. **2** is a simplified diagram illustrating an alternative nitride-based power photodiode die that has been prepared according to an embodiment of the present disclosure.

FIG. **3** is a simplified diagram illustrating another alternative nitride-based power photodiode structure that has been prepared according to an embodiment of the present disclosure.

FIG. **4** is a simplified diagram illustrating the definition of the fill factor for a photodiode according to an embodiment of the present disclosure.

FIG. **5** is a simplified diagram illustrating the illuminated current-voltage behavior and fill factor of a photodiode according to a first comparative embodiment of the present disclosure.

FIG. **6** is a simplified diagram illustrating the illuminated current-voltage behavior and fill factor of a photodiode according to a second comparative embodiment of the present disclosure.

FIG. **7** is a simplified diagram showing a schematic illustration of semiconductor layers within a photodiode structure according to an embodiment of the current disclosure.

FIGS. **8**A, **9**A, and **10**A are simplified diagrams showing photocurrent as a function of applied voltage for a photodiode structure according to embodiments of the current disclosure.

FIGS. **8**B, **9**B, and **10**B are simplified diagrams showing local band structure as a function of position within a photodiode structure according to embodiments of the current disclosure.

FIG. **11** is a simplified diagram showing photocurrent as a function of applied voltage for an illuminated photodiode according to an embodiment of the current disclosure.

FIG. **12** is a simplified diagram showing photocurrent as a function of applied voltage for an illuminated packaged photodiode according to an embodiment of the current disclosure.

FIGS. **13**A and **13**D are simplified diagrams illustrating another alternative nitride-based power photodiode structure and photodiode die, respectively, that have been prepared according to an embodiment of the present disclosure.

FIGS. **13**B and **13**C are simplified diagrams illustrating methods to remove a substrate from a nitride-based power photodiode structure according to embodiments of the present disclosure.

FIGS. **14**A, **14**B, and **14**C are simplified diagrams illustrating alternate photodiode structures and a photodiode die, respectively, that have been prepared according to an embodiment of the present disclosure.

FIG. **15** includes a table of the illuminated I-V performance characteristics of InGaN/GaN photodiode structures according to one or more embodiments of the present disclosure.

FIGS. **16**A, **16**B, and **16**C are simplified diagrams illustrating alternate photodiode die that have been prepared according to an embodiment of the present disclosure.

FIG. **17**A is a simplified diagram illustrating an alternate photodiode die that has been prepared according to an embodiment of the present disclosure.

FIG. **17**B is a simplified diagram illustrating an alternate photodiode die that has been prepared according to an embodiment of the present disclosure.

FIGS. **18**A and **18**B are simplified diagrams showing side views of a photodiode die according to an embodiment of the present disclosure.

FIGS. **18**C and **18**D are simplified diagrams showing cross sections of a photodiode die according to an embodiment of the present disclosure.

FIG. **18**E is a simplified diagram showing a plan view of a photodiode die according to an embodiment of the present disclosure.

FIGS. **19**A, **19**B, **19**C, **19**D, and **19**E are simplified diagrams illustrating the optical path into and within a photodiode die according to an embodiment of the present disclosure.

FIGS. **20**A and **20**B are simplified diagrams showing side views of a photodiode die according to an alternative embodiment of the present disclosure.

FIGS. **20**C and **20**D are simplified diagrams showing cross sections of a photodiode die according to an alternative embodiment of the present disclosure.

FIG. **20**E is a simplified diagram showing a plan view of a photodiode die according to an alternative embodiment of the present disclosure.

FIGS. **21**A and **21**B are simplified diagrams illustrating the optical path into and within a photodiode die according to an alternative embodiment of the present disclosure.

FIGS. **22**A and **22**B are simplified diagrams showing side views of a photodiode die according to another alternative embodiment of the present disclosure.

FIGS. **22**C and **22**D are simplified diagrams showing cross sections of a photodiode die according to another alternative embodiment of the present disclosure.

FIG. **22**E is a simplified diagram showing a plan view of a photodiode die according to another alternative embodiment of the present disclosure.

FIG. **23**A is a simplified diagram showing a cross section of a photodiode die according to yet another alternative embodiment of the present disclosure.

FIG. **23**B is a simplified diagram showing a cross section of an array of photodiode dies according to yet another alternative embodiment of the present disclosure.

FIGS. **24**A, **24**B, and **24**C are simplified diagrams illustrating configurations of a power-over-fiber module according to several embodiments of the present disclosure.

FIGS. **25**A, **25**B, **25**C, and **25**D are simplified diagrams illustrating configurations of a power-over-fiber module incorporating both power and a modulated signal according to several embodiments of the present disclosure.

FIG. **26** is a simplified diagram showing detailed-balance model efficiency calculations as a function of semiconductor bandgap at temperatures of 300, 400, 500, and 600 degrees Kelvin.

FIGS. **27**A and **27**B are simplified diagrams showing cross sections of a photodiode die according to yet another alternative embodiment of the present disclosure.

FIG. **28** is a simplified diagram of a power-over-fiber module coupled to a lighting system according to an embodiment of the present disclosure.

FIGS. **29**A and **29**B are simplified diagrams showing an optical absorption model for a packaged photodiode according to an embodiment of the present disclosure.

FIG. **30** is a simplified diagram showing a patterned substrate according to an embodiment of the present disclosure.

FIGS. **31**A and **31**B are simplified diagrams showing side and side-cross-sectional views of a packaged photodiode coupled to an optical fiber according to an embodiment of the present disclosure.

FIGS. **31**C and **31**D are simplified diagrams showing top and top-cross-sectional views of a packaged photodiode coupled to an optical fiber according to an embodiment of the present disclosure.

FIG. **31**E is a simplified diagram showing a bottom view of a packaged photodiode coupled to an optical fiber according to an embodiment of the present disclosure.

FIG. **32** is a simplified diagram showing a side-cross-sectional view of a packaged photodiode coupled to an optical fiber according to an embodiment of the present disclosure.

FIGS. **33**A-**33**I are simplified diagrams showing side cross sectional views of a packaged photodiode coupled to an optical fiber according to alternate embodiments of the present disclosure.

FIGS. **34**A-**34**I are simplified diagrams showing side cross sectional views of a packaged photodiode coupled to an optical fiber according to alternate embodiments of the present disclosure.

FIGS. **35**A-**35**F are simplified diagrams showing side cross sectional views of a packaged photodiode and a separate photodetector coupled to an optical fiber according to embodiments of the present disclosure.

FIG. **36** is an isometric view of a fixture used to support a photodiode die and optical fiber according to an embodiment of the present disclosure.

To facilitate understanding, identical reference numerals have been used, where possible, to designate identical elements that are common to the figures. It is contemplated that elements and features of one embodiment may be beneficially incorporated in other embodiments without further recitation.

DETAILED DESCRIPTION

According to the present disclosure, techniques related to manufacturing and applications of power photodiode struc-

tures and devices based on group-III metal nitride and gallium-based substrates are provided. More specifically, embodiments of the disclosure include techniques for fabricating photodiode devices comprising one or more of GaN, AlN, InN, InGaN, AlGaN, and AlInGaN, structures and devices. Such structures or devices can be used for a variety of applications including optoelectronic devices, photodiodes, power-over-fiber receivers, and others.

As noted previously, lasers and photodiodes are better developed in the GaAs material system. One of the key differences in materials properties between the arsenide and nitride systems is that the bandgap may be varied readily with minimal impact on lattice constant in the case of the arsenides, e.g., via AlGaAs, but not in the case of the nitrides. Traditional photodiode package architectures incorporating nitride absorber layers may require an absorber layer thickness on the order of several hundred nanometers to absorb the large majority of the incident light. Assuming an absorber layer absorption coefficient of 1×10^5 cm^{-1}, the light absorbed in a single pass is approximately 39%, 63%, 87%, 95%, and 98% for thicknesses of 50, 100, 200, 300, and 400 nm, respectively. In the case of the nitrides, such a thickness of InGaN, with sufficient indium (In) to efficiently absorb blue or violet light, may be too strained to avoid relaxation by dislocation generation or by cracking. The inventors have discovered an approach to circumvent this problem, involving delivering electromagnetic radiation along long optical paths through an absorber layer to achieve near-100% optical absorption even when a relatively thin absorber layer containing power photodiode structure is provided. Additional benefits of the new approach include excellent heat dissipation, zero or very low grid shadow losses, and long effective minority carrier lifetimes. Here, the effective minority carrier lifetime includes photon recycling, defined as reabsorption of photons emitted by the absorber layer. The term "light" and "optical radiation" are often used herein interchangeably and are both intended to generally describe electromagnetic radiation at one or more wavelengths unless otherwise noted in the context of the discussion.

In order to take proper advantage of geometries involving long optical paths through the absorber layer, novel optical coupling geometries, fixtures, and methods are disclosed herein. Additional benefits of the novel optical coupling methods include improved ease and precision of alignment and improved efficiency, robustness, durability, and lifetime.

In addition, photodiode structures, such as a stack of epitaxially-grown layers, have both similarities and differences to structures for light-emitting diodes (LEDs) and laser diodes (LDs). For example, both LED and LD structures commonly include electron blocking layers within a p-type layer, to minimize electron loss from the active region and promote radiative carrier recombination within the active region. However, such structures may increase the series resistance for photodiode structures and may be counter-productive. Similarly, LD structures commonly include one or more of cladding layers, optical confinement layers, and separate confinement heterostructure (SCH) layers that may detract from the performance of the photodiodes, as their design is driven by different considerations than the present application.

For purposes of designing effective epitaxial structures for a photodiode, both in general and for the specific case where the active layer includes or consists of InGaN or Ga(In)N, high levels of active layer optical absorption and of the collection efficiency for minority carriers will increase the detection sensitivity and the operating current, I_{mp}. Low concentrations of defects, both point defects and extended defects, such as dislocations and stacking faults, will reduce Shockley-Read-Hall nonradiative recombination and thereby result in higher operating voltages V_{mp}. Low concentrations of defects may also enable improved photodiode performance under high light conditions (i.e., high optical power (Watts) conditions). The efficiency η of a photodiode may be written as $\eta=V_{mp}\times I_{mp}/P_{in}$, where P_{in} is the input radiative power.

Another way of expressing the efficiency η of a photodiode is $\eta=V_{oc}\times I_{sc}\times FF/P_{in}$, as illustrated schematically in FIG. **4**, where V_{oc} is the open-circuit voltage, I_{sc} is the short-circuit current, and FF is the fill factor. Still another way of expressing the efficiency of a semiconductor photodiode is $\eta=(eV_{oc}/E_g)\times OA\times IQE\times FF\times E_g/(hv)$, where e is the charge of an electron, E_g is the band gap of the semiconductor, OA is the optical absorption (or fraction of incident photons absorbed in the absorber layer), IQE is the internal quantum efficiency (fraction of absorbed photons producing an electron-hole pair that is collected), h is Planck's constant, and v is the photon frequency. In preferred embodiments, the FF is greater than 50%, greater than 60%, greater than 70%, greater than 80%, or greater than 90%.

Relative to prior art photodiodes designed for much lower photon fluxes, mostly fabricated using GaN-on-sapphire structures, the inventive photodiodes, including GaN-on-GaN structures, feature high conversion efficiency due to careful optimization of the composition and doping of the semiconductor layers and to large area p-side and n-side electrical contacts with high reflectivity for use with a many-reflection excitation architecture and with very low contact resistance to minimize lateral ohmic losses at high current densities. In certain embodiments, the current photodiode structures are designed for applications where illumination is provided by a single laser or multiple lasers and enters the structure though an edge or through an aperture, as schematically illustrated in FIG. **2**. In certain embodiments, the laser light is coupled into an edge of the photodiode structure or into an aperture formed in the photodiode structure using optical fibers, lenses, or waveguides. In certain embodiments, the inventive photodiode structures further incorporate a much lower dislocation density, with longer minority carrier diffusion lengths for higher current plus longer minority carrier lifetimes for higher open circuit voltage and fill factor. In addition, the inventive devices may include electrically conductive substrates, enabling vertical transport in vertically oriented power devices for a simpler design and reduced series resistance, and transparent substrates with a very similar refractive index of that of the absorber layers, minimizing optical losses. In certain embodiments, the substrate has a nonpolar or semipolar crystallographic orientation, enabling tuning of polarization fields for optimum device performance.

FIGS. **1** and **3** depict simplified diagrams of group III-metal nitride based photodiode structures **1000**, and FIG. **2** depicts a simplified diagram of a group III-metal nitride based photodiode die **1002**. Referring to FIG. **1**, a substrate **101** is provided. In certain embodiments, substrate **101** comprises single-crystalline group-III metal nitride, gallium-containing nitride, or gallium nitride. Substrate **101** may be grown by HVPE, ammonothermally, or by a flux method. In certain embodiments, substrate **101** is a template, where a single-crystalline group-III metal nitride layer **1104** has been deposited or grown on a template substrate **1101** that consists of or includes a material such as sapphire (Al_2O_3), silicon carbide (SiC), or silicon. In alternative embodiments, template substrate **1101** may consist of or

include gallium arsenide, germanium, a silicon-germanium alloy, $MgAl_2O_4$ spinel, ZnO, ZrB_2, BP, InP, AlON, $ScAlMgO_4$, $YFeZnO_4$, MgO, Fe_2NiO_4, $LiGa_5O_8$, Na_2MoO_4, Na_2WO_4, In_2CdO_4, lithium aluminate ($LiAlO_2$), $LiGaO_2$, $Ca_8La_2(PO_4)_6O_2$, gallium nitride (GaN), aluminum nitride (AlN), or the like. One or both large area surfaces of substrate **101** may be polished and/or chemical-mechanically polished. A large-area surface **102** of substrate **101** may have a crystallographic orientation within 5 degrees, within 2 degrees, within 1 degree, or within 0.5 degree of (0001) +c-plane, (000-1) −c-plane, {10-10} m-plane, {11-2±2}, {60-6±1}, {50-5±1}, {40-4±1}, {30-3±1}, {50-5±2}, {70-7±3}, {20-2±1}, {30-3±2}, {40-4±3}, {50-5±4}, {10-1±1}, {1 0 −1±2}, {1 0 −1±3}, {2 1 −3 ±1}, or {3 0 −3 ±4}. It will be understood that plane {3 0 −3 ±4} means the {3 0 −3 4} plane and the {3 0 −3 −4} plane. Large-area surface **102** may have an (h k i l) semipolar orientation, where i=−(h+k) and l and at least one of h and k are nonzero. In certain embodiments, template substrate **1101** consists of or includes sapphire and has a large-area surface **102** that has a crystallographic orientation within 5 degrees, within 2 degrees, within 1 degree, or within 0.5 degree of (0001), (10-10), (10-12), (22-43), or (11-23). In certain embodiments, template substrate **1101** consists of or includes sapphire and has a large-area surface **102** that is misoriented from (0001) by an angle between about 0.5 degree and about 8 degrees, or between about 2 degrees and about 4 degrees, toward the {11-20} a-plane, toward the {10-10} m-plane, or toward a-plane intermediate between a-plane and m-plane. In certain embodiments, template substrate **1101** has a cubic structure and a large-area surface **102** that has a crystallographic orientation within 5 degrees, within 2 degrees, within 1 degree, or within 0.5 degree of {111}, {100}, {110}, or {114}. Other orientations may also be chosen.

In certain embodiments, surface **1102** of template substrate **1101** is patterned, to facilitate light transmission between template substrate **1101**, and a stack of n-type first non-absorber layer **105**, absorber layer **107**, optional second non-absorber layer **109**, and p-type layer or p-type non-absorber layer **111**. Referring to FIG. **30**, surface **1102** may include a patterned array of features **1106**. Features **1106** may include or consist of cones, domes, hemispheres, triangular pyramids, square pyramids, hexagonal pyramids, or the like. Other shapes are also possible. Features **1106** may be characterized by a pitch **1108**, a height **1110**, and a width **1112**. Features **1106** may be arranged in a square array, a rectangular array, or a hexagonal array across surface **1102**. Other patterns of features **1106** are also possible. Pitch **1108** may be between about 0.2 micrometer and about 10 micrometers, or between about 1 micrometer and about 5 micrometers. Height **1110** may be between about 0.1 micrometer and about 10 micrometers, or between about 1 micrometer and about 3 micrometers. Width **1112** may be between about 0.1 micrometer and about 10 micrometers, or between about 1 micrometer and about 5 micrometers. In certain embodiments, template substrate **1101** consists of or includes sapphire, and has a surface **1102** that has a crystallographic orientation within about 5 degrees of (0001). The template substrate **1101** may be referred to as a patterned sapphire substrate, as is known in the art, in certain embodiments.

Large-area surface **102** may have a maximum dimension between about 0.2 millimeter and about 600 millimeters and a minimum dimension between about 0.2 millimeter and about 600 millimeters and substrate **101** may have a thickness between about 10 micrometers and about 10 millimeters, or between about 100 micrometers and about 2 millimeters. In certain embodiments, substrate **101** is substantially circular, with one or more orientation flats. In alternative embodiments, substrate **101** is substantially rectangular. In certain embodiments, large-area surface **102** has a maximum dimension of about 50 mm, 100 mm, 125 mm, 150 mm, 200 mm, 250 mm, or 300 mm. The variation in the crystallographic orientation of the large-area surface **102** may be less than about 5 degrees, less than about 2 degrees, less than about 1 degree, less than about 0.5 degrees, less than about 0.2 degrees, less than about 0.1 degrees, or less than about 0.05 degrees relative to the average orientation at the large area surface.

Large-area surface **102** of substrate **101** may have a threading dislocation density less than about 10^{10} cm^{-2}, less than about 10^9 cm^{-2}, less than about 10^8 cm^{-2}, less than about 10^7 cm^{-2}, less than about 10^6 cm^{-2}, less than about 10^5 cm^{-2}, less than about 10^4 cm^{-2}, less than about 10^3 cm^{-2}, or less than about 10^2 cm^{-2}. Large-area surface **102** of substrate **101** may have a stacking-fault concentration below about 10^4 cm^{-1}, below about 10^3 cm^{-1}, below about 10^2 cm^{-1}, below about 10 cm^{-1} or below about 1 cm^{-1}. Large-area surface **102** of substrate **101** may have a symmetric x-ray rocking curve full width at half maximum (FWHM) less than about 500 arcsec, less than about 300 arcsec, less than about 200 arcsec, less than about 100 arcsec, less than about 50 arcsec, less than about 35 arcsec, less than about 25 arcsec, or less than about 15 arcsec. Large-area surface **102** of substrate **101** may have a crystallographic radius of curvature greater than 0.1 meter, greater than 1 meter, greater than 10 meters, greater than 100 meters, or greater than 1000 meters, in at least one or at least two independent or orthogonal directions. In a specific embodiment, large-area surface **102** of substrate **101** has a threading dislocation density less than about 10^5 cm^{-2}, a stacking-fault concentration below about 10 cm^{-1}, and a symmetric x-ray rocking curve full width at half maximum (FWHM) less than about 50 arcsec. The reduced dislocation density in the substrate **101**, relative to most prior art photodiodes, is expected to result in a reduced dislocation density in the semiconductor layers of the photodiode and to a higher open-circuit voltage V_{oc} and a higher efficiency at high current densities.

In some embodiments, the substrate **101** may include regions having a relatively high concentration of threading dislocations separated by regions having a relatively low concentration of threading dislocations. The concentration of threading dislocations in the relatively high concentration regions may be greater than about 10^5 cm^{-2}, greater than about 10^6 cm^{-2}, greater than about 10^7 cm^{-2}, or greater than about 10^8 cm^{-2}. The concentration of threading dislocations in the relatively low concentration regions may be less than about 10^6 cm^{-2}, less than about 10^5 cm^{-2}, or less than about 10^4 cm^{-2}. Substrate **101** may also or separately include regions having a relatively high electrical conductivity separated by regions having a relatively low electrical conductivity. Substrate **101** may have a thickness between about 10 microns and about 100 millimeters, or between about 0.1 millimeter and about 10 millimeters. Substrate **101** may have a dimension, including a diameter, of at least about 5 millimeters, at least about 10 millimeters, at least about 25 millimeters, at least about 50 millimeters, at least about 75 millimeters, at least about 100 millimeters, at least about 150 millimeters, at least about 200 millimeters, at least about 300 millimeters, at least about 400 millimeters, or at least about 600 millimeters. In a specific embodiment, substrate **101** has a thickness between about 250 micrometers and about 600 micrometers, a maximum lateral dimension or diameter between about 15 millimeters and about 160 millimeters,

and includes regions where the concentration of threading dislocations is less than about 10^4 cm^{-2}.

Substrate **101** may include a release layer **1103** for facile separation of single-crystalline group-III metal nitride layer **1104** from the balance of the substrate, such as a template substrate **1101**. In some embodiments, the release layer **1103** has an optical absorption coefficient greater than 1000 cm^{-1} at least one wavelength where the template substrate is substantially transparent, with an optical absorption coefficient less than 50 cm^{-1}, thereby enabling substrate removal by a laser lift-off technique, for example, after fabrication of at least one device structure. In certain embodiments, release layer **1103** includes or consists of GaN that is heavily doped with Co, increasing its optical absorption coefficient to greater than 5000 cm^{-1} over the entire visible spectrum. In one specific embodiment, Co-doped release layer **1103** having a thickness between 0.5 micrometer and 50 micrometers is formed ammonothermally on template substrate **1101**, with CoF_2 as an additive to the mineralizer and template substrate **1101** consisting of a high quality GaN seed crystal. In another specific embodiment, Co-doped release layer **1103** is formed by MOCVD on a template substrate **1101** (e.g., high-quality GaN substrate), using at least one of cyclopentadienylcobalt dicarbonyl ($(C_5H_5)Co(CO)_2$), cobalt (II) acetylacetonate ($Co(CH_3C(O)CHC(O)CH_3)_2$), cobalt tricarbonyl nitrosyl ($Co(CO)_3NO$), dicobalt octacarbonyl ($Co_2(CO)_8$), and tetracobalt dodecacarbonyl ($Co_4(CO)_{12}$) as a dopant precursor. In still another specific embodiment, Co-doped release layer **1103** is formed by hydride vapor phase epitaxy (HVPE) on a template substrate **1101**, such as a high quality GaN substrate, using at least one of cyclopentadienylcobalt dicarbonyl ($(C_5H_5)Co(CO)_2$), cobalt (II) acetylacetonate ($Co(CH_3C(O)CHC(O)CH_3)_2$), cobalt tricarbonyl nitrosyl ($Co(CO)_3NO$), dicobalt octacarbonyl ($Co_2(CO)_8$), and tetracobalt dodecacarbonyl ($Co_4(CO)_{12}$) as a dopant precursor. Further details are described in U.S. Pat. No. 8,148,801, which is hereby incorporated by reference in its entirety. In some embodiments, the release layer **1103** includes or consists of InGaN, thereby enabling substrate removal by a photoelectrochemical etching technique, for example, after fabrication of at least one device structure. In some embodiments, the InGaN-containing release layer has a thickness between about 2 nanometers and about 100 nanometers or between about 5 nanometers and about 50 nanometers. In some embodiments, the release layer has a bandgap less than that of the absorber layer **107** described below. In a specific embodiment, release layer **1103** includes or consists of a strained-layer superlattice of InGaN and GaN or AlGaN. In some embodiments, the percent (%) indium (In) in the strained-layer superlattice is greater than that in the absorber layer **107**, and is grown by MOCVD on a template substrate **1101**, such as a high quality GaN substrate. Further details of an InGaN release layer are described in more detail in U.S. Pat. No. 8,866,149 and in U.S. Patent Application publication no. US2019/0088495, each of which are hereby incorporated by reference in their entirety.

In certain embodiments, substrate **101** consists of or includes a single-crystalline group-III metal nitride layer **1104** bonded to or formed on a surface of a template substrate **1101**. The single-crystalline group-III metal nitride layer **1104** may include gallium. The single-crystalline group III metal nitride layer **1104** may be deposited by HVPE, by metalorganic chemical vapor deposition (MOCVD), molecular beam epitaxy (MBE), or the like. The single-crystalline group-III metal nitride layer **1104** may have a thickness between about 1 micrometer and about 100 micrometers, between about 2 micrometers and about 25 micrometers, or between about 3 micrometers and about 15 micrometers. In certain embodiments, the single-crystalline group-III metal nitride layer **1104** has a wurtzite crystal structure and a crystallographic orientation within 5 degrees, within 2 degrees, within 1 degree, or within 0.5 degree of (0001) +c-plane, (000-1) −c-plane, {10-10} m-plane, {11-2±2}, {60-6±1}, {50-5±1}, {40-4±1}, {30-3±1}, {50-5±2}, {70-7±3}, {20-2±1}, {30-3±2}, {40-4±3}, {50-5±4}, {10-1±1}, {1 0 −1 ±2}, {1 0 −1 ±3}, {2 1 −3 ±1}, or {3 0 −3 ±4}. In certain embodiments, a nucleation layer (not shown) is present at the interface between the template substrate **1101** and the single-crystalline group-III metal nitride layer **1104**. In certain embodiments, the nucleation layer consists of or includes one or more of aluminum nitride, gallium nitride, and zinc oxide. In certain embodiments, the nucleation layer is deposited on the template substrate **1101** by at least one of low-temperature MOCVD, sputtering, and electron-beam evaporation. In certain embodiments, the nucleation layer has a thickness between about 1 nanometer and about 200 nanometers or between about 10 nanometers and about 50 nanometers. In certain embodiments, the substrate further includes one or more strain-management layers, for example, an AlGaN layer or a strained-layer superlattice.

In certain embodiments, large-area surface **102** has atomic impurity concentrations of at least one of oxygen (O), and hydrogen (H) above about 1×10^{16} cm^{-3}, above about 1×10^{17} cm^{-3}, or above about 1×10^{18} cm^{-3}. In certain embodiments, a ratio of the atomic impurity concentration of H to the atomic impurity concentration of O is between about 0.3 and about 2, between about 1.1 and about 1000, or between about 5 and about 100. In certain embodiments, large-area surface **102** has impurity concentrations of at least one of lithium (Li), sodium (Na), potassium (K), fluorine (F), chlorine (CI), bromine (Br), or iodine (I) above about 1×10^{15} cm^{-3}, above about 1×10^{16} cm^{-3}, or above about 1×10^{17} cm^{-3}, or above about 1×10^{18} cm^{-3}. In certain embodiments, large-area surface **102** has impurity concentrations of O, H, carbon (C), Na, and K between about 1×10^{16} cm^{-3} and about 1×10^{19} cm^{-3}, between about 1×10^{16} cm^{-3} and about 2×10^{19} cm^{-3}, below 1×10^{17} cm^{-3}, below 1×10^{16} cm^{-3}, and below 1×10^{16} cm^{-3}, respectively, as quantified by calibrated secondary ion mass spectrometry (SIMS). In another embodiment, large-area surface **102** has impurity concentrations of O, H, C, and at least one of Na and K between about 1×10^{16} cm^{-3} and 1×10^{19} cm^{-3}, between about 1×10^{16} cm^{-3} and about 2×10^{19} cm^{-3}, below 1×10^{17} cm^{-3}, and between about 3×10^{15} cm^{-3} and about 1×10^{18} cm^{-3}, respectively, as quantified by calibrated secondary ion mass spectrometry (SIMS). In still another embodiment, large-area surface **102** has impurity concentrations of O, H, C, and at least one of F and Cl between about 1×10^{16} cm^{-3} and about 1×10^{19} cm^{-3}, between about 1×10^{16} cm^{-3} and about 2×10^{19} cm^{-3}, below 1×10^{17} cm^{-3}, and between about 1×10^{15} cm^{-3} and about 1×10^{19} cm^{-3}, respectively, as quantified by calibrated secondary ion mass spectrometry (SIMS). In some embodiments, large-area surface **102** has impurity concentrations of H between about 5×10^{17} cm^{-3} and 1×10^{19} cm^{-3}, as quantified by calibrated secondary ion mass spectrometry (SIMS). In a specific embodiment, substrate **101** has an infrared absorption peak at about 3175 cm^{-1}, with an absorbance per unit thickness of greater than about 0.01 cm^{-1}.

Substrate **101** may be characterized by a wurtzite structure substantially free from any cubic entities or other crystal structures, the other structures being less than about 0.1% A in volume in reference to the substantially wurtzite structure.

Substrate **101** may be characterized by a total thickness variation (TTV) of less than about 25 micrometers, less than about 10 micrometers, less than about 5 micrometers, less than about 2 micrometers, or less than about 1 micrometer, and by a macroscopic bow that is less than about 200 micrometers, less than about 100 micrometers, less than about 50 micrometers, less than about 25 micrometers, or less than about 10 micrometers. Substrate **101** may have a concentration of macro defects on the large-area surface **102**, with a diameter or characteristic dimension greater than about 100 micrometers, of less than about 2 cm^{-2}, less than about 1 cm^{-2}, less than about 0.5 cm^{-2}, less than about 0.25 cm^{-2}, or less than about 0.1 cm^{-2}. The variation in miscut angle across a large-area surface **102** of substrate **101** may be less than about 5 degrees, less than about 2 degrees, less than about 1 degree, less than about 0.5 degree, less than about 0.2 degree, less than about 0.1 degree, less than about 0.05 degree, or less than about 0.025 degree in each of two orthogonal crystallographic directions. The root-mean-square surface roughness of large-area surface **102**, as measured over an area of at least 10 μm×10 μm, may be less than about 0.5 nanometers, less than about 0.2 nanometers, less than about 0.15 nanometers, less than about 0.1 nanometers, or less than about 0.05 nanometers. Substrate **101** may be characterized by n-type electrical conductivity, with a carrier concentration between about 1×10^{17} cm^{-3} and about 3×10^{19} cm^{-3} and a carrier mobility greater than about 100 cm^2N-s. In certain embodiments, substrate **101** is highly transparent, with an optical absorption coefficient at a wavelength of 405 nanometers, or of 450 nanometers, that is less than about 10 cm^{-1}, less than about 5 cm^{-1}, less than about 2 cm^{-1}, less than about 1 cm^{-1}, less than about 0.5 cm^{-1}. less than about 0.2 cm^{-1}, or less than about 0.1 cm^{-1}.

In certain embodiments, one or more n-type first non-absorber layers **105**, comprising $Al_uIn_vGa_{1-u-v}N$ layers, where $0\leq u, v, u+v\leq 1$, is deposited on the substrate. In certain embodiments, n-type first non-absorber layers **105** are deposited immediately following deposition of single-crystalline group-III metal nitride layer **1104**, that is, without interrupting the growth process or removing substrate **101** or template substrate **1104** from the deposition reactor. In certain embodiments, one or more additional layers are deposited to help manage stress in the overall structure. The carrier concentration in n-type first non-absorber layer **105** may lie in the range between about 10^{16} cm^{-3} and 10^{20} cm^{-3}. In certain embodiments, silicon, germanium, or oxygen is the n-type dopant in n-type first non-absorber layer **105**. In certain embodiments, germanium is selected as the n-type dopant. In certain embodiments, the n-type carrier concentration in n-type first non-absorber layer **105** lies in the range between 5×10^{17} cm^{-3} and 10^{20} cm^{-3} or between 2×10^{18} cm^{-3} and 6×10^{19} cm^{-3}. A high doping level may be particularly desirable if substrate **101** has a (0001) +c-plane orientation, as piezoelectric fields may more effectively be screened for efficient carrier collection. A high doping level may also be desirable if template substrate **1101** is electrically insulating or highly resistive. Abrupt or graded composition or doping profiles may be incorporated at interfaces within the n-type first non-absorber layer **105**. The deposition may be performed using metalorganic chemical vapor deposition (MOCVD) or molecular beam epitaxy (MBE). For example, the substrate may be placed on a susceptor in an MOCVD reactor. After closing, evacuating, and back-filling the reactor, the susceptor may be heated to a temperature between about 800 and about 1350 degrees Celsius in the presence of a nitrogen-containing gas. In one specific embodiment, the susceptor is heated to approximately 1185 degrees Celsius under flowing ammonia. A flow of a gallium-containing metalorganic precursor, such as trimethylgallium (TMG), triethylgallium (TEG), or triisopropylgallium may be initiated, in a carrier gas, at a total rate between approximately 1 and 50 standard cubic centimeters per minute (sccm). The carrier gas may comprise hydrogen, helium, nitrogen, or argon. The ratio of the flow rate of the group V precursor (ammonia) to that of the group III precursor (trimethylgallium, triethylgallium, trimethylindium, trimethylaluminum) during growth is between about 2000 and about 12000. A flow of disilane in a carrier gas, with a total flow rate of between about 0.1 and 10 sccm, may be initiated. In certain embodiments, doping is achieved by adding one or more of SiH_4, Si_2H_6, SiH_2Cl_2, $SiHCl_3$, $SiCl_4$, GeH_4, $GeCl_4$, O_2, and H_2O to the input gases. In certain embodiments, one or more n-type first non-absorber layer **105** and second non-absorber layer **109** is a metamorphic buffer layer and facilitates accommodation of lattice constant differences between layers. In certain embodiments, the doping level in the n-type first non-absorber layer **105** may be non-uniform, with two or more levels of doping and/or graded doping levels. In certain embodiments, the substrate temperature is varied during the deposition of the n-type first non-absorber layer **105**. In certain embodiments, the substrate temperature is held at a high value, for example, between 1100 and 1350 degrees Celsius for a first portion of the n-type first non-absorber layer **105**, then reduced to a lower value, for example, the same temperature as the temperature at which the absorber layer **107** is deposited, for a second portion of the n-type first non-absorber layer **105**, for example, between about 700 and about 950 degrees Celsius. In certain embodiments, the thickness of the second portion of the n-type first non-absorber layer **105** is between about 1 nanometer and about 20 nanometers.

Following deposition of the n-type first non-absorber layer **105** for a predetermined period of time, so as to achieve a predetermined thickness, an absorber layer **107** is deposited. In certain embodiments, the absorber layer **107** is deposited by MOCVD, at a substrate temperature between about 700 and about 950 degrees Celsius. Indium may be added to the absorber layer **107** by using at least one of trimethylindium (TMIn), triethylindium (TEIn), and triisopropylindium as a precursor in MOCVD. The deposition rate for the absorber layer **107** may be chosen to lie between about 0.005 and about 1 nanometer per second, or between about 0.01 and about 0.5 nanometer per second, or between about 0.02 and about 0.2 nanometer per second. In certain embodiments, the absorber layer **107** is unintentionally doped. In certain embodiments, the absorber layer **107** is n-type doped, using oxygen, silicon, or germanium, as a dopant, with a dopant concentration between about 5×10^{15} cm^{-3} and about 5×10^{19} cm^{-3}, or between about 5×10^{16} cm^{-3} and about 5×10^{18} cm^{-3}. In certain embodiments, the absorber layer **107** is p-type doped, using Mg as a dopant, with a dopant concentration between about 5×10^{15} cm^{-3} and about 5×10^{19} cm^{-3}, or between about 5×10^{16} cm^{-3} and about 5×10^{18} cm^{-3}. In some embodiments, the absorber layer **107** has a bandgap wavelength that is between about 400 nanometers and about 550 nanometers, such as a bandgap wavelength that is between about 440 nanometers and about 500 nanometers. The absorber layer **107** may comprise a single quantum well or multiple quantum wells, with 2-50 quantum wells (not shown). In some embodiments, the absorber layer **107** includes between about 10 and about 30 quantum wells. The quantum wells may comprise InGaN well layers and GaN barrier layers. In other embodiments, the quantum

wells may comprise $Al_wIn_xGa_{1-w-x}N$ well layers and $Al_yIn_zGa_{1-y-z}N$ barrier layers, respectively, where 0≤w, x, y, z, w+x, y+z≤1, where w<u, y and/or x>v, z so that the bandgap of the well layer(s) is less than that of the barrier layer(s) and of the n-type first non-absorber layer **105** and second non-absorber layer **109**. The well layers and barrier layers may each have a thickness between about 0.5 nanometer and about 20 nanometers. In certain embodiments, the barrier layers have a thickness between about 1 nanometer and about 3 nanometers, between about 3 nanometers and about 5 nanometers, between about 5 nanometers and 10 nanometers, or between about 10 nanometers and 15 nanometers. In certain embodiments, the well layers have a thickness between 0.5 nanometer and about 1.5 nanometer, between about 1.5 nanometer and about 2.5 nanometers, between about 2.5 nanometers and about 3.5 nanometers, between about 3.5 nanometers and about 4.5 nanometers, or between about 4.5 nanometers and about 10 nanometers. In another embodiment, the absorber layer **107** includes or consists of a double heterostructure, with an InGaN or $Al_wIn_xGa_{1-w-x}N$ layer about 20 nm to about 500 nm thick surrounded by GaN or $Al_yIn_zGa_{1-y-z}N$ layers, where w<u, y and/or x>v, z. In certain embodiments, the thickness of the double heterostructure is between about 10 nanometers and about 25 nanometers, between about 25 nanometers and about 40 nanometers, between about 40 nanometers and about 60 nanometers, between about 60 nanometers and about 100 nanometers, between about 100 nanometers and about 200 nanometers, or thicker than about 200 nanometers. Abrupt or graded composition or doping profiles may be incorporated at interfaces within the absorber layer **107**. The composition and structure of the active layer are chosen to provide light absorption at a preselected wavelength, for example, at 405 nanometers or at 450 nanometers. In certain embodiments, the wavelength is selected to lie between about 400 nanometers to about 500 nanometers. The absorber layer **107** may be characterized by photoluminescence spectroscopy. In certain embodiments, the composition of the absorber layer **107** is chosen such that the photoluminescence spectrum has a peak that is longer in wavelength than the desired absorption wavelength of the photodiode structure **1000** by between 5 nanometers and 50 nanometers or by between 10 nanometers and 25 nanometers. In certain embodiments, the quality and layer thicknesses within the absorber layer **107** are characterized by x-ray diffraction.

In some embodiments, one or more optional second non-absorber layers **109** is deposited next. Second non-absorber layer **109** may comprise $Al_sIn_tGa_{1-s-t}N$, where 0≤s, t, s+t≤1, with a higher bandgap than the absorber layer **107**, and may be doped p-type or may be unintentionally doped. In one specific embodiment, second non-absorber layer **109** comprises AlGaN. In another embodiment, second non-absorber layer **109** comprises an AlGaN/GaN multi-quantum barrier (MQB), comprising alternating layers of AlGaN and GaN, each with a thickness between about 0.2 nm and about 5 nm. In certain embodiments, one or more second non-absorber layer **109** is a metamorphic buffer layer and facilitates accommodation of lattice constant differences between layers of the photodiode structure **1000**. Abrupt or graded composition or doping profiles may be incorporated at interfaces within the second non-absorber layer **109**. In some embodiments, the optical designs of the second non-absorber layers **109** are tuned to achieve greater than about 70% optical reflection of light transmitted from the substrate through the absorber layers **107**.

Next, a p-type layer, or p-type non-absorber layer, **111**, formed of $Al_qIn_rGa_{1-q-r}N$, where 0≤q, r, q+r≤1, is deposited above the absorber layer **107** and, if present, the second non-absorber layer **109**. The p-type layer **111** may be doped with Mg, to a level between about 10^{16} cm^{-3} and 10^{21} cm^{-3} and may have a thickness between about 5 nanometers and about 1 micrometer, between about 20 nanometers and about 400 nanometers, or between about 100 nanometers and about 250 nanometers. In certain embodiments, the concentration of Mg in the p-type layer **111** closest to the absorber layer **107** is between 10^{18} cm^{-3} and 10^{21} cm^{-3}, between 3×10^{18} cm^{-3} and 3×10^{20} cm^{-3}, or between 10^{19} cm^{-3} and 2×10^{20} cm^{-3}. A high doping level may be particularly desirable if substrate **101** has a (0001) +c-plane orientation, as piezoelectric fields may more effectively screened for efficient carrier collection. The outermost 1-30 nanometers of the p-type layer **111** may be doped more heavily than the rest of the p-type layer **111**, so as to enable an improved electrical contact. In certain embodiments, the substrate temperature is varied during the deposition of the p-type layer **111**. In certain embodiments, the substrate temperature is held at a low value, for example, the same temperature as the temperature at which the absorber layer **107** is deposited, for a first portion of the p-type layer **111**, for example, between about 700 and about 950 degrees Celsius. Then the substrate temperature is raised to a higher level, for example, between about 750 and about 1000 degrees Celsius, for a second portion of the p-type layer **111**. In certain embodiments, the thickness of the first portion of the p-type layer **111** is between about 1 nanometer and about 20 nanometers, or between about 20 nanometers and 40 nanometers.

In a specific embodiment, a tunnel junction and another n-type layer (not shown) are deposited on top of the p-type layer **111**. In certain embodiments, one or more additional non-absorber layers and additional absorber layers are deposited overlying the tunnel junction.

The semiconductor layers, which include the n-type first non-absorber layer **105**, absorber layer **107**, one or more optional second non-absorber layers **109**, p-type layer **111**, and may also include additional absorber layers, one or more n-type cladding layers, and one or more p-type cladding layers, have the same crystallographic orientation, to within about two degrees, within about one degree, or within about 0.5 degree, as the crystallographic orientation of large-area surface **102** of substrate **101**, have a very high crystalline quality, comprise nitrogen, and may have a surface dislocation density below 10^9 cm^{-2}. The semiconductor layers may have a surface dislocation density below 10^{10} cm^{-2}, below 10^9 cm^{-2}, below 10^8 cm^{-2}, below 10^7 cm^{-2}, below 10^6 cm^{-2}, below 10^5 cm^{-2}, below 10^4 cm^{-2}, below 10^3 cm^{-2}, or below 10^2 cm^{-2}. In some embodiments, the semiconductor layers are substantially transparent, with an optical absorption coefficient below 100 cm^{-1}, below 50 cm^{-1} or below 5 cm^{-1} at wavelengths between about 400 nm and about 3077 nm and at wavelengths between about 3333 nm and about 6667 nm.

In a specific embodiment, the semiconductor layers have an orientation within five degrees of m-plane and the FWHM of the 1-100 x-ray rocking curve of the top surface is below 300 arc sec, below 100 arc sec, or below 50 arc sec. In another specific embodiment, the semiconductor layers have an orientation within five degrees of a-plane and the FWHM of the 11-20 x-ray rocking curve of the top surface is below 300 arc sec, below 100 arc sec, or below 50 arc sec. In yet another specific embodiment, the semiconductor layers have an orientation within five degrees of a semipolar orientation selected from {1 −1 0 ±1}, {1 −1 0 ±2}, {1 −1 0 ±3}, {2 0 −2±1}, {3 0−3 ±1}, or {1 1 −2 .+−.2} and the FWHM of the lowest-order semipolar symmetric x-ray

rocking curve of the top surface is below 300 arc sec, below 100 arc sec, or below 50 arc sec. In another specific embodiment, the semiconductor layers have an orientation within five degrees of (0001) c-plane and the FWHM of the 0002 x-ray rocking curve of the top surface is below 300 arc sec, below 100 arc sec, or below 50 arc sec. In still another specific embodiment, the semiconductor layers have an orientation within ten degrees of (000-1) c-plane and the FWHM of the 0002 x-ray rocking curve of the top surface is below 300 arc sec, below 100 arc sec, or below 50 arc sec.

In certain embodiments, for process development purposes, it may be useful to fabricate structures with one or more of the above-described layers missing. For example, the p-type layer **111** and the absorber layer **107** could be omitted for purposes of developing or optimizing a p-side reflective electrical contact **113**, as described below. One or more of the p-side reflective electrical contact **113** and the p-type layer **111** could be omitted for purposes of developing or optimizing the electrical, optical and material properties of the absorber layer **107**.

The crystallographic orientation of the semiconductor layers and the doping and bandgap profile may have a major impact on the performance of a photodiode, including one or more of a photodiode structure, a photodiode die, or a packaged photodiode. It is well known that for +c-plane GaN-based devices containing heterostructures, spontaneous and piezoelectric polarization, due to the strong polarity of the Ga—N bond and the lack of inversion symmetry in the wurtzite crystal structure, can create strong electric fields that can result in unfavorable device performance. It is believed that these fields can negatively impact the performance of photodiodes, particularly at high current densities, and have identified and disclosed herein several approaches to overcome these effects.

The use of +c-plane substrates, that is, where the crystallographic orientation is within 5 degrees, within 2 degrees, within 1 degree, or within 0.5 degree of (0001), has several advantages for high-power photodiodes, including 1) a more mature commercial supply chain with large-area, epi-ready substrates, 2) well-established, stable epitaxy growth conditions, and 3) relative ease in controlling dopant concentrations over many orders of magnitude. However, as illustrated in the Comparative Examples below, the use of relatively-standard LED-type structures may not enable photodiodes with high fill factors.

In certain embodiments, the deleterious effects of spontaneous and piezoelectric fields in +c-plane photodiodes, which become progressively more severe as the indium (In) percent in the absorber layer **107** is increased, are mitigated by the use of high doping levels on both the n-side and the p-side of the absorber layer **107**. The impacts of bandgap alignment and spontaneous and piezoelectric fields on photodiode performance at high current densities has been investigated. The semiconductor layers used in the analysis of the performance of a photodiode structure **1000** of a photodiode die are shown schematically in FIG. **7**. In the simplified model, absorber layer **730** is positioned between n-type doped layer **710** and p-type doped layer **750**. Optionally, an n-type non-absorber layer (or cladding layer) **720** is interposed between n-type doped layer **710** and absorber layer **730**. Optionally, a p-type non-absorber layer (or cladding layer) **740** is interposed between absorber layer **730** and p-type doped layer **750**. For simplicity, the absorber layer **730** was modeled as a double heterostructure, with a thickness of 40 nanometers, but similar effects are expected when the absorber layer consists of or includes multiple quantum well (MQW) structures.

In the case of absorber layers **730** containing one or more layers that include $In_{0.18}Ga_{0.82}N$, which are appropriate for absorption of light having a wavelength of about 473 nanometers or less, the short-circuit current and fill factor are very low when the doping level of the n-type doped layer **710** in contact with a first side of the absorber layer **730** is 2.0×10^{19} cm^{-3} and the doping level of the p-type doped layer **750** in contact with a second side of the absorber layers **730** is 2.0×10^{19} cm^{-3}, as shown in FIG. **8**A. This very poor performance is believed to be due to poor screening of the electric fields related to the polarization discontinuity and band offsets between InGaN and GaN, as shown in FIG. **8**B. However, when the doping level of the n-type doped layer **710** in contact with a first side of the absorber layer **730** is raised to 3.5×10^{19} cm^{-3} and the doping level of the p-type doped layer **750** in contact with a second side of the absorber layers **730** is raised to 6.0×10^{20} cm^{-3}, the illuminated I-V performance is much better, as shown in FIG. **9**A. This greatly improved performance is due to much better screening of the electric fields in the absorber layer **730** and in close proximity to the GaN—InGaN interface, as shown in FIG. **9**B. As shown in the table illustrated in FIG. **15**, improvements in fill factor FF can be achieved by increasing the doping levels in both layers in contact with the absorber layer **730**. In particular, fill factors above 90% can be achieved by doping in the n-type doped layer **710**, or the n-type non-absorber layer **720**, if present, at a concentration of about 3.5×10^{19} cm^{-3} or higher and by the activated doping level in the p-type doped layer **750**, or the p-type non-absorber layer **740**, if present, at a concentration of about 2.0×10^{20} cm^{-3} or higher.

Referring back to FIG. **1**, in some embodiments, the photodiode structure **1000** includes an n-type first non-absorber layer **105**, at least one absorber layer **107**, and a p-type layer **111** that each have a threading dislocation density below 10^7 cm^{-2}. The photodiode structure **1000** may also include one or more absorber layers **107**, an n-type first non-absorber layer **105**, and a p-type layer **111** that have a crystallographic orientation that differs from (000-1) −c-plane by between 2 degrees and 5 degrees. The photodiode structure **1000** may also include one or more absorber layers **107**, an n-type first non-absorber layer **105**, and a p-type layer **111** that have a crystallographic orientation within 5 degrees of {10-10} m-plane and each of the n-type first non-absorber layer **105** and p-type layer **111** are characterized by a dopant concentration of at least 4×10^{18} cm^{-3}. The photodiode structure **1000** may also include one or more absorber layers **107**, an n-type first non-absorber layer **105**, and a p-type layer **111** that have a crystallographic orientation within 5 degrees of a semipolar plane selected from {10-1-2}, {10-1-1}, {20-2-1}, {30-3-1}, and {40-4-1} and each of the n-type first non-absorber layer **105** and p-type layer **111** are characterized by a dopant concentration of at least 2×10^{18} cm^{-3}.

FIG. **15** includes the illuminated I-V performance characteristics of InGaN/GaN photodiodes having the structure indicated schematically in FIG. **7**. For simplicity, the absorber layer is modeled as a 40 nanometer thick double heterostructure.

In the case of absorber layers **730** containing one or more layers that include $In_{0.12}Ga_{0.88}N$, which are appropriate for absorption of light having a wavelength of about 435 nanometers or less, the fill factor is below 60% when the doping level of the n-type doped layer **710** or the n-type cladding layer **720**, if present, in contact with a first side of the absorber layers **730** is 2.0×10^{19} cm^{-3} and the doping level of the p-type doped layer **750** or the p-type cladding

layer **740**, if present, in contact with a second side of the absorber layers **730** is 8.0×10^{18} cm^{-3}. However, when the doping level of the p-type doped layer **750** or the p-type cladding layer **740**, if present, in contact with the second side of the absorber layers **730** is raised to 2.0×10^{19} cm^{-3}, the fill factor is raised to almost 80%, and when the doping level of the p-type doped layer **750** or the p-type cladding layer **740**, if present, in contact with the second side of the absorber layers **730** is raised further to 1.0×10^{20} cm^{-3}, the fill factor is raised to about 93%. The results in the table of FIG. **15** show that if the doping level in a p-type cladding layer **740** adjacent to the absorber layer **730** is reduced, relative to the doping level in the p-type doped layer **750**, the fill factor is reduced significantly. This result is significant because it may be difficult to achieve full doping all the way up to deposition of the undoped absorber layer **730**, thus producing a sharp transition in the doping profile, and immediately upon switching from an undoped absorber layer **730** deposited at a temperature below 950 degrees Celsius to a p-type doped layer **750**, which is deposited at considerably higher temperature, that has a desired doping level. However, as also shown in the table of FIG. **15**, improvements in the fill factor FF can also be achieved by introducing n-type cladding layer **720** and/or p-type cladding layer **740** on one or both of the n-type and p-type sides of the absorber layer **730**, respectively, particularly when the p-type cladding layer **740** has an indium concentration intermediate between that of the absorber layer **730** and of the n-type doped layer **710** and/or the p-type doped layer **750**. The intermediate indium concentration in the cladding layer may be uniform, continuously graded, or step graded. The n-type cladding layer **740** may include a strained layer superlattice. In some embodiments, the photodiode structure **1000** includes at least one of an n-type cladding layer and a p-type cladding layer, wherein the n-type cladding layer **720** lies between an n-type doped layer **710** and one or more absorber layers **730**, and wherein the n-type cladding layer **720** has a dopant concentration of at least 2×10^{19} cm^{-3}, and the p-type cladding layer **740** lies between the one or more absorber layers **730** and a p-type doped layer **750**, and wherein the p-type cladding layer **740** has a dopant concentration of at least 5×10^{19} cm^{-3}.

In certain embodiments, the deleterious effects of spontaneous and piezoelectric fields in +c-plane-oriented photodiodes are mitigated by use of a −c-plane substrate that has a crystallographic orientation that is within 10 degrees, such as within 6 degrees, within 5 degrees, within 4 degrees, within 3 degrees, within 2 degrees, or within 1 degree of (000-1). In certain embodiments, the substrate and the semiconductor layers have a crystallographic orientation that differs from (000-1) by between 1 degree and 10 degrees or between 2 degrees and 5 degrees. In certain embodiments, the substrate and the semiconductor layers are misoriented from (000-1) toward a <10-10> m-direction. In certain embodiments, the substrate and the semiconductor layers are misoriented from (000-1) toward a <11-20> a-direction. Referring again to the table of FIG. **15**, it has been found that doping concentrations of 1.0×10^{16} cm^{-3} or 1.0×10^{17} cm^{-3} or 1.0×10^{18} cm^{-3} in the n-type doped and the p-type doped layers, which are immediately adjacent to the absorber layer **730**, are sufficient to achieve a high fill factor for both 12% and 18% indium concentrations in the absorber layer **730**. It is believed that a fill factor greater than 85% can be achieved if the doping concentration in the n-type doped layer **710** and p-type doped layer **750** is between 1.0×10^{16} cm^{-3} and 1.0×10^{20} cm^{-3} for absorber Indium concentrations greater than 8% in the case where the substrate and the semiconductor layers each have a −c crystallographic orientation. In one example, the photodiode is characterized by a fill factor of at least 50% under an illumination level producing a current density of at least 10 A cm^{-2}.

In certain embodiments, the deleterious effects of spontaneous and piezoelectric fields in +c-plane photodiodes are mitigated by use of an m-plane substrate, that is, with an orientation within where the crystallographic orientation is within 5 degrees, within 2 degrees, within 1 degree, or within 0.5 degree of (10-10). Referring again to the table of FIG. **15**, it has been found that a doping concentration of 2.0×10^{19} cm^{-3} in the n-type doped layer **710** or the n-type cladding layer **720**, if present, and the p-type doped layer **750** or the p-type cladding layer **740**, if present, which are immediately adjacent to the absorber layer, are sufficient to achieve a fill factor above 90% for both 12% and 18% indium concentrations in the absorber layer.

In certain embodiments, the deleterious effects of spontaneous and piezoelectric fields in +c-plane photodiodes are mitigated by use of semipolar substrate that has a crystallographic orientation that is within 5 degrees, within 2 degrees, within 1 degree, or within 0.5 degree of {20-2-1} or {30-3-1}. Referring again to the table of FIG. **15**, it has been found that a doping concentration of 8.0×10^{18} cm^{-3} in the n-type doped and the p-type doped layers, which are immediately adjacent to the absorber layer, are sufficient to achieve a fill factor above about 90% for both 12% and 18% indium concentrations in the absorber layer.

In certain embodiments, in order to reduce the carbon content in N-polar or semipolar InGaN layers, triethylgallium (TEG) and triethylindium (TEIn) are used as the metalorganic precursors rather than the more conventional trimethyl gallium (TMG) and trimethylindium (TMIn). For example, the carbon concentration in the semiconductor layers may be less than 1×10^{18} cm^{-3} or less than 1×10^{17} cm^{-3}. In certain embodiments, the ratio of hydrogen (H_2) and nitrogen (N_2) carrier gas, the substrate temperature, and the pressure are optimized to minimize formation of hillocks in the N-polar semiconductor layers.

In certain embodiments, the semiconductor layers are annealed to electrically activate the p-type dopant. In certain embodiments, the annealing is performed in situ in the MOCVD reactor used to deposit the semiconductor layers, for example, under flowing N_2 to a temperature between about 500 degrees Celsius and about 900 degrees Celsius. In certain embodiments, the annealing is performed in a furnace or in a rapid thermal annealing (RTA) oven, for example, under flowing N_2 to a temperature between about 400 degrees Celsius and about 900 degrees Celsius. In certain embodiments, the atmosphere during the annealing process may also contain an oxidizing gas such as O_2. In certain embodiments, the fraction of the oxidizing gas within the annealing atmosphere is between about 5% and about 95%. In certain embodiments, the duration of the annealing process is between about one second and about five hours, or between about 10 seconds and about one hour. In certain embodiments, after annealing, the surface of the semiconductor layers is cleaned to prepare them for additional deposition. In certain embodiments, the cleaning includes or consists of one or more of treatment by a mineral acid, such as hydrochloric acid, nitric acid, or aqua regia, a piranha etch, a buffered oxide etch, by dry etching, or by treatment with a plasma, such as an argon plasma.

In certain embodiments, a transparent conductive layer is deposited on the p-type semiconductor layer. In certain embodiments, the transparent conductive layer comprises a transparent conductive oxide (TCO) such as indium tin

oxide or aluminum zinc oxide. In certain embodiments, the transparent conductive layer is deposited by a one or more of thermal evaporation, electron-beam evaporation, and sputtering. In certain embodiments, the deposited TCO layer is annealed in a controlled atmosphere containing oxygen at a temperature between about 300 and 700 degrees Celsius, so as to co-optimize the optical/transparency and electrical properties of the TCO layer. In certain embodiments, the transparent conductive layer has a thickness between about 10 nanometers and about 1000 nanometers.

Each of the photodiode structures **1000** described in the present disclosure are intended for use in a photodiode die **1002** of a packaged photodiode with a multiple-reflection geometry. The packaged photodiode contains a photodiode die **1002** and may also contain one or more of a heat sink, an enclosure, a separate photodetector, an optical entrance aperture, solder bumps, wire bonds, or encapsulation consisting of or including a polymer such as an epoxy or a silicone. In some embodiments the packaged photodiode may further include one or more components for coupling light into or out of the photodiode die **1002** and for enabling more reflections.

In order to maximize the efficiency of the packaged photodiode, it may be important to maximize the reflectivity of the front and back faces of the photodiode structure **1000** of a photodiode die **1002**. A photodiode die **1002** is generally cut, by singulation or dicing, into discrete dimensions (e.g., rectangular pieces) from a photodiode structure **1000** that includes one or more non-absorber layers **105**, **109**, an absorber layer **107**, p-side reflective electrical contact **113**, and n-side reflective electrical contact **114**. A photodiode die **1002** consists of or includes a device cavity region, which may include at least one of a substrate and an optically transmissive member and may be bounded by edge structures, such as an optical window and reflective coatings. A device cavity region is formed of at least two opposing reflective members and an optically transmissive member between the two opposing reflective members. Electromagnetic radiation entering through an optical window into the device cavity region passes through the optically transmissive member and is internally reflected between the reflective members at least two or more times. Luminescent light emitted from the one or more absorber layers may also be internally reflected between the reflective members at least two or more times.

In some embodiments, the two opposing surfaces are parallel to each other. In some other embodiments, the two opposing surfaces are not parallel to each other. In the photodiode structure **1000** shown in FIG. **1**, the optically transmissive member is substrate **101** and the reflective members are p-side reflective electrical contact **113** and n-side reflective electrical contact **114** described below.

In addition, in order to maximize the efficiency of the packaged photodiode, it is important to minimize the electrical resistance of the contacts in the photodiode structure. Referring again to FIG. **1**, a p-side reflective electrical contact **113** may be deposited on the p-type layer **111**. In a preferred embodiment, the average reflectivity of the reflective p-side electrical contact is greater than 70%, greater than 80%, greater than 85%, greater than 90%, greater than 95%, greater than 97%, or greater than 98% at a specific angle or range of angles at which light is incident during operation. In general, the term "average reflectivity" as used herein is intended to broadly describe a reflectance value that is calculated by averaging at least two reflectance measurement data points on a surface at a specific wavelength between 390 nanometers and 460 nanometers and at one or more angles with respect to the surface of the layer that are representative of the range of incident angles during device operation. During operation of a packaged photodiode, in some embodiments, light (or optical radiation) is coupled into a vertical edge, or approximately vertical edge, of the photodiode die **1002** and the angle of incidence of the light on the reflective layers (e.g., p-side reflective electrical contact **113** or n-side reflective electrical contact **114** in FIGS. **1** and **2**) internally is between about 0 and about 30 degrees, between about 0.2 and about 20 degrees, or between about 0.3 and about 10 degrees, as measured from the plane of the reflective layers (e.g., a plane parallel to the large-area surface **102** in FIG. **2**). In one example, the light receiving surface **252**, which is illustrated in FIG. **2**, is oriented as a vertical edge of the photodiode die **1002** or a vertical plane within the photodiode die **1002** that is at an angle with respect to the large-area surface **102** (e.g., 90° angle). In some embodiments of the photodiode die **1002**, light is coupled into a non-vertical edge of the photodiode die **1002** and the angle of incidence on the reflective layers internally is between about 0.1 and about 60 degrees, between about 0.2 and about 40 degrees, or between about 0.3 and about 20 degrees, as measured from the plane of the reflective layers. In other embodiments of the photodiode die **1002**, light is coupled into a large area surface of the photodiode die **1002** through an aperture, and the angle of incidence on the reflective layers internally is between about 30 and 90 degrees, between about 45 and 90 degrees, or between about 60 and 90 degrees, as measured from the plane of the reflective layers (e.g., a plane parallel to the large-area surface **102** in FIG. **2**). In still other embodiments of the photodiode die **1002**, light is coupled into a large area surface of the photodiode die **1002** through an aperture and undergoes internal reflection at an oblique angle, and the angle of incidence on the reflective layers internally is between about 0.1 and about 45 degrees, between about 0.3 and about 30 degrees, or between about 0.5 and about 20 degrees, as measured from the plane of the reflective layers. The contact resistance of the p-side reflective electrical contact is less than 3×10^{-3} Ωcm^2, less than 1×10^{-3} Ωcm^2, less than 5×10^{-4} Ωcm^2, less than 2×10^{-4} Ωcm^2, less than 10^{-4} Ωcm^2, less than 5×10^{-5} Ωcm^2, less than 2×10^{-5} Ωcm^2, or less than 10^{-5} Ωcm^2. In preferred embodiments, the contact resistance is less than 1×10^{-4} Ωcm^2. The p-side reflective electrical contact may include at least one of silver, gold, aluminum, nickel, platinum, rhodium, palladium, titanium, chromium, germanium, ruthenium, magnesium, scandium, or the like. In some embodiments, the p-side reflective electrical contact may include or consist of at least two layers, with a first layer providing a good electrical contact and comprising platinum, nickel, aluminum, or titanium and having a thickness between 0.1 and 5 nanometers, and a second layer providing superior optical reflectivity and comprising silver, gold, or nickel and having a thickness between 0.4 nanometer and 1 micrometer. In certain embodiments, the p-side reflective electrical contact may include or consist of at least three layers, at least four layers, or at least five layers. In certain embodiments, the p-side reflective electrical contact comprises three layers, with the first layer comprising silver, with a thickness between about 1 nanometer and about 200 nanometers, a second layer comprising a moderately oxophilic metal, with a thickness between about 0.5 nanometer and about 2 nanometers, and a third layer comprising silver, with a thickness between about 50 nanometers and about 200 nanometers. In certain embodiments, the moderately oxophilic metal includes or consists of nickel. In certain embodiments, the moderately

oxophilic metal includes or consists of or includes one or more of copper, cobalt, iron, and manganese. In certain embodiments, the reflective p-side electrical contact is annealed after deposition to improve its reflectivity and/or to reduce its contact resistance. In certain embodiments, the annealing is performed in a rapid thermal anneal (RTA) furnace, to a temperature between about 300 degrees Celsius and about 1000 degrees Celsius. In certain embodiments the p-side reflective electrical contact is annealed to a temperature between about 500 and about 900 degrees Celsius under a controlled atmosphere containing oxygen at a partial pressure between about 0.1 Torr and about 200 Torr, so as to cause interdiffusion between the moderately oxophilic metal and silver and introduction of a controlled concentration of oxygen atoms into the p-side reflective electrical contact layer. In preferred embodiments, the partial pressure of oxygen is reduced below about 10^{-4} Torr before cooling the p-side reflective electrical contact below a temperature of about 250 degrees Celsius, so as to avoid formation of excess silver oxide. In certain embodiments, the p-side reflective electrical contact includes oxygen with a maximum local concentration between about 1×10^{20} cm^{-3} and about 7×10^{20} cm^{-3}. Further details are described in U.S. Pat. No. 9,917,227, which is hereby incorporated by reference in its entirety. The p-side reflective electrical contact may be deposited by thermal evaporation, electron beam evaporation, sputtering, or another suitable technique. In a preferred embodiment, the p-side reflective electrical contact serves as the p-side electrode for the power photodiode. In certain embodiments, the p-side reflective electrical contact is planar and parallel to the semiconductor layers, which may be useful for maximizing its reflectivity. In alternative embodiments, the p-side reflective electrical contact is patterned or textured, which may be useful for admission or extraction of light, for example, within an aperture.

In certain embodiments, a reflectance measurement of a particular reflective surface may be performed by preparing at least two sample types, with one having the reflective surface left intact and the other having the reflective surface removed. Both samples may be fabricated such that measurement probe light is coupled in with low reflectance through a first surface, undergoes reflection and refraction from a second surface corresponding to the reflective surface that is to be measured, and is coupled out with low internal reflectance through a third surface. In some embodiments, reflections at the first and third surfaces are minimized by application of a dielectric anti-reflective coating tuned to the wavelength of a probe light, which has a similar wavelength as the wavelength that is to be used during operation of the power photodiode device. Reflections at the first and third surfaces can be reduced further by fabricating the samples such that light transmits through the first and third surfaces at near normal incidence. The optical power transmitted out of the surface corresponding to the reflective surface and the third surface are measured for both sample types and used to calculate the reflectance of the reflective surface according to methods that are well known in the art.

Referring again to FIG. **1**, in certain embodiments, an n-side reflective electrical contact **114**, with an average reflectivity greater than about 70%, is deposited on the back side of substrate **101**. In a preferred embodiment, the average reflectivity of the reflective n-side electrical contact is greater than 80%, greater than 85%, greater than 90%, greater than 95%, greater than 97%, or greater than 98% at a specific angle or range of angles at which light is incident during operation. The contact resistance of the reflective n-side electrical contact is less than 1×10^{-3} Ωcm^2, less than 5×10^{-4} Ωcm^2, less than 2×10^{-4} Ωcm^2, less than 10^{-4} Ωcm^2, less than 5×10^{-5} Ωcm^2, less than 2×10^{-5} Ωcm^2, or less than 10^{-5} Ωcm^2. In preferred embodiments, the contact resistance is less than 5×10^{-5} Ωcm^2. The reflective n-side electrical contact may comprise at least one of silver, gold, aluminum, nickel, platinum, rhodium, palladium, titanium, chromium, or the like. In some embodiments, the reflective n-side electrical contact may include or consist of at least two layers, with a first layer providing a good electrical contact and comprising aluminum or titanium and having a thickness between 0.1 and 5 nanometers, and a second layer providing superior optical reflectivity and comprising aluminum, nickel, platinum, gold, or silver and having a thickness between 10 nanometers and 10 micrometers. In certain embodiments, the n-side reflective electrical contact may include or consist of at least three layers, at least four layers, or at least five layers, so as to co-optimize the reflectivity (maximized), the contract resistance (minimized), and the robustness (maximized). The reflective n-side electrical contact may be deposited by thermal evaporation, electron beam evaporation, sputtering, or another suitable technique. In certain embodiments, the n-side reflective electrical contact serves as the n-side electrode for the power photodiode. In certain embodiments, the n-side reflective electrical contact is planar and is aligned parallel to the semiconductor layers, which may be useful for maximizing its reflectivity. In alternative embodiments, the n-side reflective electrical contact is patterned or textured, which may be useful for admission or extraction of light, for example, within an aperture.

In certain embodiments, particularly embodiments where the n-side reflective electrical contact includes aluminum, in order to reduce the contact resistance of the n-side reflective electrical contact, the back side of substrate **101** is processed by reactive ion etching (RIE) using a chlorine-containing gas or plasma. In one specific embodiment, the chlorine-containing gas or plasma includes $SiCl_4$. In certain embodiments, in order to reduce the contact resistance of the n-side reflective electrical contact, further cleaning steps are performed. In certain embodiments, the further cleaning steps include or consist of one or more of treatment by a mineral acid, such as hydrochloric acid, nitric acid, or aqua regia, a buffered oxide etch, by dry etching, or by treatment with a plasma, such as an argon plasma.

In some embodiments, as shown in FIG. **2**, the p-side reflective electrical contact comprises a two-component mirror/p-electrode, including a discontinuous p-electrode **215** and a p-side reflective electrical contact **113**, which is shown as a p-side reflective electrical contact layer that is deposited over the discontinuous p-electrode **215** elements. The discontinuous p-electrode **215** is optimized as an electrical contact and can be made, for example, of a nickel/gold, or a platinum/gold stack where the nickel, or platinum is about 20 to 200 nm thick and the gold is about 100 nm to 1 micron thick. In one suitable embodiment, the discontinuous p-electrode **215** is a gridded electrode having grid openings of between about 1 micron and 0.1 cm on a side. The p-side reflective electrical contact **113** may comprise at least one of silver, gold, aluminum, platinum, rhodium, palladium, chromium, or the like, and may be deposited over the p-type layer **111** and over the gridded discontinuous p-electrode **215**. Preferably, the p-side reflective electrical contact is deposited after any annealing processing of the discontinuous p-electrode to reduce interdiffusion. Optionally, a diffusion barrier layer such as nickel, rhodium, platinum, palladium, iridium, ruthenium, rhenium, tungsten, molybdenum, niobium, tantalum, or $MC_xN_yO_z$ (where M includes

a metallic element such as aluminum, boron, silicon, titanium, vanadium, chromium, yttrium, zirconium, lanthanum, or a rare earth metal, and x, y, z are each between 0 and 3) is disposed between the discontinuous p-electrode **215** and the p-side reflective electrical contact **113**. Assuming an operating current density of 10 A/cm^2, a sheet resistance of 4×10^5 Ω/sq for the p-type layers, and that current is conducted from the p-type layer only to the gridded, discontinuous p-electrode **215** and not directly to the p-side reflective electrical contact **113**, the calculated percent power loss due to lateral conduction within the p-type layers is approximately 0.6, 3.6, and 14.5% for 2, 5, and 10 micron grid finger spacing, respectively. Rather than a grid configuration, the discontinuous p-electrode **215** can alternatively be arranged as an array of dots, rectangles, circles, or the like that are positioned in a plane that is parallel to large-area surface **102**. The separation between the discontinuous p-electrode **215** is preferably between about 1 micron and 0.1 cm. The use of a reflective metal p-electrode or combination of reflective electrical contact and discontinuous electrode enables fabrication of large area power photodiodes without necessitating lateral carrier transport through p-doped layers over large distances, thus minimizing lateral ohmic losses and the series resistance in the device. Parasitic optical absorption by a discontinuous p-electrode can be minimized by designing the electrode pattern and orienting the light propagation path so that light incident on the discontinuous p-electrode pattern is largely avoided.

The photodiode structure may include a p-side reflective electrical contact disposed over the p-type layer, wherein the p-side reflective electrical contact has an average reflectance of at least 80% at a specific angle or range of angles at which light is incident during operation for wavelengths between 390 nanometers and 460 nanometers and a contact resistance below 1×10^{-3} Ωcm^2.

As noted above, the photodiode structures **1000** described in the present disclosure are intended for use in a photodiode die and in a packaged photodiode with a multiple-reflection geometry. In some embodiments, during operation a photodiode die disposed within a packaged photodiode is configured to receive one or more wavelengths of radiation, which is also referred to herein as light, from an illumination source **251**. The illumination source **251** may include a laser, an optical fiber, or other useful radiation source. In order to optimize the power efficiency of a packaged photodiode, it is important to maximize the reflectivity of the front and back faces of the photodiode die, and also the sides of individual photodiode die after singulation. In addition, it is important to minimize the electrical resistance of the contacts and to optimize the configuration between the light receiving surface **252** of the photodiode die and the reflective contact structures (for example, the p-side reflective electrical contact and the n-side reflective electrical contact). Referring again to FIG. **2**, light of a desired wavelength, for example, 405 nanometers or 450 nanometers may enter the photodiode structure **1000** through an aperture or a window (not shown) and enters the light receiving surface **252**, such that light propagates within substrate **101** and the semiconductor layers, and is reflected from the p-side reflective electrical contact **113** and the n-side reflective electrical contact **114** and from an edge reflector (not shown). The light receiving surface **252** generally includes a portion of the photodiode device (or photodiode die) that is positioned and aligned to provide the radiation emitted from the illumination source **251** to a region of the photodiode die disposed between the p-side reflective electrical contact **113** and the n-side reflective electrical contact **114**, as shown in FIG. **2**. The light receiving surface **252**, in some embodiments, may include a region on an edge of the photodiode die, such as shown schematically in FIG. **2**. In other embodiments, the light receiving surface **252** may include an open region on one of the surfaces **255** or **256**, which does not include portions of the materials used to form the p-side reflective electrical contact **113** or the n-side reflective electrical contact **114**, respectively. In this configuration, the open region is designed to allow the radiation emitted from the illumination source **251** to enter the region of the photodiode die disposed between the p-side reflective electrical contact **113** and the n-side reflective electrical contact **114**. In some embodiments, the light receiving surface **252** is aligned relative to the photodiode die to cause light delivered from the illumination source **251** to be reflected at least once, at least twice, at least three times, or at least five times between the p-side reflective electrical contact **113** and the n-side reflective electrical contact **114**. The light delivered from the illumination source **251** can, for example, have at least one wavelength between 390 nanometers and 460 nanometers.

In certain embodiments, as also shown in FIG. **2**, an n-side reflective electrical contact comprises a two-component mirror/n-electrode including a discontinuous n-electrode **217** and an n-side reflective electrical contact **114**. The discontinuous n-electrode **217** is optimized as an electrical contact and can be made, for example, of a titanium/aluminum or a titanium/aluminum/gold stack where the titanium is about 5 to 200 nm thick and the aluminum or gold is about 100 nm to 1 micron thick. In one suitable embodiment, the discontinuous n-electrode **217** is a gridded electrode having grid openings of between about 1 micrometer and 1 centimeter on a side. In certain embodiments, the portion of the surface beneath the gridded electrode is roughened, for example, using a wet etching treatment, prior to deposition of the gridded electrode. In certain embodiments, a roughened surface has a root-mean-square roughness between about 300 nanometers and about 1 millimeter, or between about 1 micrometer and about 200 micrometers. Assuming an operating current density of 10 A/cm^2 and a sheet resistance of 0.27 Ω/sq for an n-type GaN substrate, the calculated percent power loss due to lateral conduction within the substrate layers is approximately 0.4, 2.5, and 9.8% for 0.2, 0.5, and 1 cm grid finger spacing, respectively. In certain embodiments, n-side reflective electrical contacts on the side of a singulated die prepared from this structure are added in addition to or instead of the backside n-side reflective electrical contact. In certain embodiments, n-contacts and p-contacts are added to the same side of the die, after formation of trenches to the n-type doped layer or the p-type doped layer, respectively, as needed. The trenches may be formed by lithography and dry or wet etching, as is well known in the art and described in further detail below. The n-side reflective electrical contact **114** may comprise at least one of silver, gold, aluminum, platinum, rhodium, palladium, chromium, or the like, and may be deposited over the back side of substrate **101** and over the gridded discontinuous n-electrode **217**. Preferably, the electrical contact is deposited after any annealing processing of the discontinuous n-electrode to reduce interdiffusion. Optionally, a diffusion barrier layer such as nickel, rhodium, platinum, palladium, iridium, ruthenium, rhenium, tungsten, molybdenum, niobium, tantalum, or $MC_xN_yO_z$ (where M includes a metallic element such as aluminum, boron, silicon, titanium, vanadium, chromium, yttrium, zirconium, lanthanum, or a rare earth metal, and x, y, z are each between 0 and 3) is disposed between the discontinuous n-electrode **217** and

the n-side reflective electrical contact **114**. Rather than a grid configuration, the discontinuous n-electrode **217** can be arranged as an array of dots, rectangles, circles, or the like that are positioned in a plane that is parallel to large-area surface **102**. The separation between the discontinuous n-electrode **217** is preferably between about 1 micron and 0.1 cm. The use of a reflective metal n-electrode or combination of reflective electrical contact and discontinuous electrode enables fabrication of large area power packaged photodiodes without necessitating lateral carrier transport through substrate **101** over large distances, which may be important if the carrier concentration of substrate **101** is low in order to optimize transparency or if it is quite thin, for example, less than about 100 micrometers, less than about 50 micrometers, or less than about 25 micrometers. Parasitic optical absorption by a discontinuous n-electrode can be minimized by designing the electrode pattern and the light propagation path so that light incident on the discontinuous n-electrode pattern is largely avoided.

The photodiode structure **1000** may include an n-side reflective electrical contact that has an average reflectance of at least 80% at a specific angle or range of angles at which light is incident during operation for wavelengths between 390 nanometers and 460 nanometers and has a contact resistance below 5×10^{-4} Ωcm^2.

In some embodiments, as illustrated in FIG. **3**, at least one of the p-side reflective electrical contact and the n-side reflective electrical contact further includes a semi-transparent current-spreading layer **321**. The semi-transparent current-spreading layer **321** may consist of or include at least one of nickel oxide (NiO), nickel oxide/gold (NiO/Au), NiO/Ag, indium tin oxide (ITO), p-type zinc oxide (ZnO), ruthenium oxide (RuO_2), another transparent conductive oxide, or the like. The semi-transparent current-spreading layer **321** facilitates electrical contact to the p-type layer **111** or to the substrate **101**, for example, ohmic or quasi-ohmic behavior. To minimize light absorption in the semi-transparent current-spreading layer **321**, this layer has a thickness which is preferably between about 1 nm and about 100 nm, with more than 70% light transmission. Assuming an operating current density of 10 A/cm^2 and a sheet resistance of 25 Ω/sq for the semi-transparent current-spreading layer **321** overlying the p-type layers, the calculated percent power loss due to lateral conduction within the current spreading layer is approximately 0.4, 2.3, and 9.1% for 0.02, 0.05, and 0.1 cm grid spacing, respectively.

In some embodiments, a transparent dielectric **319** is disposed on a portion of the semi-transparent current-spreading layer **321** and between discontinuous p-electrode **315** and/or discontinuous n-electrode **317**. The transparent dielectric may comprise at least one of TiO_2, Ta_2O_5, ZrO_2, SiO_2, SiO_x, SiN_x, Si_3N_4, SiO_xN_y, Al_2O_3, or MgF_2. The transparent dielectric **319** may be a quarter-wave thick, that is, have a thickness approximately equal to one-quarter of the incident photon wavelength in air divided by the refractive index of the dielectric medium. For example, in the case that the photodiode structure **1000** has a design wavelength of 405 nanometers and the transparent dielectric consists of Ta_2O_5, with a refractive index of approximately 2.28, the thickness of the transparent dielectric **319** may be chosen as about 405/2.28/4=44 nanometers. The transparent dielectric **319** includes open areas in which a discontinuous p-electrode **315** or a discontinuous n-electrode **317** is disposed. The discontinuous p-electrode **315** and the discontinuous n-electrode **317** may comprise at least one of nickel (Ni), nickel oxide (NiO), titanium-tungsten/gold (Ti—W/Au). In a preferred embodiment, the discontinuous p-electrode **315** and/or the discontinuous n-electrode **317** does not extend over the transparent dielectric. A p-side reflective electrical contact **113** is disposed over the transparent dielectric and the electrical contact material and electrically interconnects the discontinuous p-electrode **315** in the various grid openings. An n-side reflective electrical contact **114** is disposed over the transparent dielectric and the electrical contact material and electrically interconnects the discontinuous n-electrode **317** in the various grid openings. The p-side reflective electrical contact **113** and n-side reflective electrical contact **114** also cooperate with the transparent dielectric **319** to define a reflector for reflecting light within the device. Further variations of the reflective metallic contact are described in U.S. Pat. No. 7,119,372, which is hereby incorporated by reference in its entirety.

In another set of embodiments, as illustrated schematically in FIGS. **13**A, **13**B, and **13**C, the semiconductor layers are transferred to one or more carrier substrates **1313** and the template substrate **1101** removed. By comparison to the structure illustrated schematically in FIG. **3**, the p-side electrical contact may similarly comprise a semi-transparent current-spreading layer **321** and a discontinuous p-electrode **315**, and may further comprise a transparent dielectric **319** disposed on portions of the semi-transparent current-spreading layer **321** (FIG. **13**A). A carrier substrate **1313** is then bonded to one or more of the p-type layer **111**, the semi-transparent current-spreading layer **321**, if present, the discontinuous p-electrode **315**, if present, and the transparent dielectric **319**, if present. The bonding of carrier substrate or optically transmissive member **1313** may be achieved by means of an adhesive, by means of a thermo-compression bond between one or more adhesion layers (not shown) deposited on at least one of a first surface of carrier substrate **1313** and the layer to which it is to be bonded, or by alternative bonding methods that are known in the art. In certain embodiments, carrier substrate **1313** and the adhesion layers are transparent at the wavelengths of interest for the packaged photodiode, for example, between 390 nanometers and 460 nanometers. In certain embodiments, carrier substrate **1313** includes or consists of one or more of a glass, a transparent ceramic, silica glass, borosilicate glass, aluminosilicate glass, quartz, sapphire, $MgAl_2O_4$ spinel, zinc oxide, or aluminum oxynitride. The adhesion layers may include or consist of one or more of SiO_x, GeO_x, SiN_x, AlN_x, GaO_x, Al_2O_3, Sc_2O_3, Y_2O_3, B_2O_3, R_2O_3, where R is a rare earth element, MgO, CaO, SrO, HfO_2, ZrO_2, Ta_2O_5, or B, Al, Si, P, Zn, Ga, Si, Ge, Au, Ag, Ni, Ti, Cr, Zn, Cd, In, Sn, Sb, Tl, or Pb, or an oxide, nitride, or oxynitride thereof. The adhesion layers may be deposited by thermal evaporation, electron-beam evaporation, sputtering, chemical vapor deposition, plasma-enhanced chemical vapor deposition, or the like, or by thermal oxidation of a deposited metallic film. The thickness of the adhesion layers may between about 1 nanometer and about 10 microns, or between about 10 nanometers and about 1 micron. The adhesion layer(s) may be annealed, for example, to a temperature between about 300 degrees Celsius and about 1000 degrees Celsius. In some embodiments, at least one adhesion layer is chemical-mechanically polished. In a preferred embodiment, the root-mean-square surface roughness of at least one adhesion layer is below about 0.5 nanometer, or below about 0.3 nanometer over a 20×20 μm^2 area. In certain embodiments, the thermo-compression bonding is performed in a clean room, with less than 10,000, less than 1,000, less than 100, or less than 10 particles per cubic centimeter in the air. Particles may be removed from at least one of the surfaces immediately prior to wafer bonding by spraying, brushing,

or rinsing with ionized nitrogen, a CO_2 jet, CO_2 snow, high-resistivity water, an organic solvent, such as methanol, ethanol, isopropanol, acetone, or the like. In some embodiments, the opposing surfaces are brought into contact while immersed in a liquid. Optionally, at least one of the surfaces is exposed to a plasma to enhance wafer bonding. The pressure between opposing surfaces during the thermo-compression bonding process may be between about 0.1 megapascals and about 100 megapascals, and the temperature may be held at between about 30 degrees Celsius and about 950 degrees Celsius, between about 30 degrees Celsius and about 400 degrees Celsius, or between about 30 degrees Celsius and about 200 degrees Celsius for a period between about 1 minute and about 10 hours.

A p-side reflector layer **1315** may be deposited on the opposite surface of carrier substrate **1313** from the photodiode structure **1000**. P-side reflector layer **1315** may include or consist of one or more of silver, a dielectric mirror, and a distributed Bragg reflector (DBR). P-side reflector layer **1315** may have a reflectivity, at a specific angle or range of angles at which light is incident during operation, above about 80%, above about 85%, above about 90%, above about 95%, above about 97%, or above about 98% at the design wavelength of the packaged photodiode, for example, between 360 nanometers and 460 nanometers.

The photodiode structure **1000** may be separated from the template substrate **1101** by a laser lift-off method, as shown schematically in FIG. **13**B. A laser beam **1321** may be rastered over the backside of substrate **101**. In certain embodiments, where single-crystalline group-III metal nitride layer **1104** is deposited on a template substrate **1101**, such as a sapphire substrate, and an ultraviolet laser beam is focused on the interface between single-crystalline group-III metal nitride layer **1104** and template substrate **1101**, to cause localized decomposition of the backside of single-crystalline group-III metal nitride layer **1104** and formation of micro- or nano-bubbles of N_2 and resulting in separation of template substrate **1101** from the balance of the photodiode structure **1000**. In certain embodiments, where single-crystalline group-III metal nitride layer **1104** is deposited on a release layer **1103** having an optical absorption coefficient greater than 1000 cm^{-1} at at least one wavelength where the balance of template substrate **1101** is substantially transparent, with an optical absorption coefficient less than 50 cm^{-1}, laser beam **1321** having a wavelength where release layer **1103** is strongly absorbing may be focused on release layer **1103**, causing localized decomposition and formation of micro- or nano-bubbles of N_2 and resulting in separation of template substrate **1101** from the balance of the photodiode structure **1000**. The optimal degree of weakening of the interface, without causing undesired damage to the high quality epitaxial layer or the semiconductor structure, may achieved by adjusting the temperature of the photodiode structure **1000**, the laser power, the laser spot size, the laser pulse duration, and/or the number of laser pulses. The laser fluence to effect separation may be between 300 and 900 millijoules per square centimeter or between about 400 mJ/cm^2 and about 750 mJ/cm^2. The uniformity of the laser beam **1321** may be improved by inclusion of a beam homogenizer in the beam path, and the beam size may be about 4 mm by 4 mm. In some embodiments, the laser beam **1321** is scanned or rastered across the release layer rather than being held stationary. Separation may be performed at a temperature above the melting point of the metal produced by decomposition, e.g., above about 30 degrees Celsius in the case of gallium metal.

Alternatively, the photodiode structure **1000** may be separated from the template substrate **1101** by photoelectrochemical etching, as shown schematically in FIG. **13**C. In certain embodiments, release layer **1103** comprises InGaN and has a bandgap less than that of the absorber layer. Trenches **1322** may be formed between adjacent carrier substrates **1313** though each of the semiconductor layers down to release layer **1103**, forming mesas. Trenches **1322** may be formed by dry etching or wet etching following conventional lithography, as is well known in the art. The photodiode structure **1000** is then immersed in a photoelectrochemical etching solution and may be illuminated with light having wavelengths that are strongly absorbed by the release layer **1103** but not by at least some of the other semiconductor layers. In certain embodiments the etch solution includes one or more of potassium hydroxide (KOH) potassium persulfate ($K_2S_2O_8$), sodium hydroxide (NaOH), hydrogen peroxide (H_2O_2), ethylene glycol, and tetramethylammonium hydroxide (TMAH). The KOH may have a concentration between 0.01 and 10 molar or between about 0.1 molar and about 2 molar. In certain embodiments, the light source includes a broadband source such as a mercury arc lamp, a mercury-xenon lamp, a tungsten lamp, or an LED. In certain embodiments, the light source is coupled with a filter to exclude wavelengths that are strongly absorbed by one or more of the semiconductor layers. The fluence of the light source may be between about 1 W/cm^2 and about 50 W/cm^2. In certain embodiments, the photodiode structure **1000** is connected electrically to an anode, with a separate cathode immersed in the etch solution. In certain embodiments, an electrical current is passed between the cathode and the anode to cause dissolution of the release layer **1103**, beginning from the bases of the trenches **1322** and extending laterally. In other embodiments, the photoelectrochemical etching process is electrodeless. In certain embodiments, oxidation and dissolution of the release layer is driven by an oxidizing agent present in the etch solution such as $K_2S_2O_8$. After etching for a predetermined time, release layer **1103** is substantially dissolved, enabling easy removal of the photodiode structures **1000** from template substrate **1101**.

After removal of template substrate **1101**, n-side reflective electrical contact **1319**, with a reflectivity greater than about 70%, greater than about 80%, greater than about 90%, greater than about 95%, greater than about 97%, or greater than about 98% at a specific angle or range of angles at which light is incident during operation, may deposited on the freshly-exposed back side surface **1317** of single-crystalline group-III metal nitride layer **1104**, as shown schematically in FIG. **13**D and described above. In some embodiments, surface **1317** is cleaned, by one or more of a wet process or a dry process, prior to deposition of n-side reflective electrical contact **1319**. During operation, light from illumination source **251** passes through an aperture or light receiving surface **1352**, enters carrier substrate **1313** as beam **1353**, and is multiply reflected between A-side reflector layer **1315** and n-side reflective electrical contact **1319**.

Variations of the template substrate removal and carrier substrate bonding process are possible. For example, a first carrier substrate **1411**, which may or may not be transparent, may be bonded to p-side reflective electrical contact **113**, as shown schematically in FIG. **14**A. First carrier substrate **1411** may include or consist of one or more of sapphire, silicon carbide, zinc oxide, silicon, SiO_2, glass, copper, silver, and aluminum. Then, following removal of template substrate **1101** by a process similar to that described above and shown schematically in FIGS. **13**B and **13**C, a semi-

transparent current-spreading layer **321** may be deposited on the freshly-exposed back side surface **1417** of single-crystalline group-III metal nitride layer **1104**, as shown schematically in FIG. **14**B and described above. The semi-transparent current-spreading layer **321** facilitates electrical contact to the single-crystalline group-III metal nitride layer **1104**, for example, ohmic or quasi-ohmic behavior. In some embodiments, a transparent dielectric **319** is disposed on a portion of the semi-transparent current-spreading layer **321** and between discontinuous n-electrode **317**. In certain embodiments, discontinuous n-electrode **317** is highly reflective and transparent dielectric **319** is an anti-reflection layer. A first surface of a second carrier substrate **1413**, transparent at the wavelengths of interest, may then be bonded to single-crystalline group-III metal nitride layers **1104**, semi-transparent current-spreading layer **321**, discontinuous n-electrode **317**, and/or transparent dielectric **319**, as shown in FIG. **14**C. An n-side reflector layer **1414** may then be deposited on a second surface of the second carrier substrate **1413**, which can function as an optically transmissive member. Now, light from illumination source **251** passes through an aperture or light receiving surface **1452**, enters carrier substrate **1313** as beam **1453**, and is multiply reflected between p-side reflective electrical contact **113** and n-side reflector layer **1414**.

In certain embodiments, as shown schematically in FIGS. **16**A, **16**B, and **16**C, both n-type and p-type electrical contacts are placed on the same side of an optically transmissive member. In certain embodiments, the optically transmissive member includes or consists of the substrate on which the semiconductor layers were deposited. In other embodiments, the semiconductor layers are removed from the substrate and subsequently bonded to an optically transmissive member. The substrate or the optically transmissive member, together with semiconductor layers and dielectric layers, if present, can define a device cavity region **1669** through which light is multiply reflected as it undergoes absorption within the absorber layer **107**. In certain embodiments the device cavity region **1669** may comprise a portion of an optical cavity region, which may include regions that are filled with air or a gaseous or liquid fluid or a dielectric in addition to the device cavity region **1669**. Some embodiments of optically transmissive members and lateral electrical contacts are described in further detail below.

In one specific embodiment, as shown in FIG. **16**A, electrical contacts are placed on device layers overlying template substrate **1101** and are positioned adjacent to mesas **1651** on template substrate **1101**, which can define a device cavity region **1669**. In the device cavity region **1669**, the optically transmissive member is substrate **101** and the reflective members are p-side reflective electrical contact **113** and n-side reflector layer **1414**. Such a configuration may be advantageous, for example, when template substrate **1101** is electrically insulating. Subsequent to deposition of p-type layer **111** and optional semi-transparent current-spreading layer **321**, trenches **1653** may be formed between adjacent mesas **1651** by lithography and dry etching, using processes that are well known in the art. The depth of trenches **1653** may be chosen so that regions of n-type first non-absorber layer **105** are exposed but such that most of the thickness of n-type first non-absorber layer **105** remains intact under trench **1653**, enabling good lateral electrical conduction with a minimum of ohmic losses. P-side reflective electrical contact **113** may be deposited either before or after formation of trenches **1653**. N-side electrical contacts **1657** may be deposited on exposed portions of n-type first non-absorber layer **105**. An insulating dielectric layer **1655** is disposed between the p-side reflective electrical contact **113** and the n-side electrical contacts **1657**. Insulating dielectric layer **1655** may be deposited, for example, by plasma-enhanced chemical vapor deposition (PECVD), by atomic layer deposition (ALD), or by high density plasma chemical vapor deposition (HDPCVD), and may comprise SiO_2, SiN_x, Al_2O_3, or the like. In some embodiments, insulating dielectric layer **1655** is deposited after one or both of p-side reflective electrical contact **113** and n-side electrical contacts **1657**. In some embodiments, insulating dielectric layer **1655** is deposited before one or both of p-side reflective electrical contact **113** and n-side electrical contacts **1657**. The contact resistance of the n-side electrical contact **1657** is less than 1×10^{-3} Ωcm^2, less than 5×10^{-4} Ωcm^2, less than 2×10^{-4} Ωcm^2, less than 10^{-4} Ωcm^2, less than 5×10^{-5} Ωcm^2, less than 2×10^{-5} Ωcm^2, or less than 10^{-5} Ωcm^2. In preferred embodiments, the contact resistance is less than 5×10^{-5} Ωcm^2. The n-side electrical contact **1657** may comprise at least one of silver, gold, aluminum, nickel, platinum, rhodium, palladium, titanium, chromium, or the like. In certain embodiments, the surface on which the n-side electrical contact is placed is exposed to a $SiCl_4$ plasma to reduce electrical contact resistance prior to deposition of the n-side electrical contact. An n-side reflector layer **1414** may then be deposited on the backside surface **1659** of template substrate **1101**. N-side reflector layer **1414** may include or consist of one or more of silver and aluminum. If necessary, backside surface **1659** is ground and/or polished and, optionally, chemical-mechanically polished prior to deposition of n-side reflector layer **1414** in order to enable a reflectivity greater than 80%, greater than 85%, greater than 90%, greater than 95%, greater than 97%, or greater than 98%. In preferred embodiments, the width of mesas **1651** is much larger than that of trenches **1653** after die singulation, so that very little of light reflected internally between p-side reflective electrical contact **113** and n-side reflector layer **1414** is lost out the sides of the device. In certain embodiments, n-side electrical contacts **1657** may be highly reflective, with a reflectivity greater than 70%, greater than 80%, greater than 90%, or greater than 95%.

In certain embodiments, the device is flip-chipped and both p-type and n-type electrical contacts are placed on the same side of the device structure. Such a configuration may be advantageous, for example, when template substrate **1101** is optically transparent but electrically insulating. Referring to FIG. **17**A, after deposition of p-type layer **111**, two or more vias may be etched through p-type layer **111**, second non-absorber layer **109**, if present, absorber layer **107**, and into n-type first non-absorber layer **105**. The vias may be formed by conventional lithography and a dry etching process such as reactive ion etching (RIE), inductively-coupled plasma (ICP), or chemically-assisted ion beam etching (CAIBE). Insulating dielectric layer **1616** may be deposited on the side walls of the vias, for example, by plasma-enhanced chemical vapor deposition (PECVD), by atomic layer deposition (ALD), or by high density plasma chemical vapor deposition (HDPCVD), and may comprise SiO_2, SiN_x, Al_2O_3, or the like. P-side reflective electrical contact **113** may be deposited on the portion of p-type layer **111** between the vias, and n-side reflective electrical contacts **1614** may be placed within the vias. A dielectric reflector layer **1618** or a metallic n-side reflector layer, may be deposited on the back side of substrate **101**, or template substrate **1101**. Light of a desired wavelength, for example, 405 nanometers or 450 nanometers may enter the photodiode structure **1000** through an aperture or window (not shown) that may include the light receiving surface **252**,

such that emitted light propagates within substrate **101** and the semiconductor layers, and be reflected from the p-side reflective electrical contact **113**, the n-side reflective electrical contacts **1614**, from dielectric reflector layer **1618**, and from an edge reflector (not shown). Light within the device will undergo some scattering from the material disposed within the vias. However, since the areal fraction of the vias is relatively small and their depth is small compared to the thickness of substrate **101**, the scattering will be modest.

In alternative embodiments, vias are placed on the n-side rather than on the p-side, as shown schematically in FIG. **17**B. For example, referring again to FIGS. **13**C, after removal of template substrate **1101**, rather than depositing or bonding n-side reflective electrical contact **1319** to surface **1317**, as shown schematically in FIG. **13**D, instead, two or more vias may be etched through single-crystalline group-III metal nitride layer **1104**, n-type first non-absorber layer **105**, absorber layer **107**, and second non-absorber layer **109**, if present, and into p-type layer **111** or semi-transparent current-spreading layer **321**. Insulating dielectric layers **1616**, p-side reflective electrical contacts **1615**, and n-side reflective electrical contacts **1663** may be placed, analogous to the structures of the photodiode die **1002** shown in FIG. **17**A.

Referring again to FIG. **16**B, in certain embodiments electrical contacts are placed on device layers underlying and lateral to carrier substrate **1313**. Such a configuration may be advantageous when carrier substrate **1313** is optically transparent but electrically insulating, constituting another example of an optically transmissive member. For example, p-side reflective electrical contacts **1661** may be placed in contact with one or more of p-type layer **111**, semi-transparent current-spreading layer **321**, discontinuous p-electrode **315**, and transparent dielectric **319**. Gaps or trenches **1654** adjacent to or surrounding carrier substrate **1313**, into which p-side reflective electrical contacts **1661** are placed, may be formed by one or more of cutting carrier substrate **1313** using a dicing saw, wet or dry etching of carrier substrate **1313**, for example, through a residual portion left over after a saw cut, or bonding placement of multiple, discrete carrier substrates **1313** rather than a single large carrier substrate. N-side reflective electrical contact **1319** may be deposited on the underside of single-crystalline group-III metal nitride layer **1104**.

Referring again to FIG. **16**C, in certain embodiments electrical contacts are placed on device layers overlying and lateral to a second carrier substrate **1413**, which can constitute yet another embodiment of an optically transmissive member. Such a configuration may be advantageous when second carrier substrate **1413** is optically transparent but electrically insulating. For example, n-side reflective electrical contacts **1663** may be placed in contact with one or more of single-crystalline group-III metal nitride layer **1104**, semi-transparent current-spreading layer **321**, discontinuous n-electrode **317**, and transparent dielectric **319**. Gaps or trenches **1656** adjacent to or surrounding second carrier substrate **1413**, into which n-side reflective electrical contacts **1663** are placed may be formed by one or more of cutting second carrier substrate **1413** using a dicing saw, wet or dry etching of second carrier substrate **1413**, for example, through a residual portion left over after a saw cut, or bonding placement of multiple, discrete second carrier substrates **1413** rather than a single large carrier substrate.

In certain embodiments, the photodiode structure **1000** may be characterized prior to singulation. For example, the optical properties, such as transmission or reflection, may be investigated by optical absorption spectroscopy. The morphology of one or more layers may be characterized by differential interference contrast microscopy (DICM, or Nomarski) and/or by atomic force microscopy. The luminescence properties of one or more epitaxial layers may be characterized by one or more of photoluminescence spectroscopy, photoluminescence microscopy, and microfluorescence. The impurity concentrations in one or more layers may be characterized by calibrated secondary ion mass spectrometry (SIMS). The crystallinity of one or more epitaxially grown layers may be characterized by x-ray diffraction. The electrical properties of one or more layers may be characterized by Hall measurements, Van der Pauw measurements, or non-contact resistivity measurements. The contact resistance and series resistance of one or more of the p-side and n-side reflective electrical contacts and of one or more layers may be investigated by transmission line measurements (TLM). The photodiode electrical properties and power conversion efficiency may be characterized by current-voltage (I-V) measurements, either in the dark or under illumination by conventional or laser light sources of various intensities. Minority carrier collection within the photodiode structure **1000** may be quantified by quantum efficiency measurements. The photodiode structure **1000** may be further characterized by electroluminescence measurements.

After wafer-level fabrication, individual photodiode die may be separated, for example, by laser scribing and cleaving, by laser cutting, by stealth dicing, by die sawing, or the like, and packaged. The dicing or cleave direction relative to the crystal axes may be chosen to control the morphology of the edges. For example, c-plane fabricated photodiode wafers, including semiconductor layers, reflective p-type and/or n-type contacts, and other device structures, may be cleaved along the m-plane for a smooth cleaved surface, or along the a-plane for a rough cleaved surface composed of m-plane facets.

FIGS. **18**A-**18**E show simplified schematic diagrams of side views, cross sections, and a plan view of a photodiode die **1002** of a packaged photodiode designed for side illumination through a corner or edge. FIG. **18**E includes sectioning lines that illustrate the viewing position of the views shown in FIGS. **18**A-**18**D. In addition to an n-side reflective electrical contact **114** and a p-side reflective electrical contact **113**, the side edges of one or more absorber layers may be passivated (e.g., also referred to herein as the edge passivation) due to the deposition or formation of a passivation layer or by performing one or more processing techniques (e.g., exposure to plasma-generated ions or radicals, reactive annealing process, etc.) on an existing layer to reduce shunt current paths along the device edges. In certain embodiments, the passivation process includes or consists of a coating and the coating includes or consists of one or more of AlN_x, Al_2O_3, TiO_2, Ta_2O_5, ZrO_2, SiO_2, SiO_x, SiN_x, Si_3N_4, SiO_xN_y, AlO_xN_y, or $Si_uAl_vO_xN_y$. In certain embodiments, the passivation coating or layer is deposited by atomic layer deposition (ALD), chemical vapor deposition (CVD), plasma enhanced chemical vapor deposition (PECVD), high density plasma chemical vapor deposition (HDPCVD), or electron cyclotron resonance (ECR) plasma deposition. In certain embodiments, a deposited passivation layer comprises hydrogen at a concentration greater than 10^{19} cm^{-3}, which passivates dangling-bond point defects at the interface between the semiconductor layers and the passivation layer. In certain embodiments the passivation layer has a lower work function than that of the semiconductor layers. In some embodiments, edge passivation is not utilized in or formed on a photodiode die.

At one location of the edge of the photodiode die, the edge includes an optical window **912**. The optical window **912**

may be coated with an anti-reflection optical window layer **911**, while the remainder of the perimeter of the edge may be coated with an edge reflector layer **905**. In some embodiments, the optical window **912** portion of the edge includes a surface that has a desired roughness or texture, in lieu of or in addition to the anti-reflection optical window layer **911**. In certain embodiments the optical window **912** is placed at a corner. In other embodiments the optical window **912** is placed away from a corner. The area of the optical window **912** may be less than about 40%, less than about 30%, less than about 20%, less than about 10%, less than about 5%, less than about 2%, less than about 1%, less than about 0.5%, less than about 0.2%, or less than about 0.1% of the surface area of at least one absorber area, as measured in a plane parallel to large-area surface **102**. The anti-reflection optical window layer **911** may comprise at least one of MgF_2, SiO_2, Al_2O_3, HfO_2, $LaTiO_3$, Si_3N_4 or TiO_2 and may be deposited by electron beam deposition, sputtering, or other suitable deposition techniques. In certain embodiments, the anti-reflection optical window layer **911** is textured. In certain embodiments, the angle between the surface normal of the edge of the optical window **912** and the surface normal of the substrate can deviate from 90 degrees. The optical window **912** may comprise one or more planar layers and/or textured structures. In certain embodiments the orientation of the optical window **912** is parallel to the edge of the die. In other embodiments, the optical window has an outer orientation that is not parallel to the edge of the die, for example, to minimize optical losses upon coupling to a fiber at non-normal incidence angle. The edge reflector layer may comprise at least one of silver, gold, aluminum, platinum, rhodium, palladium, chromium, or the like, and may be deposited by electron beam deposition or sputtering. In certain embodiments, the edge reflector layer may include dielectric layers to enhance edge reflection. Light entering the optical window **912** makes multiple passes through the combination of semiconductor layers (including non-absorber, absorber, and p-type contact semiconductor layers) **915** (FIGS. **18**C-**18**D) that are disposed on the substrate.

The die may be attached to one or more of a lower heat sink **901** or an upper heat sink **909**. A separate submount may also be provided and positioned between the die and lower heat sing **901** or upper heat sink **909**. The heat sink and the submount may include a layer and/or a plate or other shape that comprises at least one of copper, aluminum, silicon, silicon carbide, sapphire, aluminum nitride, beryllium oxide, diamond, or the like. The photodiode die **1002** may be attached to the heat sink and/or to the submount by one of a Au/Sn eutectic, a Au/Ge eutectic, or the like bonding layer.

FIGS. **19**A, **19**B, **19**C, **19**D, and **19**E show schematic illustrations of cross-sectional and plan views, respectively, of the light path from an optical fiber **1001** into the photodiode die **1002**. The optical fiber **1001** described in relation to FIGS. **19**A-**19**E is similarly configured as the optical fiber **3180**, which is described in greater detail below. In these figures, the X-direction is chosen to lie in the plane of the photodiode die (i.e., parallel to large-area surface **102**) along a first direction, the Y-direction is chosen to lie in the plane of the die, perpendicular to the X-direction, and the Z-direction is chosen to be perpendicular to the plane of the die. The optical fiber **1001**, which may have an anti-reflection coating **1003**, is coupled to the optical window **912** at an angle α with respect to the plane of the photodiode die (cf. FIG. **19**A) and an angle β with respect to an edge **1902** of the die (cf. FIG. **19**B). The plane of the photodiode die is generally parallel to a major surface of the semiconductor layers **915**, which, in one example, is parallel to the X-Y plane in FIG. **19**A. In some embodiments, as illustrated in FIG. **19**B, the optical fiber **1001** is coupled to the photodiode die such that it also includes an angle Δ with respect to an edge **1901** (e.g., light receiving edge in FIG. **19**B of the photodiode die **1002**. Deviation of angle α from zero degrees causes the light that enters the die to undergo multiple reflections from the reflective p-type contact and from the reflective n-type contact. In certain embodiments, total internal reflection may be exploited in the top and bottom mirrors. In certain embodiments, the value of α is chosen to be between 0 and about 50 degrees, between 0 and about 40 degrees, between 0 and about 20 degrees, or between 0 and about 5 degrees, or even between 0.1 and 5 degrees. Deviation of angle β from zero degrees causes the light that enters the die to undergo multiple reflections from edge reflector layers and illuminate the entire die volume. With a relatively small value of β, the light bounces incrementally from one edge of the photodiode die to another (FIG. **19**B). With a larger value of β the light traverses the die with fewer bounces (FIG. **19**C). In certain embodiments, the value of β is chosen to be between 0 and about 60 degrees, between 0 and about 20 degrees, between 0 and about 10 degrees, between 10 and about 30 degrees, or between about 30 and about 50 degrees. In certain embodiments the die may be narrow in the Y-direction, for example, with a width between 5× and 0.5× the thickness of the die, between 2× and 0.8× the thickness of the die, or between 1.5× and 1× the thickness of the die, and the value of may be small, for example, less than about 20 degrees, less than about 10 degrees, less than about 5 degrees, or approximately zero, so that the light travels to the distal end of the die and is then reflected back along approximately the same path. In certain embodiments, efficient reflection from the edges of the die may be facilitated by making use of total internal reflection, that is, ensuring that incident angle of the internal light rays relative to the surface normal is greater than $(360/(2\pi))*\arcsin(n_1/n_2)$ degrees, where n_1 is the exterior refractive index and n_2 is the interior refractive index. In certain embodiments, the value of angle Δ is chosen to be between 0 and about 20 degrees, between 0 and about 10 degrees, or between 0 and about 5 degrees, or even between 0.1 and 5 degrees.

One or more optical fibers may be coupled to the photodiode die using a fixture that includes one or more of a connector and a ferrule by methods that are known in the art. In one embodiment, as illustrated in in FIG. **36**, a fixture **3601** includes a supporting structure **3611**, mounting plate **3610** and mounting elements **3620** that are configured to position, support and align the light emitting end **3182** of an optical fiber **3180** relative to an edge **1901** (e.g., FIGS. **19**B and **36**) or surface (e.g., n-side reflective electrical contact containing surface in FIGS. **33**A-**33**I) of a photodiode die **1002**. The optical fiber **3180** is positioned on and attached to a surface **3609** of the mounting plate **3610** by use of the mounting element **3620**. The mounting element **3620** can include a simple clamping device that is configured retain a portion of the optical fiber. However, in some embodiments, the mounting element **3620** may include one or more retaining features that are configured to support a connector or ferrule that are coupled to a portion of the optical fiber **3180**. The photodiode die **1002** is also positioned on and attached to the surface **3609** of the mounting plate **3610**. In some embodiments, the photodiode die **1002** is bonded to or clamped to the surface **3609** of the mounting plate **3610** by use of removable clamps, fastening elements, adhesives, metallic or ceramic bonding layers, or other similar devices

or device retaining methods known in the art. In some embodiments, the photodiode die **1002** includes a heat sink **901** that is disposed between the active regions of the photodiode die **1002** and the surface **3609** of the mounting plate **3610**. In some embodiments, a submount (not shown) is positioned between photodiode die **1002** and heat sink **901**. In some embodiments, the relative positions of a first end (i.e., light emitting end **3182**) of the optical fiber **3180**, the principal axis **3183**A (FIGS. **31**B and **36**) of the optical fiber, a first edge and a second edge of the photodiode die are controlled to a tolerance between about 1 micrometer and about 1 millimeter, or between about 1 micrometer and about 100 micrometers, or between about 2 micrometers and about 50 micrometers, or between about 3 micrometers and about 25 micrometers. In some embodiments, the fixture is configured to position the radiation emitting end **3182** of the optical fiber a first distance **3630** (FIG. **36**) from a surface of the optical window **912**, wherein the first distance is between about 2 micrometers and about 10 millimeters. In configurations where the radiation emitting end **3182** of the optical fiber **3180** is not parallel to an edge **1901** of the photodiode die **1002** or surface of the optical window **912**, the first distance can be measured from a point where the principal axis **3183**A extends through the radiation emitting end **3182** of the optical fiber **3180** to the center of emitted radiation that impinges on the surface of the optical window **912** or the edge **1901** of the photodiode die **1002**. Similarly, in configurations where the radiation emitting end **3182** of the optical fiber **3180** is not parallel to a light receiving surface of an optical coupling member **3187** (FIGS. **33**A-**33**E) or light receiving surface of an optical waveguide **3190** (FIGS. **31**A-**32**), the first distance (e.g., distance Di in FIG. **31**B) can be measured from a point where the principal axis **3183**A extends through the radiation emitting end **3182** of the optical fiber **3180** to the center of emitted radiation that impinges on the light receiving surface of the optical coupling member **3187** or optical waveguide **3190**.

The fixture generally provides a structure that is used for holding the relative positions of the light emitting end **3182** of the optical fiber **3180** relative to the light receiving edge **1901** of the photovoltaic die **1002** constant to within a tolerance between about 1 micrometer and about 1 millimeter. In some embodiments, the mounting plate **3610** is formed from a material that has a coefficient-of-thermal expansion (CTE) that matches the CTE of the optical fiber **3180** and/or photodiode die **1002** to help maintain the desired tolerance during operation of the photodiode package. In one example, the mounting plate **3610** includes a material such a Kovar®, Invar or other materials that have a CTE that is similar to the materials from which the optical fiber **3180** and/or photodiode die **1002** are formed.

In certain embodiments, ends of the one or more optical fibers, which may include or consist of one or more of silica, glass, and plastic and may be single mode or multimode, may be attached to a ferrule by an adhesive such as epoxy. The ferrule, which may be used in the fixture, may consist of or include a ceramic, stainless steel, aluminum, copper, or plastic. The end face of the ferrule may be polished, along with the ends (i.e., radiation emitting ends **3182**) of the one or more optical fibers. The ferrule may be attached to the fixture by means of a connector. The position of the photodiode die **1002** within the fixture may be determined by precisely controlling the lateral dimensions of the die, for example, to better than 100 micrometers, to better than 50 micrometers, to better than 25 micrometers, or to better than 10 micrometers, and by positioning a first edge (e.g., edge **1901**) and a second edge of the die, a submount to which the die is attached, or a heatsink **901** to which the submount is attached, against features in the fixture. As noted above, the photodiode die **1002** may be attached to the mounting plate **3610** of the fixture **3601** by one or more of gold-tin solder, a Au—Au-thermocompression bond, epoxy, silver epoxy, sintered silver interface material, or thermal adhesives. One or more of a submount and a heatsink may be included in the thermal and mechanical path between the photodiode die and the fixture. Each of the photodiode die and the submount, the submount and the heatsink, and the heatsink and the fixture may be bonded by one or more of gold-tin solder, a Au—Au-thermocompression bond, epoxy, silver epoxy, sintered silver interface material, or thermal adhesives. The submount may consist of or include one or more of silicon, glass, sapphire, silicon carbide, beryllium oxide, diamond, copper tungsten alloy, or aluminum nitride. The heatsink **901** may consist of or include one or more of copper and aluminum.

The edge-optical-coupling geometries shown in FIGS. **19**A-**19**D have a number of advantages, including simplicity and easy achievement of high optical reflectivities from the front and back surfaces of the device due to the high incident angle of the light received from the optical fiber **1001**. However, these geometries may also have some drawbacks, which are addressed in the alternative geometries described below. For example, without incorporating focusing optics, the optical coupling may be most efficient with an edge-coupling geometry if the device is thicker than the diameter of the optical fiber, or at least thicker than the diameter of the core of the optical fiber. As GaN, sapphire, and other substrate thicknesses are often of the order of 300 micrometers, this may be a challenge for certain optical fibers. For example, in certain embodiments, optical fiber **1001** may be a single mode fiber, with a diameter of the fiber core below about 15 micrometers. However, in other embodiments, which may be useful for high-power applications where the power being transmitted from one or more laser diodes is above 1 watt, above 2 watts, above 5 watts, above 10 watts, above 20 watts, or above 50 watts, optical fiber **1001** may be a multimode fiber, with a diameter of the fiber core between about 25 micrometers and about 500 micrometers, between about 40 micrometers and about 300 micrometers, or between about 50 micrometers and about 200 micrometers. In still other embodiments optical fiber **1001** is actually an optical fiber bundle, or fiber optic bundle, with an overall diameter between about 100 micrometers and about 5 millimeters, or between about 200 micrometers and about 2 millimeters, or between about 250 micrometers and about 1 millimeter. A second challenge is that quite precise alignment between the fiber and the device may be required to assure that a desired fraction of optical radiation is delivered to the photodiode die **1002**. A third challenge is that, due to a high intensity of light during the initial passes through the absorber layer or active region, a high density of electron and hole carriers may be generated in certain locations within the photodiode, causing a high concentration of carriers within the absorber layer and possibly-significant non-radiative Auger recombination processes that will lead to a loss of efficiency. The active region will generally include the absorber layer, which may include one or more layers that have differing compositions and/or material characteristics.

In certain embodiments, as illustrated schematically in FIG. **19**E, light is transmitted from a fiber, which is oriented approximately perpendicular to the surface of the die (i.e., the Z-direction), to a surface of a mirror **1005** and into the edges of one, two, three, four, or more die simultaneously.

This geometry may be advantageous for enhancing the optical coupling and leveraging a mature commercial supply chain for fiber coupling fixtures.

The side-entrance die geometry illustrated in FIGS. **19**A, **19**B, **19**C, and **19**D has the advantage of relative simplicity and ease of fabrication. However, in these embodiments it may be beneficial if the substrate is maintained at a thickness greater than that of the optical fiber or fiber bundle, for example, approximately 100 micrometers, 200 micrometers, 300 micrometers, or 500 micrometers. In addition, the relatively long path length, created by the orientations shown in FIGS. **19**A-**19**D of the optical radiation delivery into the side-entrance die geometry configuration, will necessitate minimizing the optical absorption coefficient of the substrate in embodiments where the substrate constitutes the optically transmissive member. In certain embodiments, as illustrated in FIGS. **27**A and **27**B, light is coupled into a second optically transmissive member **2101** affixed to the first optically transmissive member (e.g., the substrate **101**), or in some embodiments, affixed directly to the edge reflector layers **905**, to achieve efficient light spreading laterally through the device. In these embodiments the optical cavity region may include second optically transmissive member **2101** in addition to substrate **101**, the latter of which is a major component of the device cavity region. In certain embodiments, such as that shown in FIG. **14**B, substrate **101** has been removed, and second optically transmissive member **2101** may be optically coupled directly to semiconductor layers **915**. The second optically transmissive member may consist of or include SiO_2 or Al_2O_3, or the like. In certain embodiments, total internal reflection may be exploited in the second optically transmissive member. In certain embodiments, reflective structures comprised of dielectric and metal layers may be disposed on one or more of the second optically transmissive member surfaces to enhance internal reflections. In some embodiments, the interface between the second optically transmissive member and the group III-N substrate is roughened or patterned with RMS height variation between 30 nanometers and 100 micrometers, or between 50 nanometers and 10 micrometers. In some embodiments, one or more surfaces on the second optically transmissive member are roughened. In some embodiments, one or more surfaces on the second optically transmissive member are roughened. In some embodiments, dielectric anti-reflective coating layers are deposited on the group III-N surface. In certain embodiments, second optically transmissive member **2101** is chosen to be thicker than the diameter of an optical fiber coupled to it in an assembly.

FIGS. **20**A-**20**E show simplified schematic diagrams of side views, cross sections, and a plan view of a photodiode die **1002** of a packaged photodiode designed for top or bottom illumination near a corner or edge. FIG. **20**E includes sectioning lines that illustrate the viewing position of the views shown in FIGS. **20**A-**20**D. Edge passivation, anti-reflection window coating **1111**, edge reflection layers **905**, and the like, are similar to those described in conjunction with FIGS. **19**A-**19**E except for the location of the optical window (or entrance aperture) to the photodiode die. However, in certain embodiments the backside of the substrate, together with the reflective n-type electrical contact, is shaped so that light incident into the die though the optical window **1119** with an anti-reflection coating **1111** is reflected back at a different angle, causing the light to spread laterally through the die via subsequent reflections with the reflective p-type and n-type layers. In certain embodiments the orientation of the optical window **1119** is parallel to the top or bottom surface of the die. In other embodiments, the **1119** optical window has an outer orientation that is not parallel to the top or bottom surface of the die, for example, to minimize optical losses upon coupling to a fiber at non-normal incidence angle.

In certain embodiments, a reflective member **2020** (FIG. **20**C) in contact with the substrate or optically transmissive member changes the propagation direction of light within the device cavity region by more than about 30 degrees, more than about 45 degrees, or more than about 60 degrees. In some embodiments, the reflective member **2020** changes the propagation direction of first reflection of light entering the device cavity region by between about 40 degrees and about 140 degrees. These embodiments may enable efficient coupling to fibers having a diameter larger than the thickness of the substrate and may also be advantageous for the robustness and stability of the optical coupling or to leverage a mature commercial supply chain for fiber coupling fixtures.

FIGS. **21**A and **21**B are schematic illustrations of cross-sectional and plan views, respectively, of the light path from an optical fiber into the top/edge-illuminated photodiode die similar to the configuration shown in FIGS. **20**A-**20**E. The fiber is coupled to the optical window with an anti-reflection coating **1111** at an angle γ with respect to a surface normal of the photodiode die (cf. FIG. **21**A). In certain embodiments, the value of γ is chosen to be between 0 and about 60 degrees, between 0 and about 40 degrees, between 0 and about 20 degrees, or between 0 and about 5 degrees, or even between 0.1 and 5 degrees. Deviation of angle γ from zero degrees causes the light that enters the photodiode die to undergo multiple reflections from the reflective p-type contact and from the reflective n-type contact. However, in this case, due to one or more nonplanar features in the reflector (e.g., n-side reflective electrical contact **114** layer in FIG. **21**A) opposite the optical window (or entrance aperture) **1119** (FIGS. **20**E and **21**A-**21**B) formed in the p-side reflective electrical contact **113**, light is reflected in various lateral directions away from the entrance aperture **1119** (FIG. **21**B). In certain embodiments, total internal reflection may be exploited in the edge mirrors.

FIGS. **22**A-**22**E show simplified schematic diagrams of side views, cross sections, and a plan view of a photodiode die for a packaged photodiode designed for top or bottom illumination at the center or in a middle position of the die. Edge passivation, anti-reflection coatings, edge reflection layers, and the like are similar to those described in conjunction with FIGS. **18**A-**18**E except for the location of the optical window or entrance aperture to the photodiode die. However, in certain embodiments the backside of the substrate (e.g., heat sink **901** side), together with the n-side reflective electrical contact **114**, is shaped so that light incident into the die though the optical window (i.e., entrance aperture **1119**) with an anti-reflection coating **1111** is reflected back at a different angle, causing the light to spread laterally through the die via subsequent reflections with the reflective p-type and n-type layers. In certain embodiments, the reflective n-type electrical contact **114** has a conical or pyramidal feature formed therein so that light incident from the entrance aperture is reflected laterally in multiple directions away from the entrance aperture **1119**.

The top (or bottom)-entrance die geometry illustrated in FIGS. **22**A-**22**E may require fabrication that is somewhat more complicated than that of an edge-entrance design, which is discussed above (e.g., FIGS. **2**, **13**D, **14**B, **17**, **19**A, etc.). For example, non-planar features must be placed in or formed on the substrate, either before or after deposition of the semiconductor and reflective p-type contact layers and

before deposition of the reflective n-type layer. The nonplanar features (e.g., hemispherical, pyramidal or conical) may be formed by at least one of lithography, laser ablation, grinding, wet etching, and dry etching. Residual surface damage from a laser, grinding, or dry etch process may be removed by wet etching. In certain embodiments the substrate is thinned before formation of the nonplanar features, for example, to a thickness below 300 micrometers, below 200 micrometers, below 100 micrometers, below 50 micrometers, or below 25 micrometers. Substrate thinning may be performed by at least one of lapping, grinding, polishing, chemical mechanical polishing, dry etching, and wet etching. In certain embodiments, the substrate **101** is removed from the device altogether.

FIGS. **18**A-**22**E show die that have a predominantly rectangular or square perimeter. In other embodiments, the die has a triangular, trapezoidal, or hexagonal perimeter. In still other embodiments at least one portion of the edge of the die is curved, for example, following a circular or elliptical contour. Other perimeters are also possible and within the scope of this invention. In certain embodiments, one or more electrical contacts to the die are made at one or more of its edges in addition to or instead of to top or bottom surfaces.

In certain embodiments, one or more optical components are utilized to spread out optical radiation exiting from an optical fiber along at least one dimension prior to introduction into the photodiode. Such configurations may be useful, for example, to reduce the maximum carrier concentration in regions of the absorber layer near the entrance of optical radiation into the photodiode, reducing the extent of nonradiative Auger recombination and increasing the efficiency of the photodiode and of the optical system.

FIGS. **31**A-**31**E are simplified schematic diagrams of side views, cross sections, and top and bottom views of a packaged photodiode designed for side illumination through a corner or edge through an optical coupling member **3187** of an optical waveguide **3190**. FIG. **31**A is a side view of a packaged photodiode that is optically coupled to the optical fiber **3180**, as viewed by the sectioning line shown in FIG. **31**C. FIG. **31**B is a side cross-sectional view of the packaged photodiode as viewed by the sectioning line shown in FIG. **31**C. FIG. **31**C is a top view of the packaged photodiode as viewed by the sectioning line shown in FIG. **31**A. FIG. **31**D is a top cross-sectional view of the packaged photodiode as viewed by the sectioning line shown in FIG. **31**A. FIG. **31**E is a bottom view of the packaged photodiode as viewed by the sectioning line shown in FIG. **31**A.

Referring to FIG. **31**A-**31**E, in certain embodiments, an optical waveguide **3190** or light pipe having a low optical absorption coefficient at a predetermined wavelength is coupled optically to both an optical fiber **3180** and a photodiode die **1002** of a photodiode package, spreading optical radiation exiting from the optical fiber **3180** in a lateral direction (i.e., Y direction) so as to homogenize the optical radiation intensity within the device cavity region **1669**, enabling higher efficiency for a given optical power than a comparative design without the optical waveguide **3190**.

An optical fiber **3180** may include fiber core **3183** and fiber cladding **3181** and may be positioned in close proximity to one edge of the photodiode die **1002** of the packaged photodiode by means of a fixture (e.g., fixture **3601** of FIG. **36**), as is known in the art. The optical fiber **3180** includes a principal axis **3183**A, which is the central axis of fiber core **3181**, and is often referred to herein as a reference to a direction that radiation is emitted from the radiation emitting end **3182**, which is often referred to herein as the first end, of the optical fiber **3180**. Referring to FIG. **31**B, in one example, the principal axis **3183**A is parallel to the X-axis. The fiber core **3183** may include or consist of silica, glass, or plastic and the fiber cladding **3181** may include or consist of a dielectric composition, such as a glass or a plastic, having a lower refractive index than that of optical core **3183** in order to confine the optical radiation by total internal reflection, as is known in the art. At one location of the edge of the photodiode die **1002**, the edge may be coated with an anti-reflection optical window layer **911**, while the remainder of the perimeter may be coated with an edge reflector layer **905**. The photodiode die **1002** may be attached to one or more of a lower heat sink **901** or an upper heat sink **909**. The heat sink may include a layer and/or a plate or other shape that comprises at least one of copper, aluminum, or the like. The photodiode die **1002** may be attached to the heat sink **909** by one of a Au/Sn eutectic, a Au/Ge eutectic, or the like bonding layer. In preferred embodiments, optical coupling member **3187** is highly transparent at one or more wavelengths of the radiation that is absorbed by the absorber layer of the photodiode die **1002**. In certain embodiments, optical coupling member **3187** consists of or includes one or more of silica glass, borosilicate glass, aluminosilicate glass, high-refractive-index glass, another glass composition, sapphire, quartz, zinc oxide, $MgAl_2O_4$ spinel, another crystalline composition, polycarbonate, polymethylmethacrylate, or another polymer composition. In certain embodiments, one or more surfaces of optical coupling member **3187** is coated with reflective coating **3185**. Reflective coating **3185** may include one or more of silver, gold, platinum, nickel, aluminum, or a dielectric such as TiO_2, Ta_2O_5, ZrO_2, SiO_2, SiO_x, SiN_x, Si_3N_4, SiO_xN_y, Al_2O_3, or MgF_2. Reflective coating **3185** may have a reflectivity at a preselected wavelength greater than 85%, greater than 90%, greater than 95%, greater than 98%, or greater than 99% at the one or more wavelengths absorbed by the absorber layer. In some embodiments, the one or more wavelengths of the radiation are within a region between 400 nm and 550 nm. One or more of entrance aperture **3189** and the side of optical coupling member **3187** facing the photodiode die may be coated with an anti-reflection coating. The anti-reflection coating may include a material selected from a group including MgF_2, SiO_2, Al_2O_3, HfO_2, $LaTiO_3$, Si_3N_4 or TiO_2 and may be deposited by electron beam deposition, sputtering, or other suitable deposition techniques.

Referring to FIGS. **31**A and **31**B, optical radiation provided from the optical fiber **3180** is coupled into the device cavity region **1669** (FIG. **31**B) of the photodiode die **1002** without significant spreading in the Z-direction, perpendicular to the semiconductor layers of the photodiode, with an angle that is determined by the geometry of optical coupling member **3187** and is chosen to enable high reflectivity from the reflective layers and multiple passes through the absorber layer for efficient optical absorption. As discussed herein, the device cavity region **1669** will include the active region that includes one or more semiconductor layers **915**, such as one or more of the non-absorber, absorber, and p-type contact semiconductor layers, and the substrate **101**. Referring to FIGS. **31**C and **31**D, optical radiation is coupled from the optical fiber **3180** is coupled into the device cavity region **1669** of the photodiode die **1002** with significant spreading in the direction parallel to the edge of the semiconductor layers **915** of the photodiode die **1002** (i.e., Y direction), with an angle that is determined by the geometry and shape of the optical coupling member **3187** and is chosen to enable significant spreading in the lateral

dimension, a reduced carrier concentration in regions of the absorber layer close to the entrance aperture **3189**, and a high conversion efficiency.

In alternative embodiments, entrance aperture **3189** is chosen to be convex vertically (i.e., in the Z-direction (not shown)), to collimate to collimate or lightly focus the optical radiation in the vertical direction, and concave in the lateral direction (i.e., Y direction (not shown)) to spread optical radiation more rapidly laterally. In certain embodiments, curvature is added to the radiation emitting end **3182** of the optical fiber **3180** to change the angular distribution of the emitted radiation. In certain embodiments, optical coupling member **3187** and/or the photodiode die **1002** are non-rectangular in the X-Y plane. In certain embodiments, an edge of the optical coupling member **3187** and/or the photodiode die **1002** are non-linear. The optimal design will depend on photodiode parameters such as substrate absorption coefficient, substrate refractive index, active region effective absorption coefficient and thickness, n and p contact reflectivities, edge reflectance, and the like. The material for optical coupling member **3187** may be chosen for a close match to the refractive index of the device cavity region **1669**, in which case anti-reflection optical window layer **911** disposed over the optical window **912** may not be needed.

In another set of embodiments, as shown schematically in FIG. **32**, optical radiation is coupled from fiber core **3183** into the photodiode die **1002** by means of an integrating sphere **3293**. Optical radiation may enter cavity **3291** of integrating sphere **3293** through the entrance aperture **3189** and may impinge on anti-reflection optical window layer **911** of the optical window **912** disposed at the entrance to the device cavity region **1669**. In certain embodiments, integrating sphere **3293** has a shape that is a section of a sphere, an ellipsoid, a paraboloid, or other non-spherical shape. Optical radiation from device cavity region **1669** may pass through semiconductor layers **915** and substrate **101**, if present, reflect from p-side reflective electrical contact **113**, exit device cavity region **1669**, and impinge on an interior surface **3294** of the integrating sphere **3293**. In certain embodiments, reflection on an interior surface **3294** of integrating sphere **3293** is diffuse, due to the incorporation of a coating, surface texture, surface features or other light distributing features. In certain embodiments, the interior surface **3294** of integrating sphere **3293** is coated with a diffuse reflector, which may include or consist of titania (TiO_2). In certain embodiments, substrate **101** is removed, for example, as illustrated schematically in FIG. **14**B. In some embodiments, such as that illustrated schematically in FIG. **32**, the optical cavity region encompasses both the device cavity region **1669** and cavity **3291**.

In certain embodiments, the geometry of entrance aperture **3189** and integrating sphere **3293** are chosen so that light entering cavity **3291** may undergo reflection from an interior surface **3294** of integrating sphere **3293** before impinging on anti-reflection optical window layer **911**. In certain embodiments aperture **3189** includes or consists of a transparent window, which may contain an anti-reflection coating (not shown). In certain embodiments, cavity **3291** is filled with a transparent liquid or gas rather than air. In certain embodiments, the transparent liquid or gas includes or consists of one or more of a silicone, an epoxy, a perfluorinated compound, and a polymer. In certain embodiments, cavity **3291** is maintained at a sub-atmospheric pressure to avoid scattering of the optical radiation. In certain embodiments, the photodiode is flip-chipped and n-side electrical connections are made through n-type contacts **1614**, as illustrated schematically in more detail in FIGS. **17**A and **17**B.

In another set of embodiments, optical radiation at the one or more wavelengths that is provided from an optical fiber is coupled through transparent openings in the n-side electrical contact, such as the n-side reflective electrical contact **3317** shown schematically in FIGS. **33**A-**33**I. FIGS. **33**A-**33**I are simplified side views of a packaged photodiode designed for illumination through a surface of the photodiode die **1002** that includes the n-side reflective electrical contact. Referring to FIG. **33**A, in certain embodiments device cavity region **1669** of photodiode die **1002** consists of or includes substrate **101** and the semiconductor layers **915**. The optical cavity region **3301**, as described below, may include the device cavity region **1669**. In some embodiments, such as shown schematically in FIGS. **13**C and **14**B, substrate **101** has been removed and device cavity region **1669** may include semiconductor layers **915**, such as p-type layer **111**, second non-absorber layer **109**, absorber layer **105**, and n-type non-absorber layer **103** bonded to p-type reflective contact **113** or p-side reflective layer **1315** but may not include a separate optically transmissive member (FIG. **14**B). Photodiode die **1002** may include n-side reflective electrical contact **3317** and dielectric layer **3319** that are disposed on a surface of the photodiode die **1002**. In preferred embodiments, n-side reflective electrical contact **3317** has a gridded structure, with an open area greater than 50%, greater than 75%, greater than 80%, greater than 90%, or greater than 95% in a plane that is parallel to the side of the photodiode die **1002** that includes the n-side electrical contact (e.g., X-Y plane), and is highly reflective. The openings formed in n-side reflective electrical contact **3317** may be filled with dielectric layer **3319**, which may consist of or include an anti-reflection coating. Optical coupling member **3187** may have reflective coating **3185** covering most of its periphery, with anti-reflection coatings on entrance aperture **3189** and on exit aperture **3388**. Optical coupling member **3187** may have a conical, square-pyramidal, rectangular-pyramidal, triangular-pyramidal, hexagonal-pyramidal, cubic, rectangular-prism, spherical, ellipsoidal, paraboloidal, or other similar shape. Optical radiation from optical fiber core **3183** may be focused by fiber coupling lens **3390** onto entrance aperture of optical coupling member **3187**. One or both large-area surfaces of fiber coupling lens **3390** may be covered with an anti-reflection coating **3391** (e.g., MgF_2). In certain embodiments, an anti-reflection coating **3392** is present on the emitting end of fiber core **3183**. In embodiments described by FIG. **33**A, optical coupling member **3187** functions as a portion of the optical cavity region **3301**, which includes the device cavity region **1669**, in which optical radiation incident through entrance aperture **3189** undergoes multiple reflections as it undergoes optical absorption within absorber layer **107**, and optical radiation may undergo multiple passes through dielectric layer **3319** and exit aperture **3388**. Similarly, optical radiation that is emitted (e.g., luminescent light) within absorber layer **107**, that is, where electrons and holes recombine radiatively rather than being separated and collected by the p-side reflective electrical contact **113** and the n-side reflective electrical contact **3317**, may undergo multiple reflections within the optical cavity before being reabsorbed within absorber layer **107** (so-called photon recycling). The use of fiber coupling lens **3390** enables optical radiation from optical fiber core **3183** to be focused onto an area smaller than the cross sectional area of the fiber core, enabling entrance aperture **3189** to be relatively small and to

minimize loss of reflected or luminescent optical radiation outward through entrance aperture **3189**. When the medium between the fiber coupling lens and the focal plane has a refractive index of 1, the focused area can be reduced by up to a factor of NA^{-2}, relative to the area of the fiber core, where NA is the numerical aperture of the optical fiber.

Variations of this approach, where optical radiation is coupled into the photodiode die **1002** through the n-side reflective electrical contact **3317** rather than through an optical window **912**, **1119** on the edge or top of the device, are possible. For example, a transparent, index-matched adhesive **3394** may be provided between optical coupling member **3187** and n-side reflective electrical contact **3317** and dielectric layer **3319**, as shown schematically in FIGS. **33**B-**33**E. Fiber coupling lens **3390** may be provided on the end of optical fiber core **3183** rather than as a discrete element, as shown schematically in FIG. **33**C. Fiber coupling lens **3390** may be omitted, as shown schematically in FIGS. **33**D and **33**E. Optical radiation may pass from optical fiber core **3183** into entrance aperture **3189** through a transparent, index-matched adhesive **3394**, as shown schematically in FIG. **33**D, or through anti-reflection coating **3392** on the end of fiber core **3183**, as shown schematically in FIG. **33**E. In alternative embodiments, optical radiation may be coupled into the photodiode die **1002** through openings in the p-side reflective electrical contact rather than through openings in the n-side reflective electrical contact.

Rather than coupling optical radiation from an optical fiber **3180** into a relatively large area through many openings in the n-side reflective electrical contact **3317**, as in FIGS. **33**A-**33**E, the optical radiation may be coupled into photodiode entrance aperture **3396** in n-side reflective electrical contact **114**, as shown schematically in FIGS. **33**F-**33**I. Photodiode entrance aperture **3396** may be coated with an anti-reflection layer (not shown), similar to the anti-reflection optical window layer **911** of the optical window **912** described above in the discussion of FIGS. **18**A-**22**E. In these embodiments the optical cavity region **3301** encompasses device cavity region **1669**, but not an external integrating optical cavity. In preferred versions of this embodiment, device cavity region **1669** includes at least one of a substrate or an optically transmissive member, as described above. Optical radiation from optical fiber core **3183** may be focused onto photodiode entrance aperture **3396** by fiber coupling lens **3390**, either as a free-standing element (FIG. **33**F) or coupled to the end of optical fiber core **3183** (FIG. **33**G). Alternatively, optical radiation from optical fiber core **3183** may be coupled directly to entrance aperture **3396**, through an anti-reflection coating **3392** on the end of optical fiber core **3183** (FIG. **33**H) or through a transparent, index-matched adhesive **3394** (FIG. **33**I). In certain embodiments, the area of the optical window, or photodiode entrance aperture on the edge of photodiode die **1002**, is between about 1% and about 20%, or between 2% and about 10%, of the area of the edge of photodiode die **1002**.

In still another set of embodiments, optical radiation is coupled from an optical fiber **3180** to an optical window **912** on an edge of the photodiode die **1002** using additional optical elements, as shown schematically in FIGS. **34**A-**34**I. In one or more of the embodiments disclosed herein, the area of the optical window **912** can be between about one percent and about twenty percent of the surface area of the edge of the photodiode die **1002**. In one or more alternate embodiments, the area of the optical window **912** can be greater than 20 percent, such as greater than 50 percent, or between 50 and 100 percent, or even between 80 and 99.9 percent of the surface area of the edge or side of the photodiode die **1002**. FIGS. **34**A-**34**I are simplified side cross-sectional views of a packaged photodiode designed for illumination through an edge of the photodiode die **1002**. Referring to FIG. **34**A, the device cavity region **1669** includes a substrate or optically transmissive member **3401** and semiconductor layers **915** (not shown), similar to FIG. **31**A-E. Photodiode die **1002** may include n-side reflective electrical contact **114** and p-side reflective electrical contact **113**. Optical coupling member **3187** may have reflective coating **3185** covering most of its periphery, with anti-reflection coatings on entrance aperture **3189** and exit aperture **3388**. Optical coupling member **3187** may have a conical, square-pyramidal, rectangular-pyramidal, triangular-pyramidal, hexagonal-pyramidal, cubic, rectangular-prism, spherical, ellipsoidal, paraboloidal, or other similar shape. Optical radiation from optical fiber core **3183** may be focused by fiber coupling lens **3390** onto entrance aperture **3189** of optical coupling member **3187** and then enter optically transmissive member **3401** through optical window **912**, which may include an anti-reflection optical window layer **911**. One or both large-area surfaces of fiber coupling lens **3390** may be covered with an anti-reflection coating **3391**. In certain embodiments, an anti-reflection coating **3392** is present on the radiation-emitting end of fiber core **3183**. In embodiments described by FIG. **34**A, optical coupling member **3187** functions as a portion of the optical cavity region **3301**, along with substrate or device cavity region **1669**, in which optical radiation incident through entrance aperture **3189** undergoes multiple reflections as it undergoes optical absorption within absorber layer **107** (not shown). Similarly, optical radiation that is emitted within absorber layer **107**, that is, where electrons and holes recombine radiatively rather than being separated and collected by the p-side reflective electrical contact **113** and the n-side reflective electrical contact **114**, may undergo multiple reflections within the optical cavity region before being re-absorbed within absorber layer **107** (so-called photon recycling). The use of fiber coupling lens **3390** enables optical radiation from optical fiber core **3183** to be focused onto a small area, enabling entrance aperture **3189** to be relatively small and to minimize loss of reflected optical radiation outward through entrance aperture **3189**.

Variations of this approach, where optical radiation is coupled into the photodiode die **1002** through an optical window **912** on the edge of the photodiode die **1002** are possible. For example, a transparent, index-matched adhesive **3394** may be provided between optical coupling member **3187** and optical window **912**, as shown schematically in FIGS. **34**B-**34**E. Fiber coupling lens **3390** may be provided on the end of optical fiber core **3183** rather than as a discrete element, as shown schematically in FIG. **34**C. Fiber coupling lens **3390** may be omitted, as shown schematically in FIGS. **34**D and **34**E. Optical radiation may pass from optical fiber core **3183** into entrance aperture **3189** through a transparent, index-matched adhesive **3394**, as shown schematically in FIG. **34**D, or through anti-reflection coating **3392** on the end of fiber core **3183**, as shown schematically in FIG. **34**E.

Rather than coupling optical radiation from an optical fiber **3180** into a relatively large area at an edge of the photodiode die **1002**, as in FIGS. **34**A-**34**E, the optical radiation may be coupled into photodiode entrance aperture **3396**, as shown schematically in FIGS. **34**F-**34**I. In some configurations, the edge of the photodiode die **1002** will include photodiode entrance aperture **3396** that is surrounded by an edge reflector layer **905**. Photodiode entrance aperture **3396** may be coated with an anti-reflection layer

(not shown), similar to the anti-reflection optical window layer **911** of the optical window **912** described above in the discussion of FIGS. **18**A-**22**E. In these embodiments the optical cavity region **3301** encompasses device cavity region **1669**, but not an external integrating optical cavity. In some preferred versions of this embodiment, device cavity region **1669** includes at least one of a substrate or an optically transmissive member, as described above. In alternative versions of this embodiment, the optical cavity region **3301** encompasses a second optically transmissive member **2101**, as shown schematically in FIGS. **27**A and **27**B, and may or may not include a substrate **101** or a first optically transmissive member. Optical radiation from optical fiber core **3183** may be focused onto photodiode entrance aperture **3396** by fiber coupling lens **3390**, either as a free-standing element (FIG. **34**F) or coupled to the end of optical fiber core **3183** (FIG. **34**G). Alternatively, optical radiation from optical fiber core **3183** may be coupled directly to entrance aperture **3396**, through an anti-reflection coating **3392** on the end of optical fiber core **3183** (FIG. **34**H) or through transparent, index-matched adhesive **3394** (FIG. **34**I).

In certain embodiments, a packaged photodiode is desired that can convert some, but not all, of the incident optical radiation energy from a fiber to electrical power. A schematic cross section of a photodiode assembly **2301** designed for extraction of only a fraction of incident optical radiation energy generated by a laser diode or optical fiber **2401** is shown in FIG. **23**A. In certain embodiments, as illustrated in FIG. **23**A, a photodiode assembly **2301** includes reflective edge layers **1404** but optical radiation is coupled from a fiber into the top (or bottom in some alternate configurations) of the photodiode die, through p-type contact **1111**, semiconductor layers **915**, through an optically transmissive member (e.g., the substrate **101**), and through an output optical window **1412** into another adjacently positioned and similarly configured fiber (not shown). A number of such photodiode assemblies may be placed in series, such as vertically stacked, as illustrated in FIG. **23**B. In some embodiments multiple photodiode assemblies in series have approximately the same peak absorption wavelength, as determined by the indium composition in the absorber layers. In alternative embodiments the photodiode assemblies are configured to absorb optical radiation at different wavelengths, for example, by varying the indium composition in the respective absorber layers.

As noted above, a nitride-based packaged photodiode, operating at visible wavelengths, is expected to have certain advantages over arsenide-based packaged photodiodes operating in the infrared. FIG. **26** shows a schematic illustration of comparative efficiencies as a function of bandgap energy including the energies of nitride-based and arsenide-based packaged photodiodes. The efficiency is calculated assuming the detailed-balanced limit of power packaged photodiodes operating under non-degenerate conditions with input photon energies slightly above the band gap, 100% optical absorption, and 100% external quantum efficiency, using an approach described by Shockley and Queisser [Journal of Applied Physics 32, 510 (1961)]. For simplicity the input power has been assumed to be 0.1 W and the area of the optical window has been assumed to be 10^{-5} m^2, but similar results are expected for a wide range of values of these parameters. In certain embodiments, the packaged photodiode will be used at approximately room temperature. As shown in FIG. **26**, at a temperature of 300 Kelvin (room temperature) the theoretical limiting efficiency is 78.2% for a GaAs photodiode operating at a wavelength of 880 nanometers but 86.5% for an InGaN photodiode operating at a wavelength of 450 nanometers. The higher bandgap of InGaN compared to GaAs yields a higher efficiency due to the nature and shape of the Planck distribution. In certain embodiments, however, the photodiode will be employed at elevated temperatures, for example, 400 degrees Kelvin, 500 degrees Kelvin, or 600 degrees Kelvin, or at even higher temperatures. At a temperature of 400 degrees Kelvin the theoretical limiting efficiency is 71.2% for a GaAs photodiode operating at a wavelength of 880 nanometers but 82.0% for an InGaN photodiode operating at a wavelength of 450 nanometers. Although the absolute values of the efficiencies are lower at the higher temperature, the relative efficiency advantage of the InGaN photodiode over the GaAs photodiode increases from +10% to +15%. At a temperature of 500 degrees Kelvin the theoretical limiting efficiency is 64.2% for a GaAs photodiode operating at a wavelength of 880 nanometers but 77.6% for an InGaN photodiode operating at a wavelength of 450 nanometers. Although the absolute values of the efficiencies are lower the relative efficiency advantage of the InGaN photodiode over the GaAs photodiode has increased further to +21%. At a temperature of 600 degrees Kelvin the theoretical limiting efficiency is 57.4% for a GaAs photodiode operating at a wavelength of 880 nanometers but 73.2% for an InGaN photodiode operating at a wavelength of 450 nanometers. Although the absolute values of the efficiencies are lower the relative efficiency advantage of the InGaN photodiode over the GaAs photodiode has increased further to +28%.

At least one packaged, nitride-based power photodiode may be incorporated into a power-over-fiber module. The power-over-fiber module includes at least one laser diode **2401** and at least one section of optical fiber **2402** that is coupled to at least one laser diode **2401** and also to at least one photodiode **2403**, as shown schematically in FIGS. **24**A-**24**C. In some embodiments, the optical fiber **2402** includes an optical fiber bundle. In certain embodiments the power-over-fiber module comprises only one laser diode **2401**, one optical fiber **2402**, and one photodiode **2403** (FIG. **24**A). In certain embodiments, one or more branches are present in the optical fiber **2402** (or optical fiber bundle), with different optical fiber segments coupled to different photodiodes **2403** (FIG. **24**B). In certain embodiments the power-over-fiber module comprises one or more optical dispensing devices **2404**, where each optical dispensing device **2404** is capable of transmitting a controlled fraction of optical power to at least two output optical fiber branches (FIG. **24**C). In some embodiments, the optical dispensing device **2404** includes or consists of at least one of one or more galvanometric mirrors, one or more micro scanning mirrors, one or more focusing lenses, and one or more optical beam splitters.

In certain embodiments the power-over-fiber module is designed simply to transmit power optically. In other embodiments, as shown schematically in FIGS. **25**A-**25**D, the power-over-fiber module is designed to transmit both power and a signal. For example, a signal may be superimposed on the optical power by modulating the amplitude of the laser diode **2401** at one or more frequencies. In some embodiments, a control module is configured to modulate the emitted power of the laser diode at at least one controlled AC frequency and to separate the photodiode signal into a DC power component and an AC signal component at the at least one controlled frequency. An amplitude of the modulated AC component of the modulated laser diode power and power of the photodiode power can be less than 10%, less than 1%, or less than 0.1% of the corresponding DC components. The first photodiode, which is configured to convert

the DC power component into electrical power, can be further configured to detect the AC signal component at the at least one controlled frequency. In some embodiments, a separate signal photodetector device is provided, wherein the separate signal photodetector device is configured to detect the AC signal component at the at least one controlled frequency.

An amplifier system coupled to the photodiode then extracts the signal or signals at one or more frequencies. In certain embodiments, the power-over-fiber module comprises at least two laser diodes **2401** and **2405** and at least two photodiodes **2403** and **2404**, and is configured to enable signal communication in at least two different directions (FIG. **25**C). In certain embodiments, the signal is modulated at audio frequencies and the output is coupled to an audio device such as a headphone or a speaker. In certain embodiments, the AC signal component is modulated at an audio frequency and the module is coupled to a headphone or to an audio speaker. In certain embodiments the signal is modulated at kilohertz, megahertz or gigahertz frequencies (FIG. **25**D).

In certain embodiments, the modulated signal is detected using the same GaN-based photodiode device that also converts optical power to electrical power. In alternative embodiments, a separate, signal photodetector device is used to convert a portion of the modulated optical signal to a modulated electrical signal. In certain embodiments, the separate, signal photodetector device is selected from a GaN-based photodiode, a Si-based photodiode, an avalanche photodiode, an InGaAs-based photodiode, and an InP-based photodiode. In certain embodiments, the separate, signal photodetector device is edge-coupled or incorporates a resonant cavity region or refracting facet. In certain embodiments the separate, signal photodetector device has a bandwidth of at least 1 MHz, at least 10 MHz, at least 100 MHz, at least 1 GHz, at least 10 GHz, at least 25 GHz, or at least 100 GHz. In certain embodiments the separate, signal photodetector device is mounted to and receives modulated optical signal from the same optical cavity region from which a GaN-based photodiode receives DC optical power. In certain embodiments, the separate, signal photodetector device receives signal from an optical fiber connected to the same network as the GaN-based power photodiode. In certain embodiments, the separate, signal photodetector device is optically decoupled from the GaN-based power photodiode, so that stray light emission from the latter does not degrade the bandwidth of the former. In certain embodiments, a small fraction of the optical radiation from the optical fiber is routed to the separate photodetector device and the remaining, large fraction, optical radiation is routed to the GaN-based power photodiode.

FIGS. **35**A-**35**F are simplified diagrams showing side cross sectional views of a packaged photodiode and a separate, signal photodetector device **3595** coupled to an optical fiber, according to embodiments of the present disclosure. In some embodiments, optical radiation emitted from optical fiber **3180** is reflected from signal photodetector device **3595** prior to being routed to photodiode die **1002** by fiber coupling lens **3390** into entrance aperture **3189** of optical coupling member **3187**, as shown schematically in FIG. **35**A. In certain embodiments, signal photodetector device **3595** has a high-reflectivity coating **3596** that allows only a small portion of the incident optical radiation into signal photodetector device **3595**. In certain embodiments, the reflectivity of high-reflectivity coating **3596** is greater than 90%, greater than 95%, greater than 97%, or greater than 98%. In certain embodiments, high-reflectivity coating **3596** includes one or more of a metal, such as silver, and a dielectric.

In certain embodiments, a second fiber coupling lens **3390** is used to focus optical radiation from optical fiber **3180** onto signal photodetector device **3595** (FIG. **35**B), enabling the use of small lateral dimensions of signal photodetector device **3595**, which may reduce the capacitance and increase the bandwidth of the latter. In certain embodiments, a lateral dimension of signal photodetector device **3595** is less than 1 millimeter, less than 300 micrometers, less than 200 micrometers, less than 100 micrometers, or less than 50 micrometers. In certain embodiments, signal photodetector device **3595** samples optical radiation through an aperture **3598** in reflective coating **3185** on optical coupling member **3187**, as shown schematically in FIGS. **35**C-**35**F. In certain embodiments, a small internal reflector **3597** contained within optical coupling member **3187** reflects a portion of the optical radiation toward aperture **3598**. In certain embodiments, internal reflector **3597** includes one or more of a metal, such as silver, and a dielectric. In certain embodiments, internal reflector **3597** includes a bubble or void within optical coupling member **3187**. In certain embodiments, a maximum dimension of internal reflector **3597** is less than about 2 millimeters, less than about 1 millimeter, less than about 500 micrometers, less than about 200 micrometers, less than about 100 micrometers, or less than about 50 micrometers.

In certain embodiments, optical radiation exiting from optical coupling member **3187** enters an edge of photodiode die **1002** (FIG. **35**C). In other embodiments, optical radiation exiting from optical coupling member **3187** enters photodiode die **1002** through openings in n-side reflective electrical contact **3317** (FIGS. **35**D-**35**F). In certain embodiments, optical radiation from optical fiber **3180** is focused onto the entrance aperture **3189** of optical coupling member **3187** by fiber coupling lens **3390** (FIGS. **35**C-**35**E). In certain embodiments, index-matched adhesive **3394** is used to transmit optical radiation from optical coupling member **3187** to photodiode die **1002** (FIGS. **35**E, **35**F) or from optical fiber **3180** to entrance aperture **3189** (FIG. **35**F).

In certain embodiments, the power-over-fiber module is operated near room temperature, that is, less than a temperature of about 400 degrees Kelvin. In other embodiments, the power-over-fiber module is operated at a temperature between about 400 degrees Kelvin and about 500 degrees Kelvin, between about 500 degrees Kelvin and about 600 degrees Kelvin, or above about 600 degrees Kelvin.

In certain embodiments, optical coupling between the optical fiber and the photodiode may be nonrigid or non-contact, enabling easy coupling of optical power to an object that is rotating.

In certain embodiments, electrical power from the photodiode is used to power an Internet-of-Things (IoT) sensor or actuator. In certain embodiments, electrical power from the photodiode is used to power a personal electronic application or personal electronic device.

In alternative embodiments, transmission of optical power from a light source such as a laser diode to the photodiode is accomplished without a fiber, for example between satellites in space or between the ground and an airborne drone.

In certain embodiments, as shown schematically in FIG. **28**, the power-over-fiber module is integrated with a lighting system **2407**. Lighting system **2407** may include one or more of a phosphor, a heat sink, a reflective or transmissive optic for shaping the far-field distribution of light, a sensor, and a control system. Such a capability is possible with a

lighting source (e.g., laser diode) **2401** and photodiode system based on a nitride semiconductor material system but is not possible with an arsenide-based system, for example. A portion of the light injected by a light source, such as a laser diode **2401**, through an optical fiber **2402** is converted to electrical power by a photodiode **2403** and the remainder of the light is out-coupled to another optical fiber **2406** and injected into a lighting system **2407**. In some embodiments the lighting system **2407** is a luminaire. In some embodiments the lighting system **2407** is an automotive headlight. In some embodiments the luminaire contains one or more phosphors to convert a portion of the light from the optical fiber, for example, having one or more wavelengths between 400 nanometers and 460 nanometers, to emit green, yellow, and/or red light. In some embodiments the luminaire emits light approximating a solar spectrum. In some embodiments the luminaire emits light having a color temperature of approximately 2700 degrees Kelvin, approximately 3000 degrees Kelvin, approximately 4000 degrees Kelvin, or approximately 6000 degrees Kelvin. In some embodiments the luminaire emits light having a color rendition index (CRI) of approximately 80, between 80 and 90, between 90 and 95, or above 95. In some embodiments the luminaire emits collimated light with a cone angle less than 45 degrees, less and 30 degrees, less than 20 degrees, less than 10 degrees, less than 5 degrees, or less than 3 degrees. In certain embodiments electrical power from the photodiode **2403** is used to power a component in the luminaire, such as a sensor or a wireless communication device. In certain embodiments electrical power from the photodiode **2403** is used to power a control system that changes an output characteristic of the lighting system, such as the color temperature, the intensity of blue light relative to the intensity of other colors, the angular distribution of light, or the like.

One or more power-over-fiber modules may be incorporated into a power-over-fiber system. In addition to at least one laser diode light source, at least one power photodiode, and at least one section of optical fiber, the power-over-fiber system may include one or more of a control system, electrical leads to a power source such as a battery, alternator, or mains AC or DC power, a flexible jacket surrounding at least a portion of the optical fiber, at least one temperature sensor, at least one harness member to maintain a position of at least one component of a power-over-fiber module with respect to a structure within which it is placed, a means for providing cooling, such as a fan or flowing coolant liquid, and at least one sensor. The power-over-fiber system may be placed within an automobile, within an automobile engine, within a truck or truck engine, within a bus or bus engine, within a locomotive, within an aircraft or aircraft engine, within a helicopter or helicopter engine, within a house, apartment, or residential building, or within a commercial building.

In certain embodiments, such as a power-over-fiber system in an automobile or within a room in a building, the length of the fiber is relatively short, between about one centimeter and about one meter. In such a case optical attenuation within the fiber may not be performance limiting and other factors, such as turning radius and thermal stability may be more important. In other embodiments, such as a power-over-fiber system in a building where optical power is being transported from one room to another, the length of the fiber may be between one meter and one hundred meters. In this case optical attenuation within the fiber may be more important but turning radius may be less important. In other embodiments the length of the fiber may be between 100 meters and one kilometer, or greater than one kilometer.

The power-over-fiber system may have improved reliability compared to other systems. For example, relative to traditional power-over-wire systems, contacts (optical rather than contact-electrical) may be less susceptible to oxidation or other degradation, and electrical transmission noise generated by electric currents may be eliminated Relative to arsenide-based systems, the nitride-based system may have a longer operating lifetime and be less sensitive to elevated-temperature excursions.

As mentioned above, the primarily lateral propagation of light within the device cavity region of the photodiode enables a relatively thin absorber layer deposited on a relatively thick substrate to absorb the large fraction of light within the device cavity region. We have constructed an optical absorption model for the device cavity region that accounts for absorption within the substrate, non-absorber layers(s), absorber layer(s), and top and bottom reflective contacts in order to quantify the trade-offs between various design parameters for the photodiode. Inputs to the model include the substrate and absorber layer absorption coefficients, refractive indices, and thicknesses, along with the reflectance of the and bottom reflective contacts. With these inputs, the fraction of optical absorption can be calculated as a function of the light propagation angle relative to the plane of the absorber layer(s). As an example, FIGS. **29**A-**29**B shows the cumulative optical absorption in the substrate, absorber layer, top p-contact mirror, and bottom p-contact mirror as a function of lateral propagation distance, along with the input parameters for this calculation. A 15 degree light propagation angle maximized optical absorption within the absorber layer for the set of parameters shown in FIG. **29**A.

EXAMPLES

Embodiments provided by the present disclosure are further illustrated by reference to the following comparative examples and exemplary process examples. It will be apparent to those skilled in the art that many modifications, both to materials, and methods, may be practiced without departing from the scope of the disclosure.

Comparative Example 1

As a point of comparison, a +c-plane, GaN-on-GaN die was harvested from a commercial LED emitting at approximately 405 nanometers and utilized as a photodiode. The LED structure is believed to include an AlGaN electron blocking layer underlying a p-type GaN layer and a multi-quantum-well MQW structure comprising InGaN well layers and GaN barrier layers. The LED structure is believed not to include either highly-doped layers or doped, reduced-bandgap layers directly adjoining the MQW layers. The reverse current-voltage characteristics were recorded under dark and light conditions, where illumination was provided by a commercial 405 nm laser diode. The results are shown in FIG. **5** as the "LIV" curve. From the measured results, V_{oc} was evaluated as 2.74 V, E_g=3.06 eV, I_{sc}=2.6 A/cm^2, eV_{oc}/E_g=0.89, and FF=46%. The values of V_{oc} and of I_{sc} are seen to be relatively good, whereas the low value for the fill factor indicates that improved device designs are needed. By contrast, a curve with a relatively high fill factor is shown for comparison in FIG. **5**.

Comparative Example 2

An epitaxial structure, including a 500 nanometer n-type doped GaN layer containing Si dopant at a concentration of

2×10^{18} cm^{-3}, followed by a 100 nanometer n-type doped GaN layer containing Si dopant at a concentration of 4×10^{18} cm^{-3}, followed by an unintentionally doped absorber layer, followed by a 90 nanometer p-type doped layer containing Mg at a concentration of 1×10^{19} cm^{-3}, followed by a 10 nanometer p+-type doped layer containing Mg at a concentration of 1×10^{20} cm^{-3}, was deposited on a bulk GaN substrate miscut from (0001) by approximately 0.4 degrees toward [10-10]. The absorber layer was unintentionally doped and consisted of a 7 nanometer GaN layer followed by 10 alternating layers of 4 nanometer $In_{0.14}Ga_{0.86}N$ well layers and 7 nanometer GaN barrier layers. The structure was characterized by an electroluminescence peak at approximately 447 nanometers. The reverse current-voltage characteristics were recorded under dark and light conditions, where illumination was provided by a commercial 405 nm laser diode. The results are shown in FIG. **6**. From the measured results, V_{oc} was evaluated as 2.32 V, E_g=2.77 eV, $I_{sc}=6.5\times10^{-3}$ A, e V_{oc}/E_g=0.84, and FF=33%. The values of V_{oc} and of I_{sc} are seen to be relatively good, whereas the low value for the fill factor indicates that improved device designs are needed.

Comparative Example 3

An epitaxial structure, including a 1000 nanometer n-type doped GaN layer containing Si dopant at a concentration of 2.0×10^{18} cm^{-3}, followed by a 30 nanometer n-type doped GaN layer containing Si dopant at a concentration of 2×10^{19} cm^{-3}, followed by an unintentionally doped absorber layer, followed by a 50 nanometer p-type doped layer containing Mg at a concentration of 2×10^{19} cm^{-3}, followed by a 10 nanometer p+-type doped layer containing Mg at a concentration of 1×10^{20} cm^{-3}, was deposited on a bulk GaN substrate miscut from (0001) by approximately 0.4 degrees toward [10-10]. The absorber layer was unintentionally doped and consisted of a 40 nanometer double-heterostructure $In_{0.13}Ga_{0.87}N$ layer. The structure was characterized by an electroluminescence peak at approximately 435 nanometers. The reverse current-voltage characteristics were recorded under dark and light conditions, where illumination was provided by a commercial 405 nm laser diode. The results are shown in FIG. **11**. From the measured results, V_{oc} was evaluated as 2.43 V, E_g=2.85 eV, I_{sc}=0.013 A, eV_{oc}/E_g=0.85, and FF 38%. The values of V_{oc} and of I_{sc} are seen to be relatively good, whereas the low value for the fill factor indicates that improved device designs are needed.

Comparative Example 4

An epitaxial structure, including a 1000 nanometer n-type doped GaN layer containing Si dopant at a concentration of 2.0×10^{18} cm^{-3}, followed by a 100 nanometer n-type doped GaN layer containing Si dopant at a concentration of 5.0×10^{17} cm^{-3}, followed by an unintentionally doped absorber layer, followed by a 50 nanometer p-type doped layer containing Mg at a concentration of 2×10^{20} cm^{-3}, followed by a 10 nanometer p+-type doped layer containing Mg at a concentration of 1×10^{20} cm^{-3}, is deposited on a bulk GaN substrate miscut from (0001) by approximately 0.4 degrees toward [10-10]. The absorber layer is unintentionally doped and consists of a 40 nanometer double-heterostructure $In_{0.18}Ga_{0.82}N$ layer. The structure is characterized by an electroluminescence peak at approximately 473 nanometers. The reverse current-voltage characteristics are recorded under dark and light conditions, where illumination is provided by a commercial 405 nm laser diode. From the measured results, V_{oc} is evaluated as 2.20 V, E_g=2.62 eV, eV_{oc}/E_g=0.84, and FF 45%. The value of V_{oc} is seen to be relatively good, whereas the low value for the fill factor indicates that improved device designs are needed.

Example 1

An epitaxial structure, including a 1000 nanometer n-type doped GaN layer containing Si dopant at a concentration of 2.0×10^{18} cm^{-3}, followed by a 30 nanometer n-type doped GaN layer containing Si dopant at a concentration of 3.0×10^{19} cm^{-3}, followed by an unintentionally doped absorber layer, followed by a 50 nanometer p-type doped layer containing Mg at a concentration of 3×10^{19} cm^{-3}, followed by a 10 nanometer p+-type doped layer containing Mg at a concentration of 1×10^{20} cm^{-3}, is deposited on a bulk GaN substrate miscut from (0001) by approximately 0.4 degrees toward [10-10]. The absorber layer is unintentionally doped and consists of a 40 nanometer double-heterostructure $In_{0.13}Ga_{0.87}N$ layer. The structure is characterized by an electroluminescence peak at approximately 435 nanometers. The reverse current-voltage characteristics are recorded under dark and light conditions, where illumination is provided by a commercial 405 nm laser diode. From the measured results, V_{oc} is evaluated as 2.43 V, E_g=2.85 eV, eV_{oc}/E_g=0.85, and FF 85%.

Example 2

An epitaxial structure, including a 1000 nanometer n-type doped GaN layer containing Si dopant at an average concentration of 2.0×10^{18} cm^{-3}, followed by a 30 nm n-type doped GaN layer containing Si at an average concentration of 4.0×10^{19} cm^{-3}, followed by an unintentionally doped absorber layer, followed by a 50 nanometer p-type doped layer containing Mg at a concentration of 2×10^{20} cm^{-3}, is deposited on a bulk GaN substrate miscut from (0001) by approximately 0.4 degrees toward [10-10]. The absorber layer is unintentionally doped and consists of a 40 nanometer double-heterostructure $In_{0.18}Ga_{0.82}N$ layer. The structure is characterized by a photoluminescence peak at approximately 473 nanometers. The reverse current-voltage characteristics are recorded under dark and light conditions, where illumination is provided by a commercial 405 nm laser diode. From the measured results, V_{oc} is evaluated as 2.20 V, E_g=2.62 eV, eV_{oc}/E_g=0.84, and FF 91%.

Example 3

An epitaxial structure, including a 1000 nanometer n-type doped GaN layer containing Si dopant at an average concentration of 2.0×10^{18} cm^{-3}, followed by a 100 nm n-type doped GaN layer containing Si at an average concentration of 5.0×10^{17} cm^{-3}, followed by an approximately 6 nm thick compositionally-graded InGaN layer with an initial composition of GaN and final composition of approximately $In_{0.18}Ga_{0.72}N$ and a Si dopant concentration of approximately 5.0×10^{17} cm^{-3} followed by an unintentionally doped absorber layer, followed by a 50 nanometer p-type doped layer containing Mg at a concentration of 2×10^{20} cm^{-3}, is deposited on a bulk GaN substrate miscut from (0001) by approximately 0.4 degrees toward [10-10]. The absorber layer is unintentionally doped and consists of a 40 nanometer double-heterostructure $In_{0.18}Ga_{0.82}N$ layer. The structure is characterized by a photoluminescence peak at approximately 473 nanometers. The reverse current-voltage characteristics are recorded under dark and light conditions,

where illumination is provided by a commercial 405 nm laser diode. From the measured results, V_{oc} is evaluated as 2.20 V, E_g=2.62 eV, eV_{oc}/E_g=0.84, and FF 85%.

Example 4

An epitaxial structure, including a 300 nanometer n-type doped GaN layer containing Si dopant at an average concentration of 3.5×10^{18} cm^{-3}, followed by an InGaN—GaN strained-layer-superlattice (SLS), followed by an approximately 6 nm thick compositionally-graded InGaN layer with an initial composition of approximately $In_{0.04}Ga_{0.96}N$ and final composition of approximately $In_{0.2}Ga_{0.8}N$ and a Si dopant concentration of approximately 4.0×10^{17} cm^{-3}, followed by a 9-period multi-quantum well structure comprised of 3 nm $In_{0.2}Ga_{0.8}N$ wells and 9 nm GaN barrier layers containing Si dopant at a concentration of approximately 3×10^{17} cm^{-3}, followed by a 100 nanometer p-type doped layer containing Mg at a concentration of approximately 2×10^{20} cm^{-3}, was grown on a sapphire substrate with the substrate surface normal within 5 degrees of the [0001] of the nitride epitaxial layers. The absorber layer consisted of the 9-period multi-quantum well structure. The structure was characterized by a photoluminescence peak at approximately 457 nanometers. The reverse current-voltage characteristics of fabricated devices were recorded under dark and light conditions, where illumination was provided by a commercial 405 nm laser diode. The results are shown in FIG. **12**. From the measured results, V_{oc} was evaluated as 2.34 V, E_g=2.71 eV, I_{sc}=0.0114 A, eV_{oc}/E_g=0.86, and FF 78%. The values of V_{oc}, I_{sc}, and FF are seen to be relatively good. The measured FF is artificially low due to series resistance arising from the method of electrically probing the n metal contact.

Example 5

An epitaxial structure, including a 1000 nanometer n-type doped GaN layer containing Si dopant at an average concentration of 1.0×10^{18} cm^{-3}, followed by an unintentionally-doped, 20-period multi-quantum well structure comprised of 2 nm $In_{0.18}Ga_{0.82}N$ wells and 4 nm GaN barrier layers, followed by a 50 nanometer p-type doped layer containing Mg at a concentration of approximately 2×10^{18} cm^{-3}, is deposited on a bulk GaN substrate miscut from (000-1) by approximately 4 degrees toward [10-10]. The absorber layer consisted of the 9-period multi-quantum well structure. The structure is characterized by a photoluminescence peak at approximately 470 nanometers. The reverse current-voltage characteristics are recorded under dark and light conditions, where illumination is provided by a commercial 405 nm laser diode. From the measured results, V_{oc} is evaluated as 2.20 V, E_g=2.63 eV, eV_{oc}/E_g=0.84, and FF 88%.

Example 6

An epitaxial structure, including a 1000 nanometer n-type doped GaN layer containing Si dopant at an average concentration of 5.0×10^{18} cm^{-3}, followed by an unintentionally-doped, 20-period multi-quantum well structure comprised of 2 nm $In_{0.18}Ga_{0.82}N$ wells and 4 nm GaN barrier layers, followed by a 100 nanometer p-type doped layer containing Mg at a concentration of approximately 1×10^{19} cm^{-3}, is deposited on a bulk GaN substrate having a crystallographic orientation within 0.1 degree of (30-3-1). The structure is characterized by a photoluminescence peak at approximately 470 nanometers. The reverse current-voltage characteristics are recorded under dark and light conditions, where illumination is provided by a commercial 405 nm laser diode. From the measured results, V_{oc} is evaluated as 2.20 V, E_g=2.63 eV, eV_{oc}/E_g=0.84, and FF 88%.

While the foregoing is directed to embodiments of the present disclosure, other and further embodiments of the disclosure may be devised without departing from the basic scope thereof, and the scope thereof is determined by the claims that follow.

What is claimed is:

1. An optical device, comprising:

a die comprising a substrate and one or more absorber layers disposed between an n-type layer and a p-type layer, each of the one or more absorber layers, the n-type layer, and the p-type layer comprising $Al_xIn_yGa_{1-x-y}N$, where $0\leq x, y, x+y\leq1$ and having a dislocation density below about 10^{10} cm^{-2}; wherein

the one or more absorber layers each have a thickness, measured in a first direction, and an absorber layer surface that is oriented normal to the first direction,

the one or more absorber layers have a bandgap corresponding to a wavelength between about 400 nanometers and about 550 nanometers, and

the substrate has a thickness, measured in the first direction, between 10 micrometers and 10 millimeters,

the die further comprises an optical cavity region having an optical window, the optical cavity region comprising the substrate, a p-side reflective electrical contact, and an n-side reflective electrical contact,

electromagnetic radiation entering through the optical window passes through the one or more absorber layers at least two or more times, and

the n-type layer overlies a first side of the substrate, the n-side reflective electrical contact is in electrical contact with a second side of the substrate opposite the first side of the substrate, and the p-side reflective electrical contact is in electrical contact with the p-type layer.

2. The optical device of claim **1**, wherein the optical cavity region is further configured to cause internal reflection of luminescent light emitted from the one or more absorber layers due to the electromagnetic radiation passing through the one or more absorber layers.

3. The optical device of claim **1**, wherein the area of the optical window is less than 40% of the surface area of the absorber layer surface of one of the one or more absorber layers.

4. The optical device of claim **1**, wherein the absorber layer surface is parallel to a first plane and the optical cavity region is configured to cause the electromagnetic radiation passing through the one or more absorber layers to propagate in a direction within 20 degrees of the first plane.

5. The optical device of claim **1**, wherein the absorber layer surface is parallel to a first plane and the optical cavity region is configured to cause the electromagnetic radiation passing through the one or more absorber layers to propagate in a direction that is between 20 degrees and 80 degrees from the first plane.

6. The optical device of claim **1**, wherein the absorber layer surface is parallel to a first plane and the optical cavity region is configured to cause the electromagnetic radiation passing through the one or more absorber layers to propagate in a direction within 10 degrees of a normal to the first plane.

7. The optical device of claim **1**, wherein the crystallographic orientation of each of the one or more absorber

layers and each of the n-type layer and the p-type layer is within 5 degrees of (0001) or of (000-1).

8. The optical device of claim **1**, wherein the crystallographic orientation of each of the one or more absorber layers and each of the n-type layer and the p-type layer is within 5 degrees of one of {1 0 −1 0} and of {1 1 −2 0}.

9. The optical device of claim **1**, wherein the crystallographic orientation of each of the one or more absorber layers and each of the n-type layer and the p-type layer is within 5 degrees of one of {11-2±2}, {60-6±1}, {50-5±1}, {40-4±1}, {30-3±1}, {50-5±2}, {70-7±3}, {20-2±1}, {30-3±2}, {40-4±3}, {50-5±4}, {10-1±1}, {1 0 −1±2}, {1 0 −1±3}, {2 1 −3±1}, or {3 0 −3±4}.

10. The optical device of claim **1**, wherein each of the one or more absorber layers, the n-type layer and the p-type layer have a dislocation density less than about 10^8 cm^{-2}.

11. The optical device of claim **10**, wherein at least one of the p-side reflective electrical contact or the n-side reflective electrical contact comprises a discontinuous or gridded electrode and a reflective metal layer.

12. The optical device of claim **10**, wherein at least one of the n-side reflective electrical contact and the p-side reflective electrical contact comprises a dielectric layer, the dielectric layer comprising at least one of TiO_2, Ta_2O_5, ZrO_2, SiO_2, SiO_x, SiN_x, Si_3N_4, SiO_xN_y, Al_2O_3, or MgF_2.

13. The optical device of claim **10**, wherein the n-side reflective electrical contact and the p-side reflective electrical contact are configured to change the propagation direction of the electromagnetic radiation passing through the one or more absorber layers within the optical cavity region by more than about 30 degrees.

14. An optical device, comprising:

a die comprising a substrate and one or more absorber layers disposed between an n-type layer and a p-type layer, each of the one or more absorber layers, the n-type layer, and the p-type layer comprising $Al_xIn_yGa_{1-x-y}N$, where 0≤x, y, x+y≤1 and having a dislocation density below about 10^{10} cm^{-2}; wherein

the one or more absorber layers each have a thickness, measured in a first direction, and an absorber layer surface that is oriented normal to the first direction,

the die further comprises an optical cavity region having an optical window, the optical cavity region comprising the substrate, a p-side reflective electrical contact, and an n-side reflective electrical contact,

electromagnetic radiation entering through the optical window passes through the one or more absorber layers at least two or more times,

the n-type layer overlies a first side of the substrate, the n-side reflective electrical contact is in electrical contact with a second side of the substrate opposite the first side of the substrate, and the p-side reflective electrical contact is in electrical contact with the p-type layer, and

wherein the first surface of the substrate has impurity concentrations of

O between about 1×10^{16} cm^{-3} and about 1×10^{19} cm^{-3},

H between about 1×10^{16} cm^{-3} and about 2×10^{19} cm^{-3},

C below 1×10^{17} cm^{-3}, and

at least one of F and Cl between about 1×10^{15} cm^{-3} and about 1×10^{19} cm^{-3}, as quantified by calibrated secondary ion mass spectrometry (SIMS).

15. An optical device, comprising:

a die comprising an optically-transmissive member, an n-side reflective electrical contact, a p-side reflective electrical contact, and one or more absorber layers disposed between an n-type layer and a p-type layer, each of the one or more absorber layers, the n-type layer, and the p-type layer comprising $Al_xIn_yGa_{1-x-y}N$, where 0≤x, y, x+y≤1 and having a dislocation density below about 10^{10} cm^{-2}; wherein

the one or more absorber layers each have a thickness, measured in a first direction, and an absorber layer surface that is oriented normal to the first direction,

the one or more absorber layers have a bandgap corresponding to a wavelength between about 400 nanometers and about 550 nanometers,

the optically-transmissive member has a thickness, measured in the first direction, between 10 micrometers and 10 millimeters,

the die further comprises an optical cavity region having an optical window, the optical cavity region comprising the optically-transmissive member and at least one of the p-side reflective electrical contact and the n-side reflective electrical contact, wherein electromagnetic radiation entering through the optical window passes through the one or more absorber layers at least two or more times,

the n-side reflective electrical contact is in electrical contact with one of a second side of the optically-transmissive member opposite a first side of the optically-transmissive member or the n-type layer or a semi-transparent current spreading layer disposed on the n-type layer,

the p-side reflective electrical contact is in electrical contact with the p-type layer or a semi-transparent current spreading layer disposed on the p-type layer,

at least a portion of at least one of the n-side reflective electrical contact or the p-side reflective electrical contact is positioned in a second direction with respect to an edge of at least one of the optically-transmissive member or at least one absorber layer, and

the second direction is perpendicular to the first direction.

16. The optical device of claim **15**, wherein the optically-transmissive member comprises sapphire.

17. The optical device of claim **15**, wherein the optically-transmissive member comprises gallium nitride.

18. The optical device of claim **15**, wherein the optically-transmissive member comprises a patterned array of features at an interface between the optically-transmissive member and at least one of the n-type layer or the p-type layer.

19. The optical device of claim **18**, wherein the pitch of the features is between about 0.2 micrometers and about 10 micrometers and the features have a height between about 0.1 micrometer and about 10 micrometers and a width between 0.1 micrometer and about 5 micrometers.

20. An optical device, comprising:

a die comprising an optically-transmissive member, an n-side reflective electrical contact, a p-side reflective electrical contact, and one or more absorber layers disposed between an n-type layer and a p-type layer, each of the one or more absorber layers, the n-type layer, and the p-type layer comprising $Al_xIn_yGa_{1-x-y}N$, where 0≤x, y, x+y≤1 and having a dislocation density below about 10^{10} cm^{-2}; wherein

the one or more absorber layers each have a thickness, measured in a first direction, and an absorber layer surface that is oriented normal to the first direction,

the one or more absorber layers have a bandqap corresponding to a wavelength between about 400 nanometers and about 550 nanometers,

the optically-transmissive member has a thickness, measured in the first direction, between 10 micrometers and 10 millimeters,

the die further comprises an optical cavity region having an optical window, the optical cavity region comprising the optically-transmissive member and at least one of the p-side reflective electrical contact and the n-side reflective electrical contact, wherein electromagnetic radiation entering through the optical window passes through the one or more absorber layers at least two or more times,

at least one via penetrates the one or more absorber layers and at least one of the p-type layer or of the n-type layer,

the n-side reflective electrical contact makes direct electrical contact to the n-type layer or a semi-transparent current spreading layer disposed on the n-type layer, and

the p-side reflective electrical contact makes electrical contact with the p-type layer or a semi-transparent current spreading layer disposed on the p-type layer.

* * * * *